Novel Synthesis Methods Using Phosphorus and Silicon Reagents

Edward Thornton, MChem

Thesis submitted to the University of Nottingham for the degree of Doctor of Philosophy

September 2019

Chapter 1: Solution and Solid Phase Synthesis and Utility of Dioxyphosphoranes

Acknowledgements

Firstly, I would like to thank Dr Ross Denton for the opportunity to conduct this research. The advice and support over the past four years has been hugely appreciated, without which this thesis would not have been possible.

I would also like to thank my Industrial supervisors Mubina Mohamed and Niall McCreanor for all their support regarding the industrial aspects of the studentship. I am also very grateful to Niall for helping me settle into work at Astrazeneca during my CASE placement, both within the lab and in Macclesfield as a whole.

Further thanks are due to all members of the Denton group past and present. Both the academic support and humour provided served to make the work not only more successful, but also more enjoyable. A particular thanks has to go to Dean Wheeler who endured my company from day one of the PhD, and from whom it is impossible to disentangle my past four years in Nottingham.

This work would not have been possible without the help of all the analytical and technical staff of the School of Chemistry. I would also like to thank Leslie Hughes for performing the solid-state NMR analysis.

Finally, I must also acknowledge the importance of those closest to me. Frances thank you for the love and encouragement throughout all of the highs and lows. I will forever be grateful for the support you gave me and I look forward to our non-PhDing future! Last but not least I would like to thank my parents. Thank you for persevering with your problem child and making me who I am today. Without your love and support I would never have got this far.

List of Abbreviations

3c 4e	Three Centre Four Electron
AIBN	Azobisisobutyronitrile
ATP	Adenosine Triphosphate
ATR	Attenuated Total Reflectance
COD	1,5-Cyclooctadiene
COE	Cyclooctene
COT	Cyclooctatetraene
d. r.	Diastereomeric Ratio
DCE	1,2-Dichloroethane
DCM	Dichloromethane
DEAD	Diethyl Azodicarboxylate
DFT	Density Functional Theory
DIEA	*N,N*-Diisopropylethylamine
DMA	Dimethylacetamide
DMF	Dimethylformamide
DMSO	Dimethyl Sulfoxide
EDC	1-Ethyl-3-(3-dimethylaminopropyl)carbodiimide
ee	Enantiomeric Excess
HMDS	Hexamethyldisilazane
HMPA	Hexamethylphosphoramide
HOBT	Hydroxybenzotriazole

HPLC	High Performance Liquid Chromatography
HRMS	High Resolution Mass Spectrometry
IR	Infrared
m. p.	Melting Point
Ms	Methanesulfonyl
MW	Molecular Weight
NMR	Nuclear Magnetic Resonance
Oct	Octanoate
PBS	Phosphate-Buffered Saline
PIFA	(Bis(trifluoroacetoxy)iodo)benzene
ppm	Parts Per Million
r. t.	Room Temperature
s. m.	Starting Material
SuFEx	Sulfur(VI) Fluoride Exchange
TCE	1,1,2,2-Tetrachloroethane
Tf	Trifluoromethylsulfonyl
THF	Tetrahydrofuran
THP	Tetrahydropyran
TMS	Trimethylsilyl
Ts	Toluenesulfonyl

Contents

1.1 Abstract

Chapter one describes the synthesis and application of dioxyphosphoranes in both solution and solid phase reactions. Two novel monolithic dioxyphosphoranes were prepared and their efficacy demonstrated through the cyclodehydration of a diol. Characterisation of the monolithic reagents was performed using solid-state NMR analysis. Intermolecular amine-alcohol coupling reactions, using two solution phase dioxyphosphoranes, are described and efforts to overcome competitive side reactions discussed.

1.2 Introduction

1.2.1 Structure and Bonding of Phosphoranes

Phosphoranes are a class of neutral, pentavalent, phosphorus-containing compounds in the P(V) oxidation state. σ^5 phosphoranes are almost exclusively trigonal bipyramidal, with only a few square pyramidal exceptions, these mostly in the form of spirocycles (Scheme 1).[1] Within this geometry exist two distinct environments of three equatorial positions and two co-linear axial (or apical) positions. Investigations using X-ray crystallography have shown bond lengths to the apical positions to be longer than those to the equatorial positions.[2] To explain the bonding of these pentavalent species, the concept of three-centre-four-electron bonds (3c-4e) is invoked.

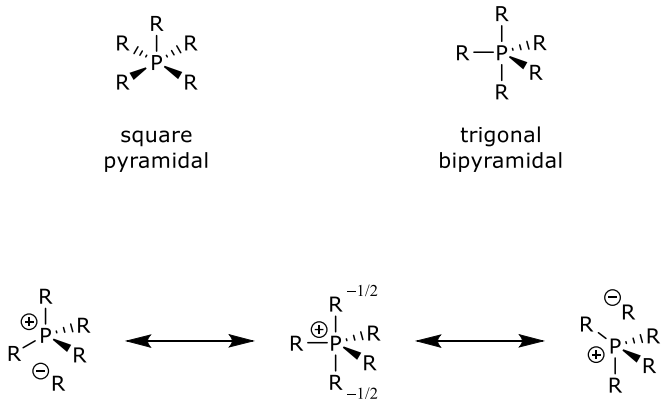

Scheme 1: Top: geometry of phosphoranes; Bottom: description of the 3c-4e bond of phosphoranes using valence bond theory.

In this theory, two electrons occupy a bonding orbital across the phosphorus atom and both apical ligands. Whilst a further two electrons are in a non-bonding orbital with electron density residing on the apical ligands.[3] Expressing this using valence bond theory, the bonding can be

depicted using the resonance forms shown in Scheme 1. Whereby, there is a formal positive charge on the phosphorus atom and half a negative charge on each apical ligand. This bonding model explains both the longer bond lengths to the apical positions, as well as the concept of apicophilicity. Apicophilicity is the phenomenon where electronegative substituents preferentially occupy the apical positions, consequently better stabilising the non-bonding electron density in these positions. Quin has suggested the order of apicophilicity of some common phosphorane substituents to be[1]:

F > H > CF_3 > PhO > Cl > MeS > MeO > Me_2N > Me > Ph

In addition to the effect of electronegativity, sterics can also be seen to play a role in this ordering. Hydrogen is an obvious anomaly if electronics were the only determining factor. This can be explained by the 90° bond angles between the apical and equatorial positions, relative to the 120° bond angles between two equatorial positions, resulting in the apical positions being more sterically congested.

Phosphoranes are often substitutionally labile towards nucleophiles. This is of great significance to the application of phosphoranes in synthesis and accordingly to this chapter. For such substitution reactions to occur, the leaving group must reside in an equatorial position to allow the attacking nucleophile to approach (attack of the axial antibonding orbital being geometrically impossible). Given that apicophilic substituents are generally better at stabilising electron density (and thus better leaving groups) this often requires a rearrangement of the phosphorane to occur. This can be achieved through either a Berry pseudorotation or an Ugi-turnstile pseudorotation (Scheme 2).[4] Both of these have a low energy barrier for acyclic phosphoranes and thus occur rapidly at room temperature.

Berry pseudorotation:

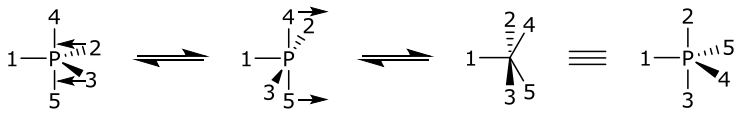

Ugi-turnstille pseudorotation:

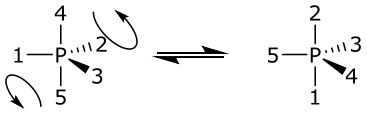

Scheme 2: Berry and Ugi-turnstile pseudorotation mechanisms for phosphorane interconversions.

Spirocyclic compounds often have a higher energy barrier for pseudorotation and thus cannot undergo geometrical rearrangements as readily. This is exemplified by the two spirocyclic coordination isomers **1** and **4** (Scheme 3).[5]

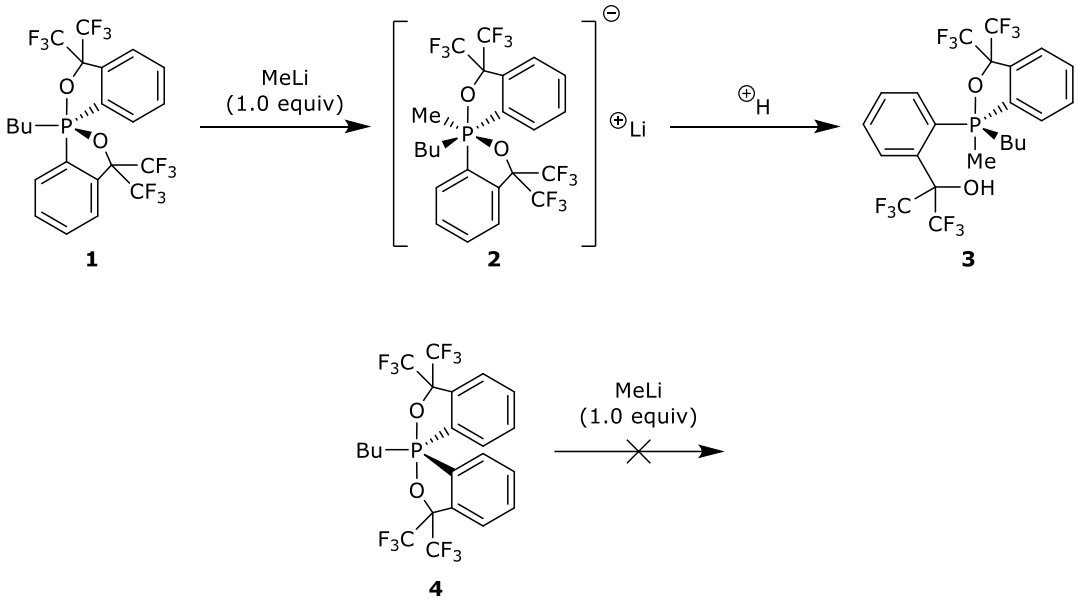

*Scheme 3: Contrasting reactivity of the two conformationally isomeric phosphoranes **1** and **4**.*[5]

The isomer bearing both apical and equatorial alkoxy ligands (**1**) reacts with methyl lithium to give **3**. Conversely, no reaction occurs using the diaxial isomer (**4**). In this latter case, the alkoxy ligands can neither be displaced in the apical positions or rearrange to an equatorial position to allow displacement.

1.2.2 Synthesis and Utility of Oxyphosphoranes

Oxyphosphoranes (phosphoranes with at least one alkoxy substituent) were initially synthesised and studied for their stereochemistry and geometry, with their synthetic utility not originally the focus of research.[6] In 1965 Denney and co-workers demonstrated the use of cyclic oxaphosphorane **5**, prepared using diethylperoxide, to ethylate benzoic acid and phenol (Scheme 4).[7]

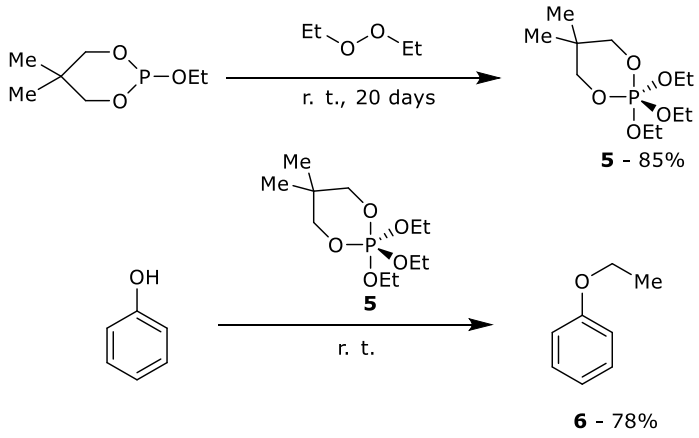

*Scheme 4: Ethylation of phenol using cyclic oxaphosphorane **5** prepared from diethylperoxide.[7] Note: Reaction duration for bottom reaction and reaction solvent for both reactions not specified.*

Building on this work, acyclic pentaethoxyphosphorane (**7**) was used to prepare tetrahydrofuran (THF) and tetrahydropyran (THP), from the

cyclodehydration of 1,4-butanediol and 1,5-pentanediol respectively (Scheme 5).[8] As with **5**, the active phosphorus reagent was prepared from the corresponding phosphite using diethylperoxide.[9]

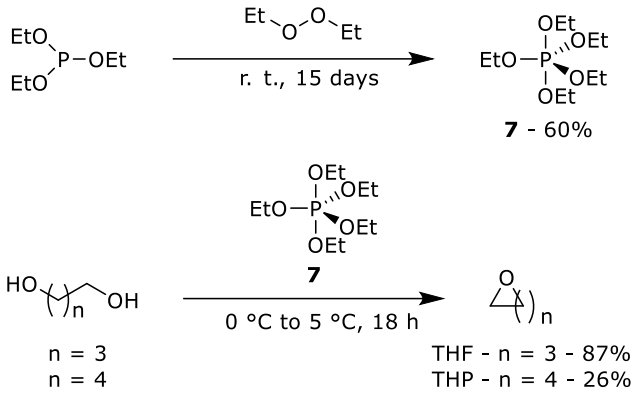

*Scheme 5: Cyclodehydration of 1,4-butanediol and 1,5-pentanediol using pentaethoxyphosphorane (**7**).[8] Note: Reaction solvents not specified.*

Evans and co-workers extensively developed this work, using diethoxytriphenylphosphorane (**8**), in a number of transformations.

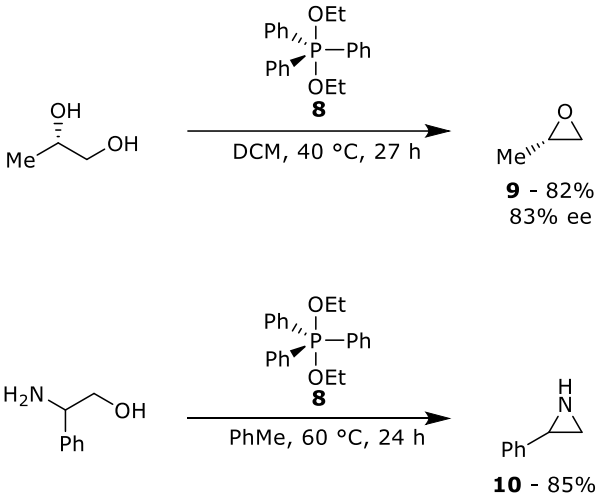

*Scheme 6: Top: Synthesis of (S)-propylene oxide (**9**) using diethoxytriphenylphosphorane (**8**);[10] Bottom: Synthesis of 2-phenylaziridine (**10**) using **8**.[11]*

Notably, chiral diols were shown to undergo cyclodehydration with >80% retention in stereochemistry (Scheme 6 top).[10] The scope of the reaction was also successfully expanded to include synthetically useful functionalised aziridines from 1,2-amino alcohols (Scheme 6 bottom).[11]

However, when attempting to synthesise cyclic sulfides from 1,2-mercapto alcohols, competitive *S*-ethylation reactions dominated.[12] In order to circumvent this, an alternative cyclic dioxyphosphorane reagent (**12**) was synthesised (Scheme 7).[13]

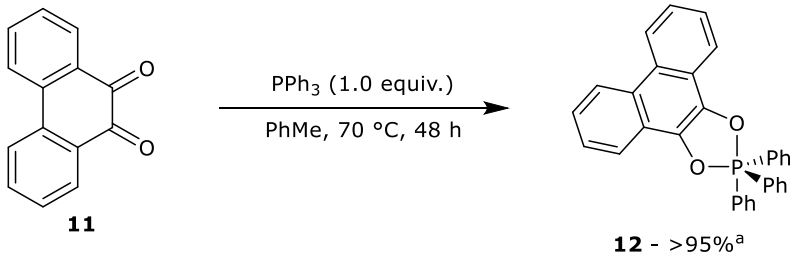

11

12 - >95%[a]

*Scheme 7: Synthesis of cyclic dioxyphosphorane **12**.*[13]

Phosphorane **12** was shown to exhibit equal to improved cyclodehydration abilities relative to **8**. Moreover, the replacement of the ethoxy substituents with a cyclic sp^2 hybridised system eliminated competitive alkylation reactions. Using **12** a number of cyclic sulfides were synthesised in excellent yields (Table 1).

*Table 1: Substrate scope of the cyclodehydration reactions mediated by the cyclic phosphorane **12**.*[13]

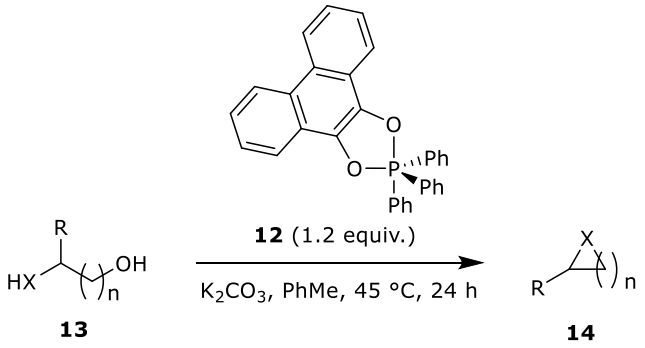

Entry	Reactant	Product	Yield / %
1	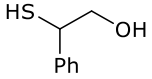		85
2	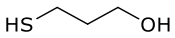		80
3	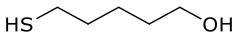		84
4	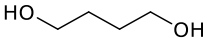		95
5	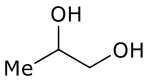	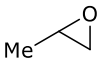	93
6	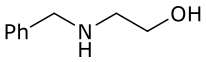	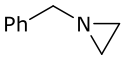	60

Dioxyphosphorane **12** was also demonstrated as an effective reagent for converting diols to cyclic ethers and 1,2-aminoalcohols to aziridines. A range of examples using **12** are given in Table 1.

It is believed that all of these transformations take place through a common mechanism (Scheme 8). In this mechanism, the reagent (**12**) attacks sequentially through each heteroatom to eliminate phenanthrene-9,10-diol (**16**). The resulting cyclic phosphorane (**17**) can tautomerise to a

reactive open chain oxyphosphonium salt (**18**) which undergoes an Arbuzov collapse to give the product.

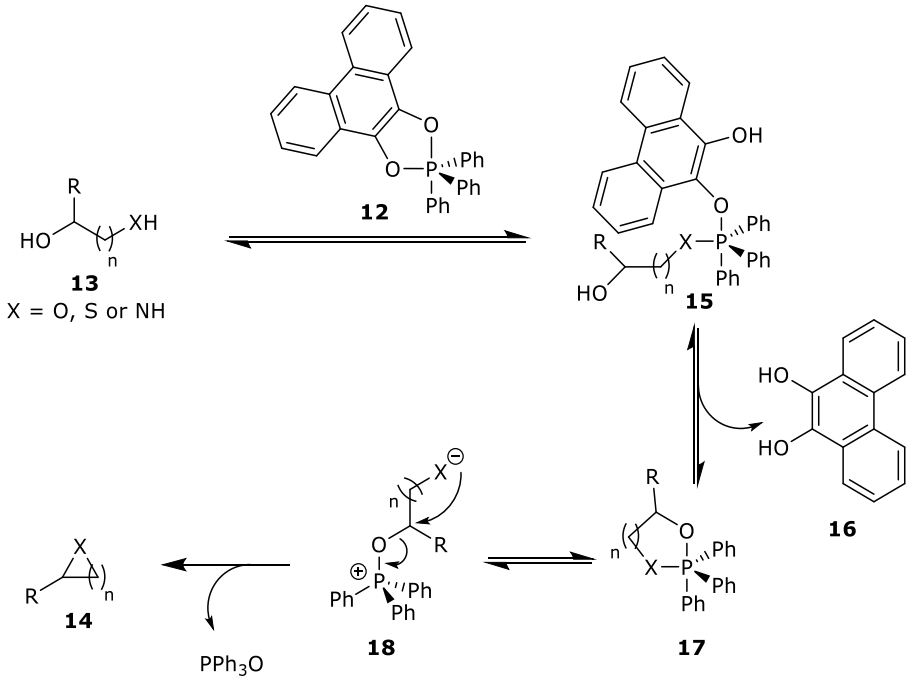

*Scheme 8: Proposed general reaction mechanism for **12**-mediated cyclodehydration reactions.*[13]

Another benefit of **12** is that it can be synthesised *via* the direct addition to a quinone, avoiding the use of hazardous and explosive peroxides.

Bis-(neopentyloxy)triphenylphosphorane (**20**) was also found to prevent competitive alkylation reactions due to the increased steric hindrance from the ^{t}Bu group. Evans and co-workers developed a 'non-peroxidic' protocol to synthesise acyclic dioxyphosphoranes such as **20**. This protocol involved the pre-formation of bromotriphenylphosphonium bromide (**19**) prior to the addition of the relevant lithium alkoxide (Scheme 9).[14,15]

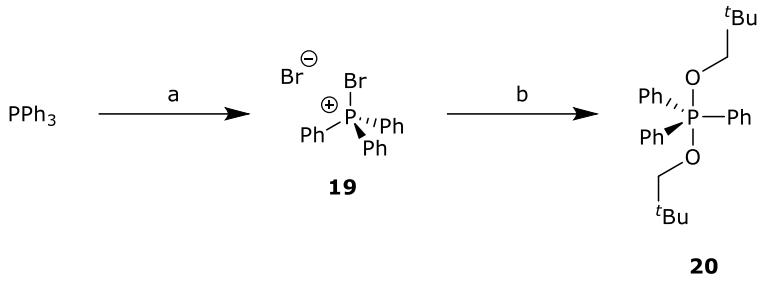

*Scheme 9: Synthesis of bis-(neopentyloxy)triphenylphosphorane (**20**) using a non-peroxidic approach.[15] Reagents and conditions: a) Br_2, DCM, −78 °C; b) $^tBuCH_2OLi$, DCM, PhMe, −78 °C to r. t., 65%[a] (over two steps); [a]Yield determined by ^{31}P NMR spectroscopy. Note: Reaction times not specified.*

Ishikawa and co-workers hypothesised that substituting the phosphorus centre with electron withdrawing substituents would allow for the synthesis of more stable dioxyphosphoranes.[16] To this end two novel dioxyphosphoranes (**21** and **22**) were synthesised with axial fluoroalkoxy ligands (Figure 1). Ishikawa also utilised a non-peroxidic approach, generating bromotriphenylphosphonium bromide in the presence of the relevant sodium alkoxide.

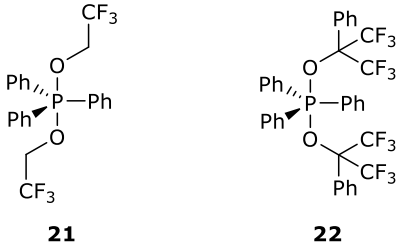

*Figure 1: Structures of the bis-(fluoroalkoxy)triphenylphosphoranes **21** and **22**.[16]*

Phosphorane **22** was found to be very stable and could be isolated as a crystalline solid, however it was too stable to be susceptible to nucleophilic attack. Conversely **21** was not isolable, but was found to be a useful reagent for the introduction of the medicinally significant trifluoroethyl group, when used in solution.[17] Reactions using **21** with alcohols and

carboxylic acids formed trifluoro ethers and esters respectively, in good yields (Scheme 10).[18]

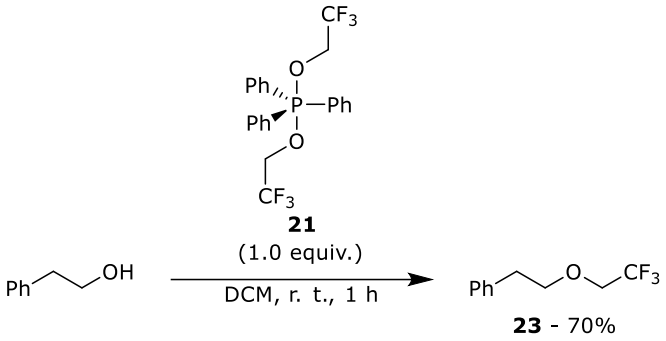

*Scheme 10: Synthesis of ether **23** using bis-(trifluoroethoxy)triphenylphosphorane (**21**).*[18]

The proposed mechanism for this transformation begins with pseudorotation of **21** to the reactive conformer **24** (Scheme 11). Ligand exchange to form the mixed dioxyphosphorane **25** allows elimination of the ether **27** and formation of triphenylphosphine oxide.

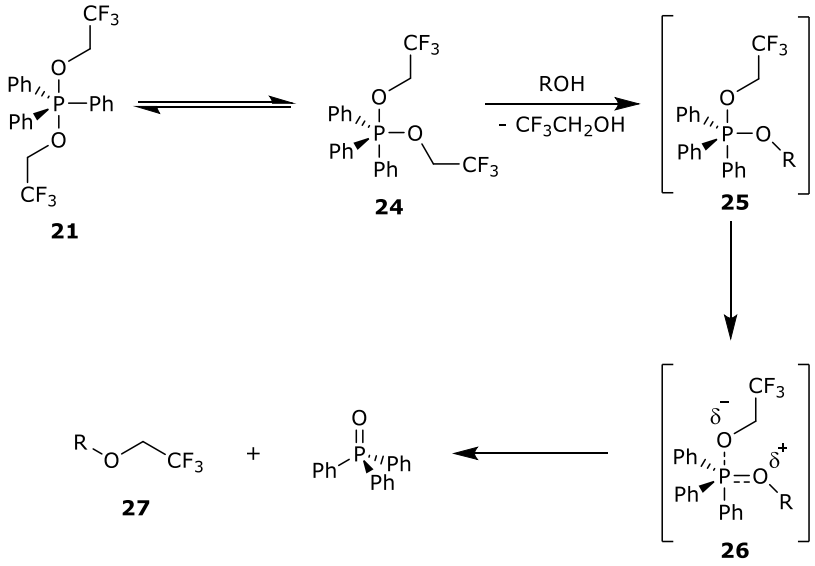

Scheme 11: Ishikawa's proposed mechanism for the trifluoroethylation of an alcohol.[18]

Additionally, **21** was found to be a versatile reagent capable of mediating the synthesis of non-symmetrical sulfides and ketones. As predicted by Ishikawa, the order of reactivity of these three dioxyphosphoranes (**20**>**21**>**22**) reflects the electronegativity of the alkoxy ligands. This observation is in agreement with the concept of apicophilicity, wherein the more electronegative alkoxy ligands occupy the axial positions to a greater degree, thus lowering the reactivity of the dioxyphosphorane. (see section 1.2.1).

Perhaps most significantly, secondary amines were synthesised in high yields using **21** (Table 2).[18]

*Table 2: Substrate scope of amine/alcohol couplings mediated by the Ishikawa phosphorane (**21**).*[18]

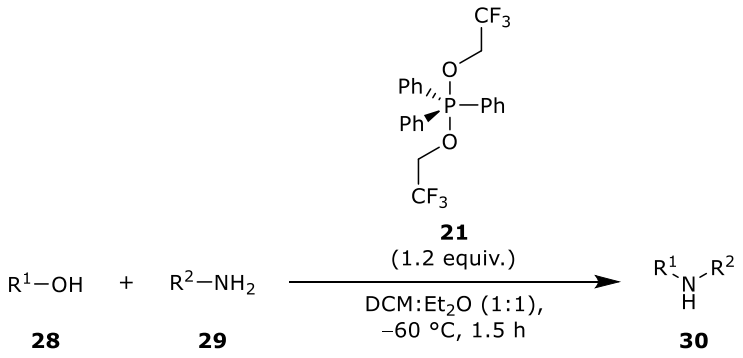

Entry	R^1	R^2	Yield / %
1	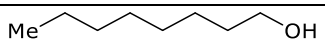	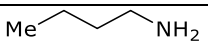	73
2	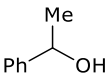	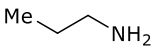	73
3	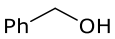	Ph—NH_2	71
4	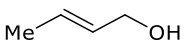	Ph—NH_2	64
5	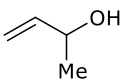	Ph—NH_2	66

Both aliphatic and aromatic alcohols and amines were active using this protocol. One major advantage of this method is the lack of activating

groups required, in contrast to the Fukuyama Mitsunobu protocol which requires a nosyl group (see section 1.2.3).[19] Amines and alcohols were coupled without the need for any protections, deprotections or redox chemistry.

Ishikawa proposed the amination reactions proceed *via* the same alcohol ligand exchange as the alcohol trifluoroethylation reactions. The secondary amine product is then formed from the direct attack of the primary amine nucleophile on **31** (Scheme 12)

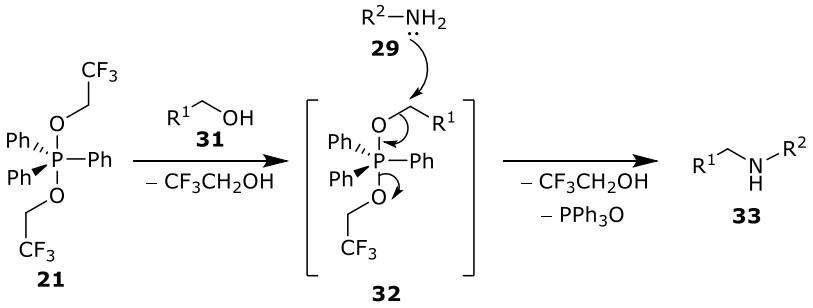

*Scheme 12: Ishikawa's proposed mechanism for **21**-mediated amine alkylation.*[18]

It is stated that the reduced temperature used in the amination reactions slows the competitive trifluoroethylation reactions. Possibly this can be explained by the intermediate **32** being unable to overcome the energy barrier for pseudorotation at this temperature. However, once again no spectroscopic evidence is provided to corroborate this mechanism.

Interestingly, no comment was made with regards to the formation of trifluoroethylated amines. These could reasonably be expected to arise, from the direct nucleophilic attack on the more electrophilic carbon of the trifluoroethoxy ligand. Similarly, overalkylation to the corresponding

tertiary amines was not mentioned. Presumably this is controlled kinetically by the near stoichiometric amount of dioxyphosphorane used.

Recently Denton and co-workers revisited this work and demonstrated that **21** was capable of performing Mitsunobu esterification reactions with inversion of stereochemistry (Scheme 13).[20]

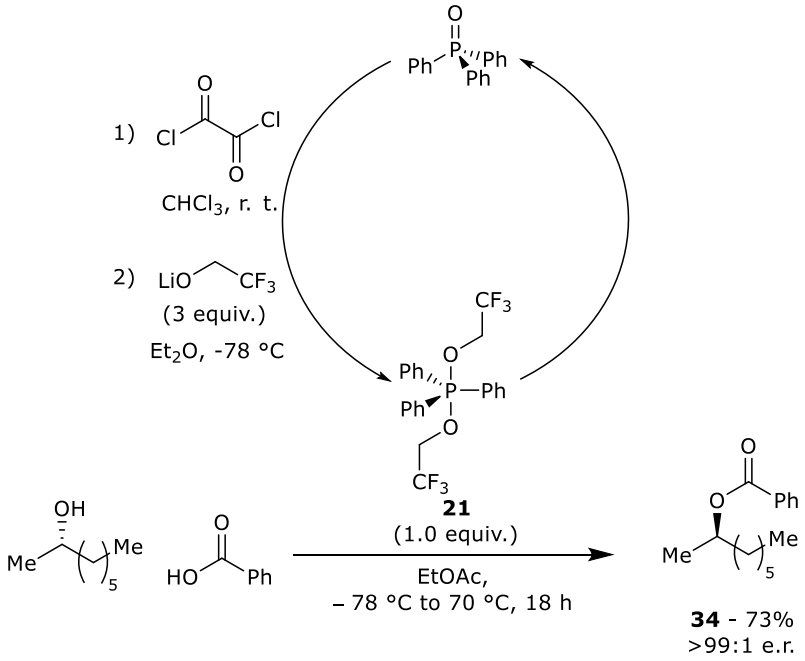

*Scheme 13: Stereospecific synthesis of the ester **34** using **21**.*[20]

A novel synthesis route to **21** was also outlined from triphenylphosphine oxide, as opposed to triphenylphosphine traditionally used. In this method, addition of oxalyl chloride generates a chlorophosphonium salt, subsequent addition of the relevant alkoxides then forms the dioxyphosphorane **21**. The use of oxalyl chloride is certainly more practical and less hazardous than elemental bromine (as used by Ishikawa and Evans). However, the main advantage of this method arises from the use of triphenylphosphine oxide. Since **21** forms triphenylphosphine oxide as it is consumed, no net

phosphorus waste is generated in these reactions. Indeed, subsequent recovery of phosphorus oxide was demonstrated successfully (in 86% yield), which was then re-used without the need for any redox chemistry.

A multinuclear NMR study was also undertaken to gain an insight into the mechanism of the reaction. Upon alcohol addition to **21** no mixed octanol/trifluoroethanol dioxyphosphorane (**32**) was observed (by ^{19}F and ^{31}P NMR spectroscopy) as had been suggested by Ishikawa for the alcohol trifluoroethylation reactions. However, upon addition of benzoic acid an alkoxyphosphonium salt with a carboxylate counter anion (**35**) was observed by ^{31}P NMR spectroscopy at 53.4 ppm. This suggests the reaction proceeds *via* an S_N2 attack of the carboxylate counterion, resulting in inversion of stereochemistry (Scheme 14).

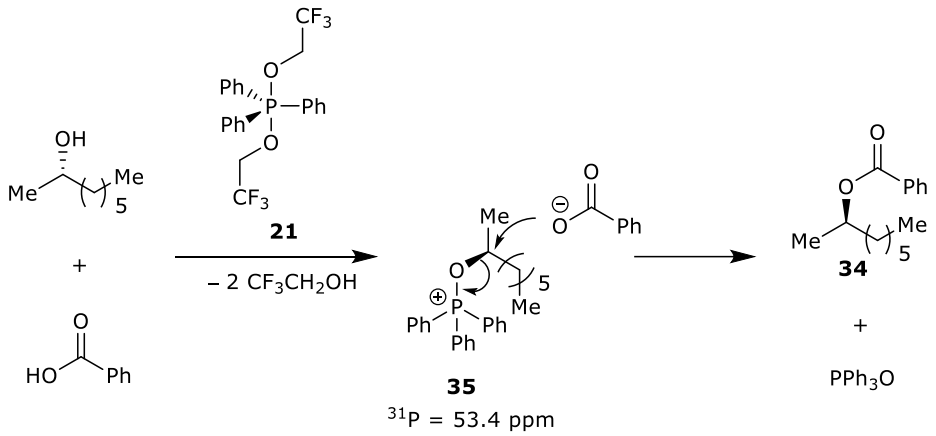

*Scheme 14: Proposed mechanism for the **21**-mediated synthesis of the ester **34** via an alkoxyphosphonium salt (**35**).*[20]

1.2.3 Existing Synthesis Routes to Amines

Reductive amination is one of the most widely used methods to prepare secondary amines.[21] In this method, a primary amine is reacted with an

aldehyde to form an imine, subsequent reduction with a suitable reducing agent then forms the secondary amine product (Scheme 15). Although typically a versatile and high yielding reaction, there are a number of drawbacks for this method. Firstly, the need for a stoichiometric reducing agent decreases the atom economy of the reaction. Secondly, many aldehydes are susceptible to oxidation to the corresponding carboxylic acid, thus making them relatively inconvenient reagents to work with.

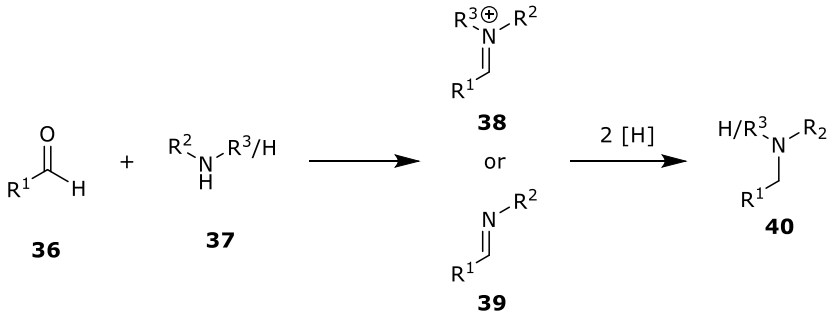

Scheme 15: General scheme for reductive amination.

Direct *N*-alkylation using alkyl halides is the most common technique for synthesising secondary or tertiary amines.[22] However, whilst attractive in its simplicity, direct alkylation reactions often give rise to over-alkylated side products (Scheme 16).[23] Consequently, when a secondary amine product is desired, a large excess of amine is often employed which must be removed at the end of the reaction. Additionally, the use of hazardous alkylating agents is a concern and their complete removal must be ensured for applications in medicinal chemistry.

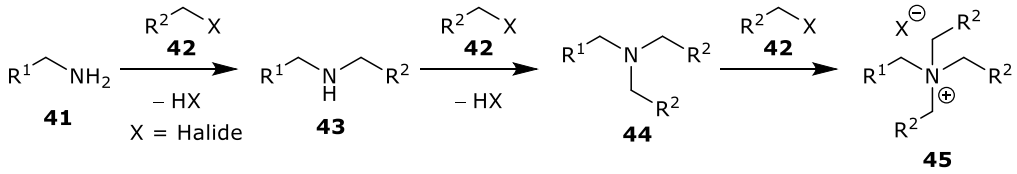

Scheme 16: General reaction scheme depicting over-alkylated side product when using alkyl halides.

Transition metal-catalysed condensation reactions using alcohols as alternatives to alkyl halides have been widely demonstrated in the literature (example in Scheme 17).[24–26]

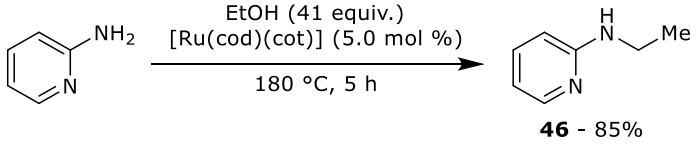

*Scheme 17: Synthesis of N-ethylpyridin-2-amine (**46**) using 'borrowing hydrogen' methodology.*[26]

Mechanistically it is believed the metal acts as an oxidant to generate an aldehyde *in situ*. Subsequent imine formation occurs from the condensation of the aldehyde and amine, prior to reduction by the metal (Scheme 18).

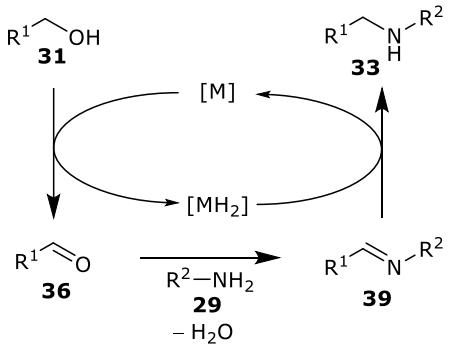

Scheme 18: General scheme for amine alkylation using 'borrowing hydrogen' methodology.

Therefore, these reactions can be said to be somewhat analogous to more traditional reductive amination reactions. As the metal effectively both removes and supplies H_2 to the molecule, the metal is said to be 'borrowing hydrogen'. These reactions have the benefit of greater selectivity towards the mono-alkylated product, in addition to avoiding the use of often toxic and mutagenic alkyl halides. However, the application of a poorly abundant late transition metal such as rhodium, iridium or ruthenium increases the cost of the reaction, whilst also being undesirable from a sustainability perspective.[24,25]

Secondary amines can also be readily prepared from alcohols using a Mitsunobu approach with an activated primary amine.[27] One commonly used example of this is the Fukuyama-Mitsunobu reaction. This involves the coupling of an alcohol and secondary sulfonamide (**47**) under Mitsunobu conditions. The sulfonamide group is then removed, under basic conditions using a thiol, at the end of the reaction (Scheme 19).[19]

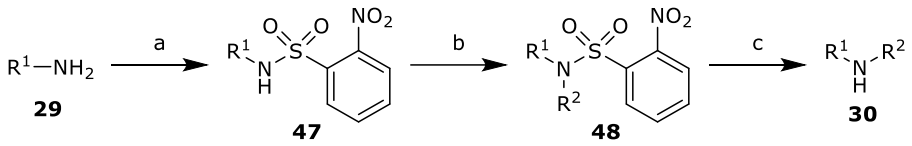

Scheme 19: General reaction scheme for the Fukuyama-Mitsunobu reaction. Reagents and conditions a) 2-Nitrobenzenesulfonyl chloride, Et_3N, DCM; b) R^2-OH, DEAD, PPh_3, DCM; c) PhSH, K_2CO_3, DMF.

The Fukuyama-Mitsunobu reaction is a widely used, high yielding and versatile reaction. However, the need for an activating group as well as stoichiometric triphenylphosphine and diethylazodicarboxylate (DEAD)

renders the reaction rather wasteful, with a poor atom economy. Secondly, the addition and removal of the activating group adds steps to a synthesis. Moreover, the use of explosive DEAD and toxic thiophenol limits the large-scale applicability of this method.

Palladium catalysed cross couplings of amines with aryl halides, known as Buchwald-Hartwig reactions, are another very powerful method for amine synthesis.[28–30] Primary and secondary aliphatic or aromatic amines may be used, with a stoichiometric base, whilst the palladium catalyst often has chelating phosphine ligands such as BINAP (Scheme 20).[31]

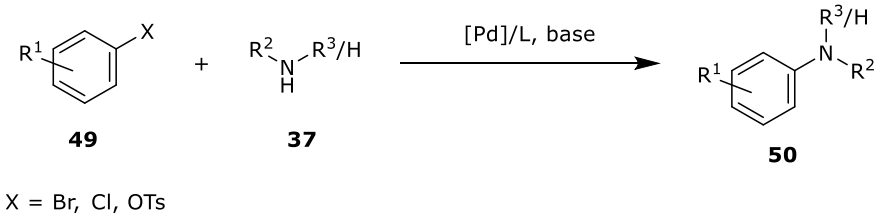

49 **37** **50**

X = Br, Cl, OTs

Scheme 20: General scheme for the Buchwald-Hartwig amination.

The Buchwald-Hartwig amination is a particularly useful tool for the synthesis of aryl amines, which can be difficult to synthesise using alternative methods.[32] Given the extremely widespread nature of this class of compounds, the Buchwald-Hartwig amination is very commonly used within industry.[33]

1.2.4 Monolithic Phosphorus Reagents in Flow Chemistry

Throughout current research there is considerable interest in the application of polymer bound reagents. Chiefly this interest is due to the relative ease of purification; time consuming and wasteful work-ups and

column chromatography can often be replaced by a simple filtration. Consequently, large excesses of polymer-bound reagents may be used to help drive a reaction to completion, without contaminating the product with residual starting material. This is particularly useful for triphenylphosphine-mediated transformations where the triphenylphosphine oxide by-product is often difficult to separate.[34,35] In addition to this, risks associated with hazardous reagents can be minimised by immobilising them on polymers.[36]

1.2.4.1 Polymeric Triphenylphosphine

Polymer-bound triphenylphosphine (**53**) was first synthesised in 1961 by Braun.[37] In this work a polymer-bound aryl iodide (**51**) undergoes a lithium halogen exchange prior to reacting with chlorodiphenylphosphine (Scheme 21).

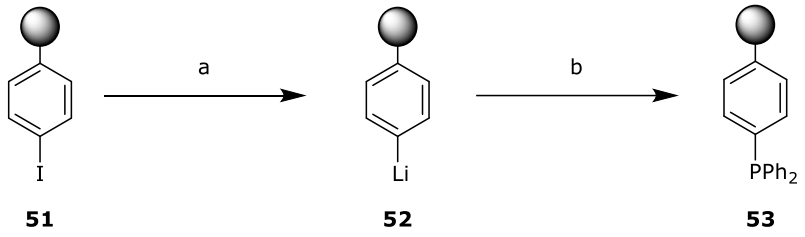

Scheme 21: Braun's post-polymerisation functionalisation strategy for the synthesis of polymer-bound triphenylphosphine.[37] Reagents and conditions a) n-BuLi; b) PPh_2Cl. Note: Reaction solvents, times, temperatures and yields not specified.

In 1972 McKinley and co-workers demonstrated the use of polymer-bound triphenylphosphine (**53**) in a number of Wittig reactions.[38] In this work two methods were described for the preparation of the polymeric reagent. Firstly, the same post-polymerisation functionalisation strategy as Braun (differing only in the use of an aryl bromide not iodide). Secondly a pre-

polymerisation functionalisation method is described where a copolymer of Diphenyl(4-vinylphenyl)phosphine (**54**), styrene and divinylbenzene was synthesised (Scheme 22). This later method offers a more simple and direct approach and eliminates the need to perform multiple reactions on the polymer support before the desired reagent is produced. For these reasons, polymerisation of a phosphorus-containing monomer is the more commonly employed strategy in the recent literature.

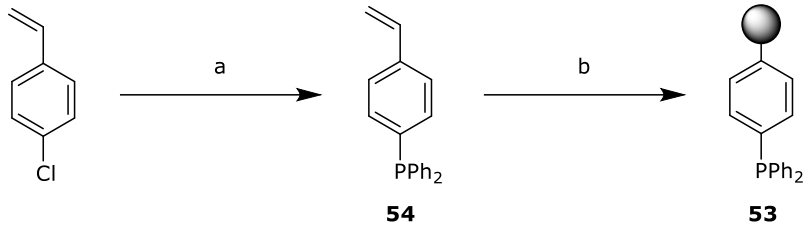

Scheme 22: McKinley's pre-polymerisation functionalisation strategy for the synthesis of polymer-bound triphenylphosphine.[38] Reagents and conditions a) Mg, EtBr, THF, 50 °C then PPh_2Cl, THF, 50 °C, 50%; b) styrene, divinylbenzene. Note: Reaction solvent and temperature for step b, and reaction time for both steps not specified.

More recent work has shown the versatility of polymer bound triphenylphosphine in a plethora of different reactions. An overview of this can be found in an excellent review by Guinó and Hii.[39]

1.2.4.2 Monolithic Polymers

Monolithic polymers were first synthesised in 1992 for separations science applications.[40] They are best described as being continuous, porous, polymeric solids with channels through which liquids can pass. In theory a monolithic polymer consists of a single covalently bonded molecule. Monoliths with an internal void space > 74.05 % are referred to as 'high internal phase monoliths' (HIPE), these have since found applications in

synthetic chemistry due to their increased mass transfer by convection. [41–43] When passing a solution through traditional polymer beads the majority of the solution travels through the particle void space without interacting with the polymer. In contrast to this, by using a uniform porous monolith the solution must pass through the polymer framework itself.

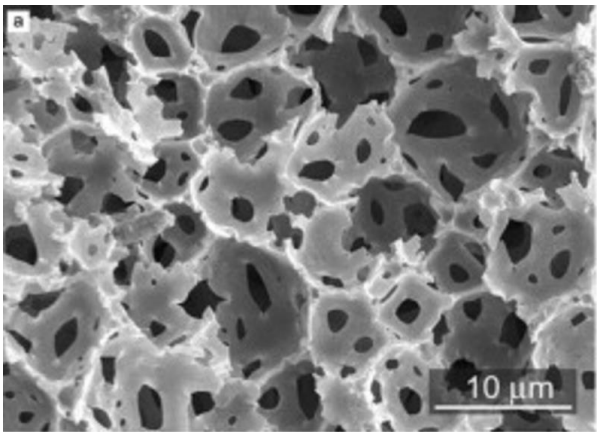

Figure 2: SEM image of a typical polyHIPE copolymer of styrene and divinylbenzene.[44]

In terms of synthesis chemistry, this ensures the immobilised reagent and the reagent(s) in solution come into closer contact. This allows for a more efficient reaction system.

The first monolithic triphenylphosphine polymer was prepared by Baxendale and co-workers in 2011.[45] A radical polymerisation of **54** is described with divinylbenzene as the crosslinker and 4,4'-azobis(4-cyanovaleric acid) as the initiator. The inclusion of 1-dodecanol as a porogen gave rise to the characteristic macroporous framework and can be easily removed post polymerisation. This monolithic triphenylphosphine

(**53**) in combination with an azide transfer monolith, was used to give an excellent Staudinger aza-Wittig flow reactor.

1.2.4.3 Flow Chemistry

The efficiency benefits of immobilised reagents can be further enhanced by their incorporation into a flow system. Flow chemistry is a topic of great current interest due to the associated time, safety and ease of scale up benefits.[46–48] A major proponent of flow chemistry, Ley has helped establish the field as a realistic alternative to conventional batch techniques. Most notably, Ley reports the total synthesis of natural products such as (±)-oxomaritidine (**61**) in flow, with extensive use of immobilised reagents (Scheme 23)[49,50]

More recently, Ley and co-workers have further developed bromination chemistry originally described by Toy.[34] Immobilisation of the active bromotriphenylphosphine bromide (**62**) as a monolithic polymer in a flow reactor allowed formation of alkyl bromides (**64**) in high yields, with no purification necessary (Scheme 24).[51] The aforementioned benefits in reactor efficiency when using a monolithic reagent were also observed. Indeed, Ley commented that when using an analogous polymeric bead column, conversion in the case of cinnamyl bromide was a mere 29% for a single pass through the column. This is in stark contrast to the 100% conversion achieved with the monolithic reagent.

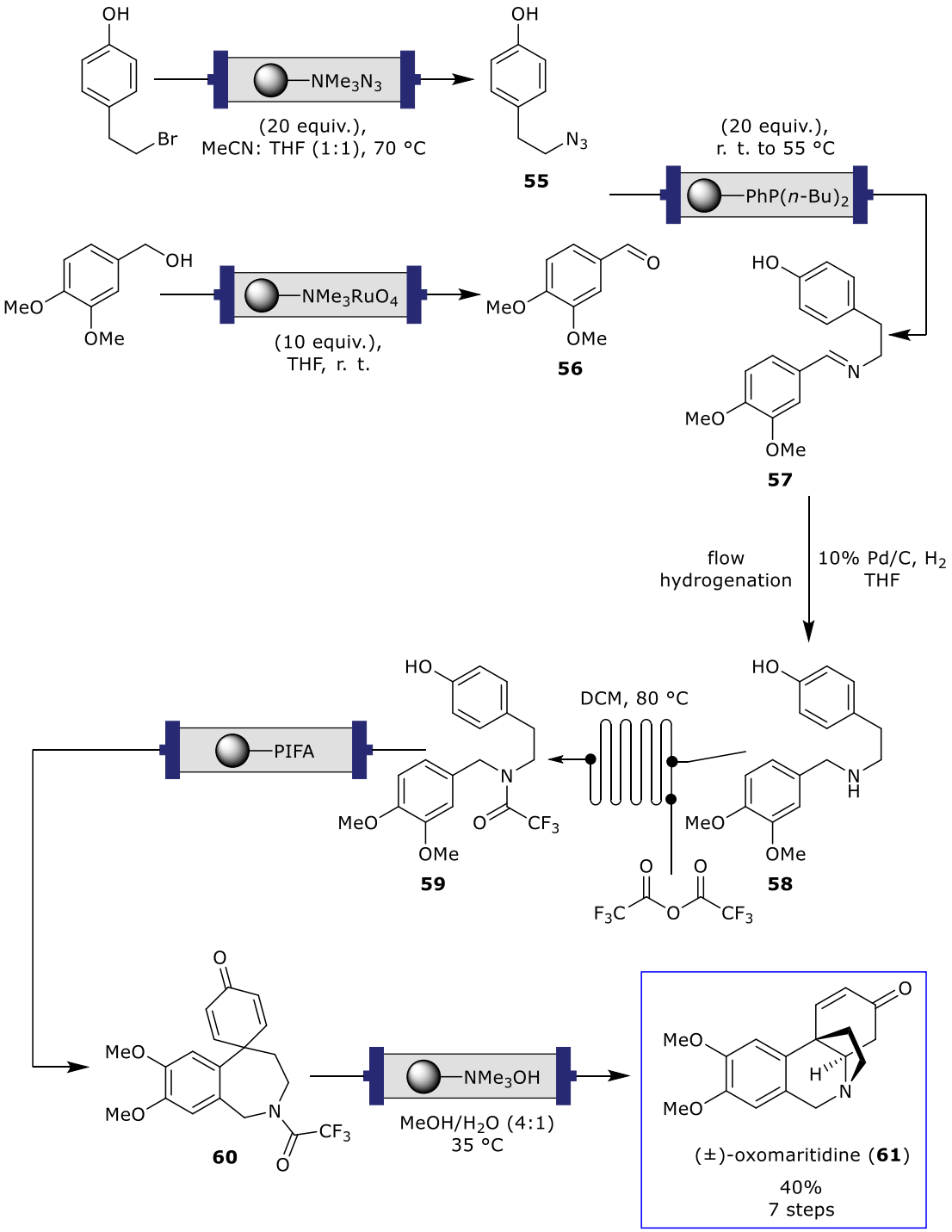

*Scheme 23: Synthesis of (±)-oxomaritidine (**61**) using exclusively flow chemistry with numerous immobilised reagents.*[49]

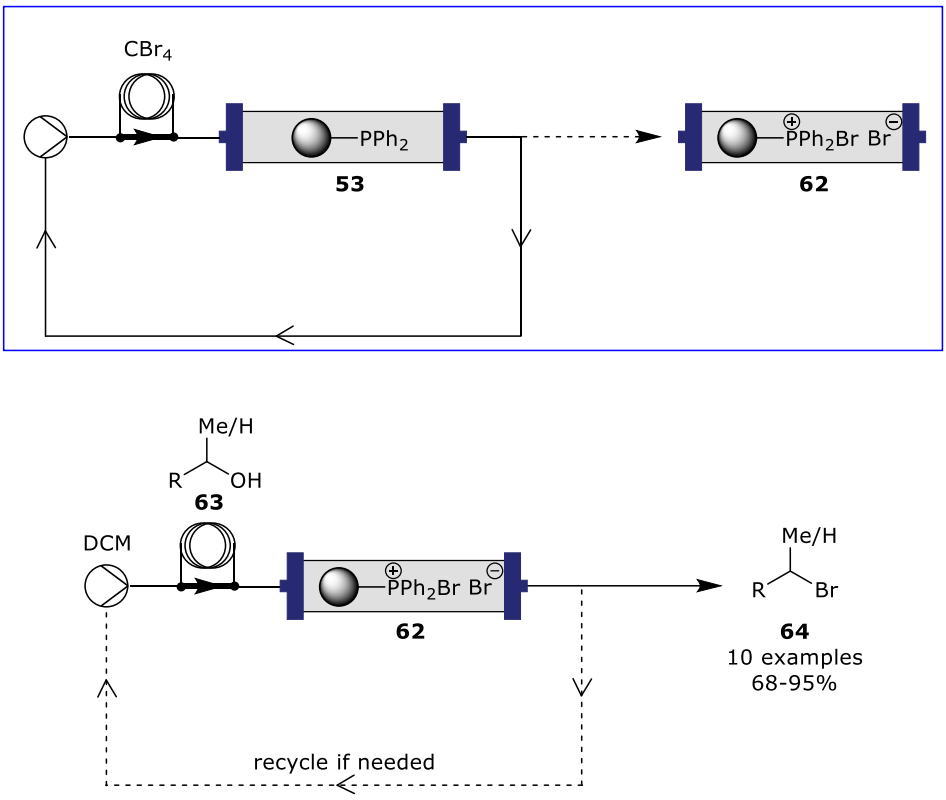

Scheme 24: Flow Appel synthesis of bromides using a monolithic bromotriphenylphosphine reagent.[51] *Note: Reactions performed at r. t., 1-14 h.*

Several more traditional amine alkylation strategies have been modified to use immobilised reagents with potential flow applications. *N*-alkylation reactions can be performed cleanly and without over-alkylation by using immobilised primary amine scavengers.[52] Immobilised cyanoborohydride has been used successfully in reductive aminations,[53] whilst Mitsunobu reactions have also been adapted to include the use of polymer bound DEAD.[54] However to date Evans' synthesis of diethoxydiphenylpolystyrylphosphorane (**65**) (Scheme 25) is the only example of an immobilised dioxyphosphorane reagent.[55]

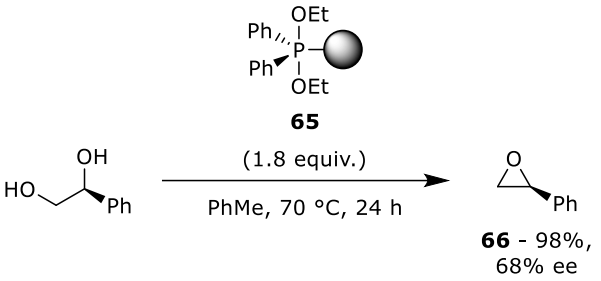

*Scheme 25: Synthesis of the epoxide **66** using diethoxydiphenylpolystyrylphosphorane (**65**).*[55]

Phosphorane **65** was used to perform cyclodehydration reactions of a range of diols. Yields were comparable to that obtained from the analogous solution phase reagent (**8**). Interestingly, the synthesis of **66** was enantioselective (68% ee) whilst the same reaction performed by **8** gave a mixture of enantiomers (Scheme 25). This selectivity could be due to neighbouring group participation from other phosphorus sites, which are situated in close proximity within the polymer. Alternatively, increased steric hindrance could help prevent the rotation of intermediates which would lead to product mixtures. Regardless, this selectivity highlights another potential benefit of polymeric reagents.

Whilst these results are impressive, there is clearly an extensive range of dioxyphosphorane-mediated reactions which have yet to be explored using immobilised reagents.

1.2.5 Project Aims

As previously outlined, despite the importance of synthesising substituted amines, the traditional methods have a number of shortcomings. The aim of this project was to develop a new, efficient, safe and clean protocol for amine alkylation.

The work of Ishikawa and co-workers has demonstrated the ability of dioxyphosphoranes to facilitate amine/alcohol coupling reactions. However, this chemistry is poorly developed and forms difficult to separate phosphine oxides.

We proposed that implementation of a novel monolithic dioxyphosphorane into an "*N*-cube" benchtop flow reactor would enable the desired coupling reactions to take place cleanly and efficiently, with no need for separation of the dioxyphosphorane coupling agent (Scheme 26). In addition to the monolithic reagent, the flow reactor will include a desiccant cartridge to prevent hydrolysis, as well as a flow IR cell for in-line analysis.

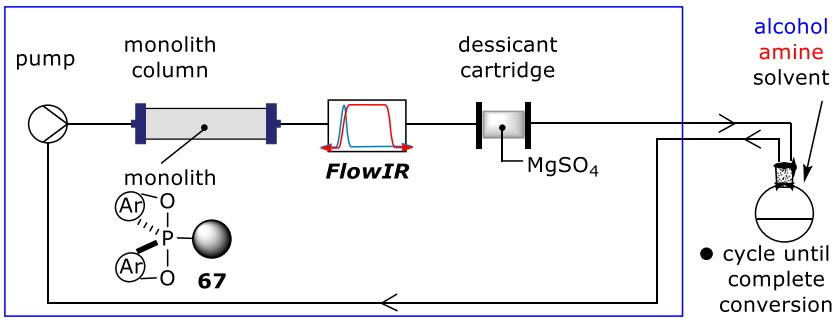

Scheme 26: Proposed 'N-cube' benchtop reactor setup.

It was then proposed to utilise this novel reactor to synthesise a range of valuable amines in flow, demonstrating the value of this methodology (Scheme 27).

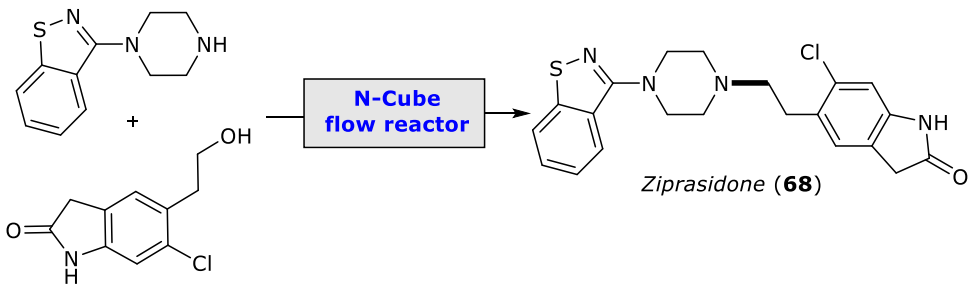

Scheme 27: Development of the 'N-Cube' reactor for direct amine/alcohol coupling.

1.3 Results and Discussion

1.3.1 Synthesis and Utility of Bis(2,2,2-trifluoroethoxy)triphenylphosphorane

Initial work into phosphorus-mediated amine/alcohol couplings focussed on bis(2,2,2-trifluoroethoxy)triphenylphosphorane (**21**). As **21** had the most literature precedent for amine/alcohol coupling, it was considered the best option to explore and better understand the chemistry prior to developing it.

Phosphorane **21** was synthesised using the more recent literature published method from triphenylphosphine oxide (Scheme 28).[20] Initial experiments yielded inconsistent results with varying degrees of conversion. However, by using an excess of the lithium alkoxide (3 equiv. instead of 2), scaling up the reaction and the inclusion of an internal indicator in the alkoxide solution these issues were overcome. Using this protocol stock solutions of **21** in toluene, chloroform and ethyl acetate were prepared with >95% conversion (by ^{31}P NMR spectroscopy).

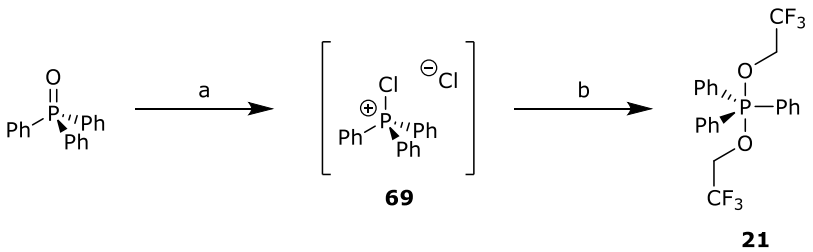

*Scheme 28: Synthesis of bis(2,2,2-trifluoroethoxy)triphenylphosphorane (**21**). Reagents and conditions a) $(COCl)_2$, $CHCl_3$, r. t., 1 h; b) F_3CCH_2OLi, $CHCl_3$, Et_2O, −78 °C to r. t, 3.5 h >95%[a]. [a]Yield determined by ^{31}P NMR spectroscopy.*

Prior to undertaking amine/alcohol coupling reactions we first looked to trial trifluoroethylation reactions of alcohols. Whilst acting as a simpler

reaction with which to test our stock solutions of **21**, the introduction of the trifluoroethyl group is also a useful transformation for medicinal chemistry.[17] Initially stock solutions of **21** in anhydrous ethyl acetate were prepared as described in the literature for Mitsunobu transformations.[20] Unfortunately, when attempting to perform a trifluoroethylation reaction with 1-decanol, significant quantities of decyl acetate were formed. This transesterification reaction does not occur in the absence of the dioxyphosphorane, it is presumably facilitated by phosphoranes containing decanol ligands. Evidently ethyl acetate was not a suitably inert solvent for use in this chemistry. Further stock solutions of **21** were prepared in either anhydrous toluene or chloroform.

Benzyl alcohol underwent trifluoroethylation in toluene, at room temperature, with a conversion of 43% after 24 hours to give the ether **70** (Scheme 29). Changing the solvent to chloroform and heating to 50 °C increased the conversion to 77% after 3 hours by ^{1}H NMR spectroscopy.

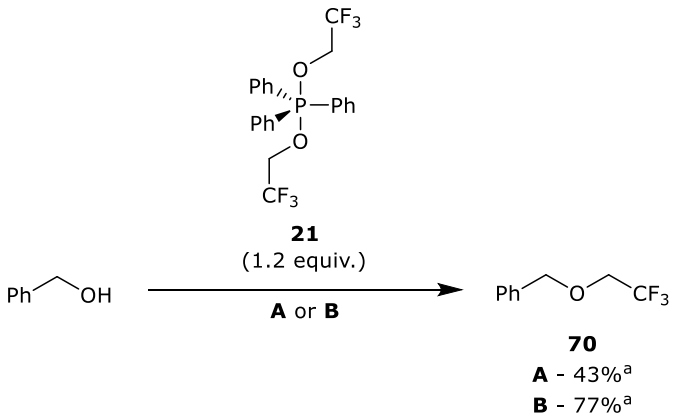

*Scheme 29: Trifluoroethylation of benzyl alcohol using **21**. Reaction conditions: **A**) $CHCl_3$, 50 °C, 3 h; **B**) PhMe, r. t., 24 h; [a]Yield determined by ^{1}H NMR spectroscopy; [b]$CHCl_3$ conditions*

Moving forward with a stock solution of **21** in chloroform we turned our attention to the coupling of amines and alcohols. Aniline was successfully

coupled with benzyl alcohol to give *N*-benzylaniline (**71**) in 12% yield (Scheme 30). However, this yield is considerably lower than was reported in the literature (71%).[18]

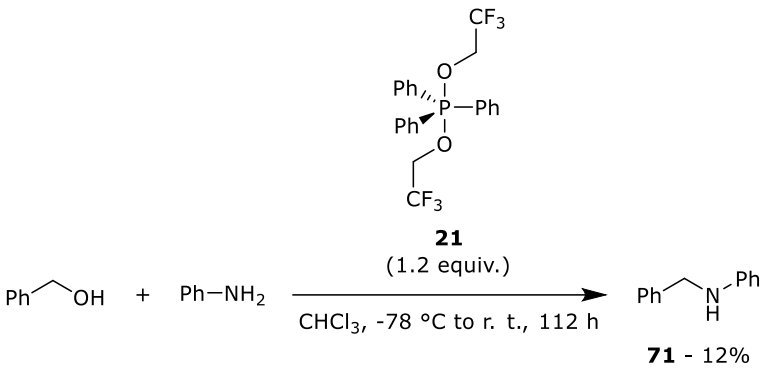

*Scheme 30: Synthesis of N-benzylaniline (**71**) using **21.***

On subsequent repeats of this reaction the competitive trifluoroethylation of benzyl alcohol was found to be the dominant reaction. Further experiments were undertaken aiming to eliminate this side reaction, the results of which are summarised in Table 3.

By using two equivalents of aniline (Table 3 entry 2) selectivity towards **71** was favoured relative to the initial conditions employed (Table 3 entry 1). Although the trifluoroethylation side reaction was not eliminated, the improvement in selectivity was encouraging.

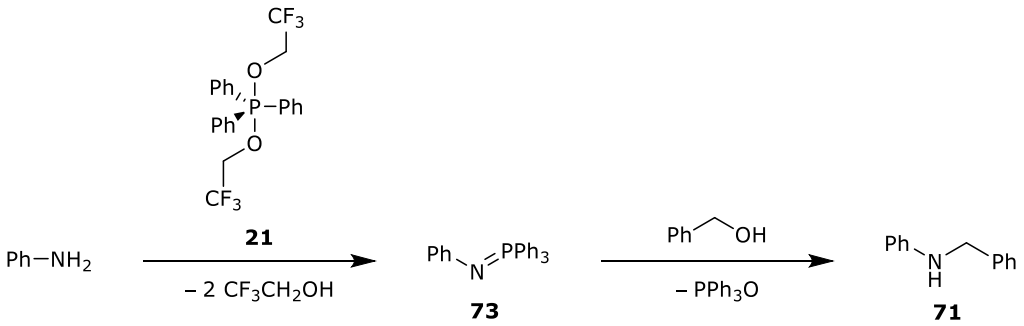

*Scheme 31: Proposed alternative mechanism for the **21**-mediated synthesis of amine **71** via an iminophosphorane **73**.*

*Table 3: Optimisation of conditions for the **21**-mediated coupling of benzyl alcohol and aniline.*

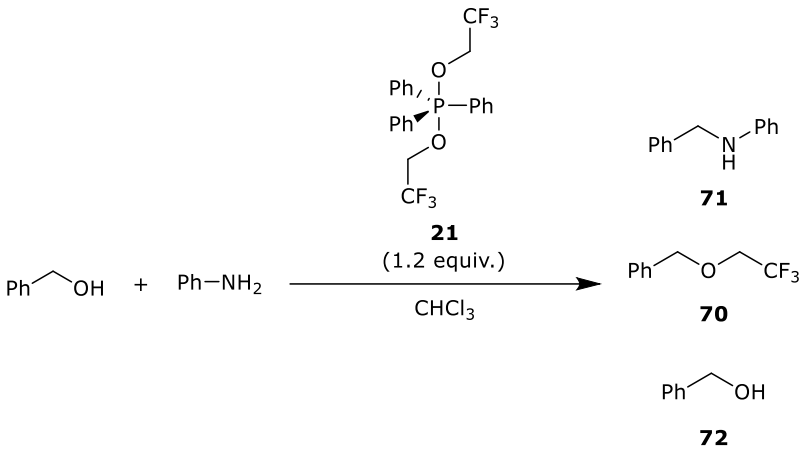

Entry	Addition conditions	Time / hours	Temp / °C	Product Distribution / %[a]		
				71	**70**	**72**
1	A	115	-78 to r. t.	9	79	12
2	B	115	-78 to r. t.	27	25	48
3	C	115	-78 to r. t.	1	31	68
4	D	24	-61 to r. t.	8	41	51
5	D	24	-41 to r. t.	6	42	52
6	E	24	r. t.	15	46	39
7	E	3	50	20	40	40
8	F	3	50	10	53	37

*Addition conditions: **A**) Aniline added and stirred at r. t. for 30 min. Cooled to -78 °C, benzyl alcohol added dropwise over 5 min and held 1.5 hour prior to warming to r. t. Held at r. t. for 113.5 hours. **B**) As for **A** but 2 equivalents of aniline used **C**) As for **A** but aniline stirred at r. t. for 48 h. **D**) Aniline added and stirred r. t. for 10 min. Cooled and benzyl alcohol added over 1 hour. Allowed to warm to r. t. after 1 hour and held a further 23 hours at r. t. **E**) Aniline and benzyl alcohol added simultaneously. **F**) Aniline added and stirred at r. t. for 30 min, heated to 50 °C and benzyl alcohol added over 1 hour; [a]Determined by ^{1}H NMR spectroscopy.*

One alternative mechanism to that proposed by Ishikawa (Scheme 12) for the **21**-mediated amination of alcohols is *via* an iminophosphorane (**73**) (Scheme 31). In an attempt to pre-form this iminophosphorane species, aniline was added to **21** for 48 hours prior to the addition of benzyl alcohol

(Table 3 entry 3). In this case the iminophosphorane was formed, however only in 15% conversion (by ^{31}P NMR spectroscopy). This reaction showed the poorest selectivity as well as having the largest quantity of unreacted benzyl alcohol. This result likely suggests that the iminophosphorane is unreactive in this reaction and is not an intermediate in the formation of the **71**. Once benzyl alcohol was added the amount of **21** was lower than in previous reactions due to the iminophosphorane formation (and possibly hydrolysis). Upon benzyl alcohol addition **21** then reacted preferentially with the benzyl alcohol, which by that stage would have been in excess forming **70**.

Higher temperatures of −61 °C and −41 °C were used with the aim to improve overall conversion of benzyl alcohol (Table 3 entries 4 and 5 respectively). In both of these examples, benzyl alcohol was added slowly over an hour in an attempt to reduce the trifluoroethylation side reaction. Unfortunately, the prolonged addition time gave no improvement in selectivity and reduced overall conversion. Presumably this was due to increased hydrolysis of **21** during the addition, similar to the aforementioned experiment (Table 3 entry 3).

Reactions at room temperature and 50 °C both gave a similar improvement in yield and selectivity relative to the original conditions (Table 3 entries: 6, 7 and 1 respectively). Whilst slow addition of benzyl alcohol at 50 °C showed a slight deterioration in yield and selectivity (Table 3 entry 8).

For all of the experiments performed, **21** had been completely consumed by the end of the reaction. This is in spite of the fact that the benzyl alcohol is never fully consumed. Evidently despite rigorously anhydrous

conditions being employed, there was always a degree of hydrolysis occurring which negatively impacted the overall mass conversion.

N-Benzyl-4-nitroaniline was also synthesised using the same conditions as Table 3 entry 1 (Table 4). However, similarly poor selectivity and yields were observed. Whilst the formation of some secondary amine product (**74**) shows potential for the expansion of the reaction scope, the selectivity issues surrounding these couplings must first be overcome.

*Table 4: Synthesis of N-benzyl-4-nitroaniline (**21**).*

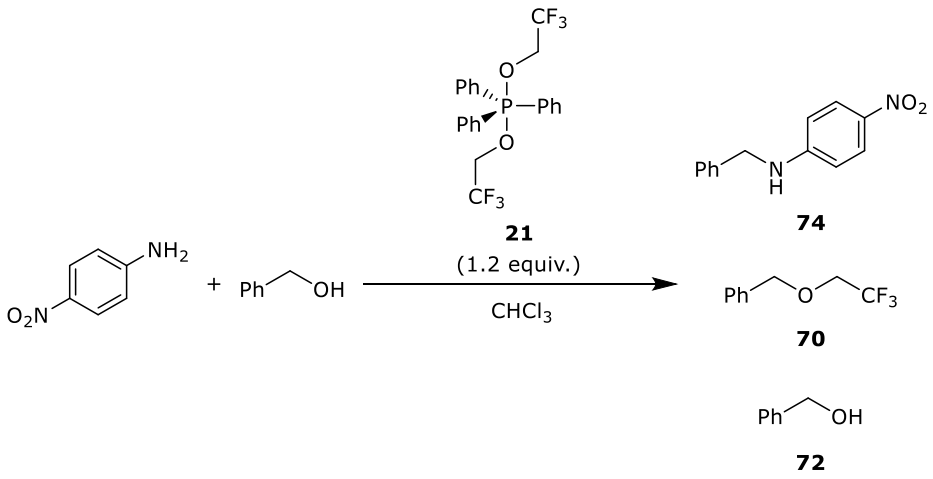

Addition conditions	Time / hours	Temp / °C	Product distribution / %[a]		
			74	**70**	**72**
A	115	-78 to r. t.	7	58	35

*Addition conditions: **A**) 4-Nitroaniline added and stirred at r. t. for 30 min. Cooled to −78 °C, benzyl alcohol added dropwise over 5 min and held 1.5 hours prior to warming to r. t. Held at r. t. for 113.5 hours; [a]Determined by ^{1}H NMR spectroscopy.*

1.3.2 Synthesis of Cyclic Dioxyphosphoranes

When faced with competitive alkylation reactions in the synthesis of thiiranes, Evans and co-workers overcame the issue by using an alternative cyclic dioxyphosphorane (**12**) (Table 1).[13] By replacing the oxygen bound sp^3 carbon of the alkoxy substituent with an aromatic sp^2

carbon, sulfur alkylation was eliminated and the intended cyclisation reaction was favoured. This competitive heteroatom alkylation reaction can be seen to be analogous to our own alcohol trifluoroethylation side reaction. Therefore, work was undertaken to explore the use of cyclic dioxyphosphoranes in the coupling of amines and alcohols.

Initially the monocyclic quinone **75** was used to access the corresponding dioxyphosphorane **76**. The main incentive to use **75** in preference to the quinone whose use was reported previously (**11**),[13] is the reduced mass of **75**, consequently giving superior atom economy. The quinone **75** was accessed in high yield *via* oxidation of 4-*tert*-butylcatechol using sodium periodate (Scheme 32).

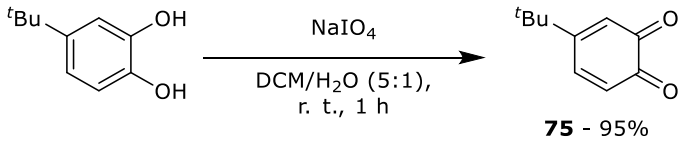

75 - 95%

*Scheme 32: Synthesis of 4-tert-Butyl-1,2-Benzoquinone (**75**).*

Synthesis of the corresponding dioxyphosphorane (**76**) from **75** was achieved using triphenylphosphine (Table 5). After 2 hours at room temperature the reaction stopped proceeding with no further formation of product observed, despite 34% triphenylphosphine remaining (Table 5 entry 1).

Table 5: Optimisation of conditions for the synthesis of 42.

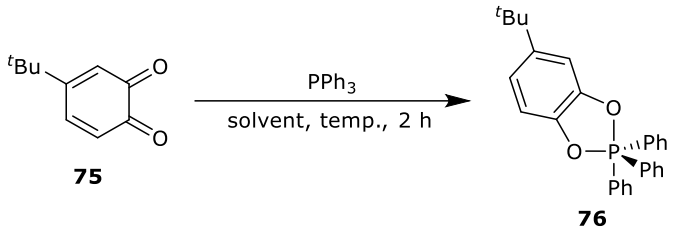

75 **76**

Entry	Solvent	Temperature / °C	**75** equiv.	Conversion / %[a]			
				PPh_3	**76**	Zwitterion (**77**)	PPh_3O
1	PhMe	r. t.	1	34	49	17	0
2	PhMe	50	1	11	54	10	26
3	PhMe	70	1	17	45	14	25
4	DCM	r. t.	1	43	18	34	5
5	hexane[b]	50	1	-	-	-	-
6	PhMe	r. t.	2	4	34	41	21
7	PhMe[c]	r. t.	2	0	68	15	17

[a]Determined by ^{31}P NMR spectroscopy; [b]Reagents insoluble; [c]¼ concentration of entries 1-6.

Consequently, work was undertaken to optimise the synthesis. Initially higher temperatures were explored to drive the reaction further to completion (Table 5 entries 2 and 3). Whilst consumption of triphenylphosphine was driven, there was no appreciable rise in product (**76**) and significant quantities of triphenylphosphine oxide were formed. This indicates that more product is forming in total, but greater levels of hydrolysis result in no net increase in product obtained.

In all examples, a new unexpected peak was observed in the ^{31}P NMR spectra at 21.2 ppm. This species was successfully isolated and characterised as a tetra-aryl phosphonium salt (**77**). A similar structure obtained from the reaction of triphenylphosphine with p-benzoquinone has been reported in the literature (**78**), which has a ^{31}P NMR resonance at 21.8 ppm (Scheme 33).[56]

77
^{31}P: 21.2 ppm

78
^{31}P: 21.8 ppm

*Scheme 33: Isolated Zwitterion **77** and a similar species (**78**) reported by Hu and co-workers.[56]*

The use of EPR experiments has previously shown the formation of zwitterions such as **78** to proceed through a radical mechanism.[57] Therefore, it is plausible that **77** is formed though an analogous pathway as shown in Scheme 34.

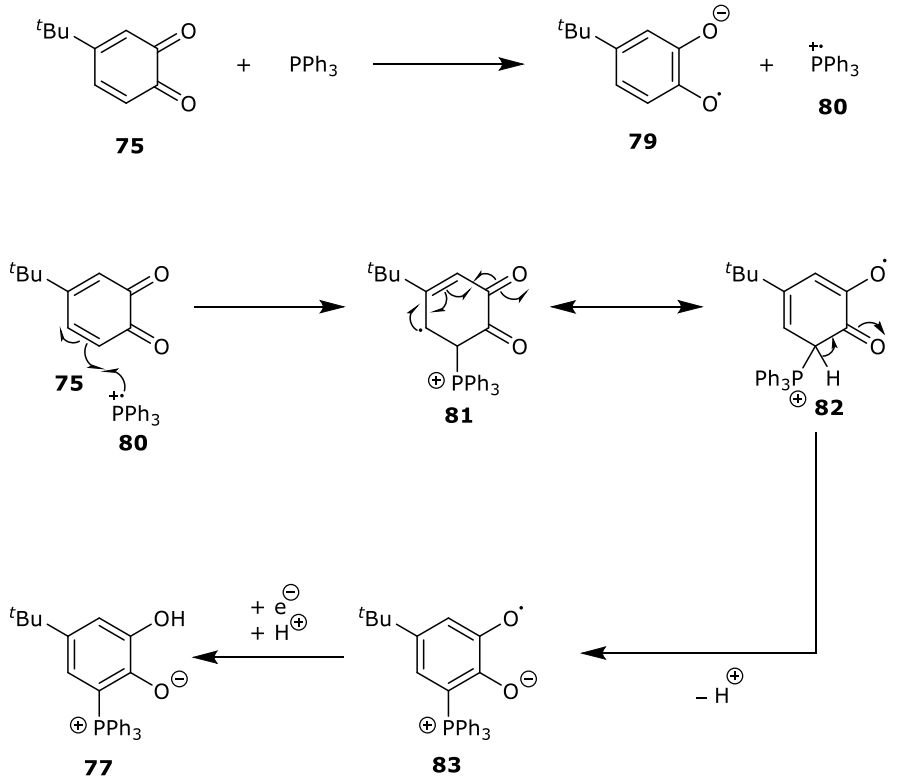

*Scheme 34: Proposed mechanism for the formation of the side-product **77**.*

In this mechanism an electron transfer from the phosphine generates a radical phosphinium cation (**80**) which attacks the neutral quinone **75**. Subsequent aromatisation gives the radical zwitterion **83**, which yields the observed, isolated, zwitterion **77** upon electron transfer from **79** and protonation. The zwitterion **77** was not active in any of the transformations outlined in section 1.3.4, thus we aimed to eliminate its formation.

Using a more polar solvent lowered the consumption of triphenylphosphine and favoured the formation of the zwitterion **77** (Table 5 entry 4). Therefore, hexane was used as an alternative non-polar solvent to toluene, however the reagents were insoluble in this case and no reaction could take place (Table 5 entry 5).

The quinone **75** was found to dimerise in solution to give **85**, presumably *via* a [4+2] cycloaddition (Scheme 35).

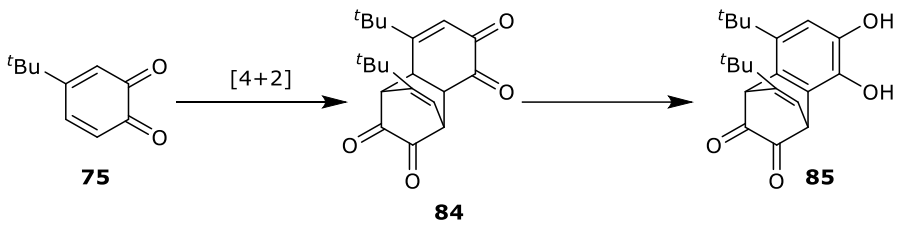

*Scheme 35: Dimerisation of **75** to form **85**.*

This explains the failure to fully consume the triphenylphosphine in Table 5 entries 1-5, as **75** is lost in the side reaction. Therefore 2 equivalents of **75** were employed to overcome the side reaction and drive the dioxyphosphorane formation (Table 5 entry 6). Although almost all the triphenylphosphine was consumed in this example, the formation of **77** became the dominant reaction occurring. By using an excess of the polar

quinone reagent the polarity of the reaction mixture was increased. With the knowledge that using a polar solvent favours **77** formation (Table 5 entry 4), it was rationalised this increase in polarity from excess **75** was facilitating the formation of **77**. Consequently, the reaction concentration was reduced to ¼ of the previous examples (0.14 M with respect to PPh_3 instead of 0.57 M), this had the intended result with the desired dioxyphosphorane product (**76**) obtained in 68% conversion (by ^{31}P NMR spectroscopy).

Given that the quinone **75** was chosen in preference to **11** for superior atom economy, the use of excess **75** diminishes this benefit. Therefore, **11** was used to form the corresponding dioxyphosphorane **12**. A literature procedure was followed and the desired product was obtained in 94% conversion (by ^{31}P NMR spectroscopy) after 18 hours at 70 °C (Scheme 36).[13] Although the literature reaction time was 48 hours, no increase in conversion was observed after 18 hours .

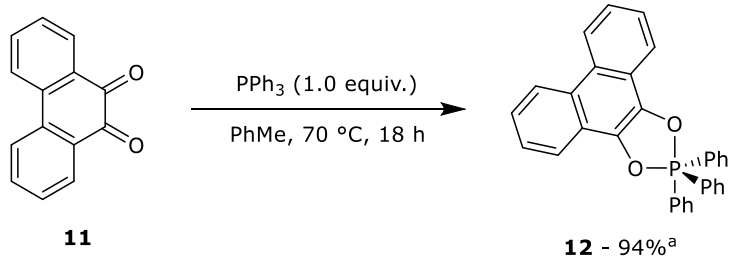

11

12 - 94%[a]

*Scheme 36: Synthesis of dioxyphosphorane **12** via the addition of triphenylphosphine to 9,10-phenanthrenequinone (**11**). [a]Conversion determined by ^{31}P NMR spectroscopy.*

1.3.3 Preparation of Phosphorus-Containing Monoliths

1.3.3.1 Monolithic Triphenylphosphine

Initial work focussed on relatively simple phosphorus-containing monoliths. Although there are known methods to install phosphorus functionality into an existing monolith, we have not explored this approach.[38] Instead we opted for the strategy of synthesising a co-polymer with a phosphorus-containing monomer. Synthesis of the monomeric form of triphenylphosphine (**54**) was undertaken using a known method (Scheme 37).[34] The reaction proceeds in good yield (63%), comparable to that reported in the literature (53%).

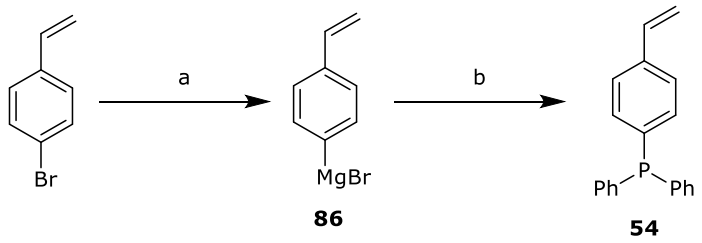

*Scheme 37: Synthesis of **54** via a Grignard addition. Reagents and conditions a) Mg, THF, r. t., 1 h; b) PPh_2Cl, THF, 0 °C to r. t., 20 h, 63% (over two steps).*

Subsequent work found this to be a capricious reaction, giving variable yields at different scales and ambient temperatures. This was overcome however using a lithium-halogen exchange protocol (Scheme 38).

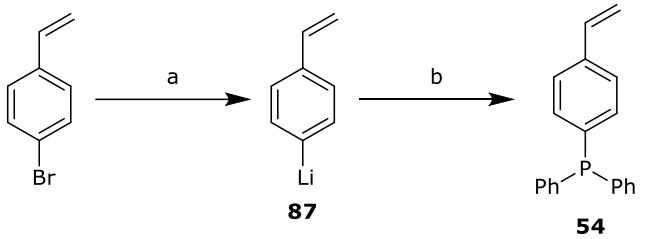

*Scheme 38: Synthesis of **54** via lithium halogen exchange. Reagents and conditions a) n-BuLi, THF, −78 °C, 30 min; b) PPh_2Cl, THF, − 78 °C to r. t., 4 h, 71% (over two steps).*

Consequently, a good quantity of material was available with which to explore its subsequent polymerisation.

Initially triphenylphosphine-containing monoliths (**53**) were synthesised using the same radical polymerisation conditions as reported in the literature (Table 6 entry 1).[51] Although polymerisation was successful, the monoliths appeared to have low porosity. Consequently, solutions did not flow through easily. In order to improve our understanding of the monolith synthesis, a number of reactions were performed altering the quantities of the initiator (azobisisobutyronitrile, AIBN) and porogen (dodecan-1-ol) (Table 6).

*Table 6: Triphenylphosphine monolith (**53**) polymerisation optimisation.*

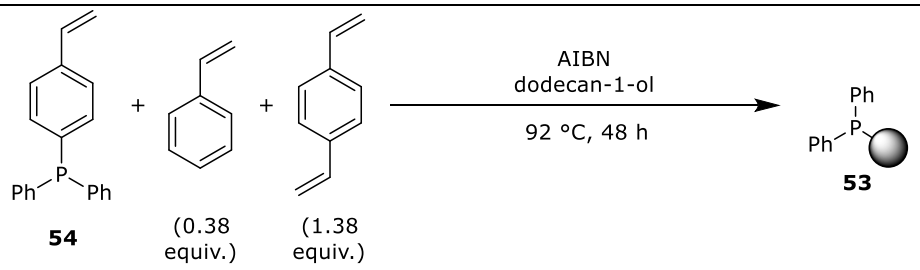

Entry	AIBN / mol%[a]	Dodecan-1-ol / equiv.	Outcome
1	1.57	2.10	Porous, slow flow
2	1.57	1.05	Not porous, no flow
3	1.57	3.00	Polymerisation failed
4	0.92	2.10	V. Porous, fast flow

[a]*With respect to total monomers*

Halving the quantity of porogen unsurprisingly yielded a much harder less porous monolith (Table 6 entry 2). Indeed, solutions could not be passed through this monolith even under applied pressure. Conversely, increasing the porogen by 50% resulted in a failure to polymerise to form a single homogenous monolith (Table 6, entry 3). The quantity of porogen in this reaction mixture was such that the concentration of monomers was too

low. Consequently, only small masses of polymer formed which were dispersed throughout the porogen. Reducing the quantity of initiator is known to increase pore size by reducing polymerisation rate and resulting in earlier phase separation.[58] Satisfyingly, this proved to be the case and a homogeneous porous monolith was synthesised which allowed solutions to flow-through easily (Table 6 entry 4). Solid state ^{31}P NMR analysis found a single peak at −6.5 ppm confirming triphenylphosphine incorporation. No corresponding phosphine oxide peak (expected at ~29 ppm) was present.

Unfortunately, with different batches of styrene dissimilar results are often observed, necessitating a re-optimisation of the conditions. This is most likely due to a variability in the concentration of 4-*tert*-butylcatechol inhibitor present. However, balancing this with the loading of initiator allows the preparation of porous monoliths to be achieved.

To confirm phosphorus incorporation into the monolith a batch reaction was performed with **53**. Benzyl azide underwent a Staudinger reduction in 95% conversion (by ^{1}H NMR spectroscopy) demonstrating **53** is an active source of PPh_3 (Scheme 39).

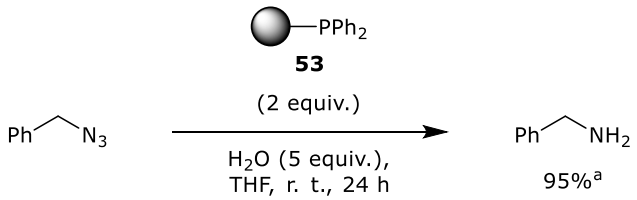

*Scheme 39: Staudinger reduction of benzyl azide using a monolithic triphenylphosphine reagent (**53**); [a]Yield determined by ^{1}H NMR spectroscopy.*

Although the monolith was partially broken apart and two equivalents were used, this reaction went some way to confirming that a significant portion of the phosphorus was accessible to the reagents in solution.

1.3.3.2 Monolithic Triphenylphosphine Oxide

Triphenylphosphine oxide as the intended precursor to chlorotriphenylphosphonium chloride and acyclic dioxyphosphoranes was the next species to be immobilised. Initially it was hoped that oxidation of **54** and subsequent polymerisation would yield a macroporous monolithic triphenylphosphine oxide.

Functionalisation prior to polymerisation is beneficial for three reasons. Firstly, product characterisation of solution phase chemistry using NMR spectroscopy and mass spectrometry is much simpler than solid state techniques. Secondly, the ability to purify the monomeric phosphorus reagent would be advantageous. Finally, solution phase transformations would likely be faster and guarantee full conversion relative to the corresponding heterogeneous reactions, in which phosphorus sites may be more difficult to access.

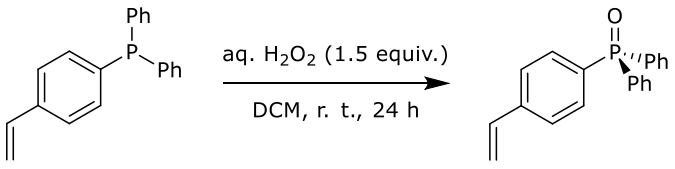

54 **88** - 75%

*Scheme 40: Synthesis of the triphenylphosphine oxide monomer **88**.*

Oxidation of **54** with aqueous hydrogen peroxide gave **88** in 75% yield (Scheme 40).

Unfortunately, polymerisation attempts under the same conditions as the previous triphenylphosphine monolith syntheses yielded a non-porous glassy solid. Evidently **88** has different polymerisation characteristics to **54**, significant optimisation work would be required to obtain a suitably porous triphenylphosphine oxide monolith. For this reason, subsequent work has focussed on transformations of monolithic triphenylphosphine (**53**).

Oxidation of **53** using aqueous hydrogen peroxide in both batch and flow processes was successful and characterised by ^{31}P NMR spectroscopy and ATR-IR (Scheme 41). It is of note that this oxidation resulted in full conversion, demonstrating that the phosphorus sites of the monolith are very accessible to reagents in solution. Therefore, any unsatisfactory results obtained using our phosphorus containing monoliths cannot be ascribed to a low effective concentration of the monolithic reagent.

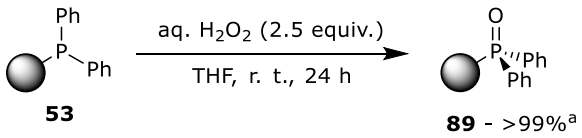

53 **89** - >99%[a]

*Scheme 41: Oxidation of monolithic triphenylphosphine (**53**) to monolithic triphenylphosphine oxide (**89**); [a]Yield determined by solid state ^{31}P NMR spectroscopy.*

1.3.3.3 Monolithic Chlorotriphenylphosphonium Chloride

Formation of the monolithic chlorophosphonium salt (**91**) was achieved using oxalyl chloride in both batch and flow reactions (Scheme 42). Gas evolution was observed as carbon dioxide and carbon monoxide formed, whilst the P=O stretch in the ATR-IR spectrum disappeared.

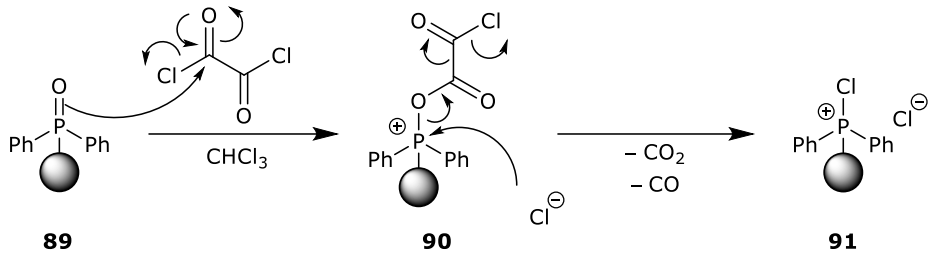

*Scheme 42: Mechanism for the formation of monolithic chlorotriphenylphosphonium chloride (**91**).*

Formation of 1-chlorodecane (**92**) in an Appel reaction with 1-decanol in flow confirmed the successful formation of active **91** (Scheme 43).

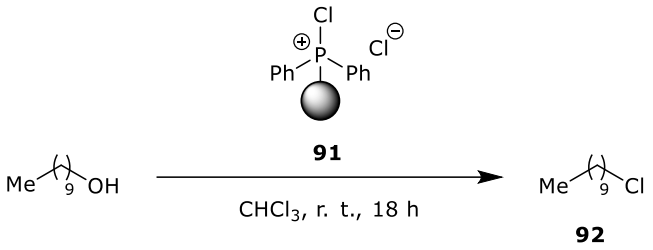

*Scheme 43: Synthesis of 1-chlorodecane (**92**) using a monolithic chlorophosphonium salt (**91**). Note: Large excess of decanol used, conversion not determined.*

Stability testing of **91** revealed slow hydrolysis to the corresponding oxide monolith (**89**). After ten days in an open atmosphere it had yet to completely revert to the oxide by ATR-IR, only after 30 days had complete hydrolysis occurred. In contrast to this, solution phase chlorotriphenylphosphonium chloride (**69**) hydrolyses in approximately 10 minutes (Scheme 44).

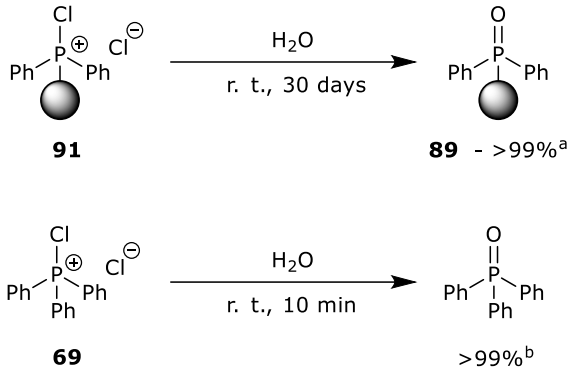

*Scheme 44: Comparison in hydrolytic stability for monolithic and solution phase chlorophosphonium salts **91** and **69**; [a]Yield determined by ATR-IR (indistinguishable spectra from pure **89**), [b]Yield determined by ^{31}P NMR spectroscopy.*

This increased hydrolytic stability is another benefit of immobilised reagents relative to the analogous homogenous chemistry. This is provided the intended reaction's rate isn't retarded to the same extent. If this is indeed the case, then it bodes well for monolithic dioxyphosphoranes, some of which are so sensitive they cannot be isolated without the use of Schlenk equipment or a glovebox.[18,20]

1.3.3.4 Monolithic Dioxyphosphoranes

Upon addition of a lithium 2,2,2-trifluoroethan-1-olate solution to crushed monolithic chlorotriphenylphosphonium chloride (**91**), a new IR absorption was observed at 1146 cm^{-1}. Unfortunately, there is no literature IR data for **21** due to the difficulty regarding its isolation. However, it is known that P-O-C linkages of phosphonates and phosphinites absorb at 1030-1064 cm^{-1}. Furthermore cyclic dioxyphosphorane **95**, previously synthesised in the group absorbs at 1246 cm^{-1} (Scheme 45).[59] Therefore, it seems reasonable to suggest the absorption at 1146 cm^{-1} is characteristic of the P-O-C linkage in the expected product **94**. Additionally, upon washing with water,

as anticipated, the peak at 1146 cm^{-1} disappeared and the phosphine oxide peak grew dramatically.

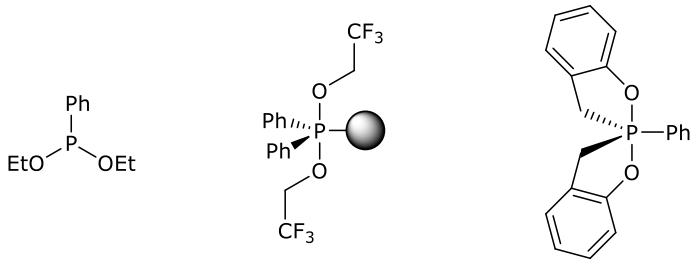

93 1042 cm^{-1} (P-O-C)

94 1146 cm^{-1} (P-O-C)

95 1246 cm^{-1} (P-O-C)

*Scheme 45: IR absorption frequencies of diethyoxyphenylphosphine (**93**), monolithic bis(2,2,2-trifluoroethoxy)triphenylphosphorane (**94**) and 2-Phenyl-2,3,3'-trihydro-2λ^5-2,2'-spirobi[benzo[d][1,2]oxaphosphole (**95**).*

All attempts to utilise **94** in batch reactions failed to give any observable products. Therefore, all subsequent work focussed on the use of the previously described cyclic dioxyphosphoranes. Consequently, the corresponding monolithic variants of the two cyclic dioxyphosphoranes dioxyphosphoranes (**12** and **76**) described in section 1.3.2 were prepared. Synthesis of **96** and **97** was achieved under identical reaction conditions, with the exception of reaction duration (Scheme 46). These species were generated and used *in situ* with no analysis performed.

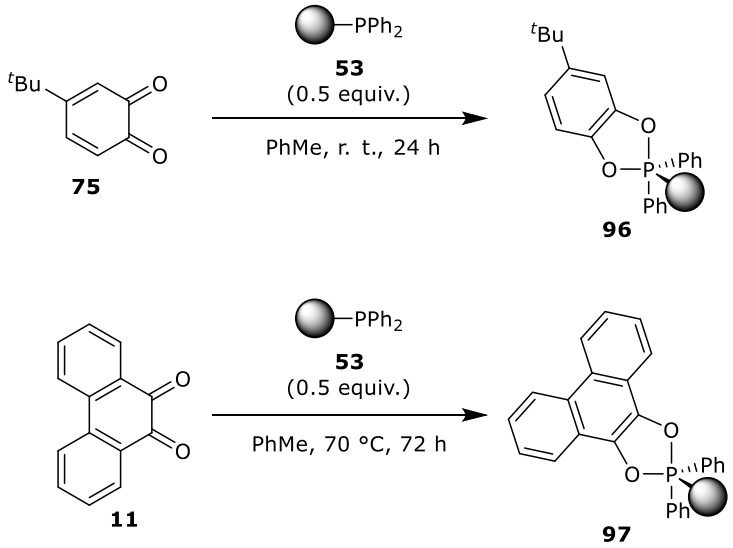

*Scheme 46: Synthesis of monolithic cyclic phosphoranes **96** and **97**.*

1.3.4 Cyclic Dioxyphosphorane-Mediated Reactions

1.3.4.1 Cyclic Dioxyphosphorane-Mediated Cyclodehydrations

Cyclic dioxyphosphorane **12** has been shown to perform cyclodehydration reactions of diols and amino alcohols in addition to mercapto alcohols.[13] All four of the previously described cyclic dioxyphosphoranes (**12**, **76**, **96** and **97**) were used to successfully synthesise tetrahydrofuran (THF) *via* the cyclodehydration of 1,4-butanediol (Table 7). In all cases complete conversion of 1,4-butanediol to THF was observed by ^{1}H NMR spectroscopy. It is noteworthy that in the case of **96** only trace product was observed after 48 hours at room temperature (with full conversion observed after 168 hours), whilst **97** showed full conversion after just 18 hours (Table 7 entries 3 and 4 respectively).

*Table 7: Synthesis of tetrahydrofuran using cyclic dioxyphosphorane monoliths **76, 12, 96** and **97**.*

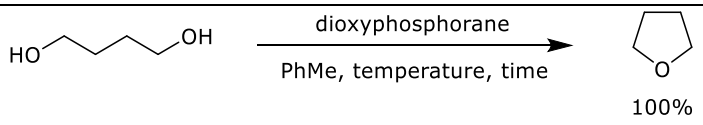

Entry	Dioxyphosphorane	Temperature / °C	Time	Conversion / %[a]
1	**76**	r. t.	72	100
2	**12**	70	3	100
3	**96**	r. t.	168	100
4	**97**	r. t.	18	100

[a]determined by [1]H NMR spectroscopy.

Industrial production of tetrahydrofuran is most commonly achieved using an acid catalyst with temperatures in excess of 100 °C.[60] Therefore this ability to achieve full conversion at room temperature with an immobilised reagent, capable of being regenerated, is very promising. Due to the apparent increased reactivity and higher conversion **12** was chosen in preference to **76** for all future transformations.

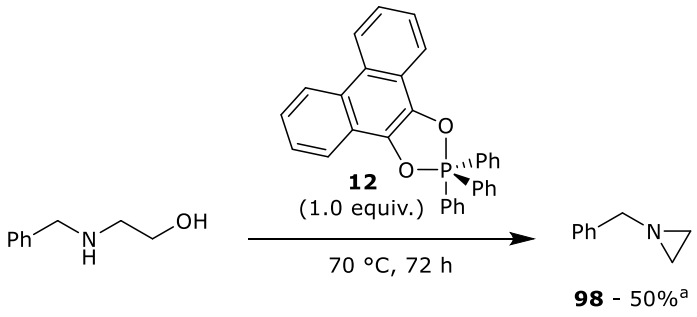

*Scheme 47: Synthesis of N-Benzylaziridine (**98**) via the cyclodehydration of N-Benzylethanolamine. [a]Yield determined by [1]H NMR spectroscopy.*

Cyclodehydration of amino alcohols to form nitrogen heterocycles has also been described in the literature.[13] As the analogous intramolecular reaction to our intended intermolecular amine/alcohol couplings, this was next explored. *N*-Benzylethanolamine was successfully converted to *N*-

benzylaziridine (**98**) in 50% conversion by ^{1}H NMR spectroscopy (Scheme 47). This is roughly comparable with the literature yield of 60% for which no reaction conditions are given. Given that when we performed the reaction a 1:1 ratio of starting material and product were observed, we attempted to increase this conversion by using 2 equivalents of **12**. In this case 61% conversion was observed after 24 hours at 70 °C. However, after a further 24 hours the conversion had decreased to 39% as the aziridine product reverted to the starting material. Nevertheless, having confirmed the reactivity of **12** we began our investigations into intermolecular amine/alcohol couplings.

1.3.4.2 Cyclic Dioxyphosphorane-Mediated Amine/Alcohol Couplings

A test reaction with 3-phenylpropanol and morpholine was devised to screen reaction conditions for the desired transformation. 3-Phenypropanol was chosen due to the limited electronic effects on the alcohol, combined with its ease of handling and commercial availability. Morpholine's great importance in pharmaceutical applications, combined with being a secondary amine (thus minimising over-alkylation) make it an ideal candidate.[61,62]

Using an equimolar ratio of amine and alcohol with 1.2 equivalents of the dioxyphosphorane (**12**) the desired product (**99**) was obtained in 23% yield after 24 hours at room temperature (Scheme 48).

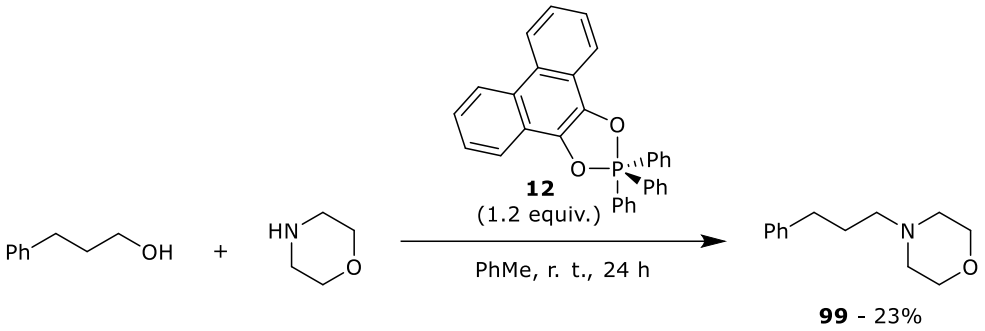

*Scheme 48: Synthesis of 4-(3-phenylpropyl)morpholine (**99**).*

This represents the first example of an intermolecular amine/alcohol coupling mediated by a cyclic dioxyphosphorane. Moreover, with the exception of **21**, it is the first example of such a transformation mediated by any class of dioxyphosphorane. A range of reaction conditions were explored to optimise the yield of the reaction, the results of which are summarised in Table 8.

For all the reactions in Table 8 no remaining alcohol was present at the end of the reaction (with the exception of entries 4 and 5). Therefore, it was apparent that the alcohol must be consumed in an unwanted side reaction given the poor yields. Both the mono and di-alkylated catechol species (Scheme 49) were isolated which explained the poor yields obtained. The two side products (**100** and **101**) were generally observed in a 1:1 ratio and constituted the remaining mass balance.

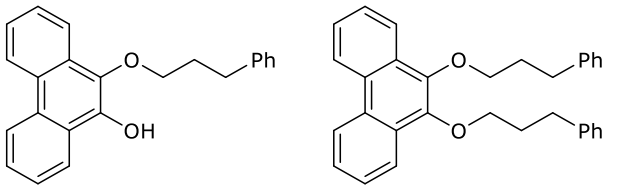

100 **101**

*Scheme 49: Structures of the two isolated side products **100** and **101**.*

By using 3 equivalents of morpholine it was hoped that the competitive side reaction would be minimised. However, the isolated yield of **99** was only marginally increased to 28% (Table 8 entry 2). Switching to a more polar solvent, DCM, reduced the yield to just 7% (Table 8 entry 3), presumably by preferentially stabilising the formation of the side products.

*Table 8: Optimisation of conditions for the synthesis of 4-(3-phenylpropyl)morpholine (**99**).*

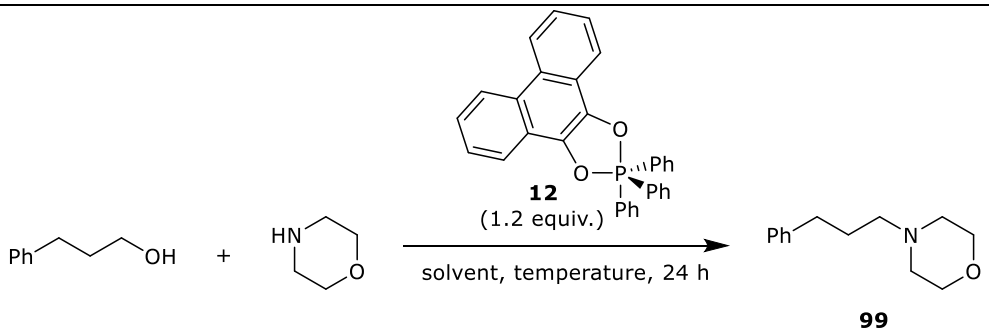

Entry	Solvent	Temperature / °C	Alcohol / equiv.	Amine / equiv.	**12** / equiv.	**99** yield / %
1	PhMe	r. t.	1.0	1.0	1.2	23
2	PhMe	r. t.	1.0	3.0	1.2	28
3	DCM	r. t.	1.0	1.0	1.2	7
4[a]	PhMe	0 to r. t.	1.0	1.0	1.2	7
5[a,b]	PhMe	0 to r. t.	1.0	1.0	1.2	8
6	PhMe	r. t.	2.0	1.0	2.0	16

[a]Residual alcohol present; [b]Alcohol added via syringe pump over 1 hour.

By reducing the reaction temperature both the intended reaction and competitive side reactions were outcompeted by hydrolysis with adventitious water. Consequently, all the dioxyphosphorane was consumed yielding just 7% product (Table 8 entry 4). Slowing the addition of the alcohol, to keep a lower relative concentration, did not decrease the formation of the unwanted side products (Table 8 entry 5). Finally, an excess of alcohol and dioxyphosphorane was used in an attempt to ensure there was alcohol present for the morpholine to react with (Table 8 entry 6). However, this merely increased the quantity of unwanted side products formed with no increase in the yield of **99**.

It had been hoped that oxygen alkylated products would not be observed in these reactions due to the aromatic sp^2 system. Although the mechanism for these side reactions is not known, presumably the 3-phenypropanol is acting as the electrophile. This is despite the poor nucleophilicity of the phenolic oxygen. A control reaction was performed with 3-phenylpropanol and **12**, which confirmed both side products **100** and **101** were formed in the absence of morpholine.

In the literature proposed mechanism for **12**-mediated cyclodehydrations, 9,10-phenanthrenediol (**16**) is eliminated which is oxidised to the quinone (**11**) in the presence of oxygen (Scheme 50). Assuming therefore that the 9,10-phenanthrenediol (**16**) is the reactive species present in the formation of the unwanted side products, then exposure of the reaction to oxygen should eliminate this. Consequently, a reaction was performed under an oxygen atmosphere with molecular sieves present to remove water formed. Although **16** was readily oxidised in solution, the dioxyphosphorane (**12**) was not stable under such conditions. As a result,

neither product nor the oxygen alkylated side products were recovered at the end of the reaction.

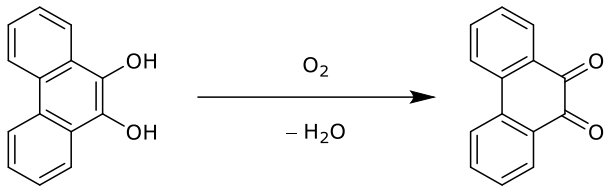

16 **11**

*Scheme 50: Oxidation of 9,10-phenanthrenediol (**16**) to 9,10-phenanthrenequinone (**11**) under atmospheric conditions.*

Whilst the confirmation that **12** can be used to couple amines and alcohols intermolecularly was significant, further work would be required to make this a viable process.

1.3.4.3 Application of Monolithic Cyclic Dioxyphosphoranes in Flow

Reactions using immobilised dioxyphosphoranes have to date only been carried out in a batch process, with one polymeric dioxyphosphorane (**65**), as described in section 1.2.4.3.[55] We aimed to demonstrate the first use of an immobilised dioxyphosphorane in a flow, with the use of **97**.

To characterise the monolithic dioxyphosphorane, a batch reaction in toluene was performed (as was previously shown in Scheme 46), with a portion of the monolith quickly removed and analysed by solid state ^{31}P NMR spectroscopy. The major peak observed was that corresponding to the triphenylphosphine monolith (**53**) at −6.5 ppm, with the second major peak being due to the oxide (**89**) at 25.2 ppm. However, when this was overlaid with the spectrum of another subsequently prepared sample, a distinct shoulder can be observed at around −20 ppm (Figure 3). This is in

the expected region of the desired product (solution chemical shift: −16.4 ppm). Therefore, it is likely that the product (**97**) has formed; the inherent increased broadness of solid-state NMR has caused the two peaks (which only have ~10 ppm separation in the solution phase) to coalesce. Additionally, the formation of the oxide will be due to the hydrolysis of the dioxyphosphorane. Whilst this could be occurring during the reaction, it could also take place throughout the process of sample removal, homogenising and packing into the rotor for analysis.

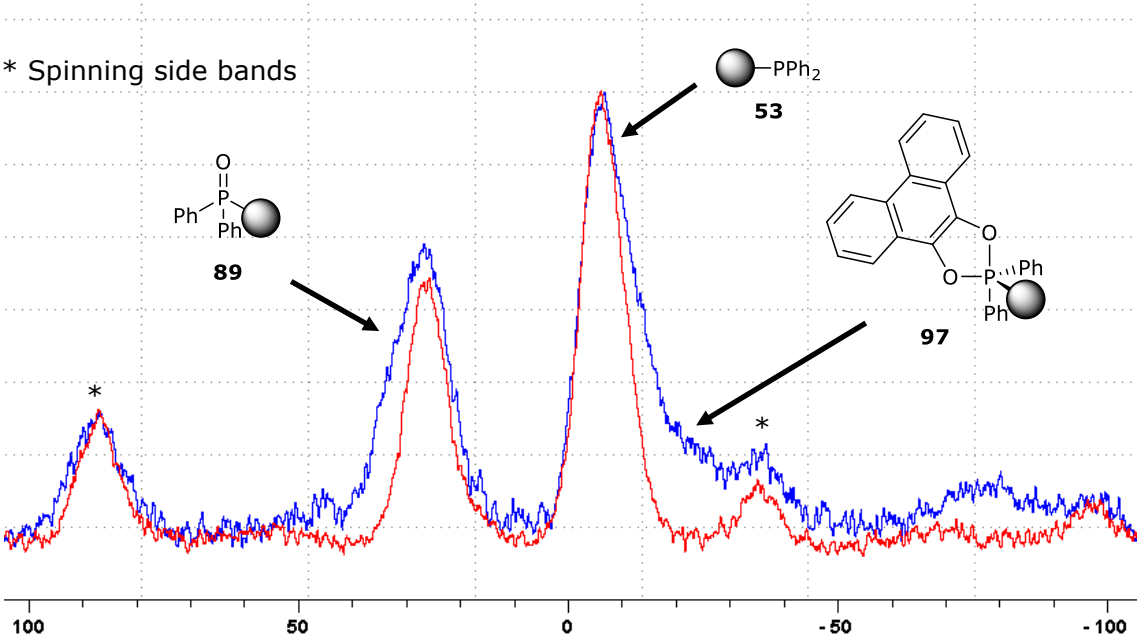

*Figure 3: Solid-state NMR spectrum for the preparation of monolithic dioxyphosphoranes. Blue trace: batch preparation of **97** in toluene. Red trace: hydrolysed preparation of **97**.*

If the latter case is true and hydrolysis is occurring upon analysis, then a significant quantity of the active reagent could have been formed, which could be applied as a reagent in a flow process.

A simple flow reactor setup was devised using a peristaltic pump and empty biotage™ column to contain the monolith (Figure 4)

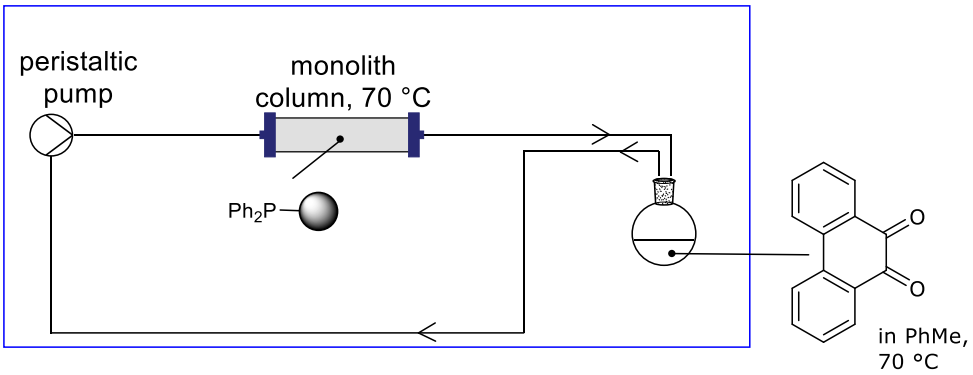

*Figure 4: Initial reactor setup for the synthesis of monolithic dioxyphosphorane **97** in flow.*

Initial attempts to synthesise **97** in flow using toluene, with the monolith column heated to 70 °C (as was successful in batch) proved unsuccessful. This was due to severe blockages that formed upon the quinone solution cooling in the tubing. In spite of the greater dilution of this experiment to the batch reactions (26 mM vs 67 mM), the quinone solubility in toluene at room temperature proved prohibitive. With no equipment available to heat the tubing, alternative solvents were explored.

Successful batch formation of the analogous solution phase dioxyphosphorane (**12**) in DCM was achieved. This combined with its ability to solubilise the quinone at room temperature, suggested it to be a suitable replacement.

Using DCM with the same setup as previously, no product was observed by solid state ^{31}P NMR spectroscopy, whilst a large peak for the corresponding oxide was observed. This suggested a greater degree of hydrolysis of **97**

was occurring, however it cannot be certain if this occurred during preparation for analysis. Additionally, the use of the more volatile solvent DCM led to solvent evaporation causing the system to run dry, leading to blockages and flow being stopped. Despite extensive efforts to better seal the joints and the system as a whole, this loss of solvent could never be fully eliminated. However, through the use of less volatile solvents, this issue could be somewhat alleviated.

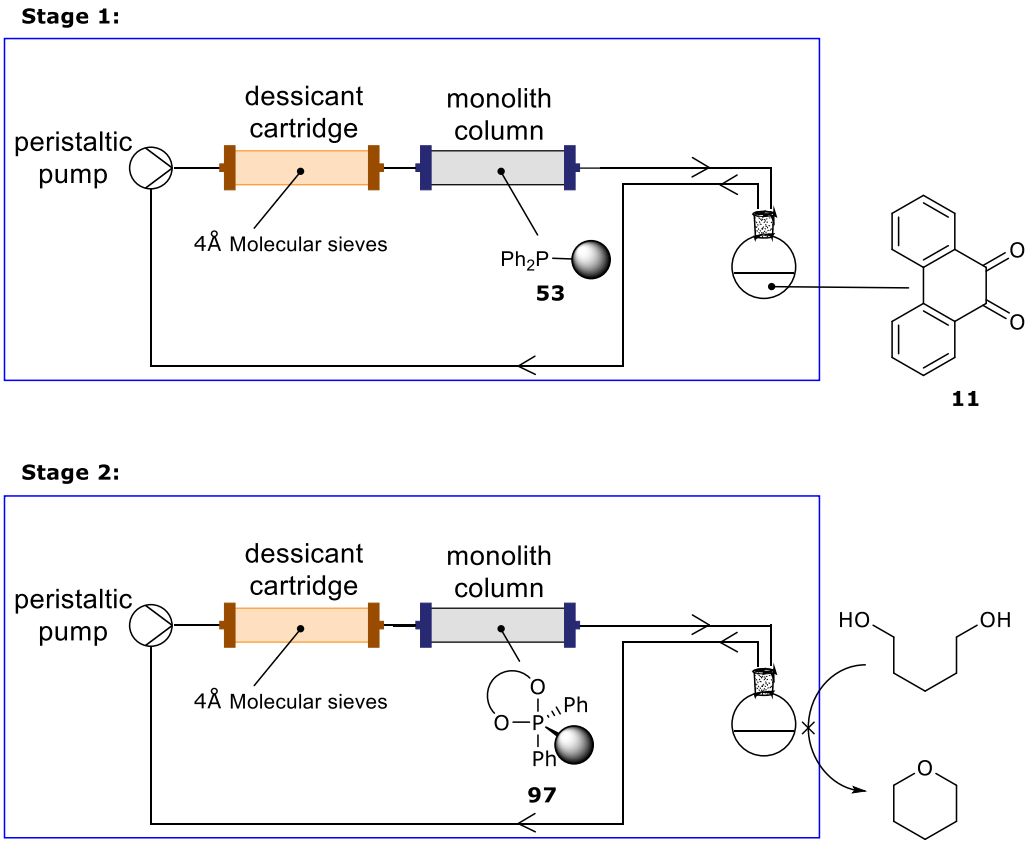

*Figure 5: Schematic of the preparation of monolithic dioxyphosphorane **97** (stage 1) and a subsequent test reaction for the cyclodehydration of 1,5-pentanediol (stage 2). Reaction conditions: Stage 1A: DCE, r. t., 24 h; Stage 1B: DMF, 50 °C, 24 h; Stage 2A: DCE, r. t., 20 h; Stage 2B: DMF, 50 °C, 20 h.*

Two preparations of **97** were attempted using DCE and DMF using the setup shown in Figure 5. No isolation for analysis was attempted to limit the opportunity for hydrolysis to occur, whilst molecular sieves were

implemented in a desiccant cartridge to aid in this regard. After cycling the quinone solution for 24 hours, 1,5-pentanediol was added and the reaction continued a further 20 hours (Figure 5). For both reactions only starting material was observed with no tetrahydropyran present. Evidently the flow setup developed was not capable of maintaining the rigorously anhydrous conditions required for this extremely sensitive chemistry, which is usually performed using Schlenk apparatus.

1.4 Conclusions and Outlook

Porous monolithic triphenylphosphine, triphenylphosphine oxide and chlorotriphenylphosphonium chloride reagents have been synthesised and characterised by solid state NMR and/or infrared spectroscopy. Their synthetic utility has been demonstrated through successful test reactions.

The dioxyphosphorane bis(2,2,2-trifluoroethoxy)triphenylphosphorane has been synthesised and its capacity to perform trifluoroethylation reactions demonstrated. Dioxyphosphorane-mediated amine/alcohol coupling reactions have been achieved with limited success due to competing trifluoroethylation reactions.

Two cyclic dioxyphosphoranes were synthesised and tested in an attempt to avoid competitive alkylation reactions. The more active of the two (derived from triphenylphosphine and 9,10-phenanthrenequinone) was used to successfully synthesise 4-(propyl)morpholine. However, competitive alkylation reduced the efficacy of the process.

Novel monolithic variants of both cyclic phosphoranes were synthesised and successfully used to synthesise THF by cyclodehydration, in batch reactions. Synthesis of the immobilised dioxyphosphorane was achieved (with low conversion) in flow, but competitive hydrolysis prevented its use for cyclodehydration reactions.

Further work in this area should focus on the application of more rigorously anhydrous flow equipment, enabling hydrolytically labile dioxyphosphoranes to be used in flow. Alternatively, further dioxyphosphoranes could be prepared with a view to optimising the desired reactivity over unwanted side reactions (including hydrolysis).

1.5 Experimental

1.5.1 General Experimental Procedures

Unless stated otherwise, all reactions were carried out under an atmosphere of argon. All glassware was flame dried or oven dried and allowed to cool under a stream of argon before use. Cooling to 0 °C was effected using an ice-water bath. Cooling to temperatures below 0 °C was effected using dry ice-acetone mixtures. The term petroleum ether refers to the fraction with boiling point of 40 to 60 °C.

Commercially available solvents and reagents were used as supplied with the following exceptions. Toluene, THF and diethyl ether were collected from a solvent tower, where a degassed solvent was passed through two columns of activated alumina and a 7 micron filter under a 4 bar pressure. $CHCl_3$ was stirred with phosphorus pentoxide for 2 h, distilled and stored under an argon atmosphere over activated 4 Å molecular sieves. Reactions were monitored using thin layer chromatography on Merck TLC silica gel 60 F_{254} pre-coated aluminium sheets with fluorescent indicator. Sheets were visualised using ultra-violet light (254 nm) and/or $KMnO_4$ solution, as appropriate. Flash column chromatography was performed using Aldrich silica gel 60, 40–63 μm.

Compounds for which characterisation data matches literature values are denoted by a reference next to the compound name. IR and m. p. data has only been recorded for novel compounds.

Infrared spectra were recorded on the ATR module of a Bruker Alpha spectrometer. Mass spectra were acquired on a Bruker Micromass LCTOF.

Bruker DPX 300, Bruker DPX 400, Bruker AV 400, Bruker AV (III) 400, Bruker AV (III) 400HD or Bruker AV 500 spectrometers were used to record all ^{1}H, ^{13}C, ^{19}F and ^{31}P NMR spectra of dilute solutions of the appropriate compound in the indicated deuterated solvent. All chemical shifts (δ) are reported in parts per million (ppm) relative to residual chloroform (δ_H = 7.26 ppm, δ_C = 77.2 ppm) or benzene (δ_H = 7.16 ppm, δ_C = 128.1 ppm). Coupling constants (*J*) are reported in Hertz and are recorded after averaging. The multiplicity of a ^{1}H NMR signal is designated by one of the following abbreviations: s = singlet, d = doublet, t = triplet, q = quartet and m = multiplet. Where given, reaction conversions were determined by the relative ^{1}H integrations of the product and the appropriate starting material.

Relaxation delays were not measured for solution phase ^{31}P NMR spectroscopy. Consequently, ^{31}P NMR integrals cannot be considered quantitative.

Solid state ^{31}P direct polarisation spectra were recorded on a Bruker Avance I 400WB NMR spectrometer fitted with a 4 mm HX magic angle spinning probe. The samples were packed into 4 mm zirconia rotors and spun about the magic angle at a frequency of 12 kHz. The spin lattice relaxation times were not determined for these samples but a recycle delay of 600 s was used for each. Typically, ^{31}P relaxation times can be very long, so based on experience, 600 s was considered to be sufficient time to allow full relaxation back to equilibrium following each radiofrequency pulse. The spectra were externally referenced to ammonium dihydrogen phosphate at 0.81 ppm.

Solid state ^{13}C cross polarisation magic angle spinning spectra were recorded on a Bruker Avance III 500WB NMR spectrometer fitted with a 4

mm HFX probe. The samples were spun about the magic angle at a frequency of 8 kHz. In these experiments, the spinning sidebands were suppressed using a TOSS-a (Total sideband suppression) method. The spectra were externally referenced to the peak due to the carbonyl carbon of glycine at 176.03 ppm.

Flow experiments were performed using a Cole-Palmer MasterFlex L/S peristaltic pump with an easy-load (II) pump head and PVC Masterflex transfer tubing.

*Figure 6: Typical flow reactor setup for synthesis and use of the monolithic dioxyphosphorane **97**. Three necked round bottomed flask contains reagents in solution. Empty column chromatography column contains monolithic polymer and molecular sieves.*

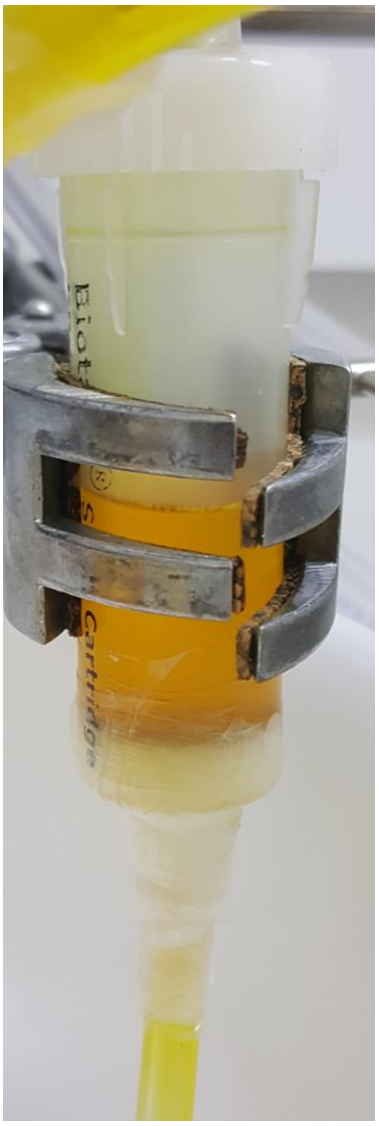

*Figure 7: Synthesis of the monolithic dioxyphosphorane (**97**) in flow. Orange solution contains 9,10-phenanthrenequinone (**11**), white solid at the bottom of column is monolithic triphenylphosphine (**53**).*

1.5.2 Experimental Data of Compounds

Bis(2,2,2-trifluoroethoxy)triphenylphosphorane (**21**)[20]

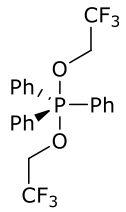

To a solution of triphenylphosphine oxide (1.11 g, 4.00 mmol) in $CHCl_3$ (6.5 mL), in a Schlenk flask, was added oxalyl chloride (340 µL, 4.00 mmol) dropwise over 1 min. The resulting solution was stirred at r. t. for 1 hour. To a separate Schlenk flask was added 2,2,2-trifluoroethanol (862 µL, 12.0 mmol), *N*-benzylbenzamide (20 mg) and Et_2O (26 mL). The resulting solution was cooled to 0 °C and *n*-BuLi (1.6M in hexanes, 7.50 mL, 12.0 mmol) was added dropwise over 1 min. (Note: upon complete formation of the alkoxide a colour change from colourless to purple was observed). The resulting alkoxide solution was transferred *via* cannula to the above described, solution of chlorotriphenylphosphonium chloride at −78 °C. The reaction mixture was stirred at −78 °C for 30 min then at r. t. for a further 3 hours. The resulting heterogenous suspension was allowed to settle before the clear, homogeneous, dioxyphoshporane solution was transferred to a final Schlenk flask *via* cannula. The solution was then concentrated *in vacuo* and the resulting solids re-dissolved in $CHCl_3$ (10.1 mL) to give a 0.396 M[a] stock solution of **21** (>95% by ^{31}P NMR spectroscopy).

[a]Concentration determined by ^1H NMR conversion in combination with known quantities of reagents and solvent used.

^{1}H NMR (300 MHz, C_6D_6) δ 8.05 – 7.94 (m, 6H), 7.19 – 7.08 (m, 9H), 2.84 (qd, *J* = 9.0, 4.3, 4H); **^{13}C{^{1}H} NMR** (101MHz, C_6D_6) δ 134.8 (d, *J* = 173.8), 132.7 (d, *J* = 10.7), 130.4 (d, *J* = 3.2), 128.3 (d, *J* = 16.1), 60.3 (dq, *J* = 34.1, 6.0); **^{19}F NMR** (376 MHz, C_6D_6) δ −74.1 (t, *J* = 9.0); **^{31}P{^{1}H} NMR** (121 MHz, C_6D_6) δ −58.7.

Note: The ^{13}C NMR signal corresponding to the trifluoromethyl groups was not observed due to excessive splitting from fluorine and phosphorus.

N-Benzylaniline (**71**)[18]

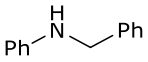

To a solution of **21** (0.396M solution in $CHCl_3$, 2.00 mL, 0.79 mmol), in a Schlenk flask, was added aniline (60 μL, 0.66 mmol) and the reaction mixture stirred at r. t. for 30 min. The reaction mixture was then cooled to −78 °C and benzyl alcohol (68 μL, 0.66 mmol) added dropwise over 5 min. The reaction mixture was stirred at −78 °C for 1.5 hours then at room temperature for 110 hours before being concentrated *in vacuo*. Flash column chromatography (1:1 petroleum ether/EtOAc) gave **71** (27 mg, 12%) as a yellow solid.

^{1}H NMR (400 MHz, C_6D_6) δ 7.45 – 7.36 (m, 5H), 7.26 – 7.22 (m, 2H), 6.78 (t, *J* = 7.2, 1H), 6.70 (d, *J* = 8.0, 2H), 4.39 (s, 2H); **^{13}C{^{1}H} NMR** (101 MHz, $CDCl_3$) δ 148.2, 139.5, 129.3, 128.7, 127.5, 127.3, 117.6, 112.9, 48.4. **HRMS** (ESI$^+$) $C_{13}H_{14}N^+$ [M+H]$^+$ calcd. 184.1126, found 184.1115.

4-*tert*-Butyl-1,2-benzoquinone (**75**)[63]

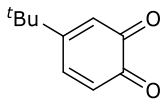

To a solution of 4-*tert*-butylcatechol (1.00 g, 6.00 mmol) in DCM (20mL) was added sodium periodate (1.28 g, 6.00 mmol) in water (6mL) and DCM (10 mL). The resulting solution was stirred at r. t. for 1 hour. The biphasic reaction mixture was separated and the aqueous layer extracted with DCM (3 × 30 mL). The combined organic layers were washed with sat. aq. $Na_2S_2O_3$ (40 mL), decolourised with charcoal, dried ($MgSO_4$) and concentrated *in vacuo* to give **75** (939 mg, 95%) as a brown solid.

^{1}H NMR (400 MHz, $CDCl_3$) δ 7.21 (dd, *J* = 10.4, 2.4, 1H), 6.41 (dd, *J* = 10.4, 0.8, 1H), 6.31 (dd, *J* = 2.4, 0.8, 1H), 1.26 (s, 9H); **^{13}C{^{1}H} NMR** (101 MHz, $CDCl_3$) δ 180.5, 180.4, 162.1, 140.0, 129.4, 123.8, 35.7, 27.8; **HRMS** (ESI^+) $C_{10}H_{13}O_2^+$ $[M+H]^+$ calcd. 165.0910, found 165.0902.

5-(*tert*-Butyl)-2,2,2-triphenyl-2λ5-benzo[*d*][1,3,2]dioxaphospholane (**76**)

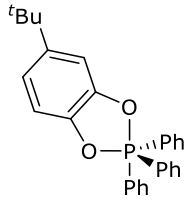

To a solution of triphenylphosphine (262 mg, 1.00 mmol) in dry toluene (7 mL), in a Schlenk flask, was added, 4-*tert*-butyl-1,2-benzoquinone (**75**) (328 mg, 2.00 mmol). The resulting solution was stirred at r. t. for 2 hours

to give **76** as a stock solution (68% purity by ^{31}P NMR). Used *in situ* without purification or further characterisation.

$^{31}P\{^{1}H\}$ NMR (121 MHz, C_6D_6) δ −20.6.

(Note: ^{1}H and ^{13}C peaks could not be distinguished from residual 4-*tert*-butyl-1,2-benzoquinone, solvent and dimeric side product **85**).

2,2,2-Triphenyl-2λ5-phenanthro[9,10-*d*][1,3,2]dioxaphospholane (**12**)[13]

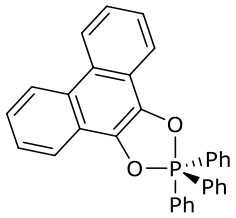

To a solution of triphenylphosphine (2.62 g, 10.0 mmol) in dry toluene (23 mL), in a Schlenk flask, was added 9,10-phenanthrenequinone (**11**) (2.08 g, 10.0 mmol). The resulting solution was heated to 70 °C for 18 hours to give **12** as a stock solution (94% purity by ^{31}P NMR). Used *in situ* without purification or further characterisation.

$^{31}P\{^{1}H\}$ NMR (162 MHz, C_6D_6) δ −16.4.

(Note: ^{1}H and ^{13}C peaks could not be distinguished from toluene solvent.)

Diphenyl(4-vinylphenyl)phosphine (**54**)[34]

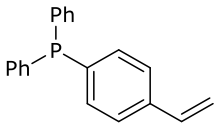

Grignard procedure:

To a suspension of magnesium turnings (481 mg, 19.8 mmol) and iodine (3 crystals) in THF (30 mL) was added 4-bromostyrene (500 µL, 3.82 mmol) dropwise over 5 min before the reaction was heated to initiation (observed by a browning in colour of the solution). Additional 4-bromostyrene (1.64 mL, 12.5 mmol) was then added dropwise over 15 min to the stirred suspension. After stirring at r. t. for 1 hour the reaction was cooled to 0 °C before chlorodiphenylphosphine (3.00 mL, 16.3 mmol) was added dropwise over 15 min. The reaction mixture was then stirred at r. t. for 20 hours. The reaction mixture was then diluted with Et_2O (100 mL) and washed sequentially with water (2 × 25 mL), 10 % aq. HCl (2 × 25 mL), saturated aqueous $NaHCO_3$ (2 × 25 mL) and brine (2 × 25 mL). The organic layer was then dried ($MgSO_4$) and concentrated *in vacuo*. Flash column chromatography (19:1, pentane/EtOAc) gave **54** (2.96 g, 63%) as a white solid.

Lithium halogen exchange procedure:

To a solution of 4-bromostyrene (3.92 mL, 30.0 mmol) in THF (110 mL) at −78 °C was added ^{n}BuLi (1.6M in hexanes, 22.5 mL, 36.0 mmol) dropwise over 15 min. The reaction mixture was stirred at −78 °C for 30 min before chlorodiphenylphosphine (5.56 mL, 30.0 mmol) was added dropwise over 10 min. The resulting solution was stirred at −78 °C for 3 hours then at r.

t. for a further 1 hour. The reaction mixture was quenched with sat. aq. NH_4Cl (60 mL) and the aqueous layer extracted with EtOAc (3 × 100 mL). The combined organic extracts were washed with sat. aq. $NaHCO_3$ (3 × 100 mL) and brine (3 × 100 mL), dried $MgSO_4$ and concentrated *in vacuo*. Flash column chromatography (19:1, pentane/EtOAc) gave **54** (2.96 g, 71%) as a white solid.

^{1}H NMR (300 MHz, $CDCl_3$) δ 7.41 – 7.26 (m, 14H), 6.73 (dd, *J* = 17.6, 10.9, 1H), 5.79 (dd, *J* = 17.6, 0.9, 1H), 5.30 (dd, *J* = 10.9, 0.9, 1H); **^{13}C{^{1}H} NMR** (101MHz, $CDCl_3$) δ 137.9, 137.2 (d, *J* = 10.8), 136.7 (d, *J* = 11.1), 136.4, 134.0 (d, *J* = 19.9), 133.7 (d, *J* = 19.8), 128.8, 128.5 (d, *J* = 7.0), 126.3 (d, *J* = 7.0), 114.7; **^{31}P{^{1}H} NMR** (121 MHz, $CDCl_3$) δ −5.8; **HRMS** (ESI$^+$) $C_{20}H_{18}P^+$ $[M+H]^+$ calcd. 289.1146, found 288.1139.

Monolithic triphenylphosphine (**53**)[51]

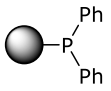

To diphenyl(4-vinylphenyl)phosphine (**54**) (637 mg, 2.21 mmol) was added styrene (89 µL, 0.77 mmol), divinylbenzene (430 µL, 3.10 mmol) and 1-dodecanol (864 mg, 4.64 mmol). The resulting heterogeneous mixture was then heated to 50 °C and stirred until homogenous. To the reaction mixture was then added azobisisobutyronitrile (9 mg, 0.06 mmol) and the resulting solution was stirred at 50 °C for 5 min. The reaction mixture was then transferred to a sealed 5 mL syringe barrel (or capped empty biotage™ column) and heated to 92 °C for 48 hours. The reaction

was cooled to r. t. and washed with DCM (20 mL) to give **53** (quantitative) as a white solid.

^{13}C NMR (126MHz, solid state), δ 144.4, 128.2, 40.3, 32.9, 32.2, 30.0, 26.3, 22.9, 18.7; **^{31}P NMR** (162 MHz, solid state) δ −6.5; **AT-IR** (neat) ν (cm^{-1}) 2923, 1600, 1485, 1435, 1404, 1185, 1119, 1018, 911, 825.

Diphenyl(4-vinylphenyl)phosphine oxide (**88**)[64]

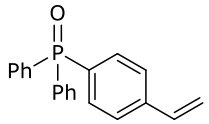

To a solution of diphenyl(4-vinylphenyl)phosphine (**54**) (288 mg, 1.00 mmol) in DCM (50 mL) was added aqueous hydrogen peroxide (30% w/v, 154 µL, 1.50 mmol) dropwise over 1 min. The resulting solution was stirred at r. t. for 20 hours then washed with sat. aq. $NaHCO_3$ (2 × 15 mL) and brine (2 × 15 mL), dried ($MgSO_4$) and concentrated *in vacuo* to give **88** (1.01 g, 75%) as a white solid.

^{1}H NMR (300 MHz, $CDCl_3$) δ 7.71 – 7.41 (m 14H), 6.73 (dd, *J* = 17.6, 10.9, 1H), 5.84 (d, *J* = 17.6, 1H), 5.36 (d, *J* = 10.9, 1H); **^{13}C{^{1}H} NMR** (101MHz, $CDCl_3$) δ 141.1 (d, *J* = 2.9), 136.0 (d, *J* = 1.7), 132.7 (d, *J* = 104.2), 132.5 (d, *J* = 10.1), 132.2 (d, *J* = 9.9), 132.0 (d, *J* = 2.8), 131.7 (d, *J* = 105.2), 128.6 (d, *J* = 12.1), 126.3 (d *J* = 12.5), 116.7; **^{31}P{^{1}H} NMR** (121 MHz, $CDCl_3$) δ 28.8; **HRMS** (ESI$^+$) $C_{20}H_{18}P^+$ $[M+H]^+$ calcd. 305.1095, found 305.1091.

Monolithic triphenylphosphine oxide (**89**)

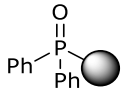

Batch procedure:

To a suspension of crushed monolithic triphenylphosphine (**53**) (720 mg, 1.43 mmol) in THF (5 mL) was added aqueous hydrogen peroxide (12.5% w/v, 0.86 mL, 3.2 mmol) dropwise over 5 min. The resulting suspension was stirred at r. t. for 24 hours. The reaction mixture was then filtered and washed sequentially with sat. aq. $NaHCO_3$ (10 mL), water (50 mL) and THF (50 mL). The resulting solid was dried *in vacuo* to give **89** (assumed quantitative) as a white solid.

Flow procedure:

Through a triphenylphosphine monolith (**53**) (1.11 g, 2.21 mmol) was circulated aqueous hydrogen peroxide (12.5% w/v, 30.0 mL, 110 mmol) continuously at r. t. for 18 hours. The monolith was then washed with acetone (100 mL) and DCM (30 mL) to give **89** (assumed quantitative) as a white solid.

^{13}C NMR (126MHz, solid state), δ 144.4, 131.4, 128.2, 40.5, 28.8, 16.8; **^{31}P NMR** (162 MHz, solid state) δ 25.2; **AT-IR** (neat) ν (cm^{-1}) 2920, 2850, 1599, 1484, 1436, 1405, 1195, 1117, 1070, 998, 827.

Monolithic chlorotriphenylphosphonium chloride (**91**)

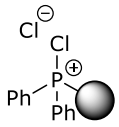

Batch procedure:

To a suspension of crushed monolithic triphenylphosphine oxide (**89**) (304 mg, 0.580 mmol) in $CHCl_3$ (5 mL) was added oxalyl chloride (75 µL, 0.88 mmol) dropwise over 1 min. The resulting suspension was stirred at r. t. for 1 hour. The reaction mixture was then filtered and washed with $CHCl_3$ (30 mL) before being dried *in vacuo* to give **91** (assumed quantitative) as a white solid. Product was used immediately without purification or further characterisation.

Flow procedure:

Through a triphenylphosphine oxide monolith (**89**) (1.13 g, 2.21 mmol) was circulated a solution of oxalyl chloride (280 µL, 3.32 mmol) in $CHCl_3$ (6 mL) at r. t. for 3 hours to give **91** as a white solid (assumed quantitative). Product was used immediately without purification or further characterisation.

AT-IR (neat) ν (cm^{-1}) 2924, 1600, 1482, 1435, 1406, 1312, 1119, 1065, 894, 824.

Monolithic Bis(2,2,2-trifluoroethoxy)triphenylphosphorane (**94**)

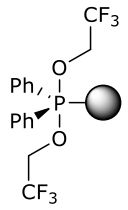

To a suspension of monolithic triphenylphosphine oxide (**89**) (417 mg, 0.800 mmol) in $CHCl_3$ (3 mL), in a Schlenk flask, was added oxalyl chloride over 1 min. The resulting suspension was stirred at r. t. for 15 hours. To a separate Schlenk flask was added 2,2,2-trifluoroethanol (106 μL, 1.47 mmol) and Et_2O (3 mL). The resulting solution was cooled to 0 °C and *n*-BuLi (1.6M in hexanes, 0.92 mL, 1.5 mmol) was added dropwise over 1 min. The resulting alkoxide solution was transferred *via* cannula to the above described, cooled (−78 °C) suspension of monolithic chlorotriphenylphosphonium chloride. The reaction mixture was stirred at −78 °C for 30 min then at r. t. for a further 48 hours. The reaction mixture was then filtered, washed with copious $CHCl_3$ and dried *in vacuo* to give **94** (assumed quantitative) as a white solid. Used *in situ* without purification or further characterisation.

AT-IR (neat) ν (cm^{-1}) 3564, 3367, 2919, 1632, 1576, 1485, 1576, 1485, 1437, 1277, 1183, 1146, 1118, 996, 846.

Monolithic 5-(*tert*-butyl)-2,2,2-triphenyl-2λ5-benzo[*d*][1,3,2]dioxaphospholane (**96**)

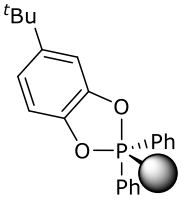

To a suspension of monolithic triphenylphosphine (**53**) (153 mg, 0.300 mmol) in dry toluene (2 mL), in a Schlenk flask, was added 4-*tert*-butyl-1,2-benzoquinone (99 mg, 0.60 mmol). The reaction mixture was stirred at r. t. for 24 hours to give **96** (assumed quantitative). Used *in situ* without purification or characterisation.

Monolithic 2,2,2-triphenyl-2λ5-phenanthro[9,10-*d*][1,3,2]dioxaphospholane (**97**)

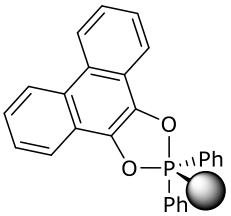

To a suspension of monolithic triphenylphosphine (**53**) (153 mg, 0.300 mmol) in dry toluene (3 mL), in a Schlenk flask, was added 9,10-phenanthrenequinone (63 mg, 0.30 mmol). The reaction mixture was heated to 70 °C for 72 hours to give **97** (assumed quantitative). Used *in situ* without purification or characterisation.

4-(Propyl)morpholine (**99**)[65]

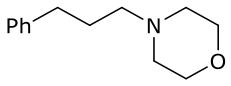

To a solution of **12** (435 mg, 0.920 mmol) in dry toluene (3 mL), in a Schlenk flask, was added 3-phenylpropanol (105 µL, 0.77 mmol) and morpholine (202 µL, 2.31 mmol). The resulting solution was stirred at r. t. for 24 hours. The reaction mixture was then extracted with 3 M HCl (3 × 10 mL). The combined aqueous layers washed with DCM (3 × 10 mL), basified with 50% NaOH (5 mL) and extracted with DCM (3 × 20 mL). The combined organic extracts were dried ($MgSO_4$) and concentrated *in vacuo* to give **99** (36 mg, 28 %) as a colourless oil.

^{1}H NMR (400 MHz, $CDCl_3$) δ 7.33 – 7.27 (m, 2H), 7.24 – 7.18 (m, 3H), 3.79 – 3.71 (m, 4H), 2.71 – 2.62 (m, 2H), 2.47 (m, 4H), 2.44 – 2.36 (m, 2H), 1.86 (m, 2H); **^{13}C{^{1}H} NMR** (101 MHz, $CDCl_3$) δ 142.1, 128.5, 128.5, 125.9, 67.1, 58.5, 53.8, 33.7, 28.3; **HRMS** (ESI^+) $C_{13}H_{20}NO^+$ $[M+H]^+$ calcd. 206.1539, found 206.1556.

1.6 References

1 L. D. Quin, *A guide to organophosphorus chemistry*, Wiley, 2000.

2 Y. Huang, A. M. Arif and W. G. Bentrude, *Phosphorus Sulfur Silicon Relat. Elem.*, 1995, **103**, 225–233.

3 G. A. Landrum, N. Goldberg and R. Hoffmann, *J. Chem. Soc. Dalton Trans.*, 1997, 3605–3613.

4 I. Ugi, D. Marquarding, H. Klusacek, P. Gillespie and F. Ramirez, *Acc. Chem. Res.*, 1971, **4**, 288–296.

5 S. Matsukawa, S. Kojima, K. Kajiyama, Y. Yamamoto, K. ya Akiba, S. Re and S. Nagase, *J. Am. Chem. Soc.*, 2002, **124**, 13154–13170.

6 E. L. Muetterties and R. A. Schunn, *Q. Rev. Chem. Soc.*, 1966, **20**, 245–299.

7 D. B. Denney and S. T. D. Gough, *J. Am. Chem. Soc.*, 1965, **87**, 138–139.

8 B. C. Chang, W. E. Conrad, D. B. Denney, D. Z. Denney, R. Edelman, R. L. Powell and D. W. White, *J. Am. Chem. Soc.*, 1971, **93**, 4004–4009.

9 D. B. Denney and L. Saferstein, *J. Am. Chem. Soc.*, 1966, **88**, 1839–1840.

10 P. L. Robinson, C. N. Barry, S. W. Bass, S. E. Jarvis and S. A. E. Jr., *J. Org. Chem.*, 1983, **48**, 5396–5398.

11 J. W. Kelly, N. L. Anderson and S. A. Evans, *J. Org. Chem.*, 1986,

51, 95–97.

12 P. L. Robinson, S. A. Evans and J. W. Kelly, *Phosphorus Sulfur Relat. Elem.*, 1986, **26**, 15–24.

13 J. W. Kelly, P. L. Robinson and S. A. Evans, *J. Org. Chem.*, 1986, **51**, 4473–4475.

14 I. Mathieu-Pelta and S. A. Evans, *J. Org. Chem.*, 1994, **59**, 2234–2237.

15 J. W. Kelly and S. A. Evans, *J. Org. Chem.*, 1986, **51**, 5490–5492.

16 T. Kubota, T. Kitazume and N. Ishikawa, *Chem. Lett.*, 1978, **7**, 889–892.

17 Y. Zhao and J. Hu, *Angew. Chem. Int. Ed.*, 2012, **51**, 1033–1036.

18 T. Kubota, S. Miyashita, T. Kitazume and N. Ishikawa, *J. Org. Chem.*, 1980, **45**, 5052–5057.

19 T. Fukuyama, C. K. Jow and M. Cheung, *Tetrahedron Lett.*, 1995, **36**, 6373–6374.

20 X. Tang, C. Chapman, M. Whiting and R. Denton, *Chem. Commun.*, 2014, **50**, 7340.

21 A. F. Abdel-Magid, K. G. Carson, B. D. Harris, C. A. Maryanoff and R. D. Shah, *J. Org. Chem.*, 1996, **61**, 3849–3862.

22 J. S. Carey, D. Laffan, C. Thomson and M. T. Williams, *Org. Biomol. Chem.*, 2006, **4**, 2337–2347.

23 C. C. Marvin, in *Comprehensive Organic Synthesis: Second Edition*, Elsevier, 2014, vol. 6, pp. 34–99.

24 M. H. S. A. Hamid, P. A. Slatford and J. M. J. Williams, *Adv. Synth. Catal.*, 2007, **349**, 1555–1575.

25 T. D. Nixon, M. K. Whittlesey and J. M. J. Williams, *Dalton Trans.*, 2009, 753–762.

26 Y. Watanabe, Y. Morisaki, T. Kondo and T. Mitsudo, *J. Org. Chem.*, 1996, **61**, 4214–4218.

27 K. C. K. Swamy, N. N. B. Kumar, E. Balaraman and K. V. P. P. Kumar, *Chem. Rev.*, 2009, **109**, 2551–2651.

28 B. H. Yang and S. L. Buchwald, *J. Organomet. Chem.*, 1999, **576**, 125–146.

29 P. Ruiz-Castillo and S. L. Buchwald, *Chem. Rev.*, 2016, **116**, 12564–12649.

30 R. Dorel, C. P. Grugel and A. Haydl, *Angew. Chem. Int. Ed.*, 2019, **58**, 17118–17129.

31 D. S. Surry and S. L. Buchwald, *Chem. Sci.*, 2011, **2**, 27–50.

32 J. F. Hartwig, *Angew. Chem. Int. Ed.*, 1998, **37**, 2046–2067.

33 S. D. Roughley and A. M. Jordan, *J. Med. Chem.*, 2011, **54**, 3451–3479.

34 M. K. W. Choi, H. S. He and P. H. Toy, *J. Org. Chem.*, 2003, **68**, 9831–9834.

35 D. H. Valentine Jr. and J. H. Hillhouse, *Synthesis*, 2003, 317–334.

36 G. L. Thomas, C. Böhner, M. Ladlow and D. R. Spring, *Tetrahedron*, 2005, **61**, 12153–12159.

37 D. Braun, *Angew. Chem.*, 1961, **73**, 197–208.

38 S. V. McKinley and J. W. Rakshys, *J. Chem. Soc. Chem. Commun.*, 1972, 134–135.

39 M. Guinó and K. K. Hii, *Chem. Soc. Rev.*, 2007, **36**, 608–617.

40 F. Svec and J. M. J. Frechet, *Anal. Chem.*, 1992, **64**, 820–822.

41 R. D. Arrua, M. C. Strumia and C. I. A. Igarzabal, *Materials (Basel).*, 2009, **2**, 2429–2466.

42 M. R. Buchmeiser, *Polymer (Guildf).*, 2007, **48**, 2187–2198.

43 S. Kovačič, D. Štefanec and P. Krajnc, *Macromolecules*, 2007, **40**, 8056–8060.

44 A. Y. Sergienko, H. Tai, M. Narkis and M. S. Silverstein, *J. Appl. Polym. Sci.*, 2004, **94**, 2233–2239.

45 C. D. C. J. Smith, C. D. C. J. Smith, N. Nikbin, S. V. Ley and I. R. Baxendale, *Org. Biomol. Chem.*, 2011, **9**, 1927–1937.

46 D. Webb and T. F. Jamison, *Chem. Sci.*, 2010, **1**, 675–680.

47 R. L. Hartman, J. P. McMullen and K. F. Jensen, *Angew. Chem. Int. Ed.*, 2011, **50**, 7502–7519.

48 J. Wegner, S. Ceylan and A. Kirschning, *Adv. Synth. Catal.*, 2012, **354**, 17–57.

49 I. R. Baxendale, J. Deeley, C. M. Griffiths-Jones, S. V. Ley, S. Saaby and G. K. Tranmer, *Chem. Commun.*, 2006, **61**, 2566.

50 R. I. Storer, T. Takemoto, P. S. Jackson and S. V. Ley, *Angew.*

Chem. Int. Ed., 2003, **42**, 2521–2525.

51 K. A. Roper, M. B. Berry and S. V. Ley, *Beilstein J. Org. Chem.*, 2013, **9**, 1781–1790.

52 W. Xu, R. Mohan and M. M. Morrissey, *Bioorganic Med. Chem. Lett.*, 1998, **8**, 1089–1092.

53 S. V. Ley, M. H. Bolli, B. Hinzen, A.-G. Gervois and B. J. Hall, *J. Chem. Soc. Perkin Trans. 1*, 1998, **266**, 2239–2242.

54 P. Lan, J. A. Porco, M. S. South and J. J. Parlow, *J. Comb. Chem.*, 2003, **5**, 660–669.

55 J. W. Kelly, P. L. Robinson and S. A. Evans Jr., *J. Org. Chem.*, 1985, **50**, 5007–5009.

56 D. V. Moiseev, B. O. Patrick, B. R. James and T. Q. Hu, *Inorganica Chim. Acta*, 2010, **363**, 3569–3574.

57 G. Boekestein and H. M. Buck, *Phosphorus Sulfur Relat. Elem.*, 1978, **5**, 61–66.

58 R. Koeck, M. Fischnaller, R. Bakry, R. Tessadri and G. K. Bonn, *Anal. Bioanal. Chem.*, 2014, **406**, 5897–5907.

59 A. Shannon-Little, PhD thesis, Univerity of Nottingham, 2013.

60 S. E. Hunter, C. E. Ehrenberger and P. E. Savage, *J. Org. Chem.*, 2006, **71**, 6229–6239.

61 K. Narinderpal, N. Junaid and B. Raman, *Res. Rev. J. Bot. Sci.*, 2013, **2**, 1–9.

62 M. Al-Ghorbani, A. Bushra Begum, Z. Zabiulla, S. V. Mamatha and S.

A. Khanum, *Res. J. Pharm. Technol.*, 2015, **8**, 611–628.

63 Z. Huang and J. P. Lumb, *Angew. Chem. Int. Ed.*, 2016, **55**, 11543–11547.

64 T. Fu, H. Qiao, Z. Peng, G. Hu, X. Wu, Y. Gao and Y. Zhao, *Org. Biomol. Chem.*, 2014, **12**, 2895–2902.

65 C. A. Goooodman, E. M. Janci, O. Onwodi, C. C. Simpson, C. G. Hamaker and S. R. Hitchcock, *Tetrahedron Lett.*, 2015, **56**, 4468–4471.

Chapter 2: Convergent Synthesis of Azetidines

1.1 Abstract

Chapter two focuses on work towards an unprecedented, single step, convergent synthesis of azetidines from isoxazolidines. Attempts to achieve this goal using phosphorus-based methodology similar to chapter one are described. Subsequent work exploits an alternative reductive system using phenylsilane as the reductant, in combination with $[Ir(COD)Cl]_2$ as a catalyst. Preliminary optimisation studies ultimately furnished the model azetidine product in 41% yield. Preparation of ten isoxazolidines and the successful ring contraction of five of these is described. Mechanistic investigations elucidate the role of an amino alcohol in the process. Furthermore, the substrate controlled stereospecificity is established.

1.2 Introduction

1.2.1 Applications of Azetidines

Azetidine (**2**) was first synthesised in 1888 by Gabriel and Weiner.[1] The treatment of 3-bromopropan-1-amine (**1**) with sodium hydroxide was found to produce a small quantity of the novel heterocycle (Scheme 1).

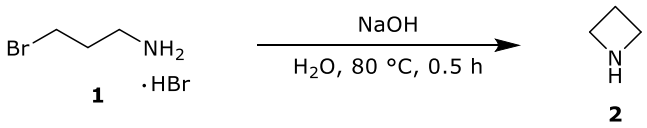

*Scheme 1: First synthesis of azetidine (**2**), via* the *base treatment of a γ-bromoamine (**1**).[1] Note: Reaction yield not specified.*

Since these early beginnings azetidines have been established as important structures across a number of fields. (*S*)-Azetidine-2-carboxylic acid (**3**) is a non-proteinogenic amino acid known to act as a plant growth regulator (Scheme 2).[2,3] First isolated from Convallaria Majalis (lily of the valley) in 1955, derivatives of **3** have since found use within the agrochemical industry.[4] 2-(Azetidinyl)oxoacetates such as **4** have been shown to be effective growth regulators for the production of rice (Scheme 2).[5] Additionally, a number of derivatives of **3** have found use as chemical hybridizing agents to induce sterilization of male plants (**5**[6], **6**[7] and **7**[8] Scheme 2).

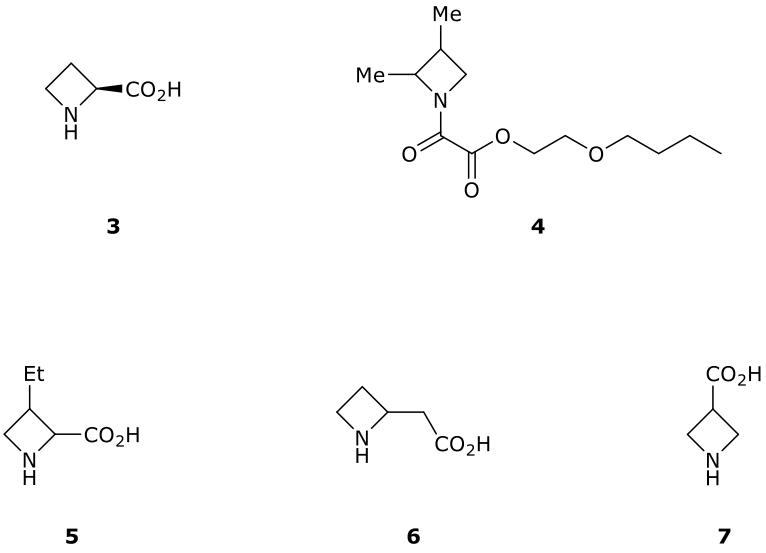

Scheme 2: Azetidines of agrochemical interest.

Derivatives of **3** have also found use in the field of pharmaceuticals. Perhaps most notable of these is Ximelagatran (**8**, also known as Exanta), a prodrug of melagatran (**9**), which was a commercialised thrombin inhibitor from Astrazeneca (Scheme 3).[9]

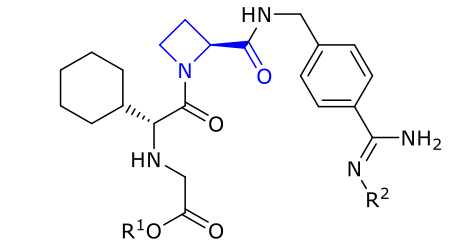

*Scheme 3: Thrombin inhibitor Melagatran (**9**) and its prodrug form Xiemelagatran (**8**).*

The azetidine carboxylic acid core is also present in **11**, an adduct of the natural product geldanamycin (**10**) and **3** (Scheme 4).[10] Inhibition of P185 phosphotyrosine in human breast cancer cells was successfully demonstrated using **11**. Interestingly in this case, a derivative of

geldanamycin with an unsubstituted azetidine (**12**) exhibited a lower IC_{50} than both **11** and geldanamycin itself. Thus, demonstrating the application of azetidine fragments in drug discovery extends beyond their use as an amino acid homologue.

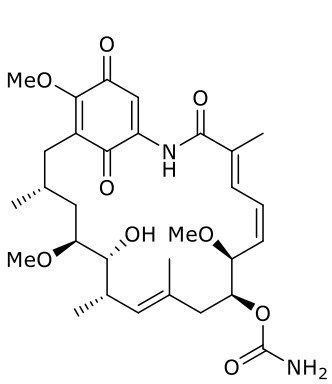

10: Geldanamycin

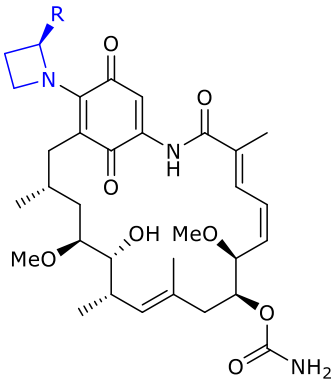

11: R = COOH
12: R = H

*Scheme 4: Geldanamycin (**10**) and its azetidine-containing derivatives (**11** and **12**).*

Whilst there is not a plethora of natural products containing the azetidine moiety, a number with pharmacological activity are known. Isolated from the marine sponge *Penares* sp., penaresidin A and B (**13** and **14** respectively) have been shown to exhibit potent activity as actomyosin ATPase activators (Scheme 5).[11]

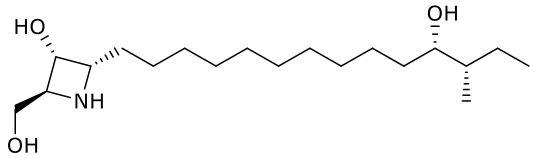

13: Penaresidin A

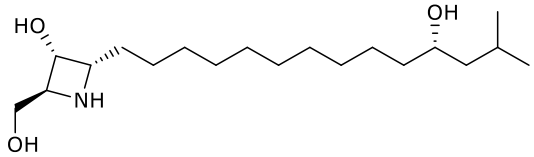

14: Penaresidin B

*Scheme 5: Marine sponge natural products penaresidin A (**13**) and B (**14**).*

Perhaps the most complex azetidine alkaloid found to date is calydaphninone (**15**), isolated in 2007 from the east Asian tree *Daphniphyllum calycillum (*Scheme 6*)*.[12] Whilst **15** has to date not been shown to exhibit any bioactivity, it represents a significant synthetic challenge.

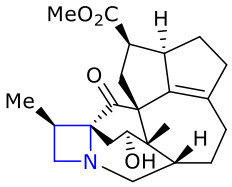

15: Calydaphninone

*Scheme 6: Azetidine-containing alkaloid calydaphninone (**15**).*

Another important application of azetidines is within the field of asymmetric catalysis, as both organocatalysts and ligands. The seminal paper by List on proline-catalysed direct asymmetric aldol reactions demonstrated that 2-azetidine carboxylic acid (**3**) was an effective catalyst, albeit inferior to its five membered analogue.[13]

The azetidine-tethered ferrocene catalyst **18** developed by Wang and co-workers has been shown to be highly effective for asymmetric addition reactions of aldehydes (Scheme 7).[14] Notably the structure of the tethered azetidine is closely related to proline.

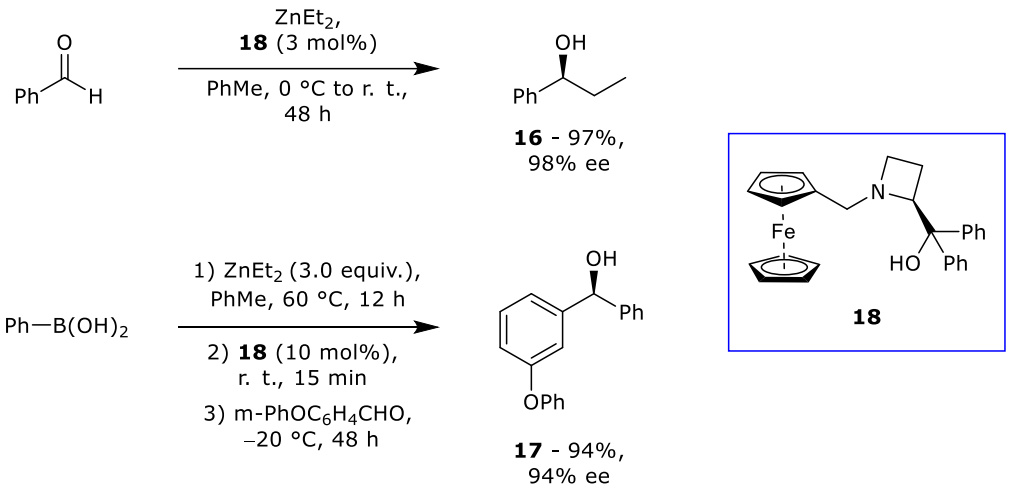

*Scheme 7: Example asymmetric alkylation and arylation reactions catalysed by ferrocene **18**.[14] Note: Reaction equivalents of $ZnEt_2$ not specified for preparation of **16**.*

Suzuki reactions have also been catalysed by azetidine-containing catalysts.[15] A number of bidentate azetidine-containing ligands, such as that used in **19**, were used to perform Suzuki couplings with great efficacy. High yields were obtained with low catalyst loadings (Scheme 8).

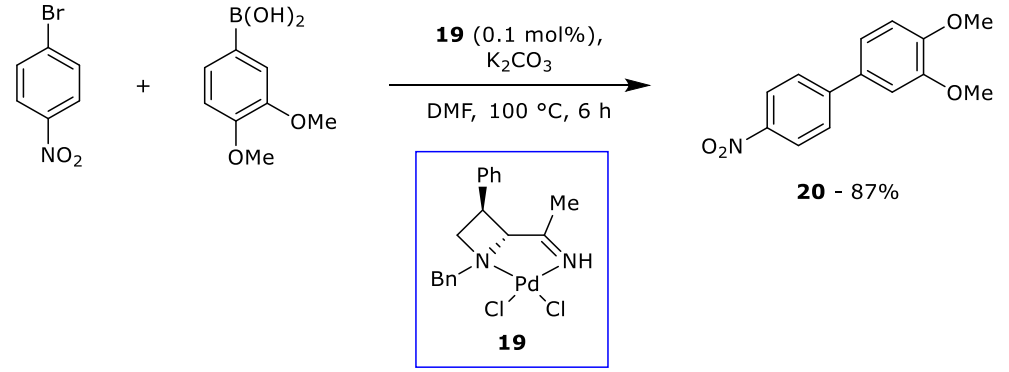

*Scheme 8: Use of an azetidine ligand-containing palladacycle precatalyst (**19**) in a Suzuki coupling.[15]*

1.2.2 Synthesis of Azetidines

1.2.2.1 Cyclisations by the nucleophilic attack of amines

By far the most common method for the synthesis of azetidines is the nucleophilic displacement of a leaving group with an amine.[16] This leaving group can be a halide as demonstrated in the first synthesis of azetidine by Gabriel and Weiner (Scheme 1).[1] Chlorides[17], bromides[18] and iodides[19] have all been used to good effect with secondary amines. The use of pseudo-halides such as tosylates[20] and mesylates[21] is also prevalent as a means of accessing azetidines *via* γ-aminoalcohols.

Addition of a primary amine to a 1,3-dielectrophile is another common method of accessing azetidines (Scheme 9).[22] This is a valuable method for constructing 1,3-substituted azetidines from easily prepared starting materials.

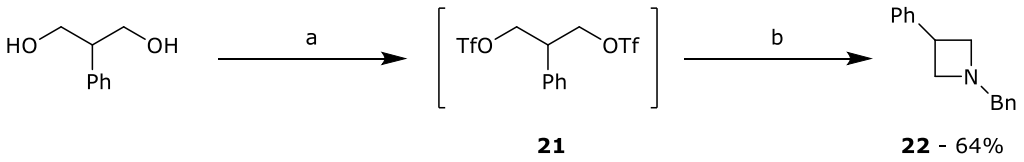

21 **22** - 64%

*Scheme 9: Synthesis of azetidine **22** from a 1,3-dielectrophile (**21**).[22] Reagents and conditions a) Tf_2O, DIEA, MeCN, −20 °C, 30 min; b) $BnNH_2$, DIEA, MeCN, 70 °C, 2 h, 64% (over two steps).*

For both the displacement of mono and di-halides, competing side reactions such as dimerization, polymerization, fragmentation and elimination are the major drawback.[23] Success of the reaction is heavily dependent on the nature of the substrate. An example of this is shown in Scheme 10, where only 14% of the desired product (**23**) was formed, with polymerization consuming the majority of the starting material.[24] Isolation

of the dimer (**24**) in 22% and the tetramer (**25**) in 2% yields supported this explanation.

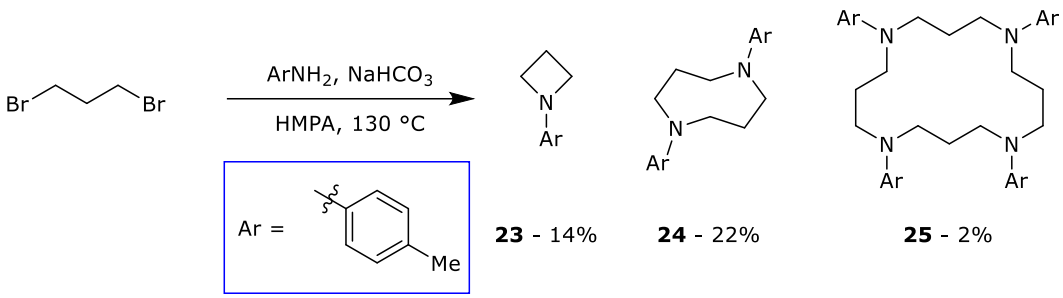

*Scheme 10: Addition of an amine to 1,3-dibromopropane generates an azetidine (**23**) and side-products **24** and **25**.*[24]

1.2.2.2 Nucleophilic attack of amines to α-haloepoxides

Another method for the synthesis of azetidines utilises α-haloepoxides. This method is effectively an extension of the previously mentioned strategy, the γ-haloamine is formed *in situ* from the nucleophilic attack of an amine to the primary epoxide. Subsequent cyclisation, as for the aforementioned method, allows the formation of azetidines in a single step. This protocol was first described by Gaertner in 1967 where a range of amines were used with epichlorohydrin (Scheme 11).[25] Low yields and long reaction times are the main drawback of this method.

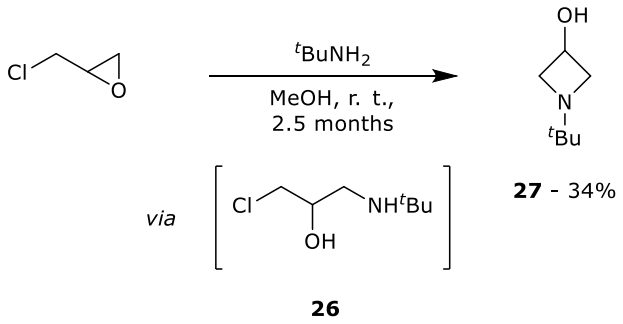

*Scheme 11: Example synthesis of azetidine **27** from epichlorohydrin via the γ-haloamine **26**.*[25]

Moreover, γ-haloamines are often isolable and in some instances better yields are obtained if they are isolated prior to ring closure.[23] Consequently, this negates one of the primary advantages of this method over that described in section 1.2.2.1.

1.2.2.3 Cyclisations of β-chloroimines

β-chloroimines (**28**) can also be used as precursors to azetidines. For this to occur a suitable nucleophile is used to attack the imine, subsequently allowing cyclisation *via* displacement of chloride (Scheme 12). Examples of nucleophiles that can be used include cyanide,[26] hydride[26] and methoxide[27] ions as well as organolithiums.[28] Isolation of the azetidines obtained from the use of methoxide was only possible in the case of aryl substituted imines, however.

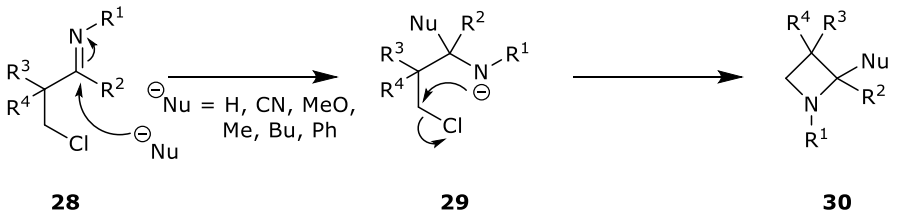

28 **29** **30**

*Scheme 12: Mechanism for the synthesis of azetidine (**30**) from the cyclisation of a β-chloroimine (**28**).*[26–28]

Whilst this method can be used to afford a range of azetidines in good yields, it is not without disadvantages. Perhaps most significant of these is the necessity for geminal alkyl substituents in the α-position of the imine, greatly reducing the scope of the reaction. Furthermore, synthesis of β-chloroimines is non-trivial and thus extends the route from commercially available materials to products.

1.2.2.4 C-C bond formation by halide displacement

Displacement of a halide with a carbanion in the α-position, relative to the amine, is another route to azetidines. One advantage of this method is the direct integration of a tertiary amine into the azetidine core. The carbanion is formed as an enolate, using a tethered ester, by deprotonation with a strong base. Bouzas and co-workers employed this strategy towards the synthesis of enantiopure (*S*) and (*R*)-azetidine-2-carboxylic acid (**3** and **34** respectively) (Scheme 13).[29] Deprotonation using LiHMDS allowed cyclisation to occur giving a mixture of two diasteromers (**32** and **33**). Separation of these diastereomers and subsequent hydrogenolysis gave both products as single enantiomers.

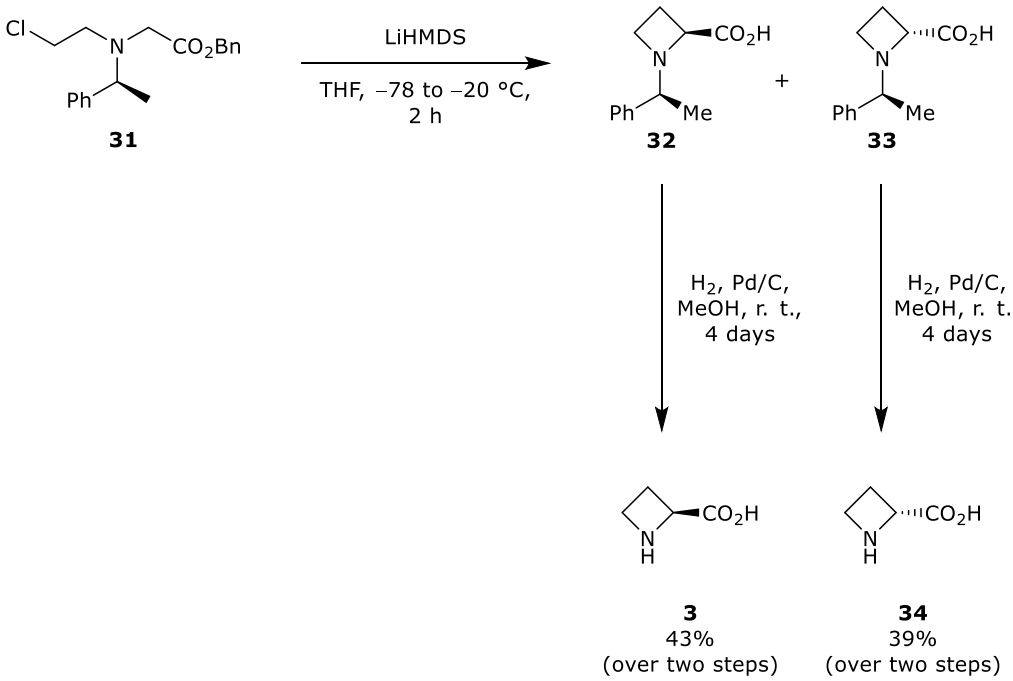

*Scheme 13: Use of the enolate C-C bond formation protocol towards the synthesis of (S) and yntyn-azetidine-2-carboxylic acid (**3** and **34** respectively).[29]*

The two primary drawbacks to this method lie in the structure of the starting material required. Firstly, the necessity of the tethered ester for

the generation of the anion results in an ester/acid present in the product which may not be desired. Secondly, whilst the direct incorporation of a tertiary amine into the azetidine product may sometimes be desirable, often it will not be. Consequently, extra steps will be added to the synthesis to install and remove a protecting group, as secondary amines are not tolerated in this method. Furthermore, a strong base is required to form the enolate, reducing functional group tolerance.

1.2.2.5 Reduction of β-lactams

The prevalence of β-lactams and their ease of synthesis make them a good starting material for the synthesis of azetidines. As a result, reduction of the carbonyl in β-lactams is one of the more common protocols chosen. Choice of reducing agent is of great importance, with some substrates being susceptible to ring-opening and formation of 3-aminopropanol derivatives. $LiAlH_4$, diborane, $NaBH_4/AlCl_3$ and Raney Nickel are all incompatible for this very reason.[23] However, the use of alternative reducing agents such as monochlorohydroalane, dichloroalane and diisobutyl aluminum hydride allows the synthesis of azetidines without breaking the ring. An example of this is shown in Scheme 14 where monochlorohydroalane was used to synthesise azetidine **36** without loss of enantiopurity.[30]

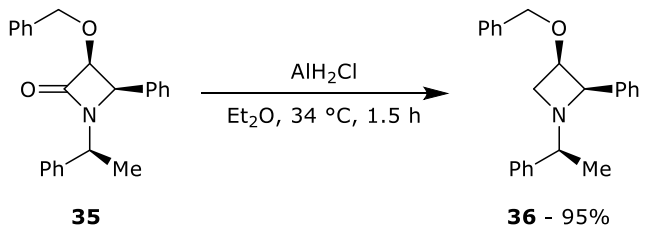

35 **36** - 95%

*Scheme 14: Reduction of β-lactam (**35**) without loss of enantiopurity using monochlorohydroalane.[30]*

Even with the use of the aforementioned milder reducing agents, a lack of functional group tolerance is the primary drawback of these reactions. As a result, reduction of β-lactams is not always suitable for the construction of complex azetidines bearing sensitive functionality.

1.2.2.6 [2+2] cycloadditions

Cycloadditions are an attractive route to azetidines being both convergent and atom economical. Unfortunately, relatively few examples are known. Whilst these examples can be high yielding and selective, they are often very substrate specific. An example of this [2+2] cycloaddition method is shown in Scheme 15 where the highly substituted azetidine **39** was synthesised in excellent yield and stereoselectivity.[31]

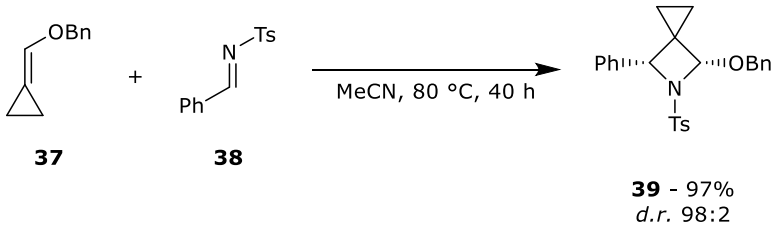

*Scheme 15: Synthesis of azetidine **39*** via a [2+2] cycloaddition.[31]

However, inclusion of the cyclopropane group in the substrate (which was hypothesized to stabilize the intermediate zwitterion) was necessary to avoid the use of more forcing conditions. Without a cyclopropane substituent, Aben and co-workers were forced to use elevated pressure of 14 kPa in their earlier study on the [2+2] reaction between imines and electron rich alkenes.[32]

1.2.2.7 Ring contractions

Conversion of larger rings into azetidines is another means of accessing the azetidine moiety. This is a particularly good method when the starting ring is itself easy to synthesise. Vinyl cyclic carbamates (**40**) have been shown to decarboxylate in the presence of a palladium catalyst, yielding azetidines with good levels of diastereoselectivity (Scheme 16).[33]

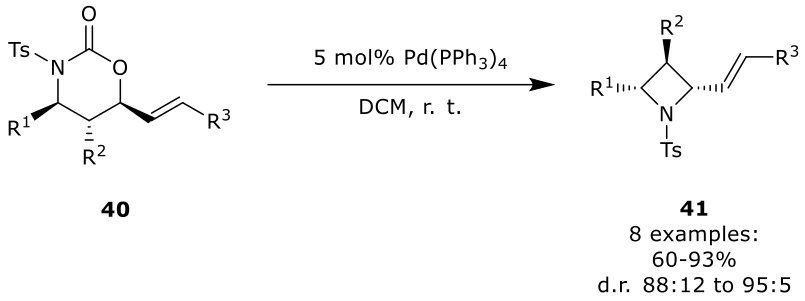

40 **41**
8 examples:
60-93%
d.r. 88:12 to 95:5

*Scheme 16: Catalytic decarboxylation of vinyl cyclic carbamates (**40**) for the synthesis of azetidines (**41**).[33]*

The starting ring system **40** is readily prepared from 1,3-aminoalcohols, thus it can be seen as an alternative strategy to that outlined in section 1.2.2.1. Whilst this is a good strategy to access these high value targets, it is not a general method. Additionally, it ultimately offers another linear approach from a well-known precursor.

Rearrangement of a larger ring has been shown as a good means to access specific, complex, azetidine-containing ring systems. Shown in Scheme 17 is a particularly elegant synthesis of an azetdidine-containing tricyclic ring system (**47** and **48**), wherein the key step is a 6π electrocyclic ring closure from the 8-membered ring (**46**).[34]

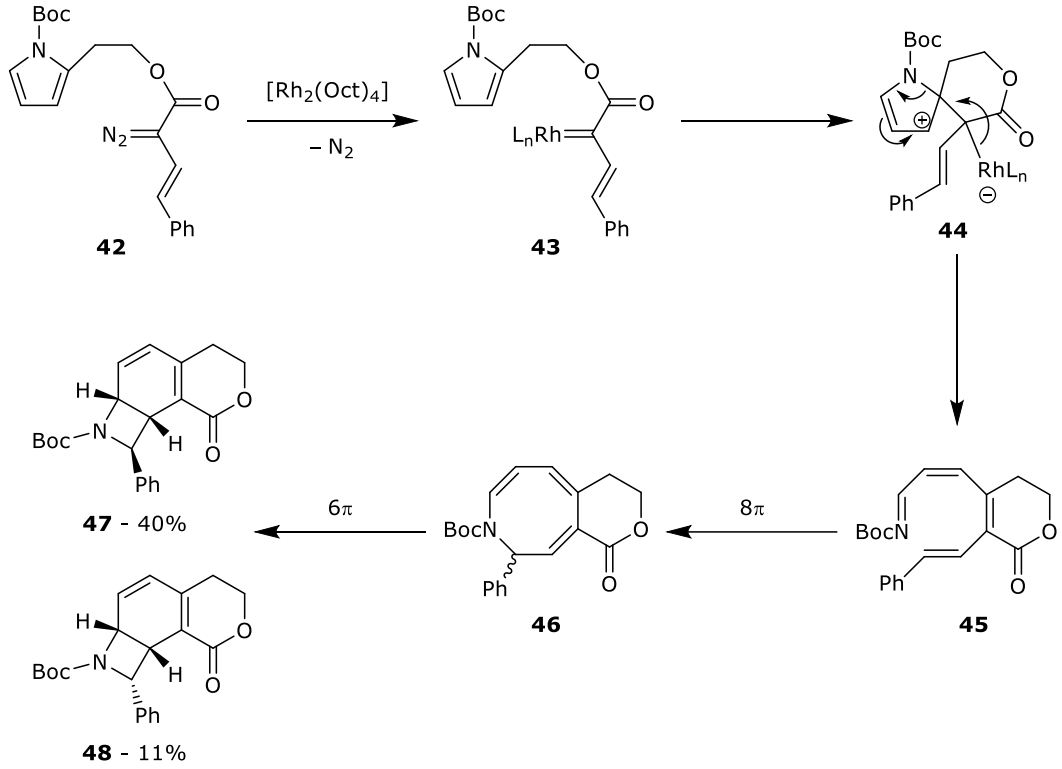

*Scheme 17: Proposed mechanism for the synthesis of the azetidine-containing tricyclic structures **47** and **48**.*[34]

1.2.3 Project Aims

As shown in section 1.2.2, synthesis routes to azetidines almost exclusively rely upon linear strategies. Given that linear synthesis routes are inherently less practical and efficient than convergent ones, development of a novel convergent strategy would be a valuable addition to the field.

To this end we envisaged a convergent method *via* the proposed reductive ring contraction of an isoxazolidine (**51**) (Scheme 18). A single step transformation of an isoxazolidine to an azetidine (**52**), such as this, is unprecedented in the literature. Isoxazolidines (**51**) can be readily obtained *via* the [3+2] cycloaddition of a nitrone (**49**) and alkene (**50**). The versatility of these reactions is very well developed.[35]

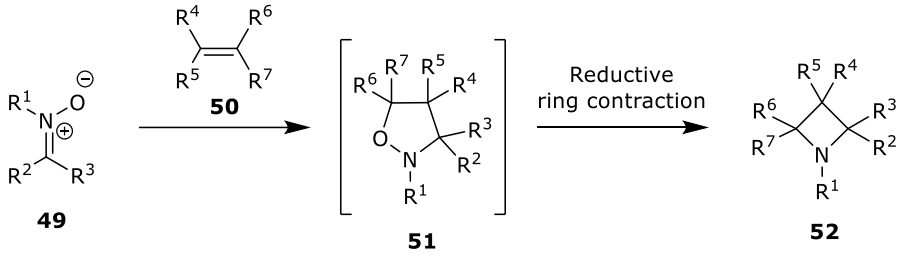

*Scheme 18: Proposed general scheme for the convergent synthesis of azetidines (**52**) via a ring contraction of an isoxazolidine (**51**).*

If a suitable reductive system can be developed to perform this desired ring contraction, a valuable synthesis strategy will be obtained, wherein the azetidine is ultimately formed from a nitrone and azetidine fragment (Scheme 19).

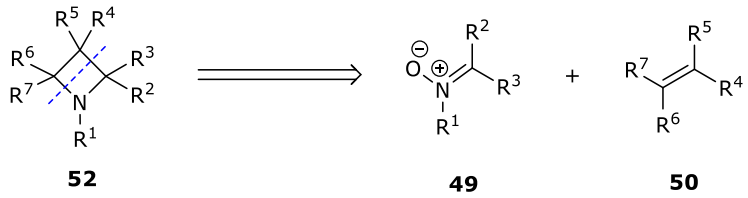

*Scheme 19: Disconnection of an azetidine (**52**) to give a nitrone (**49**) and alkene (**50**) fragment.*

1.3 Results and Discussion

1.3.1 Model Substrate Synthesis

To begin our investigations, we first needed a suitable model substrate and *cis*-2,3,5-triphenylisoxazolidine (**53**) was chosen for three main reasons.

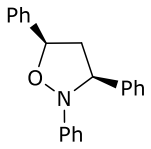

53

*Scheme 20: Structure of cis-2,3,5-triphenylisoxazolidine (**53**), the chosen model substrate for these investigations.*

Firstly, substitution at the 3 and 5 positions of the ring with a single diastereomer would allow us to explore the retention/inversion of these positions, which neighbour the heteroatom bond to be broken. Secondly, synthesis of **53** (purely as the *cis*-diastereomer) can be achieved through the combination of three high yielding literature procedures. Finally, the starting materials required to synthesise **53** (nitrobenzene, benzaldehyde and styrene) are readily available and inexpensive.

The synthesis began with the reduction of nitrobenzene using hydrazine monohydrate and rhodium on carbon to from *N*-phenylhydroxylamine (**54**) (Scheme 21). Condensation of **54** with benzaldehyde in ethanol gave the desired nitrone (**55**) in 82% yield. The final step, of central importance to this strategy, was the 1,3-dipolar cycloaddition between **55** and styrene. This was achieved with the single *cis*-diastereomer (**53**) being obtained in 89% yield, giving a combined yield of 46% over three steps.

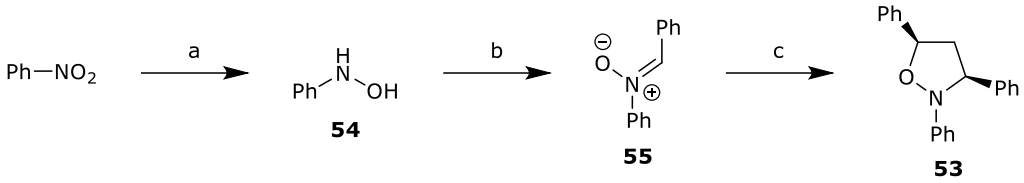

*Scheme 21: Synthesis of the model substrate **53**. Reagents and conditions a) $N_2H_4.H_2O$, Rh/C, THF, 0 °C to r. t., 3 h, 63%; b) PhCHO, EtOH, r. t., 18 h, 82%; c) $PhCHCH_2$, 60 °C, 40 h, 89%, >99:1 dr.*

With our model substrate in hand we began to explore the hypothesised, unprecedented, reductive ring contraction.

1.3.2 Phosphorus-Mediated Ring Contractions

1.3.2.1 Theoretical Basis for Experiments

As was discussed in chapter one it is well established that phosphines can undergo oxidative addition with peroxides to form dioxyphosphoranes (Chapter 1, Scheme 5). Additionally, dioxyphosphoranes can collapse to give ethers with the phosphine being oxidised. With this in mind, it was theorised that a phosphine could be used to insert into the nitrogen-oxygen single bond of an isoxazolidine. If this is indeed the case, then the relevant phosphorane intermediate (**61**) for the cyclodehydration of an amino alcohol could be formed (Scheme 22). This therefore represents an interception of the pathway used by Evans and co-workers for the synthesis of cyclic amines.[36]

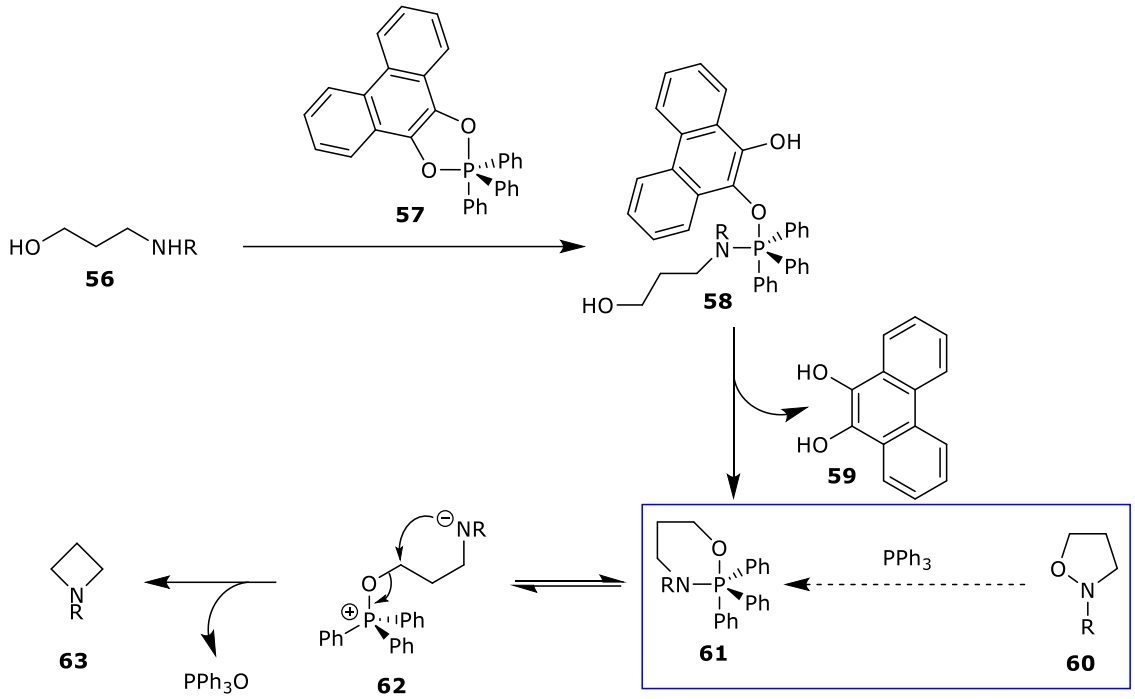

*Scheme 22: Mechanism for the dioxyphosphorane-mediated cyclodehydration of a 1,3-amino alcohol and the proposed interception of intermediate **61** via insertion of a phosphine into an isoxazolidine.*

1.3.2.2 Phosphorus-Mediated Ring Contraction of the Model Substrate

The model substrate (**53**) was heated with triphenylphosphine and tributylphosphine at reflux in three different solvents (Table 1). In all cases none of the desired azetidine product (**64**) was observed. For the reactions in DCM and toluene (Table 1 entries 1-2 and 4-5 respectively) no consumption of the starting material (**53**) was observed. In contrast to this, when reactions were performed at 150 °C in tetrachloroethane (TCE), consumption of **53** was observed. In the case of tributylphosphine (Table 1 entry 6), this was in the form of decomposition to a complex mixture of products. However, when triphenylphosphine was used the amino alcohol **65** was observed in 74% conversion (Table 1 entry 3).

*Table 1: Initial trialled conditions for the phosphine-mediated synthesis of azetidine **64**.*

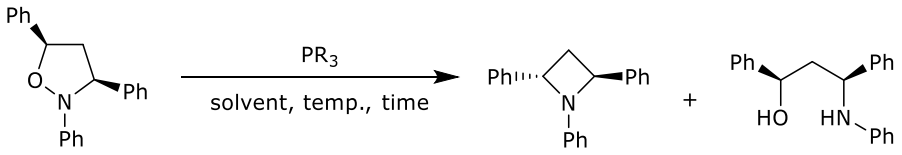

53 **64** **65**

Entry	R	Solvent	Temp. / °C	Time / h	Product distribution / %[a]		
					53	**64**	**65**
1	Ph	DCM	40	24	100	0	0
2	Ph	PhMe	110	24	100	0	0
3	Ph	TCE	150	1	26	0	74
4	Bu	DCM	40	24	100	0	0
5	Bu	PhMe	110	24	100	0	0
6	Bu	TCE	150	1	Decomposition		

[a]*Product distribution determined by ^{1}H NMR spectroscopy.*

A control experiment was performed which confirmed that this formation of **65** was due to the phosphine, not the result of a simple thermally induced ring-opening (Scheme 23).

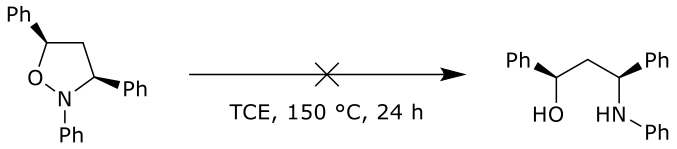

53 **65**

*Scheme 23: Control experiment for the possible thermally induced ring-opening of **53**.*

Therefore, it can be seen that the phosphine is successfully breaking the intended bond, albeit not with the desired product resulting. This is most likely due to one of two possible explanations. Firstly, the azetidine product (**64**) is forming but is unstable to the harsh reaction conditions, consequently ring-opening to give the amino alcohol **65**. Alternatively, the

desired phosphorane intermediate **61** is being successfully intercepted but cannot collapse to give the product or is outcompeted by hydrolysis. In both instances, triphenylphosphine oxide would be produced as a co-product, which is indeed observed by ^{31}P NMR spectroscopy in all cases where **65** is formed. For either of these theories to be true, adventitious water must be present in the reaction, despite anhydrous conditions being employed.

In an attempt to overcome potential product instability a screen of reaction temperatures was performed (Table 2).

*Table 2: Screen of reaction temperature for the attempted triphenylphosphine-mediated ring contraction of **53**.*

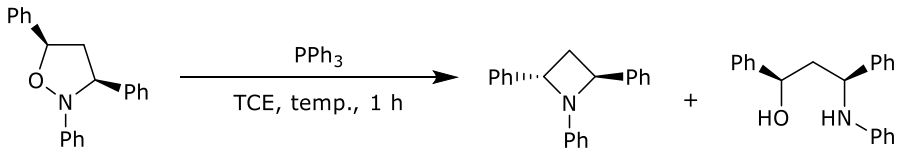

53 **64** **65**

Entry	Temp. / °C	Product Distribution / %[a]		
		53	**64**	**65**
1	60	91	0	9
2	80	81	0	19
3	100	76	0	24
4	120	55	0	45
5	150	26	0	74

[a]Product distribution determined by ^{1}H NMR spectroscopy.

Unfortunately, no product was observed in any of these reactions. Instead, the amino alcohol **65** was observed in increased amounts as the temperature was raised. To determine the cause of these observations, we returned to the dioxyphosphorane chemistry described in chapter one to directly access the proposed phosphorane intermediates.

1.3.2.3 Cyclodehydration of 1,3-Aminoalcohol Derived Dioxyphosphoranes

Dioxyphosphorane-mediated cyclodehydrations of diols have been developed to give cyclic ethers of ring sizes three to six (inclusive).[37] However, for cyclic amines only ring sizes of three and six have been demonstrated.[36] Therefore, in order to assess the feasibility of the phosphine-mediated reduction of **53**, we returned to the dioxyphosphorane chemistry described in chapter 1.

To this end, preparation of 3-(phenylamino)propan-1-ol (**66**) was achieved, in 91% yield using a literature procedure, to give a 1,3-aminoalcohol to use (Scheme 24).[38]

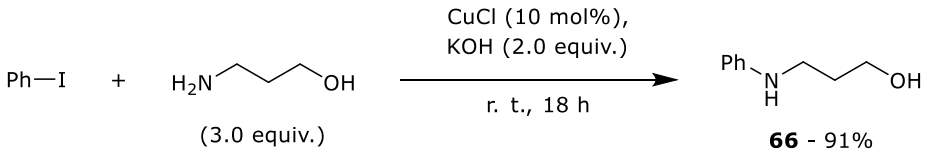

*Scheme 24: Synthesis of 1,3-aminoalcohol **66**.*

Subsequently, the desired cyclodehydration of **66**, to form the azetidine **67**, was explored using dioxyphosphorane **57** (Scheme 25).

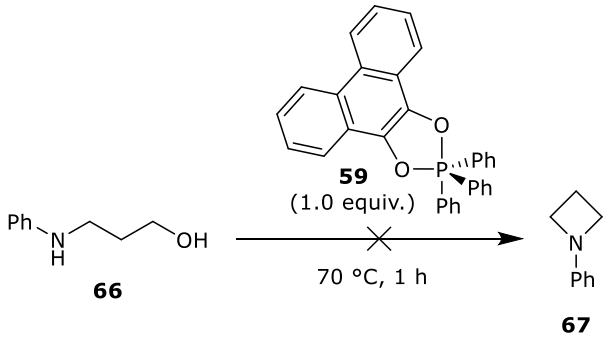

*Scheme 25: Unsuccessful cyclodehydration of **66** to give azetidine **67**.*

Full conversion of the dioxyphosphorane (**59**) to triphenylphosphine oxide was observed by ^{31}P NMR spectroscopy. However, no formation of the azetidine product (**67**) occurred. Instead a mixture of the two aromatic ethers (**68** and **69**) was observed by ^{1}H NMR spectroscopy and were subsequently isolated (Scheme 26).

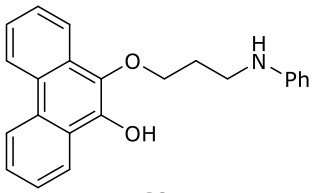

68

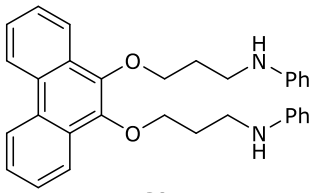

69

*Scheme 26: Aromatic ethers **68** and **69** formed from the failed cyclodehydration of **66**.*

There are two differences between the model isoxazolidine (**53**) and the amino alcohol *N*-Benzylethanolamine (**70**), used successfully in the synthesis of *N*-phenylaziridine (**71**) (Scheme 27, as described in chapter one).

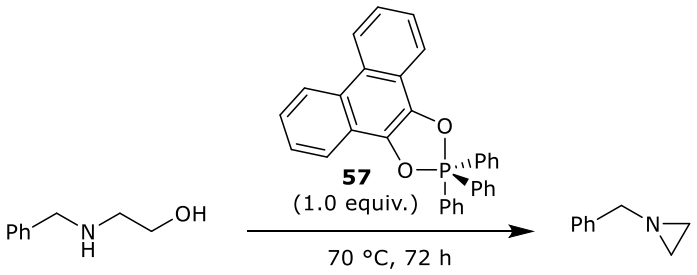

70 **57** **71** - 50%[a]

*Scheme 27: Synthesis of N-Benzylaziridine (**71**) via the cyclodehydration of N-benzylethanolamine (**70**). [a]Yield determined by ^{1}H NMR spectroscopy.*

Firstly, the extra methylene group extending the chain length between nitrogen and oxygen. Secondly, the inclusion of an *N*-phenyl substituent instead of *N*-benzyl. Consequently, **72** was synthesised (Scheme 28) as

the *N*-benzyl derivative of **66** to give a direct comparison between the propensity of 1,2 and 1,3-aminoalcohols to cyclodehydration.

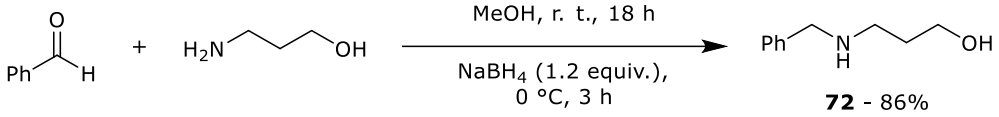

*Scheme 28: Synthesis of the 1,3-amino alcohol **72**.*

The dioxyphosphorane-mediated cyclodehydration of **72** was successful, with full conversion observed by ^{1}H NMR spectroscopy (Scheme 29).

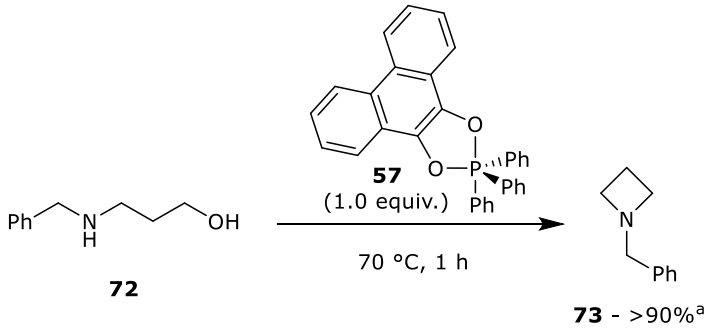

*Scheme 29: Successful cyclodehydration of **72** to give azetidine **73**. [a]Yield determined by ^{1}H NMR spectroscopy.*

This suggested that the failure of the cyclodehydration of **66** could be attributed to the *N*-phenyl substituent and was not intrinsic to all 1,3-aminoalcohols. This difference in reactivity between the amino alcohols **66** and **72** is most likely due to the reduced nucleophilicity of the aniline-type anion of the intermediate **74**, which is formed when **66** is used (Scheme 22).

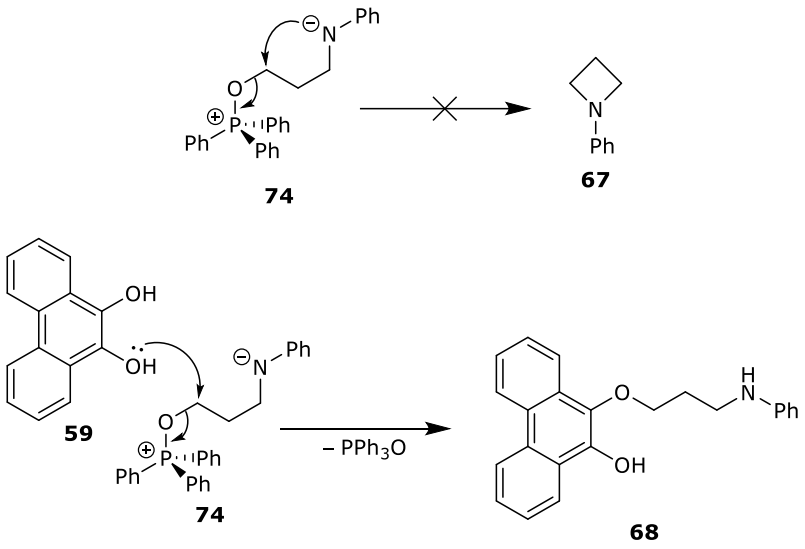

*Scheme 30: Top: failed Arbuzov collapse of the phosphonium salt **74** for the synthesis of azetidine **67**. Bottom: mechanism for the formation of the aromatic ether **68**).*

It is possible that this reduced nucleophilicity prevents the Arbuzov collapse required to form the azetidine product (**67**) (Scheme 30). Instead attack of the phosphonium salt with a phenolic hydroxyl group of phenanthrene-9,10-diol (**59**) forms the aromatic ether **68** (which can itself partake in another Arbuzov collapse to give **69**). Phenanthrene-9,10-diol (**59**) itself is formed from the substitution of the initial dioxyphosphorane **57** with the amino alcohol (Scheme 22).

With this knowledge in hand, it was determined that the desired phosphorane intermediate (**61**) from the phosphine insertion into **53**, likely cannot collapse to give the desired product (**64**). Therefore, as proved successful with the 1,3-amino-alcohols, the *N*-benzyl derivative (**76**) was synthesised (Scheme 31).

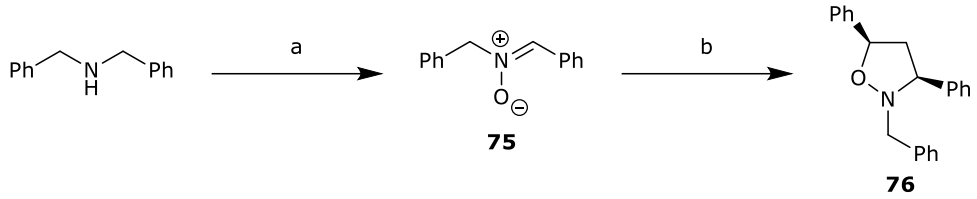

*Scheme 31: Synthesis of the N-benzyl isoxazolidine **76**. Reagents and conditions a) H_2O_2, $Na_2WO_4.2H_2O$, MeOH, 0 °C to r. t., 18 h, 74%; b) c) $PhCHCH_2$, benzene, 80 °C, 48 h, 75%, 74:26 dr.*

Unfortunately, in the case of **76** none of the desired product (**77**) was observed, nor was the possible amino-alcohol **78**. This suggests that although in this case the ring closure of the desired phosphorane intermediate may be possible, the initial insertion into the N,O-bond of **76** is not.

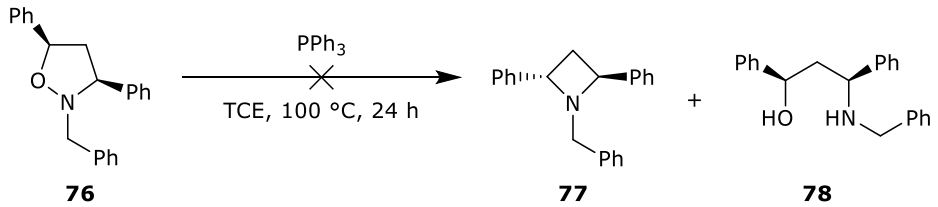

*Scheme 32: Attempted phosphine-mediated reductive ring contraction of **76**.*

It is worth noting that if this method could be made successful, in its current form, it would still have the undesirable attribute of forming stoichiometric phosphine oxide waste. As a result, it was deemed necessary to search for an alternative method to perform our desired reductive ring contraction.

1.3.3 Catalytic Ring Contractions Using Silanes as Terminal Reductants

1.3.3.1 Background and Initial Studies

Recent work within the Denton group has utilised a catalytic reductive system originally developed by Brookhart and co-workers. In the original work diethylsilane is used in combination with $[Ir(COE)_2Cl]_2$ to reduce amides (Scheme 33 top).[39] Denton and co-workers adapted this protocol and implemented it to give a one-pot synthesis of amines from carboxylic acids (Scheme 33 bottom).[40]

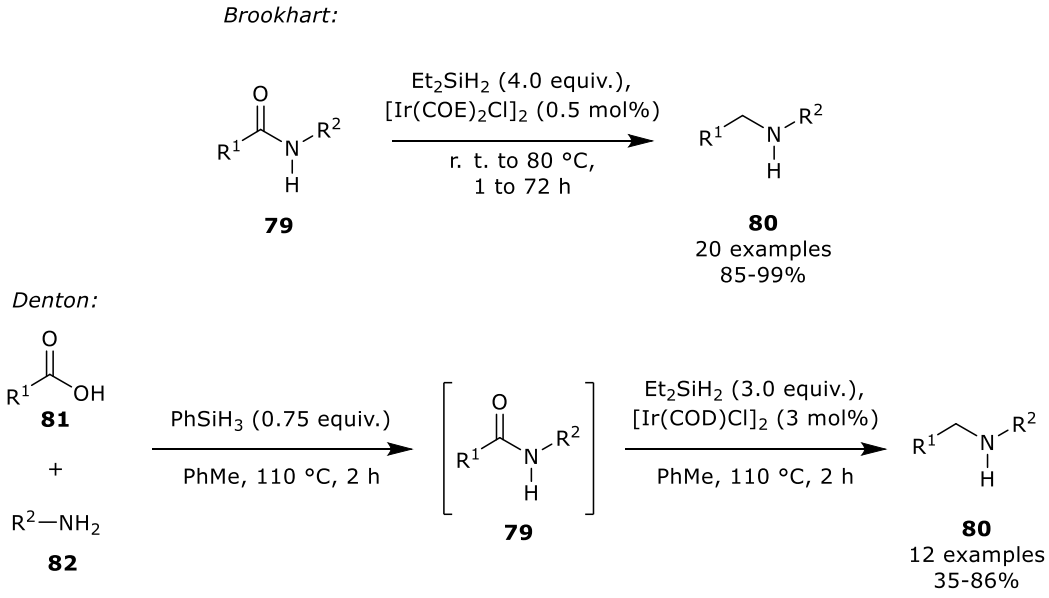

Scheme 33: Top: general scheme for the reduction of amides developed by Brookhart;[39] Bottom: general scheme for the reductive amination using carboxylic acids developed by Denton.[40]

The deoxygenating reduction of an amide can be seen to be somewhat analogous to our desired ring contraction. Whilst the work of Brookhart and Denton removes oxygen from the substrate in the form of an amidic carbonyl, our desired transformation removes oxygen from the isoxazolidine ring. Although these are very different substrates, the

powerful reducing ability of this system, combined with its relatively good functional group tolerance suggested it would be a good candidate for our work. Consequently, speculative experiments were undertaken to explore the use of this reductive system to perform the desired ring contraction.

Returning to our original model substrate **53**, we applied the conditions optimised in the aforementioned paper by Denton and co-workers (Scheme 34). Gratifyingly, the desired transformation occurred and the azetidine product (**64**) was isolated in 12% yield. The reaction was observed to proceed with inversion of stereochemistry with the *trans*-diastereomer being obtained as the major product. However, a single diastereomer of **53** was used in this reaction, showing the stereocentre is not cleanly inverted under these reaction conditions. Significantly, the *trans*-diastereomer has a C2 axis of symmetry and consequently the two protons of the azetidine methylene bridge are equivalent. Conversely, the *cis*-diastereomer does not have a C2 axis of symmetry and the methylene protons are inequivalent. Accordingly, stereochemical assignment is easily achieved by ^{1}H NMR spectroscopy.

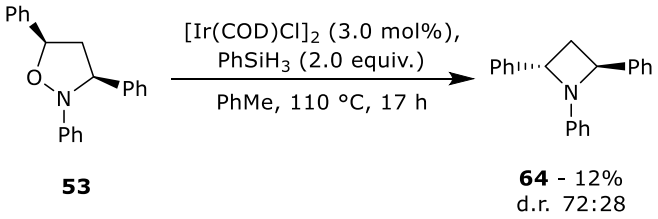

53

64 - 12%
d.r. 72:28

*Scheme 34: Catalytic reductive ring contraction of **53** to give azetidine **64**.*

As mentioned in section 1.2.3 the main advantage of this proposed synthesis methodology is its convergent nature. To exemplify this, a one-pot transformation was performed with ring formation and ring contraction

taking place with no isolation or purification (Scheme 35). In this case the desired product (**64**) was isolated in 17% yield, thus showing there is no drop off in reaction efficiency.

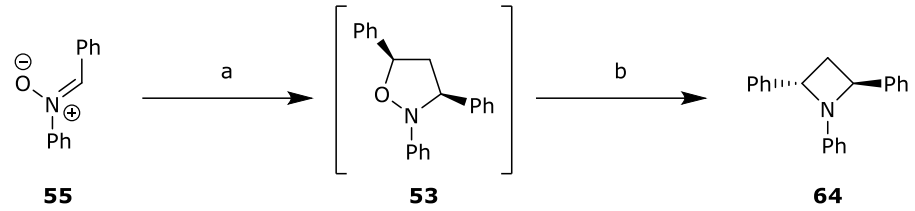

55 **53** **64**

*Scheme 35: One-pot synthesis of azetidine **64** from nitrone **55**. Reagents and conditions a) $PhCHCH_2$, 60 °C, 40 h; b) $[Ir(COD)Cl]_2$, $PhSiH_3$, PhMe, 110 °C, 24 h, 17% 78:22 dr.*

With these novel transformations acting as proof-of-concept we turned our attention to the optimisation of this process. This new methodology is perhaps most powerful as a one-pot ring formation/ring contraction process. However, to improve reproducibility and expediate the optimisation process, the reductive ring contraction step was considered in isolation.

1.3.3.2 Optimisation of Reaction Conditions

1.3.3.2.1 Control experiments and optimisation of silane loading

A control reaction performed in the absence of catalyst and another in the absence of silane showed both to be required for the reaction to occur (Scheme 36).

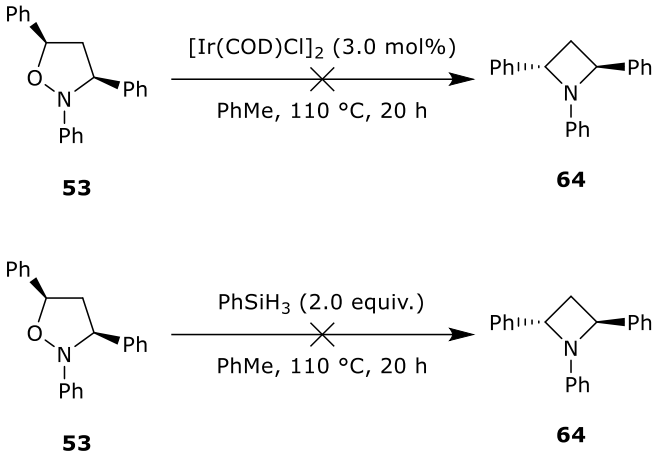

*Scheme 36: Top: control reaction in the absence of silane; Bottom: control reaction in the absence of catalyst. Both for the reductive ring contraction of **53**.*

Phenylsilane as the terminal reductant clearly plays a key role in this transformation. Consequently, the equivalents used were varied to see how this would affect conversions (Table 3, entries 1-3). Increasing the amount of phenylsilane had a positive effect on the conversion of **53** to **64**, with 70% conversion observed when three equivalents of phenylsilane were used (Table 3, entry 3). In an attempt to further increase this conversion, a reaction was heated at 110 °C for 22 hours (Table 3, entry 4). Unfortunately, in this case no product or starting material were observed due to decomposition. However, when the reaction temperature was reduced to 70 °C, a 22 hour reaction with three equivalents of phenylsilane gave full conversion to the desired product, with no signs of decomposition (Table 3, entry 5). The reaction was also shown to proceed at room temperature, albeit with low conversion (Table 3, entry 6).

*Table 3: Optimisation of the reductive ring contraction of **53**.*

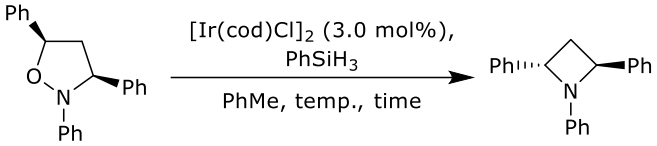

53 **64**

Entry	$PhSiH_3$ equiv.	Temp. / °C	Time / h	**53** / %[a]	**64** / %[a]
1	2.0	110	3	64	36
2	2.5	110	3	41	59
3	3.0	110	3	30	70
4	3.0	110	22	Decomposition	
5	3.0	70	22	<1	>99
6	3.0	r. t.	22	80	20
7	3.0[b]	70	20	>99	trace

[a]Product distribution determined by ^1H NMR spectroscopy; [b]Et_2SiH_2 used in place of $PhSiH_3$.

In the aforementioned work by Brookhart and co-workers, diethylsilane was used as their reductant.[39] However, when it was used for our transformation only trace product was observed (Table 3 entry 7).

Using the conditions from Table 3 entry 5, the azetidine **64** was isolated in 41% yield, a significant increase on the initial experiment (Scheme 34). Additionally, at this reduced temperature only the *trans*-diastereomer was obtained compared to the 72:28 mixture isolated before.

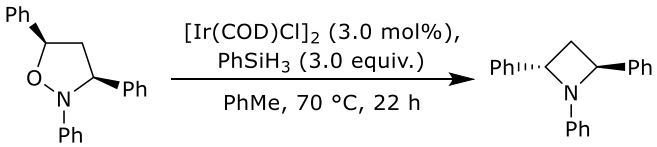

53

64 - 41%
d.r. > 99:1

*Scheme 37: Synthesis of azetidine **64** using the silane and temperature optimised conditions of Table 3 entry 5.*

1.3.3.2.2 Mass balance inconsistency – determination and possible explanations

Although this increase in yield was very encouraging, there is a noticeable discrepancy between the isolated yield and conversion calculated using ^{1}H NMR spectroscopy. Initially, this was thought to be an isolation issue with degradation of the product on purification. However, repeating the experiment depicted in Scheme 37 with the incorporation of 1,1,2,2-tetrachloroethane (TCE), as an internal standard, showed a non-linear relationship between consumption of starting material (**53**) and product (**64**) formation (Table 4).

*Table 4: Synthesis of **64** using optimised conditions from Table 3 entry 5 with TCE internal standard.*

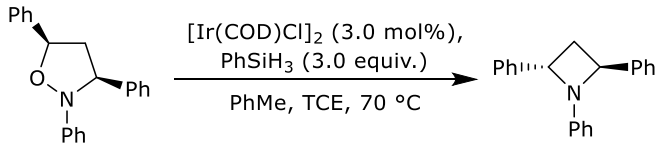

53 **64**

Entry	Time / h	**53** / %[a]	**64** / %[a]	Deficit[b] / %
1	0	100	0	0
2	16	0	32	68
3	40	0	21	79

*[a]Yields determined ^{1}H NMR spectroscopy using TCE as an internal standard; [b]Unexplained loss of starting material determined by 100 – (% of **53** + % of **64**).*

After 16 hours full consumption of **53** was observed with only 32% of **64** being formed (Table 4 entry 2). When the reaction was held for a further 24 hours the quantity of **64** present dropped to 21% (Table 4 entry 3), suggesting that the product was unstable to the reaction conditions.

A similar experiment was performed with two equivalents of phenylsilane used and earlier sampling of the reaction (Table 5).

*Table 5: Synthesis of **64** using two equivalents of phenylsilane with TCE internal standard.*

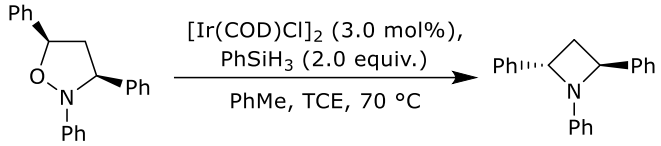

53 **64**

Entry	Time / h	**53** / %[a]	**64** / %[a]	Deficit[b] / %
1	0.0	100	0	0
2	1.5	61	14	25
3	3.0	47	18	35
4	5.0	36	19	45
5	22.0	10	11	79

*[a]Yields determined by ^{1}H NMR spectroscopy using TCE as an internal standard; [b]Unexplained loss of starting material determined by 100 – (% of **53** + % of **64**).*

This experiment showed that even after only 1.5 hours a large discrepancy between product formation and starting material consumption had appeared (Table 5 entry 1). A decline in the azetidine **64** present was also observed in this reaction, further suggesting product instability (Table 5 entries 4 and 5).

Additionally, a thermal stability test was performed where **53** was heated to 110 °C for 144 hours (considerably longer than the reaction conditions of up to 22 hours) (Scheme 38).

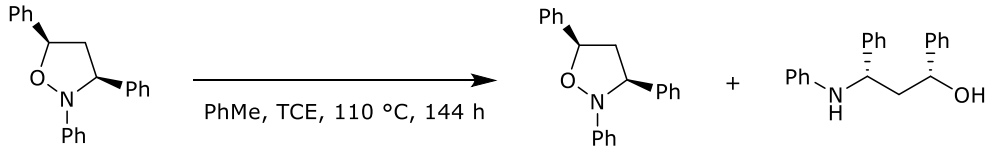

53 **53** - 86%[a] **65** - 14%[a]

*Scheme 38: Thermal stability test of **53** using TCE as an internal standard. [a]Yields determined ^{1}H NMR spectroscopy using TCE as an internal standard.*

Even after this prolonged heating only a 14% loss of **53** was observed relative to TCE as an internal standard. This was accounted for by the formation of the amino alcohol **65**. Therefore, the observed discrepancy between consumption of **53** and formation of **64** (which is much larger than 14%) cannot be due to thermal instability of **53**.

It is important to note that for these ring contraction reactions, no other species (including **65**) were isolated or observed which could explain this deficit between the internal standard and combined product and starting material integrals.

One possible explanation for this could be the formation of insoluble polymeric/oligomeric species.

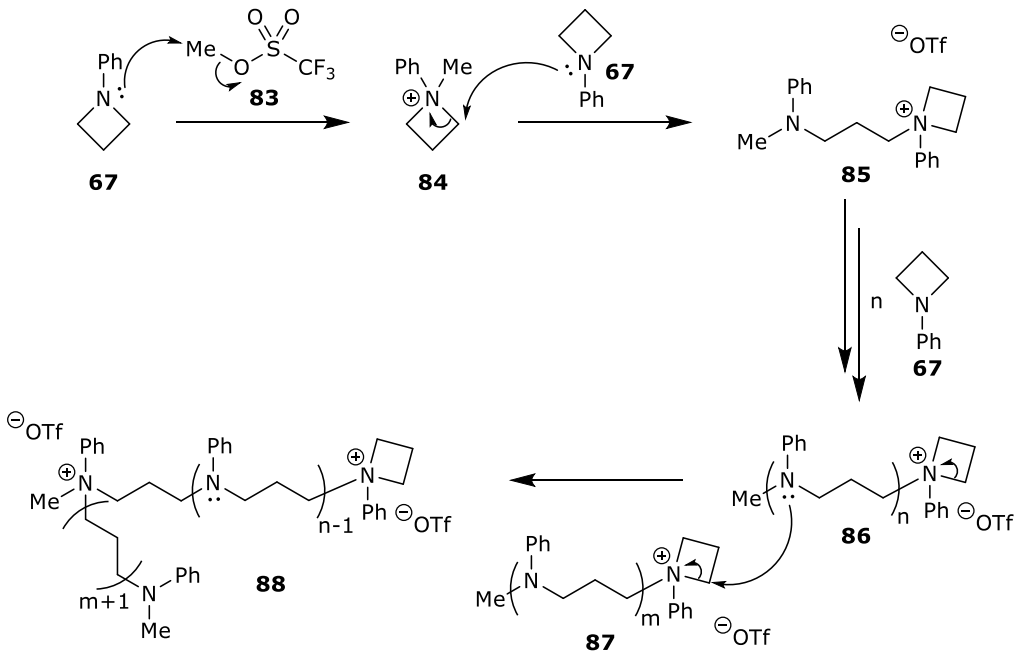

*Scheme 39: Mechanism for the cationic ring-opening polymerisation of N-phenylazetidine (**67**).*

Azetidines have been known to polymerise by a cationic ring-opening mechanism since it was first reported in 1980 by Goethals and co-

workers.[41] A more recent publication from 2000 polymerised *N*-phenylazetidine (**67**) using methyl triflate (**83**) as an initiator (Scheme 39). Methylation of **67** gives the cationic azetidinium **84** which is susceptible to ring-opening, releasing the large ring strain energy. Further ring-opening steps ultimately gives the polymer **86** which can undergo a termination step to give branched polymers such as **88**.

The polymerisation of *N*-phenylazetidine occurs readily at room temperature with only 5 mol% of **83** used. Therefore, if only a very small amount of an alkylating agent or proton source is present in the reaction, the substituted *N*-phenylazetidine **53** could be polymerising at the reaction temperature of 70 °C. These hypothesised polymeric products may be insoluble and as such neither detected nor isolated. *N*-(methanesulfonyl)azetidine has recently been shown to undergo anionic ring-opening polymerisation in the presence of a deprotonated sulfonamide.[42] Whilst this suggests another pathway for product decomposition, the weaker electron withdrawing nature of our *N*-phenyl substituent relative to the *N*-(methanesulfonyl) in the paper makes this less likely than the cationic process shown in Scheme 39.

In apparent disagreement with this theory is that when a pure sample of **64** was subjected to the reaction conditions, no decomposition was observed. Indeed, no loss of azetidine relative to the internal standard was observed even after four days (Scheme 40).

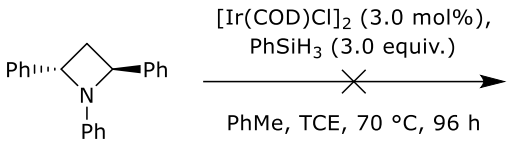

64

*Scheme 40: Product stability test of **64** under the reductive ring contraction conditions.*

This appears to be inconsistent with the previously observed decay in product shown in Table 4 and Table 5. One possible explanation for this discrepancy lies in the other species present within the reaction mixtures. For the product stability test shown in Scheme 40, only the catalyst, silane and products thereof are present to react with **64**. In contrast to this, the reductive ring contractions are likely much more complex mixtures comprising of silicon-containing by-products (e.g. silanols and siloxanes), **53** and by-products thereof. Therefore, it could be assumed that any one of these additional species present is the cause of product instability. Potentially a suitable proton source is generated to facilitate the cationic ring-opening polymerisation.

In an attempt to overcome this proposed polymerisation side reaction, further reactions were performed at lower concentrations (with respect to **53**) (Table 6). By lowering the reaction concentration, it was hoped any unwanted polymerisations would be halted by reducing the frequency of collisions between **64** and the other species responsible.

*Table 6: Effect of concentration on the transformation of **53** to **64** using [Ir(COD)Cl]$_2$.*

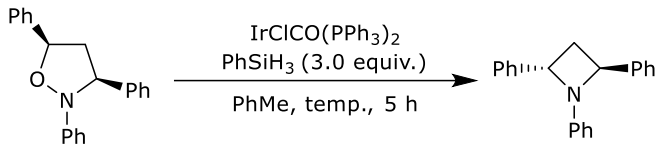

53 **64**

Entry	Concentration[a] / moldm^{-3}	Time / h	**53** / %[b]	**64** / %[b]	Deficit[c] / %
1	0.50	22	0	39	61
2	0.10	28	31	17	52
3	0.10	52	17	28	55
4	0.01	28	93	0	7
5	0.01	52	70	0	30

*[a]Concentration with respect to **53**; [b]Yields determined by ^{1}H NMR spectroscopy using TCE as an internal standard; [c]Unexplained loss of starting material determined by 100 – (% of **53** + % of **64**).*

All the reductive ring contraction reactions shown heretofore were performed at 0.5 M with respect to **53**. Lowering this concentration to 0.1 M slowed both the consumption of **53** and formation of **64** (Table 6 entries 2 and 3). Consequently, no reduction of the 'deficit' caused by unknown processes was achieved. When the transformation was undertaken at 0.01 M the consumption of **53** was greatly retarded, whilst no product was detected (Table 6 entries 4 and 5). Presumably, the rate of decomposition of **64** exceeds the rate of its formation in this example, thus it cannot be observed. As no improvements were observed at a lower concentration, all subsequent reductive ring contractions of **53** described within this chapter were performed at 0.5 M.

Another theory (to explain the non-linear conversion of **53** to **64**) is a possible retro [3+2] cycloaddition followed by reduction of the nitrone (Scheme 41 top). Retro [3+2] cycloadditions are known in the literature for isoxazolidines at elevated temperature.[43] Although in the previously

mentioned thermal stability test of **53** no nitrone was observed, it is possible the nitrone (**55**) exists in an equilibrium favouring **53**, thus preventing its observation (Scheme 38). The amine **89,** which would be produced by reduction of **55**, was observed in the reductive ring contraction by mass spectrometry and ^{1}H NMR spectroscopy in one instance. To assess the feasibility of this theory, the nitrone **55** was subjected to the reaction conditions (Scheme 41 bottom). Reduction was indeed observed with formation of the amine in 66% relative to the TCE internal standard.

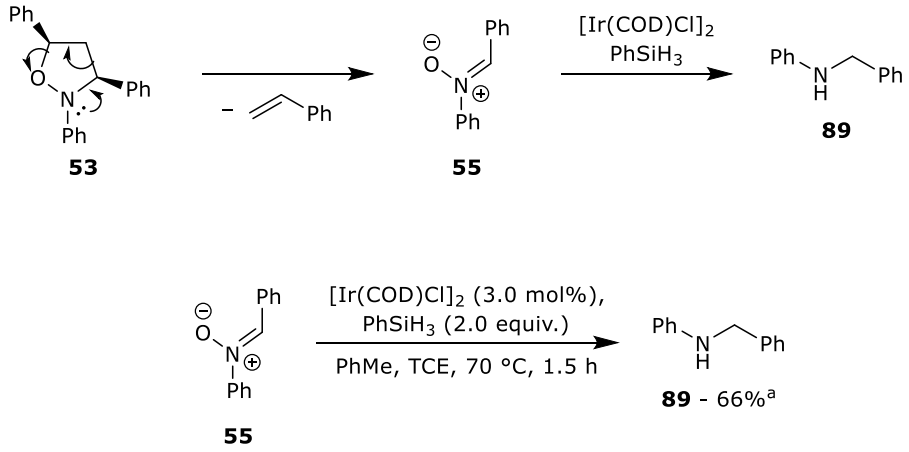

*Scheme 41: Top: proposed retro [3+2] cycloaddition and reduction of nitrone **55**; Bottom: Catalytic reduction of nitrone **55** to give amine **89**. [a]Yield determined by ^{1}H NMR spectroscopy using TCE as an internal standard.*

Interestingly, in the reduction of nitrone **55** a similar observation was made where full consumption of the starting material was observed with only 66% product present relative to the internal standard. This value dropped further to 55% after a further 24 hours, suggesting this could be another explanation for the deficit in the mass recovery of our reductive ring contractions. However, if this is indeed occurring in our reactions, it cannot account for the observed product instability. Therefore, it is not the

sole explanation for our poor yield. With these theories in mind we returned to the optimisation of the reaction.

1.3.3.2.3 Optimisation of reaction catalyst type and loading

Next to be explored was the effect of the nature and concentration of the catalyst. A small catalyst screen was conducted with three catalysts used previously as part of a reductive system with silanes. Firstly, $[Ir(COD)Cl]_2$ as used previously in this work. Secondly, $[Zn(OAc)_2]$ as used in Beller's reduction of amides[44]. Finally, Vaska's complex, $[IrClCO(PPh_3)_2]$, which has also been shown to reduce amides (Table 7).[45] Initially the reaction compositions were analysed after 1.5 hours to compare the early stages of the reactions. For $[Ir(COD)Cl]_2$, as catalyst loading was increased, both consumption of starting material and product formation rose, with full consumption of **53** observed after only 1.5 hours with 10 mol% catalyst (Table 7 entries 1-3). However, regardless of the loading, all three examples exhibited the aforementioned loss of starting material to other unknown processes. The magnitude of this loss was greater than the formation of product in all cases.

*Table 7: Catalyst screen and loading optimisation for the reductive ring contraction of **53** to **64**, observations made after 1.5 hours.*

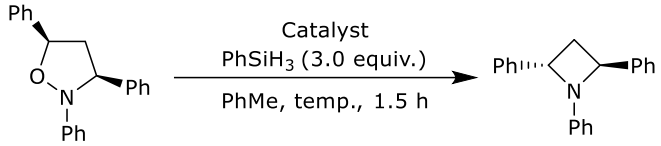

53 **64**

Entry	Catalyst	Catalyst loading / mol%	Temp. / °C	**53** / %[a]	**64** / %[a]	Deficit[b] / %
1	$[Ir(COD)Cl]_2$	1	70	89	5	6
2	$[Ir(COD)Cl]_2$	3	70	60	15	25
3	$[Ir(COD)Cl]_2$	10	70	0	20	80
4	$[Zn(OAc)_2]$	3	70	100	0	0
5	$[Zn(OAc)_2]$	10	110	98	0	2
6	$[IrClCO(PPh_3)_2]$	3	70	100	0	0
7	$[IrClCO(PPh_3)_2]$	6	70	97	0	3
8	$[IrClCO(PPh_3)_2]$	1	110	66	8	26
9	$[IrClCO(PPh_3)_2]$	3	110	0	10	90

[a]Yields determined by ^1H NMR spectroscopy using TCE as an internal standard;
*[b]Unexplained loss of starting material determined by 100 – (% of **53** + % of **64**).*

For $[Zn(OAc)_2]$ no product was observed, even at 10 mol% and 110 °C (Table 7 entry 5). Evidently very little if any reaction is occurring here as only 2% consumption of **53** was observed, a value which lies within error. Vaska's complex also showed no reaction to be occurring at 3 mol% and 70 °C (Table 7 entry 6). Increasing the catalyst loading to 6 mol% had essentially no effect on this (Table 7 entry 7). By increasing the reaction temperature to 110 °C, the desired product was observed using Vaska's complex at both 1 and 3 mol% (Table 7 entries 8 and 9). However, in both cases formation of **64** did not directly correlate to consumption of **53**. When compared to the reactions using $[Ir(COD)Cl]_2$, Vaska's complex formed less product relative to starting material consumed. Namely, entries 3 and 9 both consumed **53** entirely, but entry 3 formed double the quantity of **64**. Likewise, entries 2 and 8 can be compared where both

have an unexplained deficit of 25-26%, but the reaction using $[Ir(COD)Cl]_2$ formed almost double the amount of **64** (15% compared to 8%).

To corroborate these observations for Vaska's complex the same reactions can be compared after a more prolonged reaction time of five hours (Table 8).

*Table 8: Reaction compositions for the transformation of **53** to **64** using Vaska's complex, observations made after 5 hours.*

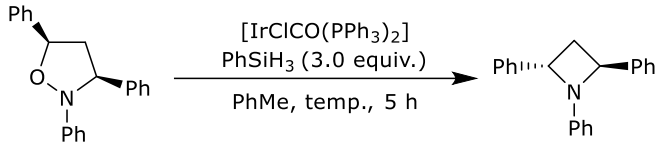

53 **64**

Entry	Catalyst loading / mol%	Temp. / °C	**53** / %[a]	**64** / %[a]	Deficit[b] / %
1	3	70	95	trace	>4
2	6	70	81	trace	>18
3	1	110	27	24	49

*[a]Yields determined by ^{1}H NMR spectroscopy using TCE as an internal standard; [b]Unexplained loss of starting material determined by 100 – (% of **53** + % of **64**).*

As seen in Table 7 entries 6 and 7, no product was observed for reactions using Vaska's complex at 70 °C (Table 8 entries 1 and 2). However, in these instances with a longer reaction time, the starting material began to be consumed by unknown side reactions. As was seen in Table 7 entry 8, a reaction at 110 °C with 1 mol% catalyst does form the desired product (Table 8 entry 3). This reaction appears to proceed well from 1.5 to 5 hours, albeit not to completion after 5 hours, with only 24% product being formed.

Given the initial reductive ring contractions using $[Ir(COD)Cl]_2$ gave best results after 22 hours (Table 3), these reactions were also compared after 22 hours (Table 9). The apparent inertness of $[Zn(OAc)_2]$ also makes analysis of these reactions after a longer reaction time more desirable.

*Table 9: Reaction compositions for the transformation of **53** to **64** using $[Ir(COD)Cl]_2$ and $Zn(OAc)_2$, observations made after 22 hours.*

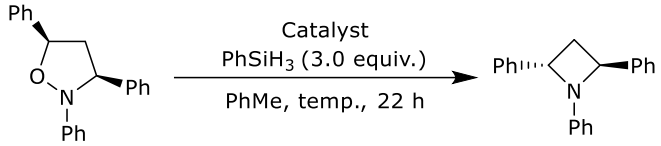

53 **64**

Entry	Catalyst	Catalyst loading / mol%	Temp. / °C	**53** / %[a]	**64** / %[a]	Deficit[b] / %
1	$[Ir(COD)Cl]_2$	1	70	32	25	43
2	$[Ir(COD)Cl]_2$	3	70	0	39	61
3	$[Zn(OAc)_2]$	3	70	100	0	0
4	$[Zn(OAc)_2]$	10	110	30	trace	>69

*[a]Yields determined by ^1H NMR spectroscopy using TCE as an internal standard; [b]Unexplained loss of starting material determined by 100 – (% of **53** + % of **64**).*

For the reaction performed with 1 mol% $[Ir(COD)Cl]_2$ there was more starting material than product after 22 hours (Table 9 entry 1). Full consumption of **53** was observed however when 3 mol% of the catalyst was used after 22 hours (Table 9 entry 2). The value of 39% product obtained for this experiment correlates closely to the 41% isolated yield shown in Scheme 37, when the same conditions were used in a preparative experiment. Evidently $[Zn(OAc)_2]$ is not an effective catalyst for this transformation, after 22 hours no reaction was observed for the 70 °C reaction using 3 mol% (Table 9 entry 3). Although consumption of **53** was observed when 10 mol% was used at 110 °C, no **64** was observed (Table 9 entry 4).

As a result of our investigations, to date, the best conditions found for the reductive ring contraction of **53** to **64** are those found in Scheme 37 (3 mol% $[Ir(COD)Cl]_2$, 3 equiv. $PhSiH_3$, PhMe, 70 °C, 22 h). It was hypothesised that **53** could have been a poor choice of model substrate, more susceptible to the unknown side reactions. Therefore, a range of

alternative isoxazolidines were synthesised and their ring contractions explored. This also serves as a preliminary study into the substrate scope of our novel transformation.

1.3.3.3 Investigations Using Alternative Substrates

1.3.3.3.1 Synthesis of alternative isoxazolidines

The *N*-benzyl derivative (**76**) of the model substrate **53** was prepared as described in Scheme 31. In section 1.3.2.3 it was deduced that the N,O-bond of **76** was more difficult to break, though once split was more likely to give the desired product. However, this work is an entirely different synthetic manifold and consequently its reactivity in this system is unknown.

Additional isoxazolidines were subsequently synthesised altering the substituents in all positions of the ring. Firstly, three different *N*-phenyl isoxazolidines (**91**, **92** and **93**) were prepared from the common nitrone **55** and the relevant alkene, this being the same method as used for the synthesis of **53** (Table 10).

Both **91** and **92** have very similar structures to that of the original model substrate **53**. It was hoped that this would increase the chance of success for the desired ring contraction, whilst exploring the tolerance of the reaction to both pyridine heterocycles and aryl halides. The latter of which would give a more synthetically useful target, the halide acting as a good handle for further derivatisation.

*Table 10: Synthesis of isoxazolidines **91**-**93** from the common nitrone **55**. [a]Epimers not assigned.*

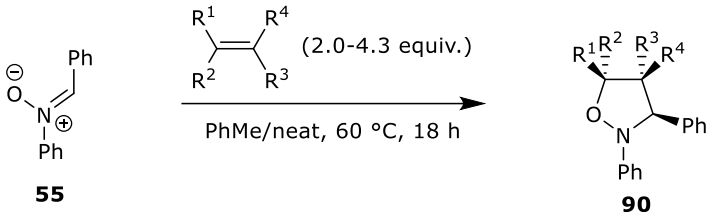

55 **90**

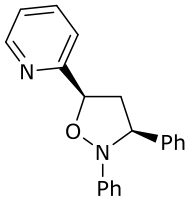

91
93%, d.r. 68:32

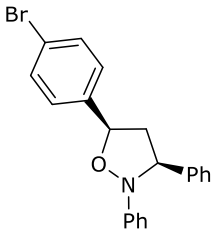

92
73%, d.r. 94:6

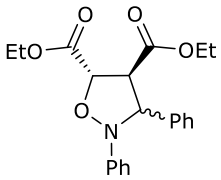

93
68%,
(97:3 ratio of epimers)[a]

The isoxazolidine **93** represents a more significant departure from **53** for the alkene derived fragment, whilst maintaining the same nitrone of the previously successful substrate. As a result, the significance of the alkene fragment will be investigated. All three isoxazolidines were isolated in good to excellent yield with moderate to excellent diastereoselectivity. In contrast to **90** and **91** the major stereoisomer of the isoxazolidine **93** was not determined, however there exists a *trans*-configuration between the two ester groups.

Further substrates were subsequently prepared, also using a 1,3-dipolar cycloaddition, with different nitrogen bound substituents. Two isoxazolidines were synthesised in order to explore the effect of varying the electronics on the nitrogen of the isoxazolidine. Bearing an electron withdrawing CF_3 group in the *para*-position, **96** would decrease the electronegativity of the nitrogen (Scheme 42). Whilst **98**, would serve as the inverse of this with an electron donating OMe group, also in the *para*-

position (Scheme 43). By incorporating the substituents in the *para*-position, the electronic effects can be analysed with minimal impact on the sterics of the substrates. Both of these compounds (**96** and **98**) were synthesised from their corresponding nitrones (**95** and **97** respectively).

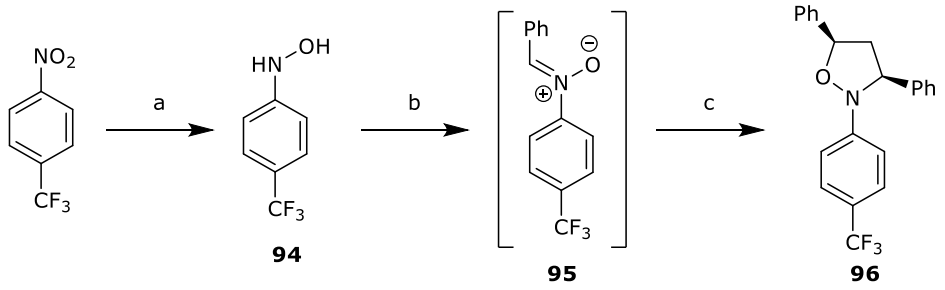

*Scheme 42: Synthesis of isoxazolidine **96**. Reagents and conditions a) $N_2H_4.H_2O$, Rh/C, THF, 0 °C to r. t., 3 h, 92%; b) PhCHO, $MgSO_4$, DCM, r. t., 2 h; c) $PhCHCH_2$, THF, 60 °C, 18 h, 65% (over two steps), 92:8 dr.*

Despite **98** appearing to be formed by ^{1}H NMR spectroscopy, it could not be isolated. This is due to it readily decomposing upon either recrystallisation or column chromatography. Presumably, this is a result of the electron donating methoxy substituent facilitating ring-opening of the isoxazolidine, thus opening up other reaction pathways. Consequently, **98** was used *in situ* in a one pot process as was outlined in Scheme 35.

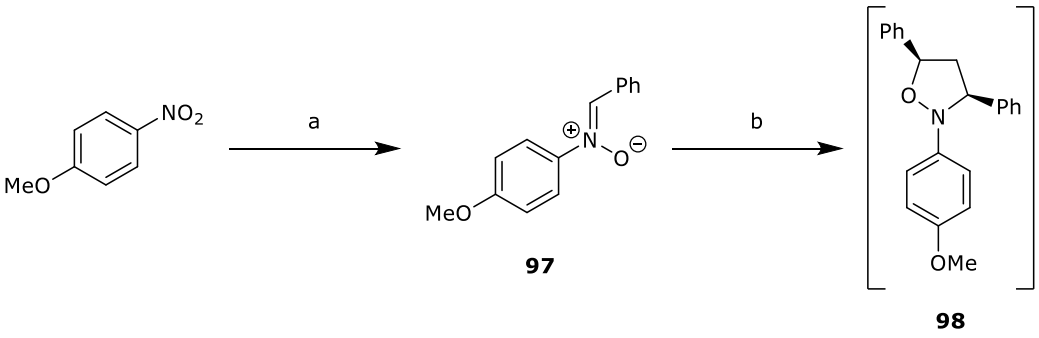

*Scheme 43: Synthesis of isoxazolidine **98**. Reagents and conditions a) PhCHO, Zn, NH_4Cl, EtOH, H_2O, r. t., 19 h, 52%; b) $PhCHCH_2$, THF, 80 °C, 21 h.*

Two further isoxazolidines (**101** and **102**) were synthesised bearing alkyl substituents at the 2 and 3 positions (Table 11). Being derived from styrene, **101** is analogous to the original model substrate **53** with only the nitrone fragment differing. Consequently, this would allow the impact of the two nitrone fragments on the reaction success to be directly compared. Both substrates were prepared from the common nitrone **99** which was used *in situ* to prevent decomposition.

*Table 11: Synthesis of isoxazolidines **101** and **102** from the common nitrone **99**. Reagents and conditions a) H_2O_2, $Na_2WO_4.2H_2O$, MeOH, 0 °C to r. t., 18 h; b) alkene, 60 °C, 88 h. [a]Yield reported over two steps.*

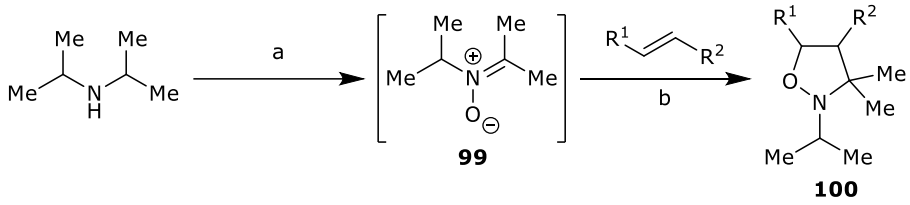

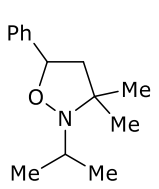

101 - 25%[a]

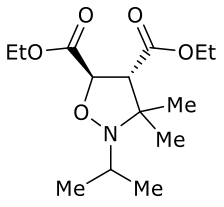

102 - 32%[a]

One final isoxazolidine was synthesised as a bicyclic substrate (**105**) *via* an intra-molecular 1,3-dipolar cycloaddition (Scheme 44). In this example, the nitrone formed is tethered to the alkene and consequently undergoes the ring forming cycloaddition *in situ*. A particularly attractive feature of this example is if combined with the one pot ring formation/ring contraction method, complex bicyclic azetidines could be synthesised from linear chain aldehydes in a single reaction.

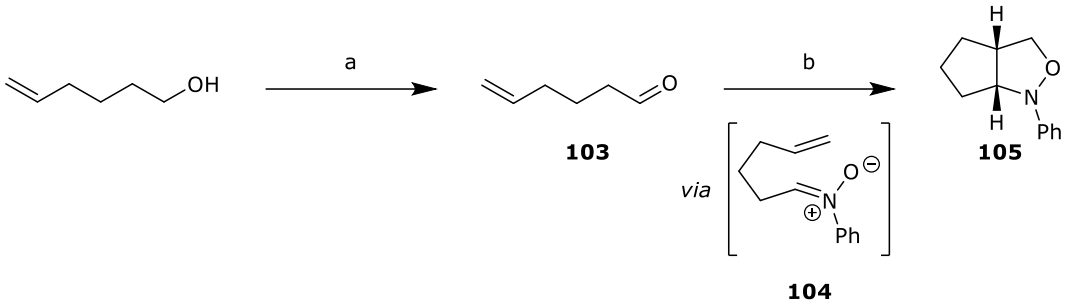

*Scheme 44: Synthesis of isoxazolidine **105** via an intramolecular [3+2] cycloaddition. Reagents and conditions a) $(COCl)_2$, DMSO, DCM, −78 °C to r. t., 1 h, 18%; b) PhNHOH, Et_2O, EtOH, r. t., 18 h then 60 °C 96 h, 49%.*

With our nine alternative substrates in hand, investigations into the ring contraction of these isoxazolidines were undertaken.

1.3.3.3.2 Ring contractions using alternative substrates

The first three isoxazolidines to be studied were those derived from the same nitrone (**55**) as the initial model substrate **53**. Replacing the phenyl ring at the 5 position with a pyridine ring (**91**) had a profound effect on the success of the reaction (Table 12).

*Table 12: Attempted reductive ring contraction of the isoxazolidine **106**.*

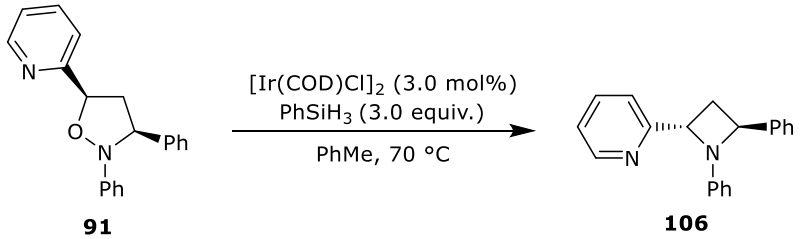

Entry	Time / h	**91** / %[a]	**106** / %[a]	Deficit[b] / %
1	1.5	96	0	4
2	3.0	94	0	6
3	5.0	94	0	6

*[a]Yields determined by ^{1}H NMR spectroscopy using TCE as an internal standard; [b]Unexplained loss of starting material determined by 100 – (% of **91** + % of **106**)*

No formation of the desired product (**106**) was observed and essentially no starting material was consumed. The fact that **91** is inert to these reaction conditions is a significant difference as a result of a minor modification. This can plausibly be explained by the pyridine acting as a coordinating ligand to the iridium catalyst, inhibiting its desired reactivity as a result.

Aryl halides appear to be well tolerated with the ring contraction of **92** being successful (Table 13). The product (**107**) being formed in 35% after 24 hours is very similar to the value of 32% obtained after 16 hours from the reaction of the original model substrate **53**, both having no starting material remaining (Table 4 entry 2).

*Table 13: Reductive ring contraction of the isoxazolidine **92**.*

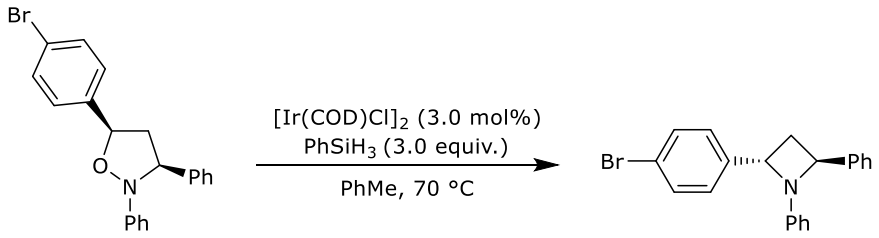

92 **107**

Entry	Time / h	**92** / %[a]	**107** / %[a]	Deficit[b] / %
1	1.5	50	15	35
2	3.0	37	19	44
3	5.0	26	23	51
4	24.0	0	35	65

*[a]Yields determined by ^{1}H NMR spectroscopy using TCE as an internal standard; [b]Unexplained loss of starting material determined by 100 – (% of **92** + % of **107**)*

Unfortunately, in the case of **93** none of the desired azetidine product was observed, whilst the isoxazolidine was gradually consumed (Table 14). In this case a complex mixture of products were observed by ^{1}H NMR spectroscopy. This is very likely to be a result of reduction of the ester

groups, consequently leading to a large number of products. In the previously mentioned paper by Denton and co-workers using this same reductive system, examples bearing ester functionality were not tolerated.[40] Moreover, the publication by Brookhart and co-workers only has one example with a methyl ester, for which comment is made that reduction of this occurs if <2 equivalents of silane are used.[39]

*Table 14: Attempted reductive ring contraction of the isoxazolidine **93**.*

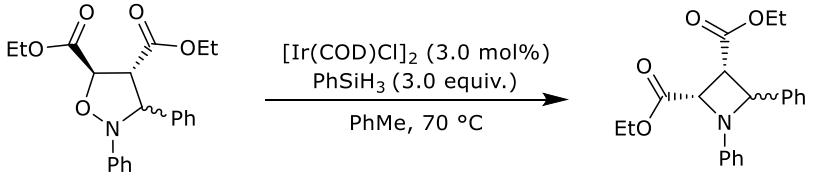

93[a] **108**

Entry	Time / h	**93** / %[b]	**108** / %[b]	Deficit[c] / %
1	1.5	85	0[d]	15
2	3.0	81	0[d]	19
3	5.0	68	0[d]	32
4	24.0	44	0[d]	56

*[a]Epimers not assigned; [b]Yields determined by ^{1}H NMR spectroscopy using TCE as an internal standard; [c]Unexplained loss of starting material determined by 100 – (% of **93** + % of **108**); [d]Complex mixture of products observed in the baseline of the ^{1}H NMR spectra.*

Introduction of an electron withdrawing substituent (in the form of a CF_3 group) to the nitrogen-bonded ring greatly slowed the reactivity (Table 15). Although **96** did successfully undergo the reductive ring contraction to form **109**, it did so with only 7% product formed and 66% starting material remaining after 22 hours (Table 15 entry 4).

*Table 15: Ring contraction of the isoxazolidine **96**.*

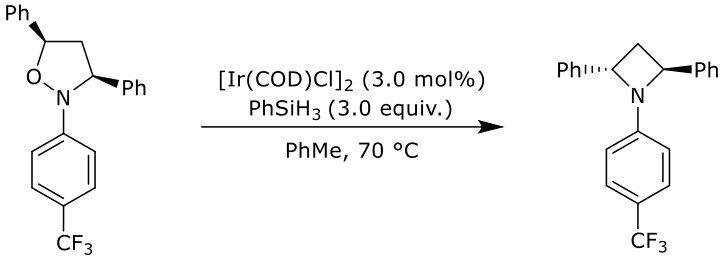

96 **109**

Entry	Time / h	**96** / %[a]	**109** / %[a]	Deficit[b] / %
1	1.5	86	trace	14
2	3.0	80	4	16
3	5.0	76	5	19
4	22	66	7	27

*[a]Yields determined by ^{1}H NMR spectroscopy using TCE as an internal standard; [b]Unexplained loss of starting material determined by 100 – (% of **96** + % of **109**).*

Perhaps this poorer reactivity can be explained by the reduced nucleophilicity of the nitrogen, impeding the ring closure step. When the reaction was monitored using ^{19}F NMR spectroscopy a number of minor signals were present between −136 and −188 ppm. One of these (−141.5 (d, *J* = 68.9 Hz) was determined to be the known compound **110** (Scheme 45).[46]

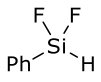

110

*Scheme 45: Structure of by-product **110**, formed in the reductive ring contraction of **96**.*

Evidently, the CF_3 group in **96** is not inert to the reaction conditions and must be the fluorine source for the formation of these unwanted side products.

As mentioned in section 1.3.3.3.1, **98** was not stable to isolation. As a result, its reductive ring contraction was performed as a one-pot reaction (Scheme 46). Attempts were made to monitor product formation throughout the reaction using an internal standard as for the previous substrates. However, as the reaction mixture contained both major and minor diastereomers for both **98** and **111**, in addition to excess styrene, no valid data could be obtained.

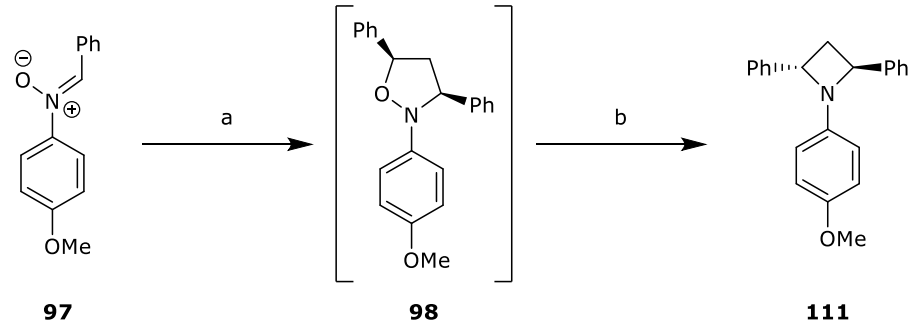

*Scheme 46: One-pot synthesis of azetidine **111** from nitrone **97**. Reagents and conditions a) $PhCHCH_2$, 80 °C, 20 h; b) $[Ir(COD)Cl]_2$, $PhSiH_3$, PhMe, TCE, 70 °C, 5 h, 9% 80:20 dr.*

Nevertheless, the desired product **111** was isolated in 9% yield (Scheme 46). Unfortunately, no valid comparisons to the synthesis of **109** may be drawn from this experiment due to the differences in reaction setup.

In the case of the *N*-benzyl substrate **76**, no product was observed, with minimal consumption of starting material (Table 16). This lack of reactivity relative to **53** is possibly explained by a greater difficulty to break open the isoxazolidine ring, as was previously observed in section 1.3.2.3; the N,O-bond of the *N*-phenyl isoxazolidine **53** is weaker due to the resonance of the nitrogen lone pair (or anion upon ring-opening) into the phenyl ring.

*Table 16: Attempted ring contraction of the N-benzyl isoxazolidine **76**.*

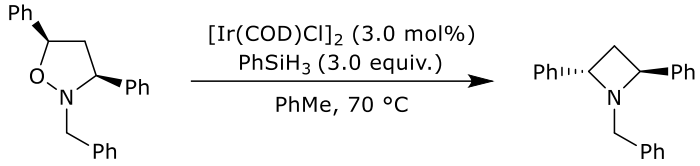

76 **77**

Entry	Time / h	**76** / %[a]	**77** / %[a]	Deficit[b] / %
1	1.5	93	0	7
2	3.0	96	0	4
3	5.0	90	0	10

*[a]Yields determined by ^{1}H NMR spectroscopy using TCE as an internal standard; [b]Unexplained loss of starting material determined by 100 – (% of **76** + % of **77**).*

Isoxazolidine **101** can be seen to be analogous to **53** sharing the same alkene fragment with the nitrone fragment differing. For **101** no product was observed after 5 hours (Table 17 entry 3). Some 15% of the starting material was consumed in the first 1.5 hours but this remained static thereafter (Table 17 entries 1-3).

*Table 17: Attempted ring contraction of the isoxazolidine **101**.*

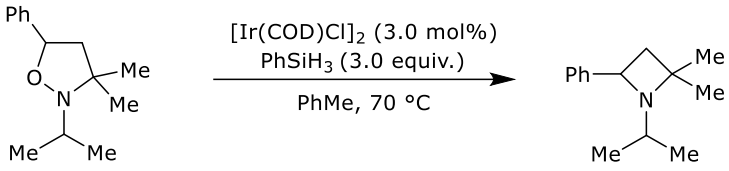

101 **112**

Entry	Time / h	**101** / %[a]	**112** / %[a]	Deficit[b] / %
1	1.5	85	0	15
2	3.0	81	0	19
3	5.0	83	0	17

*[a]Yields determined by ^{1}H NMR spectroscopy using TCE as an internal standard; [b]Unexplained loss of starting material determined by 100 – (% of **101** + % of **112**).*

In the same way that the *N*-benzyl substituent of **76** reduced reactivity relative to the *N*-phenyl substrate **53**, it would appear *N*-alkyl substituents also hinder reactivity. Therefore, the inclusion of an aromatic substituent on the nitrogen of the isoxazolidine, to stabilise electron density on nitrogen, appears to be necessary for a successful reaction under these conditions.

As was observed for **93** in Table 14, the ester groups of **102** were not tolerated under these reaction conditions. Consequently, no product was formed and a complex mixture of minor products was observed (Table 18 entries 4-6).

*Table 18: Attempted ring contraction of the isoxazolidine **102**.*

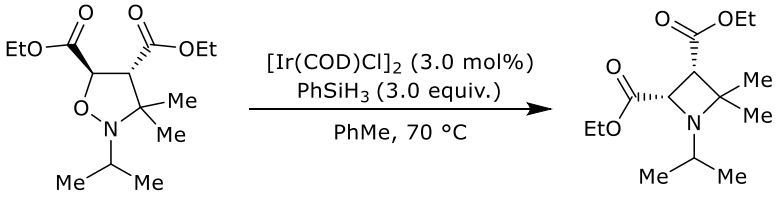

102 **113**

Entry	Time / h	**102** / %[a]	**113** / %[a]	Deficit[b] / %
1	1.5	84	0[c]	16
2	3.0	71	0[c]	29
3	5.0	61	0[c]	39

[a]Yields determined by ^{1}H NMR spectroscopy using TCE as an internal standard; [b]Unexplained loss of starting material determined by 100 – (% of s. m. + % of prod.); [c]Complex mixture of products observed in the baseline of the ^{1}H NMR spectra.

The ring contraction of the bicyclic isoxazolidine **105** gave rise to a complex mixture that could not be monitored by ^{1}H NMR spectroscopy. As a result, the reaction was purified by column chromatography after 22 hours. The desired product (**114**) was isolated in 14% yield whilst the major product isolated was the amino alcohol **115** in 35% (Scheme 47).

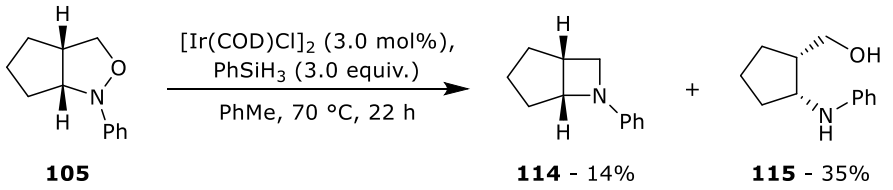

105 **114** - 14% **115** - 35%

*Scheme 47: Reductive ring contraction of **105** (derived from an intramolecular [3+2] cycloaddition) to give azetidine **114** and amino alcohol **115**.*

Interestingly, this was the first time an amino-alcohol had been isolated at the end of a ring contraction using this reductive system; indeed, they were believed to be reactive intermediates in the reaction (see section 1.3.3.4). Subjecting **115** to the reaction conditions resulted in trace product formation and a complex mixture of unknown products by ^{1}H NMR spectroscopy. Therefore, **115** was formed not in the reaction, but upon purification by hydrolysis of **114**. As a result, the total product formation prior to purification appears to be 49%, which is a good result roughly comparable to that for the model substrate **53**.

1.3.3.4 Mechanistic Studies

A number of experiments were performed to gain an insight of the mechanism of this reaction, and thus obtain a better understanding of this novel procedure.

It was previously shown that when the reductive ring contraction of the *cis*-isoxazolidine **53** was performed, the *trans*-product **64** was the major diastereomer (Scheme 48).

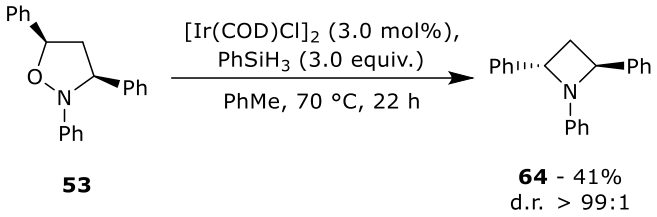

53

64 - 41%
d.r. > 99:1

*Scheme 48: Reductive ring contraction of the cis-isoxazolidine **53**, giving the trans-azetidine **64**.*

This inversion of stereochemistry at the 5 position of the isoxazolidine could have two possible explanations. Firstly, the stereocentre is inverted during the ring formation step. Secondly, the major product could be the result of an equilibration process leading to the less hindered *trans*-product. In order to determine which theory is correct, a sample of **116** (*trans*-diastereomer of **53**) was subjected to the ring contraction conditions (Scheme 49).

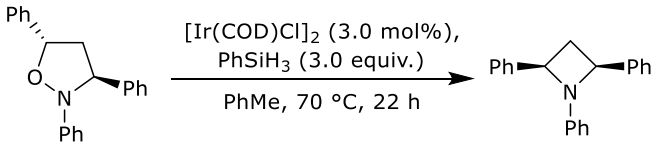

116
d.r. 63:37

117 - 36%
d.r. 67:33

*Scheme 49: Reductive ring contraction of the trans-isoxazolidine **116**, giving the cis-azetidine **117**.*

In this example the *cis*-product (**117**) was the major diastereomer formed. Consequently, the stereoselectivity of the reaction is substrate controlled. Presumably the stereocentre at the 5 position is inverted during the ring formation step.

A mechanism was proposed for these reactions based on a number of pieces of information. Firstly, the control experiments shown in Scheme 36 found that both the silane and catalyst were required for the reaction to

occur. Secondly, a silane such as phenylsilane is effectively split into a H^- component (in the form of a reducing metal hydride [MH]) and an electrophilic $^+SiR_3$ component which can readily silylate oxygen. Brookhart and co-workers have characterised the resting state of a very similar reductive system using $[Ir(COE)_2Cl]_2$ and Et_2SiH_2 (**120**, Scheme 50).[39] Scrambling of the silane bonded alkyl groups leads to a number of different dimeric complexes, all bearing metal hydrides which were observed by ^1H NMR spectroscopy.[47] Furthermore, the analogous complex (**121**), obtained using $^tBu_2SiH_2$, was characterised by X-ray crystallography. It is highly likely that our similar reductive system also forms a reducing metal hydride complex such as this.

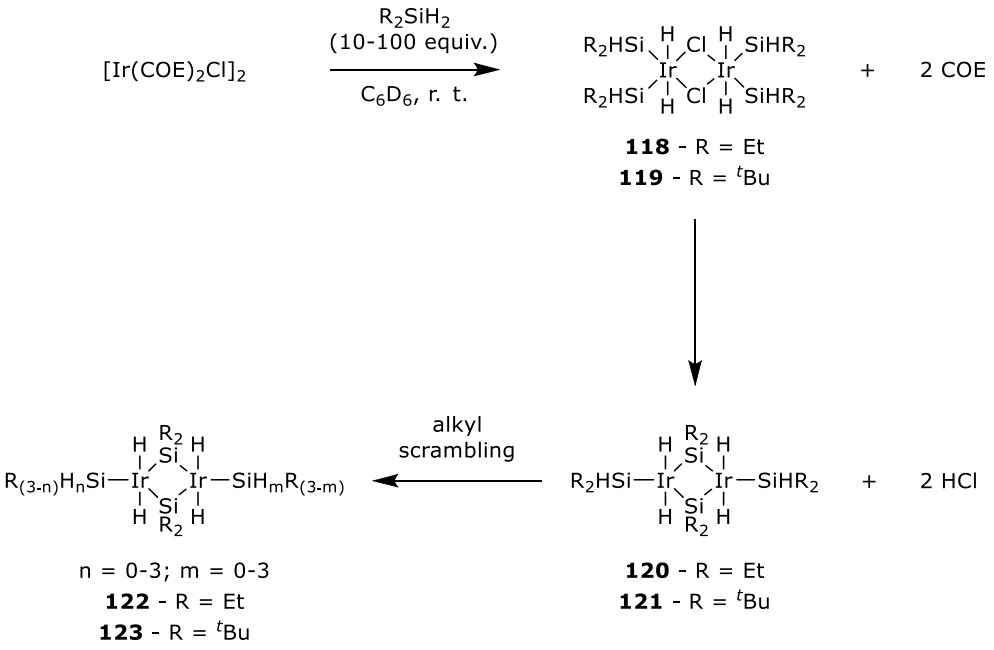

*Scheme 50: Formation of the metal hydride complexes **122** and **123** described by Brookhart.*[39]

Thirdly, gas evolution is observed when the reactions are performed suggesting generation of H_2. Finally, as mentioned previously the reaction

proceeds with inversion at the 5 position of the isoxazolidine. Based on this information the mechanism shown in Scheme 51 was proposed.

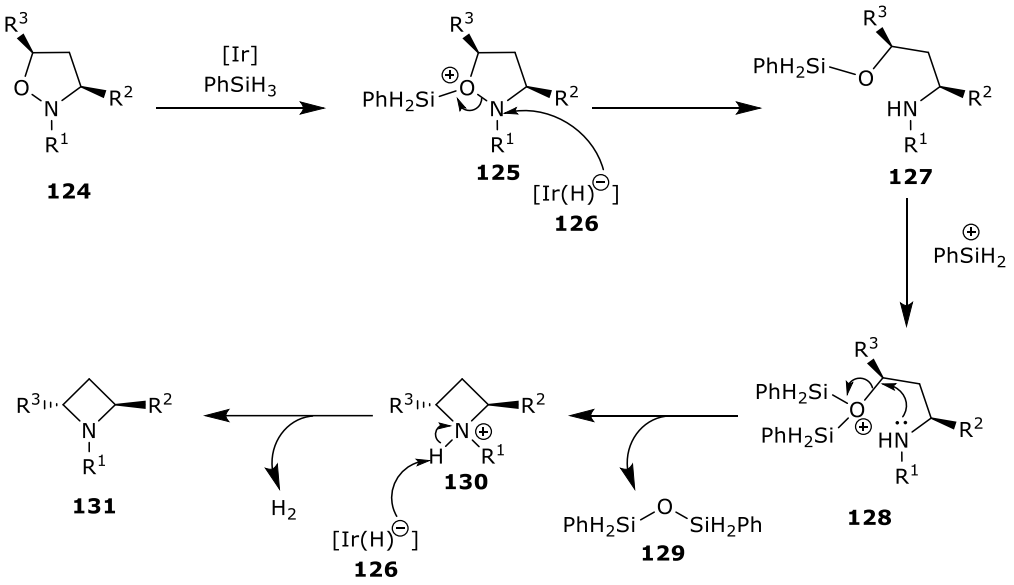

*Scheme 51: Proposed mechanism for the synthesis of azetidine **131** via the reductive ring contraction of an isoxazolidine **124**.*

The first step of this proposed mechanism involves formation of the silylated isoxazolidine **125**, after phenylsilane is activated by hydride abstraction generating a metal hydride. Subsequent attack of a reducing metal hydride species (**126**) results in heterolytic cleavage of the N,O-bond to give the silylated amino alcohol **127**. Further silylation affords **128**, ensuing ring closure *via* intramolecular attack from the amine component eliminates siloxane **129** and results in inversion of stereochemistry at the 5 position. Deprotonation of the azetidinium **130** yields the azetidine product **131** whilst evolving hydrogen gas and regenerating the iridium catalyst.

A key intermediate in this proposed mechanism is the silylated amino alcohol **127**, formed from the ring-opening of the isoxazolidine. In order to

determine if this was a viable intermediate for the reaction, the amino alcohol **65** was synthesised from ring-opening the original model substrate **53** (Scheme 52).

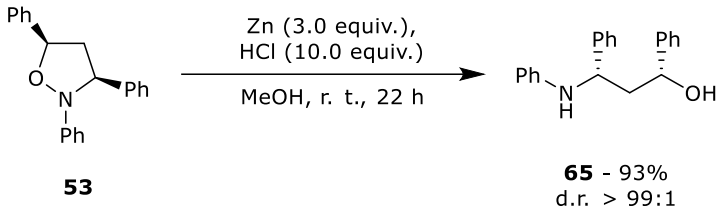

53

65 - 93%
d.r. > 99:1

*Scheme 52: Synthesis of amino alcohol **65** from the ring-opening of isoxazolidine **53**.*

Given that silylation of **65** will occur readily under the reaction conditions, it can be seen to be the precursor to the proposed intermediate **127** for the successful ring contraction of **53**. As expected, subjecting **65** to the reaction conditions gave the azetidine product **64**. Therefore, confirming the silylated amino alcohol **127** to be a likely intermediate for the ring contraction of **53**.

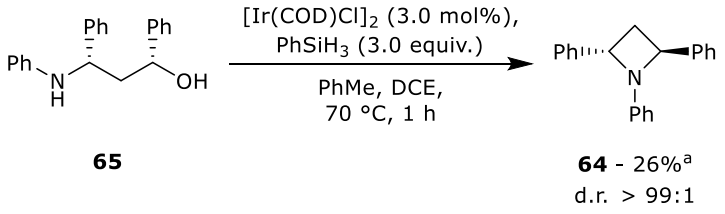

65

64 - 26%[a]
d.r. > 99:1

*Scheme 53: Synthesis of azetidine **64** from amino alcohol **65**. [a]Yield determined by ^{1}H NMR spectroscopy relative to TCE internal standard.*

From this experiment a number of other inferences can be made. Firstly, the *trans*-product was observed as the sole diastereomer, thus confirming that inversion of the stereochemistry occurs after ring-opening of the

isoxazolidine. Additionally, the reaction appeared to proceed at a much greater rate than when the isoxazolidine **53** was used as the starting material. A repeat of this reaction under milder conditions confirmed this to be the case with 20% of **64** formed and 20% **65** remaining after only 10 minutes at room temperature (Scheme 54). For comparison 60% starting material remained after 1.5 hours at 70 °C when **53** was reacted with the same silane and catalyst loadings (Table 7 entry 2).

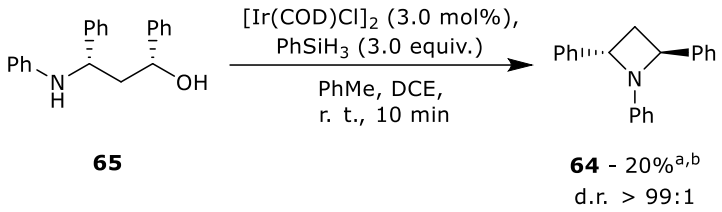

*Scheme 54: Synthesis of azetidine **64** from amino alcohol **65**. [a]Yield determined by ^{1}H NMR spectroscopy relative to TCE internal standard; [b]20% **65** remaining.*

This accelerated rate of reaction strongly suggests that breaking the N,O-bond of the isoxazolidine is the rate limiting step of the reaction. The non-linear relationship between starting material consumption and product formation was also apparent for the reaction of **65**. Therefore, the unknown pathway(s) responsible for the mass imbalance must occur after ring-opening of the isoxazolidine. Polymerisation of the azetidine product (**64**), as described in section 1.3.3.2.2, being one such theory supported by this evidence. In addition to the possible polymerisation of the azetidine product, the 1,3 amino alcohol **65** could also polymerise via intermolecular displacement of the di-silylated alcohol (**128** Scheme 51).

In order to solubilise **65** the reaction had to be performed in a 1:1 PhMe:DCE mixture and not pure PhMe as for previous reactions of **53**. Therefore, to confirm the previous conclusions made were valid, the ring

contraction of **53** was carried out also in a 1:1 PhMe:DCE mixture (Table 19).

*Table 19: Synthesis of **64** using optimised conditions from Table 3 entry 5 with TCE internal standard.*

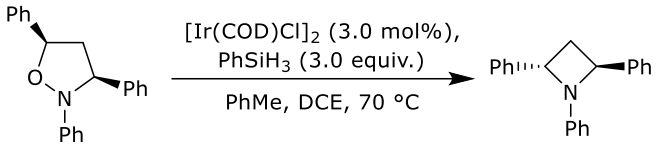

53 **64**

Entry	Time / h	**53** / %[a]	**64** / %[a]	Deficit[b] / %
1	1.5	69	9	22
2	3.0	63	11	26
3	5.0	57	14	29
4	22	37	21	42

*[a]Yields determined by ^{1}H NMR spectroscopy using TCE as an internal standard; [b]Unexplained loss of starting material determined by 100 – (% of **53** + % of **64**).*

Synthesis of **64** was successful when using a PhMe:DCE mixture, albeit with a lower conversion after 22 hours than when the reaction was performed in PhMe alone (Table 4 entry 2). This reflects the lower conversion seen in Scheme 54 for the amino alcohol **65**, suggesting the solvent is responsible. Polymerisation of *N*-phenylazetidine occurs *via* a cationic ring opening mechanism (Scheme 39), a process which is accelerated in polar solvents. Consequently, the use of DCM in the reductive ring contraction of **53** may have decreased the yield of **64** by favouring polymerisation.

1.4 Conclusions and Outlook

A novel, convergent, synthesis route to azetidines was hypothesized *via* the reductive ring contraction of isoxazolidines. Initially, it was hoped to use a variation of the dioxyphosphorane-mediated cyclodehydration methodology as described in chapter one. However, this proved unsuccessful with only amino alcohols isolated from the ring-opening of the isoxazolidine. Consequently, an alternative reductive system was required.

By using $[Ir(COD)Cl]_2$ in combination with phenylsilane the desired azetidine product was obtained. Subsequent work to optimise the reaction conditions was undertaken, resulting in a significant increase in yield. Further progress was hindered by unidentified side reactions and product instability. Nine alternative substrates were prepared, four of which were successfully contracted to the corresponding azetidines.

Investigations into the mechanism of the reaction revealed the reaction likely proceeds *via* an amino alcohol, obtained by ring-opening the isoxazolidine. The novel transformation was also found to proceed with inversion of stereochemistry, which is substrate controlled.

Further work on this exciting new methodology is currently underway within the group. In addition to a comprehensive screen of alternative catalysts and silanes, reductive ring contractions of different ring systems are being explored.

1.5 Experimental

1.5.1 General Experimental Procedures

Unless stated otherwise, all reactions were carried out under an atmosphere of argon. All glassware was flame dried or oven dried and allowed to cool under a stream of argon before use. Cooling to 0 °C was effected using an ice-water bath. Cooling to temperatures below 0 °C was effected using dry ice-acetone mixtures. The term petroleum ether refers to the fraction with boiling point of 40 to 60 °C.

Commercially available solvents and reagents were used as supplied with the following exceptions. Toluene, THF and diethyl ether were collected from a solvent tower, where a degassed solvent was passed through two columns of activated alumina and a 7 micron filter under a 4 bar pressure. $CHCl_3$ was stirred with phosphorus pentoxide for 2 h, distilled and stored under an argon atmosphere over activated 4 Å molecular sieves. Reactions were monitored using thin layer chromatography on Merck TLC silica gel 60 F_{254} pre-coated aluminium sheets with fluorescent indicator. Sheets were visualised using ultra-violet light (254 nm) and/or $KMnO_4$ solution, as appropriate. Flash column chromatography was performed using Aldrich silica gel 60, 40–63 μm.

Compounds for which characterisation data matches literature values are denoted by a reference next to the compound name. IR and m. p. data has only been recorded for novel compounds.

Infrared spectra were recorded on the ATR module of a Bruker Alpha spectrometer. Mass spectra were acquired on a Bruker Micromass LCTOF.

Bruker DPX 300, Bruker DPX 400, Bruker AV 400, Bruker AV (III) 400, Bruker AV (III) 400HD or Bruker AV 500 spectrometers were used to record all ^{1}H, ^{13}C, ^{19}F and ^{31}P NMR spectra of dilute solutions of the appropriate compound in the indicated deuterated solvent. All chemical shifts (δ) are reported in parts per million (ppm) relative to residual chloroform (δ_H = 7.26 ppm, δ_C = 77.2 ppm) or benzene (δ_H = 7.16 ppm, δ_C = 128.1 ppm). Coupling constants (*J*) are reported in Hertz and are recorded after averaging. The multiplicity of a ^{1}H NMR signal is designated by one of the following abbreviations: s = singlet, d = doublet, t = triplet, q = quartet and m = multiplet. Where given, reaction conversions were determined by the relative ^{1}H integrations of the product and the appropriate starting material.

Relaxation delays were not measured for solution phase ^{31}P NMR spectroscopy. Consequently, ^{31}P NMR integrals cannot be considered quantitative.

1.5.2 Experimental Data of Compounds

N-Phenylhydroxylamine (**54**)[48]

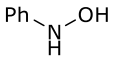

To a solution of nitrobenzene (1.23 g, 10.0 mmol) in dry THF (20 mL) at 0 °C was added 5 wt% Rh/C (25 mg, 0.10 mol% Rh) then hydrazine monohydrate (580 µL, 12.0 mmol) dropwise over 5 min. The reaction mixture was stirred at r. t. for 3 hours then filtered through a pad of celite and concentrated *in vacuo*. Recrystallisation from DCM/petroleum ether gave **54** (683 mg, 63%) as a white solid.

^{1}H NMR (400 MHz, $CDCl_3$) δ 7.33 – 7.25 (m, 2H), 7.04 – 6.93 (m, 3H); **^{13}C{^{1}H} NMR** (101 MHz, $CDCl_3$) δ 149.4, 129.0, 122.6, 114.9; **HRMS** (ESI$^+$) $C_6H_8NO^+$ $[M+H]^+$ calcd. 110.0600, found 110.0602.

(*Z*)-*N*-Benzylidenebenzenamine oxide (**55**)[48]

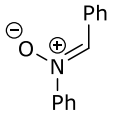

To a solution of *N*-phenylhydroxylamine (**54**) (1.93 g, 17.7 mmol) in ethanol (22 mL) was added benzaldehyde (1.79 mL, 17.7 mmol). The resulting solution was stirred at r. t. for 18 hours before being cooled to 0 °C. The resulting solids were collected by filtration and recrystalised from minimal hot ethanol to give **55** (2.86 g, 82%) as a white solid.

^{1}H NMR (400 MHz, $CDCl_3$) δ 8.44 – 8.37 (m, 2H), 7.93 (s, 1H), 7.82 – 7.75 (m, 2H), 7.54 – 7.43 (m, 6H); **^{13}C{^{1}H} NMR** (101 MHz, $CDCl_3$) δ 149.1, 134.6, 131.0, 130.7, 129.9, 129.2, 129.1, 128.7, 121.8; **HRMS** (ESI^+) $C_{13}H_{12}NO^+$ $[M+H]^+$ calcd. 198.0913, found 198.0916.

cis-2,3,5-Triphenylisoxazolidine (**53**)[49]

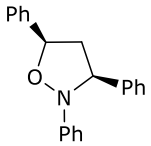

To (*Z*)-*N*-benzylidenebenzenamine oxide (**55**) (1.78 g, 9.00 mmol) was added styrene (4.45 mL, 38.7 mmol). The reaction mixture was heated to 60 °C for 40 hours then concentrated *in vacuo*. Recrystallisation from DCM/methanol gave **53** (2.42 g, 89%, >99:1 d.r.) as a white solid.

^{1}H NMR (400 MHz, $CDCl_3$) δ 7.60 – 7.53 (m, 2H), 7.48 – 7.23 (m, 10H), 7.11 – 7.03 (m, 2H), 6.98 – 6.91 (m, 1H), 5.19 (dd, *J* = 10.1, 5.7, 1H), 4.94 (apparent t, *J* = 7.9, 1H), 3.20 (ddd, *J* = 12.2, 7.9, 5.7, 1H), 2.49 (ddd, *J* = 12.2, 10.1, 7.9, 1H); **^{13}C{^{1}H} NMR** (101 MHz, $CDCl_3$) δ 152.7, 143.0, 138.0, 129.1, 129.0, 128.7, 128.5, 127.5, 127.0, 126.4, 121.5, 114.1, 80.7, 71.7, 48.9; **HRMS** (ESI^+) $C_{21}H_{20}NO^+$ $[M+H]^+$ calcd. 302.1539, found 302.1541.

3-(Phenylamino)propan-1-ol (**66**)[50]

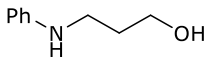

To a neat solution of iodobenzene (560 μL, 5.00 mmol) and 3-amino-1-propanol (1.15 mL, 15.0 mmol) was added copper(I) chloride (50 mg, 0.50 mmol) and potassium hydroxide (561 mg, 10.0 mmol). The resulting suspension was stirred at r. t. for 18 hours then diluted with water (10 mL) and the mixture extracted with DCM (4 × 50 mL). The combined organic extracts were dried ($MgSO_4$) and concentrated *in vacuo*. Flash column chromatography (2:1, petroleum ether/EtOAc) gave **66** (686 mg, 91%) as a brown oil.

^{1}H NMR (400 MHz, $CDCl_3$) δ 7.23 – 7.16 (m, 2H), 6.76 – 6.70 (m, 1H), 6.69 – 6.62 (m, 2H), 3.79 (t, *J* = 5.9, 2H), 3.27 (t, *J* = 6.5, 2H), 3.05 (br, 2H), 1.87 (apparent p, *J* = 6.3, 2H); **^{13}C{^{1}H} NMR** (101 MHz, $CDCl_3$) δ 148.4, 129.4, 117.7, 113.2, 61.6, 42.0, 32.0; **HRMS** (ESI^+) $C_9H_{14}NO^+$ $[M+H]^+$ calcd. 152.1070, found 152.1079.

2,2,2-Triphenyl-2λ5-phenanthro[9,10-*d*][1,3,2]dioxaphospholane (**57**)[51]

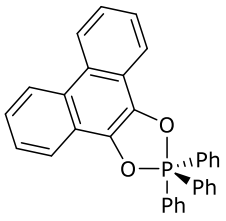

To a solution of triphenylphosphine (2.62 g, 10.0 mmol) in dry toluene (23 mL), in a Schlenk flask, was added 9,10-phenanthrenequinone (2.08 g, 10.0 mmol). The resulting solution was heated to 70 °C for 18 hours to

give **57** as a stock solution (94% purity by ^{31}P NMR). Used *in situ* without purification or further characterisation.

^{31}P{^{1}H} NMR (162 MHz, C_6D_6) δ −16.4.

(Note: ^{1}H and ^{13}C peaks could not be distinguished from toluene solvent.)

3-(Benzylamino)propan-1-ol (**72**)[52]

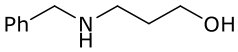

To a solution of benzaldehyde (1.02 mL, 10.0 mmol) in methanol (50 mL) was added 3-amino-1-propanol (765 µL, 10.0 mmol) and the reaction mixture stirred at r. t. for 18 hours. The reaction mixture was cooled to 0 °C and sodium borohydride (454 mg, 12.0 mmol) was added portionwise over 15 min. The reaction mixture was then stirred at r. t. for 3 hours before being concentrated *in vacuo*. To the reside was added water (50 mL) and the resulting suspension was then extracted with DCM (3 × 50 mL). The combined organic extracts were dried ($MgSO_4$) and concentrated *in vacuo* to give **72** (1.71 g, 86%) as a colourless oil.

^{1}H NMR (400 MHz, $CDCl_3$) δ 7.41 – 7.23 (m, 5H), 3.83 (t, *J* = 5.3, 2H), 3.81 (s, 2H), 3.05 (br, 2H), 2.92 (t, *J* = 5.8, 2H), 1.74 (apparent p, *J* = 5.5, 2H) ; **^{13}C{^{1}H} NMR** (101 MHz, $CDCl_3$) δ 139.7, 128.6, 128.3, 127.3, 65.4, 54.1, 48.5, 31.3.; **HRMS** (ESI^+) $C_{10}H_{15}NNaO^+$ $[M+Na]^+$ calcd. 188.1046, found 188.1044.

(*Z*)-*N*-Benzyl-1-phenylmethanimine oxide (**75**)[53]

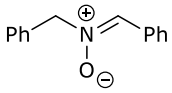

To a solution of sodium tungstate dihydrate (330 mg, 1.00 mmol) in methanol (14 mL) at 0°C was added dibenzylamine (1.92 mL, 10.0 mmol) then aqueous hydrogen peroxide (35% w/v, 2.58 mL, 30.0 mmol) dropwise over 10 min. The reaction mixture was stirred at 0°C for 15 min then r. t. for 18 hours. The reaction mixture was then concentrated *in vacuo*. The resulting aqueous solution was diluted with water (10 mL) and extracted with DCM (3 × 10 mL). The combined organic extracts were dried (Na_2SO_4) and concentrated *in vacuo*. Recrystallisation from Et_2O gave **75** (1.57 g, 74%) as a white solid.

^{1}H NMR (400 MHz, $CDCl_3$) δ 8.24 – 8.16 (m, 2H), 7.52 – 7.35 (m, 9H), 5.07 (s, 2H); **^{13}C{^{1}H} NMR** (101 MHz, $CDCl_3$) δ 134.4, 133.3, 130.6, 130.5, 129.3, 129.1, 128.7, 128.6, 127.0, 71.4; **HRMS** (ESI^+) $C_{14}H_{14}NO^+$ $[M+H]^+$ calcd. 212.1070, found 212.1067.

cis-2-Benzyl-3,5-diphenylisoxazolidine (**76**)[54]

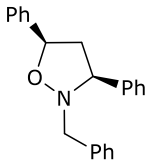

To a solution of (*Z*)-*N*-benzyl-1-phenylmethanimine oxide (**75**) (634 mg, 3.00 mmol) in benzene (15 mL) was added styrene (3.45 mL, 30.0 mmol). The reaction mixture was heated to reflux for 48 hours and then concentrated *in vacuo*. Flash column chromatography (4:1, petroleum ether/EtOAc) gave **76** (712 mg, 75%, 74:26 d.r.) as a white solid.

^{1}H NMR (400 MHz, $CDCl_3$) δ 7.53 – 7.19 (m, 15H), 5.32 – 5.22(m, 1H), 4.10 (d, *J* = 14.3, 1H), 4.13 – 4.06 (m, 1H, major), 4.00 (apparent t, *J* = 8.3, 1H, minor), 3.91 (d, *J* = 14.3, 1H), 3.15 (ddd, 12.4, 7.6, 7.1, 1H, major), 2.74 (apparent dt, *J* = 12.4, 8.5, 1H, minor), 2.59 (ddd, *J* = 12.4, 8.3, 6.3, 1H, minor), 2.42 (ddd, *J* = 12.4, 9.3, 7.5, 1H, major); **^{13}C{^{1}H} NMR** (101 MHz, $CDCl_3$, both diastereomers) δ 143.2, 139.9, 137.9, 137.5, 129.2, 129.0, 128.8, 128.8, 128.6, 128.5, 128.3, 128.0, 127.9, 127.8, 127.3, 127.2, 127.2, 126.7, 126.2, 78.8, 78.4, 71.1, 70.4, 60.4, 60.2, 48.6, 47.7; **HRMS** (ESI$^+$) $C_{22}H_{21}NNaO^+$ $[M+Na]^+$ calcd. 338.1515, found 338.1515.

trans-1,2,4-Triphenylazetidine (**64**)[55]

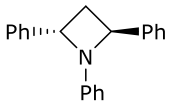

To a solution of *cis*-2,3,5-triphenylisoxazolidine (**53**) (151 mg, 0.500 mmol) and $[Ir(cod)Cl]_2$ (10 mg, 3.0 mol%) in toluene (1 mL) was added phenylsilane (185 µL, 1.50 mmol). The reaction mixture was heated to 70 °C for 22 hours before silica gel (2 g) was added. The resulting solid was then filtered and washed with a 19:1 petroleum ether/EtOAc mixture (100 mL). The filtrate was concentrated *in vacuo* and recrystalised from pentane to give **64** (59 mg, 41%, >99:1 d.r.) as a white solid.

^{1}H NMR (400 MHz, $CDCl_3$) δ 7.49 – 7.22 (m, 10H), 7.05 – 6.96 (m, 2H), 6.58 (m, 2H), 6.23 – 6.16 (m, 2H), 5.52 (t, *J* = 6.8, 2H), 2.71 (t, *J* = 6.8, 2H); **^{13}C{^{1}H} NMR** (101 MHz, $CDCl_3$) δ 146.4, 142.7, 128.9, 128.7, 127.5, 126.6, 116.4, 112.0, 64.1, 38.2; **HRMS** (ESI$^+$) $C_{21}H_{20}N^+$ $[M+H]^+$ calcd. 286.1590, found 286.1604.

cis-2,3-Diphenyl-5-(pyridin-2-yl)isoxazolidine (**91**)

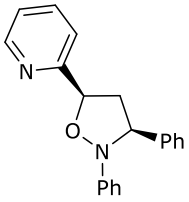

To solution of (*Z*)-*N*-benzylidenebenzenamine oxide (**55**) (592 mg, 3.00 mmol) in toluene (1.5 mL) was added 2-vinylpyridine (647 µL, 6.00

mmol). The reaction mixture was heated to 60 °C for 18 hours then concentrated *in vacuo*. Flash column chromatography (9:1, petroleum ether/EtOAc) gave **91** (846 mg, 93%, 68:32 d.r.) as a white solid.

^{1}H NMR (400 MHz, $CDCl_3$) δ 8.62 – 8.54 (m, 1H), 7.72 (apparent qd, *J* = 7.5, 1.8, 1H), 7.68 – 7.47 (m, 3H), 7.44 – 7.18 (m, 6H), 7.14 – 7.08 (m, 1H), 7.05 – 6.92 (m, 2H), 5.53 (apparent t, *J* = 7.1, 1H, minor), 5.41 (dd, *J* = 8.2, 7.0, 1H, major), 4.88 (apparent t, *J* = 7.7, 1H, major), 4.70 (dd, *J* = 8.4, 5.9, 1H, minor), 3.36 (ddd, *J* = 12.4, 8.2, 6.9, 1H, major), 3.09 (ddd, *J* = 12.3, 8.4, 7.0, 1H, minor), 2.87 (ddd, *J* = 12.3, 7.2, 5.9, 1H, minor), 2.68 (ddd, *J* = 12.4, 8.3, 7.2, 1H, major); **^{13}C{^{1}H} NMR** (101 MHz, $CDCl_3$, both diastereomers) δ 159.5, 159.3, 151.9, 150.6, 149.3, 149.2, 142.4, 141.7, 136.9, 136.8, 129.0, 129.0, 128.9, 128.6, 127.7, 127.5, 127.0, 126.6, 122.9, 122.1, 122.0, 121.4, 120.8, 116.2, 114.9, 80.6, 79.8, 71.1, 69.0, 47.0, 45.9; **HRMS** (ESI^+) $C_{20}H_{19}N_2O^+$ $[M+H]^+$ calcd. 303.1492, found 303.1494; **AT-IR** (neat) ν (cm^{-1}) 3054, 2905, 1590, 1486, 1449, 1436, 1374, 1350, 1296, 1250, 1177, 1151, 1027, 992, 913, 883, 858, 831; **m. p.** 71 – 75 °C.

<u>*cis*-5-(4-Bromophenyl)-2,3-diphenylisoxazolidine (**92**)</u>

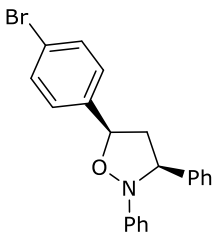

To solution of (*Z*)-*N*-benzylidenebenzenamine oxide (**55**) (249 mg, 1.26 mmol) in toluene (0.5 mL) was added 4-bromostyrene (330 μL, 2.52 mmol). The reaction mixture was heated to 60 °C for 18 hours then

concentrated *in vacuo*. Flash column chromatography (19:1, petroleum ether/EtOAc) gave **92** (352 mg, 73%, 94:6 d.r.) as a white solid.

^{1}H NMR (400 MHz, $CDCl_3$) δ 7.56 – 7.46 (m, 4H), 7.43 – 7.37 (m, 2H), 7.33 – 7.23 (m, 5H), 7.08 – 7.03 (m, 2H), 6.99 – 6.91 (m, 1H), 5.35 – 5.29 (m, 1H, minor), 5.16 (dd, *J* = 9.8, 6.0, 1H, major), 4.92 (apparent t, *J* = 7.8, 1H, major), 4.69 (dd, *J* = 8.7, 4.9 Hz, 1H, minor), 3.19 (ddd, *J* = 12.2, 8.0, 6.0, 1H, major), 2.79 – 2.64 (m, 1H, minor), 2.43 (ddd, *J* = 12.2, 9.8, 7.6, 1H, major); **^{13}C{^{1}H} NMR** (101 MHz, $CDCl_3$, both diastereomers) δ 152.4, 142.7, 137.4, 131.9, 129.2, 129.0, 128.6, 127.6, 126.4, 122.4, 121.8, 114.2, 79.9, 78.3, 71.5, 69.7, 48.8, 47.4; **HRMS** (ESI^+) $C_{21}H_{19}BrNO^+$ $[M+H]^+$ calcd. 380.0645, found 380.0655; **AT-IR** (neat) ν (cm^{-1}) 3033, 2983, 2891, 2120, 1901, 1595, 1485, 1448, 1410, 1351, 1284, 1220, 1179, 1072, 1027, 1009, 963, 935, 903, 885, 817; **m. p.** 118 – 121 °C.

Note: Only the aliphatic signals of the minor diastereomer could be identified in the ^{13}C NMR.

Diethyl 2,3-diphenylisoxazolidine-4,5-(*trans*)-dicarboxylate (**93**)[56]

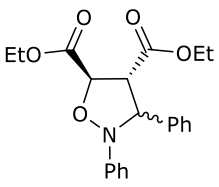

93

To (*Z*)-*N*-benzylidenebenzenamine oxide (**55**) (394 mg, 2.00 mmol) was added diethyl fumarate (1.41 mL, 8.60 mmol). The reaction mixture was

heated to 60 °C for 18 hours then concentrated *in vacuo*. Flash column chromatography (9:1, petroleum ether/EtOAc) gave **93** (500 mg, 68%, 97:3 d.r.) as a brown oil.

^{1}H NMR (400 MHz, $CDCl_3$) δ 7.49 (m, 2H), 7.39 – 7.28 (m, 3H), 7.20 (m, 2H), 7.05 – 6.95 (m, 3H), 5.10 (d, *J* = 4.7, 1H), 4.80 (d, *J* = 6.3, 1H), 4.29 (q, *J* = 7.1, 2H), 4.17 (apparent dq, *J* = 7.1, 5.1, 2H), 3.97 (dd, *J* = 6.3, 4.7, 1H), 1.31 (t, *J* = 7.1, 3H), 1.22 (t, *J* = 7.1, 3H); **^{13}C{^{1}H} NMR** (101 MHz, $CDCl_3$) δ 170.5, 170.0, 149.1, 139.5, 129.0, 128.8, 128.2, 127.2, 123.6, 117.1, 77.8, 72.8, 62.0, 61.9, 60.8, 14.3, 14.2; **HRMS** (ESI^+) $C_{21}H_{24}NO_5^+$ $[M+H]^+$ calcd. 370.1649, found 370.1654.

Note: Only peaks of the major diastereomer are reported.

N-(4-(Trifluoromethyl)phenyl)hydroxylamine (**94**)[57]

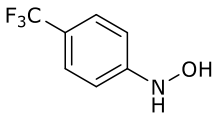

To a solution of 4-nitrobenzotrifluoride (1.91 g, 10.0 mmol) in THF (20 mL) at 0 °C was added 5 wt% Rh/C (25 mg, 0.10 mol% Rh), then hydrazine monohydrate (580 µL, 12.0 mmol) dropwise over 5 min. The reaction mixture was stirred at r. t. for 3 hours then filtered through a pad of celite and concentrated *in vacuo*. Recrystallisation from DCM/petroleum ether gave **94** (1.63 g, 92%) as a white solid.

^{1}H NMR (400 MHz, $CDCl_3$) δ 7.53 (d, *J* = 8.4, 2H), 7.04 (d, *J* = 8.4, 2H), 6.94 (br, 1H), 5.46 (br, 1H); **^{13}C{^{1}H} NMR** (101 MHz, $CDCl_3$) δ 152.7, 126.5 (q, *J* = 3.8), 124.6 (q, *J* = 271.2), 124.1 (q, *J* = 32.6), 113.8; **^{19}F NMR** (376 MHz, $CDCl_3$) δ −61.7 (s); **HRMS** (ESI^-) $C_7H_5F_3NO^-$ $[M-H]^-$ calcd. 176.0329, found 176.0330.

(*Z*)-1-Phenyl-*N*-(4-(trifluoromethyl)phenyl)methanimine oxide (**95**)[57]

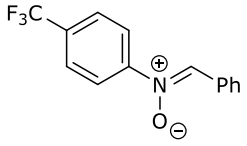

To a suspension of benzaldehyde (767 μL, 7.23 mmol) and $MgSO_4$ (957 mg, 7.95 mmol) in DCM (13 mL) was added *N*-(4-(trifluoromethyl)phenyl)hydroxylamine (**94**) (1.28 g, 7.23 mmol). The resulting suspension was stirred at r. t. for 2 hours then filtered and concentrated *in vacuo*. Trituration with petroleum ether gave **95** (1.74 g, 90%) as an impure white solid containing 4% benzaldehyde. Product used immediately without further purification or characterisation.

^{1}H NMR (400 MHz, $CDCl_3$) δ 8.48 – 8.39 (m, 2H), 7.98 (s, 1H), 7.95 (d, *J* = 8.4, 2H), 7.80 (d, *J* = 8.5, 2H), 7.57 – 7.49 (m, 2H).

cis-3,5-Diphenyl-2-(4-(trifluoromethyl)phenyl)isoxazolidine (**96**)

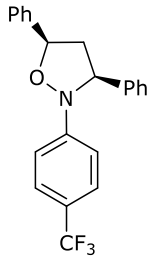

To a solution of (*Z*)-1-phenyl-*N*-(4-(trifluoromethyl)phenyl)methanimine oxide (**95**) (796 mg, 3.00 mmol) in THF (5 mL) was added styrene (690 µL, 6.00 mmol). The reaction mixture was heated to 60 °C for 18 hours then concentrated *in vacuo*. Flash column chromatography (19:1, petroleum ether/EtOAc) then recrystallisation from methanol gave **96** (833 mg, 75%, 92:8 d.r.) as a white solid.

^{1}H NMR (400 MHz, $CDCl_3$) δ 7.57 – 7.30 (m, 12H), 7.09 (d, *J* = 8.5, 2H, major), 7.01 (d, *J* = 8.4, 2H, minor), 5.39 (dd, *J* = 9.0, 6.3, 1H, minor), 5.14 (dd, *J* = 10.4, 5.5, 1H, major), 4.94 (apparent t, *J* = 8.0, 1H, major), 4.79 (dd, *J* = 9.1, 4.2, 1H, minor), 3.23 (ddd, *J* = 12.3, 8.0, 5.5, 1H, major), 2.85 (apparent dt, *J* = 12.2, 9.1, 1H, minor), 2.69 (ddd, *J* = 12.2, 6.3, 4.2, 1H, minor), 2.52 (ddd, *J* = 12.3, 10.4, 8.1, 1H, major); **^{13}C{^{1}H} NMR** (126 MHz, $CDCl_3$, both diastereomers) δ 155.1, 152.9, 142.3, 141.9, 138.5, 137.2, 129.2, 129.2, 128.8, 128.8, 128.5, 128.0, 127.8, 127.0, 126.8, 126.6, 126.4 (q, *J* = 3.8), 126.2, 126.0 (q, *J* = 3.7), 124.7 (q, *J* = 271.0), 123.1 (q, *J* = 32.6), 123.0 (q, *J* = 32.5), 114.7, 113.4, 81.2 (major), 79.2 (minor), 71.2 (major), 69.0 (minor), 48.9 (major), 47.3 (minor); **^{19}F NMR** (376 MHz, $CDCl_3$) δ −61.53 (3F, major), −61.59 (3F, minor); **HRMS** (ESI$^+$) $C_{22}H_{19}F_3NO^+$ $[M+H]^+$ calcd. 370.1413, found

370.1429; **AT-IR** (neat) ν (cm^{-1}) 3062, 3030, 2948, 2891, 2868, 1613, 1511, 1496, 1454, 1421, 1382, 1326, 1300, 1261, 1183, 1157, 1116, 1091, 1067, 1023, 1006, 940, 904, 863, 836, 826; **m. p.** 91– 94°C.

(*Z*)-*N*-(4-Methoxyphenyl)-1-phenylmethanimine oxide (**97**)[58]

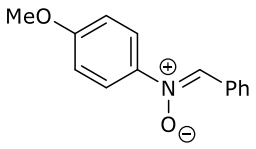

To a solution of 4-nitroanisole (1.53 g, 10.0 mmol) in a 1:1 ethanol/water mixture (70 mL) was added ammonium chloride (695 mg, 13.0 mmol) and benzaldehyde (1.02 mL, 10.0 mmol). The reaction mixture was stirred at r. t. for 5 min then zinc powder (1.31 g, 20.0 mmol) was added portionwise over 1 hour. The resulting suspension was stirred at r. t. for 18 hours then filtered through a pad of celite, diluted with water (100 mL) and extracted with DCM (3 × 100 mL). The combined organic extracts were dried ($MgSO_4$) and concentrated *in vacuo*. Recrystallisation from DCM/petroleum ether gave **97** (1.20 g, 52%) as a white solid.

^{1}H NMR (400 MHz, $CDCl_3$) δ 8.43 – 8.34 (m, 2H), 7.88 (s, 1H), 7.78 – 7.69 (m, 2H), 7.58 – 7.41 (m, 3H), 7.01 – 6.90 (m, 2H), 3.87 (s, 3H); **^{13}C{^{1}H} NMR** (101 MHz, $CDCl_3$) δ 160.8, 142.6, 133.8, 131.0, 130.9, 129.1, 128.8, 123.1, 114.2, 55.8; **HRMS** (ESI^+) $C_{14}H_{14}NO_2^+$ $[M+H]^+$ calcd. 228.1019, found 228.1015.

N-Isopropylpropan-2-imine oxide (**99**)[59]

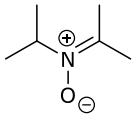

To a solution of sodium tungstate dihydrate (132 mg, 0.400 mmol) and diisopropylamine (1.40 mL, 10.0 mmol) in methanol (20 mL) at 0°C was added aqueous hydrogen peroxide (30% w/v, 3.01 mL, 30.0 mmol) dropwise over 10 min. The reaction mixture was stirred at r. t. for 18 hours then concentrated *in vacuo*. The resulting aqueous solution was diluted with DCM (100 mL), washed with brine (3 × 40 mL), dried (Na_2SO_4) and concentrated *in vacuo* to give **99** (602 mg, 69% pure) as a colourless oil. Product was unstable and used immediately without further purification or characterisation.

^{1}H NMR (400 MHz, $CDCl_3$) δ 4.46 (hept, *J* = 6.4, 1H), 2.15 (s, 3H), 2.13 (s, 3H), 1.36 (d, *J* = 6.4, 6H).

2-Isopropyl-3,3-dimethyl-5-phenylisoxazolidine (**101**)[60]

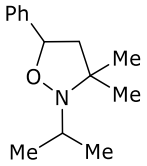

To impure *N*-isopropylpropan-2-imine oxide (**99**) (288 mg, 1.73 mmol) was added styrene (1.24 mL, 10.8 mmol). The reaction mixture was heated to 60 °C for 96 hours then concentrated *in vacuo*. Flash column

chromatography (19:1 to 9:1, petroleum ether/EtOAc) gave **101** (135 mg, 36%) as a colourless oil.

^{1}H NMR (400 MHz, $CDCl_3$) δ 7.38 (m, 2H), 7.32 (m, 2H), 7.24 (m, 1H), 4.98 (apparent t, *J* = 8.1, 1H), 3.11 (apparent hept, *J* = 6.2, 1H), 2.53 (dd, *J* = 12.2, 8.5, 1H), 2.13 (dd, *J* = 12.2, 7.8, 1H), 1.33 (s, 3H), 1.29 (s, 3H), 1.21 (d, *J* = 6.2, 3H), 1.20 (d, *J* = 6.2, 3H); **^{13}C{^{1}H} NMR** (101 MHz, $CDCl_3$) δ 142.4, 128.5, 127.3, 126.1, 76.3, 63.8, 54.9, 51.9, 25.2, 24.8, 22.2, 22.1; **HRMS** (ESI$^+$) $C_{14}H_{22}NO^+$ $[M+H]^+$ calcd. 220.1708, found 220.1696.

trans-Diethyl 2,3-diisopropylisoxazolidine-4,5-dicarboxylate (**102**)

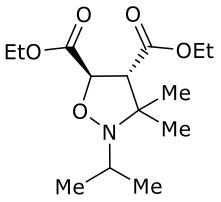

To impure *N*-isopropylpropan-2-imine oxide (**99**) (266 mg, 1.59 mmol) was added diethyl fumarate (1.62 mL, 9.89 mmol). The reaction mixture was heated to 60 °C for 96 hours then concentrated *in vacuo*. Flash column chromatography (9:1 to 4:1, petroleum ether/EtOAc) gave **102** (215 mg, 47%) as a colourless oil.

^{1}H NMR (400 MHz, $CDCl_3$) δ 4.78 (d, *J* = 6.3, 1H), 4.31 – 4.12 (m, 4H), 3.43 (d, *J* = 6.3, 1H), 3.03 (apparent hept, *J* = 6.3, 1H), 1.43 (s, 3H), 1.30 (t, *J* = 7.1, 3H), 1.27 (t, *J* = 7.1 Hz, 3H), 1.22 (d, *J* = 6.1, 3H), 1.09

(d, *J* = 6.5, 3H), 1.08 (s, 3H); **^{13}C{^{1}H} NMR** (101 MHz, $CDCl_3$) δ 172.2, 170.3, 74.8, 66.3, 63.1, 61.4, 51.5, 25.9, 22.5, 20.9, 16.8, 14.4, 14.3.; **HRMS** (ESI$^+$) $C_{14}H_{26}NO_5^+$ $[M+H]^+$ calcd. 288.1819, found 288.1805; **AT-IR** (neat) ν (cm^{-1}) 2980, 2937, 1789, 1732, 1615, 1466, 1369, 1325, 1184, 1116, 1095, 1026, 858.

Hex-5-enal (**103**)[61]

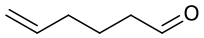

To a solution of oxalyl chloride (1.27 mL, 15.0 mmol) in DCM (24 mL) at −78 °C was added dimethyl sulfoxide (2.13 mL, 30.0 mmol) dropwise over 5 min. The reaction mixture was stirred for 10 min before hexen-1-ol (1.20 mL, 10.0 mmol) in DCM (3.5 mL) was added at −78 °C dropwise over 10 min. The reaction mixture was stirred at r. t. for 1 hour then cooled to −78 °C before triethylamine (4.18 mL, 30.0 mmol) was added dropwise over 10 min. The reaction mixture was then diluted with water (30 mL) and extracted with DCM (3 × 30 mL). The combined organic extracts were dried ($MgSO_4$) and concentrated *in vacuo*. Flash column chromatography (10:1, pentane/Et_2O) gave **103** (174 mg, 18%) as a 58% w/w solution in Et_2O.

^{1}H NMR (400 MHz, $CDCl_3$) δ 9.77 (t, *J* = 1.7, 1H), 5.77 (ddt, *J* = 17.0, 10.2, 6.7, 1H), 5.10 – 4.93 (m, 2H), 2.45 (td, *J* = 7.3, 1.7, 2H), 2.15 – 2.05 (m, 2H), 1.74 (p, *J* = 7.4, 2H); **^{13}C{^{1}H} NMR** (101 MHz, $CDCl_3$) δ 202.6, 137.7, 115.7, 43.3, 33.1, 21.3.

cis-1-Phenylhexahydro-1H-cyclopentaisoxazole (**105**)

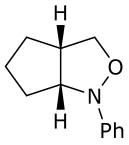

To *N*-phenylhydroxylamine (**54**) (193 mg, 1.77 mmol) was added hex-5-enal (**103**) (174 mg, 1.77 mmol) in Et_2O (190 µL) and ethanol (2.2 mL). The reaction mixture was stirred at r. t. for 18 hours then 60 °C for 96 hours before being concentrated *in vacuo*. Flash column chromatography (19:1, pentane/ Et_2O) gave **105** (165 mg, 49%) as a colourless oil.

^{1}H NMR (400 MHz, $CDCl_3$) δ 7.31 – 7.22 (m, 2H), 7.05 – 7.00 (m, 2H), 6.93 (tt, *J* = 7.5, 1.1, 1H), 4.11 (apparent dt, *J* = 8.1, 5.2, 1H), 4.02 (dd, *J* = 8.4, 7.4, 1H), 3.68 (dd, *J* = 8.4, 3.8, 1H), 3.04 (m, 1H), 1.97 – 1.87 (m, 2H), 1.89 – 1.73 (m, 2H), 1.63 (apparent tt, *J* = 11.0, 4.8, 2H); **^{13}C{^{1}H} NMR** (101 MHz, $CDCl_3$) δ 151.0, 129.0, 121.4, 114.8, 73.2, 71.4, 48.5, 33.9, 32.2, 25.7; **HRMS** (ESI^+) $C_{12}H_{16}NO^+$ $[M+H]^+$ calcd. 190.1226, found 190.1233.

trans-1-(4-Methoxyphenyl)-2,4-diphenylazetidine (**111**)[55]

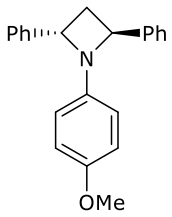

To a solution of (*Z*)-*N*-(4-methoxyphenyl)-1-phenylmethanimine oxide (**97**) (227 mg, 1.00 mmol) in THF (1.7 mL) was added styrene (230 µL, 2.00 mmol). The reaction mixture was heated to 80 °C for 20 hours then concentrated *in vacuo* at 80 °C. The resulting residue was dissolved in toluene (2 mL) and TCE added (106 µL, 1.00 mmol). A reference NMR was taken to determine isoxazoldine concentration prior to further additions (38% conversion relative to TCE internal standard by ^{1}H NMR sepctroscopy). To the resulting solution was added $[Ir(cod)Cl]_2$ (11 mg, 3.0 mol%) and phenylsilane (141 µL, 1.14 mmol). The reaction was heated to 70 °C for 5 hours then concentrated *in vacuo*. Flash column chromatography (98:2, pentane/ Et_2O) gave **111** (27 mg, 9%, 80:20 d.r.) as a colourless oil.

^{1}H NMR (400 MHz, $CDCl_3$) δ 7.63 – 7.58 (m, 1H), 7.46 – 7.29 (m, 7H), 7.29 – 7.22 (m, 2H), 6.71 – 6.65 (m, 2H), 6.61 – 6.55 (m, 2H), 6.43 – 6.38 (m, 2H), 6.14 – 6.08 (m, 2H), 4.80 (apparent t, *J* = 8.0, 2H, minor), 3.69 (s, 3H, minor), 3.64 (s, 3H, major), 3.08 (dt, *J* = 10.4, 8.0, 1H, minor), 2.68 (t, *J* = 6.7, 2H, major), 2.14 (dt, *J* = 10.4, 8.0, 1H, minor); **^{13}C{^{1}H} NMR** (101 MHz, $CDCl_3$, both diastereomers) δ 153.1, 151.3, 146.6, 143.9, 142.9, 140.9, 128.9, 128.8, 127.5, 127.5, 126.7, 126.4,

114.6 (minor), 114.6 (major), 114.1 (minor), 112.9 (major), 64.6 (minor), 64.3 (major), 55.9 (minor), 55.7 (major), 38.6 (minor), 38.0 (major); **HRMS** (ESI$^+$) $C_{22}H_{22}NO^+$ $[M+H]^+$ calcd. 316.1696, found 316.1702.

cis-6-phenyl-6-azabicyclo[3.2.0]heptane (**114**)[62]

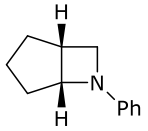

To a solution of *cis*-1-phenylhexahydro-1H-cyclopentaisoxazole (**105**) (95 mg, 0.50 mmol) and $[Ir(cod)Cl]_2$ (10 mg, 3.0 mol%) in toluene (1 mL) was added phenylsilane (185 µL, 1.50 mmol). The reaction mixture was heated to 70 °C for 22 hours then concentrated *in vacuo*. Flash column chromatography (49:1 petroleum ether/EtOAc) gave **114** (13 mg, 14%) as a brown oil.

^{1}H NMR (400 MHz, $CDCl_3$) δ 7.23 – 7.14 (m, 2H), 6.69 – 6.60 (m, 1H), 6.43 – 6.36 (m, 2H), 4.53 – 4.46 (m, 1H), 3.86 (apparent t, *J* = 7.8, 1H), 3.44 (dd, *J* = 7.4, 3.6, 1H), 2.98 (ddt, *J* = 11.2, 8.2, 3.6, 1H), 2.12 – 1.73 (m, 4H), 1.64 – 1.45 (m, 2H); **^{13}C{^{1}H} NMR** (101 MHz, $CDCl_3$) δ 149.8, 129.1, 116.1, 110.4, 69.2, 55.3, 34.4, 32.3, 30.9, 24.4.

syn-1,3-Diphenyl-3-(phenylamino)propan-1-ol (**65**)

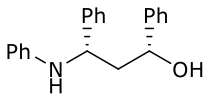

To a solution of *cis*-2,3,5-triphenylisoxazolidine (**53**) (301 mg, 1.00 mmol) in methanol (10 mL) was added zinc powder (196 mg, 3.00 mmol) then 3M HCl (3.30 mL, 10.0 mmol). The reaction mixture was stirred at r. t. for 24 hours before being neutralised with sat. aq. $NaHCO_3$ (10 mL) and extracted with EtOAc (3 × 20 mL). The combined organic extracts were washed with water (50 mL) and brine (50 mL), dried ($MgSO_4$) and concentrated *in vacuo*. Flash column chromatography (85:15, petroleum ether/ EtOAc) gave **65** (282 mg, 93%, >99:1 d.r.) as a white solid.

^{1}H NMR (400 MHz, $CDCl_3$) δ 7.39 – 7.25 (m, 9H), 7.26 – 7.18 (m, 1H), 7.14 – 7.06 (m, 2H), 6.68 (t, *J* = 7.3, 1H), 6.58 (d, *J* = 7.7, 2H), 4.87 (dd, *J* = 9.3, 3.3, 1H), 4.60 (dd, *J* = 9.0, 5.0, 1H), 2.27 (apparent dt, *J* = 14.4, 9.1, 1H), 2.07 (ddd, *J* = 14.4, 5.0, 3.3, 1H); **^{13}C{^{1}H} NMR** (101 MHz, $CDCl_3$) δ 147.3, 144.6, 143.8, 129.2, 128.9, 128.8, 127.9, 127.3, 126.4, 125.8, 118.1, 114.4, 74.0, 58.2, 47.6; **HRMS** (ESI$^+$) $C_{21}H_{22}NO^+$ $[M+H]^+$ calcd. 304.1696, found 304.1693; **AT-IR** (neat) ν (cm^{-1}) 3308, 3269, 3026, 2915, 2855, 1601, 1494, 1455, 1437, 1391, 1309, 1257, 1203, 1180, 1156, 1099, 1065, 1052, 1030, 1008, 921, 901, 876, 848, 828; **m.p.** 139 – 140 °C.

1.6 References

1 S. Gabriel and J. Weiner, *Berichte der Dtsch. Chem. Gesellschaft*, 1888, **21**, 2669–2679.

2 L. Fowden, *Phytochemistry*, 1991, **30**, 3859–3860.

3 G. Polya, *Biochemical targets of plant bioactive compounds : a pharmacological reference guide to sites of action and biological effects*, Taylor & Francis, Abingdon-on-Thames, 2003.

4 L. Fowden, *Nature*, 1955, **176**, 347–348.

5 Eu. Pat., 0469374, 1992.

6 US Pat., 4560401, 1985.

7 Eu. Pat., 0114706, 1984.

8 Eu. Pat., 0165636, 1985.

9 T. A. Brighton, *Med. J. Aust.*, 2004, **181**, 432–437.

10 R. C. Schnur, M. L. Corman, R. J. Gallaschun, B. A. Cooper, M. F. Dee, J. L. Doty, M. L. Muzzi, J. D. Moyer, C. I. DiOrio, E. G. Barbacci, P. E. Miller, A. T. O'Brien, M. J. Morin, B. A. Foster, V. A. Pollack, D. M. Savage, D. E. Sloan, L. R. Pustilnik and M. P. Moyer, *J. Med. Chem.*, 1995, **38**, 3806–3812.

11 J. Kobayashi, J.-F. Cheng, M. Ishibashi, M. R. Wälchli, S. Yamamura and Y. Ohizumi, *J. Chem. Soc., Perkin Trans. 1*, 1991, 1135–1137.

12 Y. T. Di, H. P. He, Y. S. Wang, A. B. Li, Y. Lu, J. B. Gong, X. Fang, N. C. Kong, S. N. Li, H. J. Zhu and X. J. Hao, *Org. Lett.*, 2007, **9**, 1355–

1358.

13 B. List, R. A. Lerner and C. F. Barbas, *J. Am. Chem. Soc.*, 2000.

14 M. C. Wang, W. X. Zhao, X. D. Wang and M. P. Song, *Synlett*, 2006, 3443–3446.

15 L. Keller, M. V. Sanchez, D. Prim, F. Couty, G. Evano and J. Marrot, *J. Organomet. Chem.*, 2005, **690**, 2306–2311.

16 A. Brandi, S. Cicchi and F. M. Cordero, *Chem. Rev.*, 2008, **108**, 3988–4035.

17 P. Huszthy, J. S. Bradshaw, K. E. Krakowiak, T. Wang and N. K. Dalley, *J. Heterocycl. Chem.*, 1993, **30**, 1197–1207.

18 H. Bauman and R. O. Duthaler, *Helv. Chim. Acta*, 1988, **71**, 1025–1034.

19 T. Shono, Y. Matsumura, S. Katoh and J. Ohshita, *Chem. Lett.*, 1988, **17**, 1065–1068.

20 P. W. Erhardt and A. H. Owens, *Synth. Commun.*, 1987, **17**, 469–475.

21 J. Barluenga, F. Fernández-Marí, A. L. Viado, E. Aguilar and B. Olano, *J. Org. Chem.*, 1996, **61**, 5659–5662.

22 M. C. Hillier and C. Y. Chen, *J. Org. Chem.*, 2006, **71**, 7885–7887.

23 D. E. Davies and R. C. Storr, in *Comprehensive Heterocyclic Chemistry*, 1984, vol. 7–7, pp. 237–284.

24 E. Juaristi and D. Madrigal, *Tetrahedron*, 1989, **45**, 629–636.

25 V. R. Gaertner, *J. Org. Chem.*, 1967, **32**, 2972–2976.

26 P. Sulmon, N. De Kimpe, N. Schamp, B. Tinant and J. P. Declercq, *Tetrahedron*, 1988, **44**, 3653–3670.

27 P. Sulmon, N. De Kimpe and N. Schamp, *Tetrahedron*, 1989, **45**, 2937–2955.

28 N. De Kimpe and C. Stevens, *Synthesis*, 2003, **1993**, 89–91.

29 F. Couty, G. Evano, M. Vargas-Sanchez and G. Bouzas, *J. Org. Chem.*, 2005, **70**, 9028–9031.

30 I. Ojima, M. Zhao, K. Nakahashi, T. Yamato, M. Yamashita and R. Abe, *J. Org. Chem.*, 1991, **56**, 5263–5277.

31 I. Nakamura, T. Nemoto, Y. Yamamoto and M. De Armin, *Angew. Chem. Int. Ed.*, 2006, **45**, 5176–5179.

32 R. W. M. Aben, R. Smit and J. W. Scheeren, *J. Org. Chem.*, 1987, **52**, 365–370.

33 C. Wang and J. A. Tunge, *Org. Lett.*, 2006, **8**, 3211–3214.

34 H. M. L. Davies, J. J. Matasi and G. Ahmed, *J. Org. Chem.*, 1996, **61**, 2305–2313.

35 M. Berthet, T. Cheviet, G. Dujardin, I. Parrot and J. Martinez, *Chem. Rev.*, 2016, **116**, 15235–15283.

36 J. W. Kelly, N. L. Anderson and S. A. Evans, *J. Org. Chem.*, 1986, **51**, 95–97.

37 P. L. Robinson, S. A. Evans and J. W. Kelly, *Phosphorus Sulfur Relat. Elem.*, 1986, **26**, 15–24.

38 H. Yin, M. Jin, W. Chen, C. Chen, L. Zheng, P. Wei and S. Han, *Tetrahedron Lett.*, 2012, **53**, 1265–1270.

39 C. Cheng and M. Brookhart, *J. Am. Chem. Soc.*, 2012, **134**, 11304–11307.

40 K. Andrews, D. Summers, L. Donnelly and R. Denton, *Chem. Commun.*, 2016, **52**, 1855–1858.

41 E. J. Goethals, E. H. Schacht, Y. E. Bogaert, S. I. Ali and Y. Tezuka, *Polym. J.*, 1980, **12**, 571–581.

42 L. Reisman, E. A. Rowe, Q. Liang and P. A. Rupar, *Polym. Chem.*, 2018, **9**, 1618–1625.

43 A. J. Hodges, J. P. Adams, A. D. Bond, A. B. Holmes, N. J. Press, S. D. Roughley, J. H. Ryan, S. Saubern, C. J. Smith, M. D. Turnbull and A. F. Newton, *Org. Biomol. Chem.*, 2012, **10**, 8963–8974.

44 S. Das, D. Addis, S. Zhou, K. Junge and M. Beller, *J. Am. Chem. Soc.*, 2010, **132**, 1770–1771.

45 Y. Motoyama, M. Aoki, N. Takaoka, R. Aoto and H. Nagashima, *Chem. Commun.*, 2009, 1574–1576.

46 H. Ohmura, H. Matsuhashi, M. Tanaka, M. Kuroboshi, T. Hiyama, Y. Hatanaka and K. ichi Goda, *J. Organomet. Chem.*, 1995, **499**, 167–171.

47 S. Park, B. G. Kim, I. Göttker-Schnetmann and M. Brookhart, *ACS Catal.*, 2012, **2**, 307–316.

48 D. A. Evans, H. J. Song and K. R. Fandrick, *Org. Lett.*, 2006, **8**, 3351–3354.

49 R. Huisgen, R. Grashey, H. Hauck and H. Seidl, *Chem. Ber.*, 1968, **101**, 2548–2558.

50 K. Martina, L. Rinaldi, F. Baricco, L. Boffa and G. Cravotto, *Synlett*, 2015, **26**, 2789–2794.

51 J. W. Kelly, P. L. Robinson and S. A. Evans, *J. Org. Chem.*, 1986, **51**, 4473–4475.

52 Y. Wang, X. Wen, X. Cui and X. P. Zhang, *J. Am. Chem. Soc.*, 2018, **140**, 4792–4796.

53 V. Sriramoju, S. Kurva and S. Madabhushi, *New J. Chem.*, 2018, **42**, 3188–3191.

54 T. Shimizu, M. Ishizaki and N. Nitada, *Chem. Pharm. Bull.*, 2002, **50**, 908–921.

55 L. D. S. Yadav, C. Awasthi, V. K. Rai and A. Rai, *Tetrahedron Lett.*, 2007, **48**, 8037–8039.

56 P. S. Rutledge, J. Palmer, J. L. Roberts and P. D. Woodgate, *Heterocycles*, 1976, **5**, 109.

57 E. Richmond, N. Duguet, A. M. Z. Slawin, T. Lébl and A. D. Smith, *Org. Lett.*, 2012, **14**, 2762–2765.

58 A. Hosseini and P. R. Schreiner, *Org. Lett.*, 2019, **21**, 3746–3749.

59 F. P. Ballistreri, U. Chiacchio, A. Rescifina, G. A. Tomaselli and R. M. Toscano, *Tetrahedron*, 1992, **48**, 8677–8684.

60 US Pat., 2002022724, 2002.

61 M. Liniger, C. Neuhaus, T. Hofmann, L. Fransioli-Ignazio, M. Jordi, P. Drueckes, J. Trappe, D. Fabbro and K. H. Altmann, *ACS Med. Chem. Lett.*, 2011, **2**, 22–27.

62 J. Barluenga, R. Sanz and F. J. Fañanás, *J. Org. Chem.*, 1997, **62**,

5953–5958.

Chapter 3: Novel Staudinger-Type Synthesis Methods for Carbon-Nitrogen and Nitrogen-Sulfur Bond Formation

1.1 Abstract

Chapter three describes work to expand the field of Staudinger-type synthesis methodology. Attempts to develop a novel amination protocol using alcohols is described. Additionally, a novel synthesis of sulfonamides using sulfonic acids has been developed and was utilised to prepare five sulfonamide products in yields up to 63%. A variant of the traceless Staudinger ligation using a sulfonate ester is also described. Using this method three sulfonamide products were obtained in yields up to 68%. Furthermore, a multinuclear NMR study has been performed, elucidating the mechanism of the reaction.

1.2 Introduction

1.2.1 Synthesis of Iminophosphoranes

1.2.1.1 Staudinger Reaction Outline and Scope

First described in the seminal publication of 1919 by Staudinger and Meyer, the Staudinger reaction is a transformation of significant importance.[1] This highly influential publication describes the formation of iminophosphoranes (also known as aza-ylides or phosphinimines) from the reaction between triphenylphosphine and aryl azides (Scheme 1). However, the formation of iminophosphoranes from the reaction of any organic azide and trivalent phosphorus species is referred to as a Staudinger reaction.

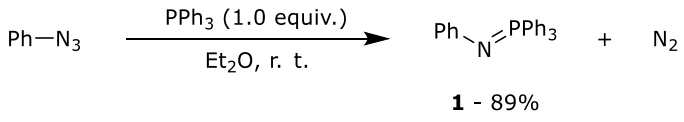

*Scheme 1: Synthesis of iminophosphorane **1** via the Staudinger reaction of phenylazide and triphenylphosphine.[1] Note: Reaction time not specified.*

A vast number of iminophosphoranes have since been prepared in the literature from a diverse array of azides and phosphorus-containing species. In addition to the aryl azides used by Staudinger originally, alkyl,[2] sulfonyl,[3] cyanogen,[4] acyl[5], imidic,[6] as well as phosphorus[7], boron[8] and tin-containing azides have since been employed (Scheme 2).[9] Although there exists this extremely varied selection of azides used in the Staudinger reaction, the majority of examples in the literature feature simple alkyl or aryl azides. The use of these two classes of azides shall be the focus of this chapter.

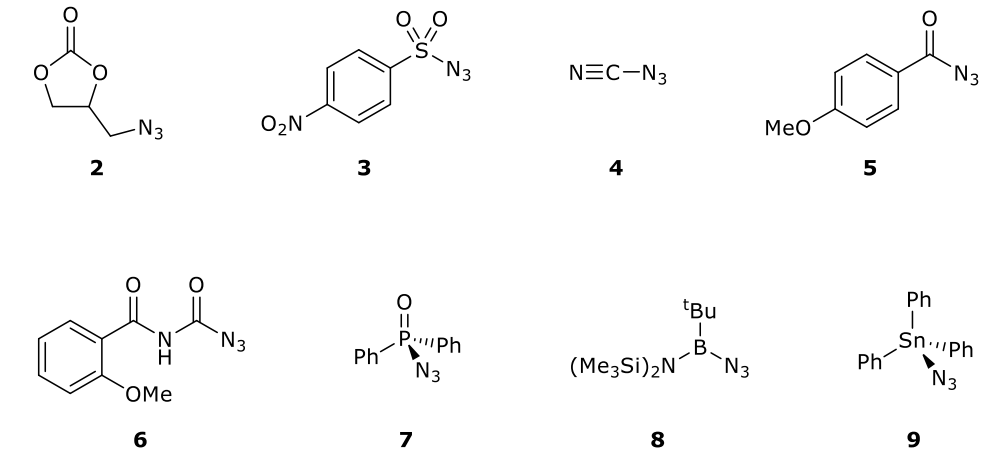

Scheme 2: Representative azides employed in Staudinger reactions.

Triphenylphosphine remains the most commonly used phosphine in Staudinger reactions due to its low cost and ease of handling.[10] However, a large number of trialkyl,[11,12] bisphosphorus,[13] polymeric[14] and cyclic,[15] phosphines have been used as precursors to iminophosphoranes (Scheme 3). In addition to phosphines, other trivalent phosphorus-containing compounds such phosphite esters[16] and exotic diazaphosphetidinones[17] are infrequently used.

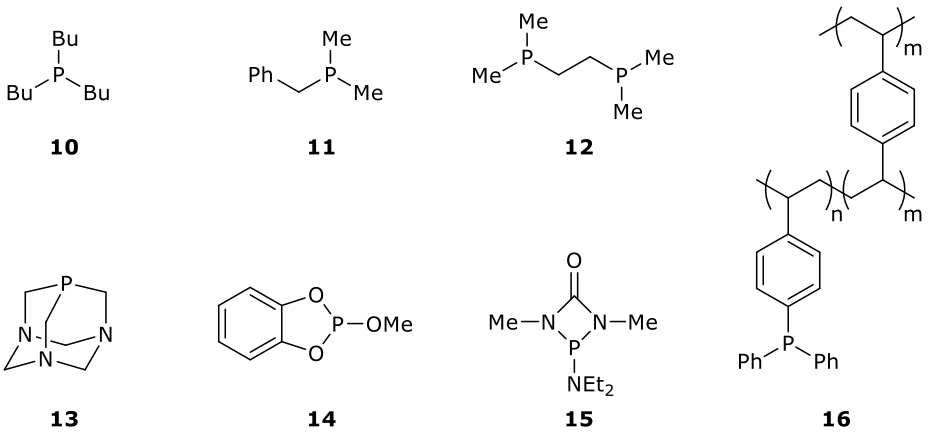

Scheme 3: Representative phosphorus-containing components employed in the Staudinger reactions.

The Staudinger reaction was the first method described in the literature for the synthesis of iminophosphoranes. To this day it remains the most commonly utilized strategy towards these compounds of great interest. Despite this, alternative synthesis routes to iminophosphoranes are sometimes used, for example the Kirsanov reaction.[18] First described in 1950, the Kirsanov reaction is the substitution reaction of a halogen-containing P(V) compound with an amine. A relatively recent example of the this is shown in Scheme 4, where a bidentate iminophosphorane ligand was synthesised.[19] In this case the HBr salt of the iminophosphorane (**19**) was stored as a stable precursor with the iminophosphorane (**20**) being generated *in situ* with base.

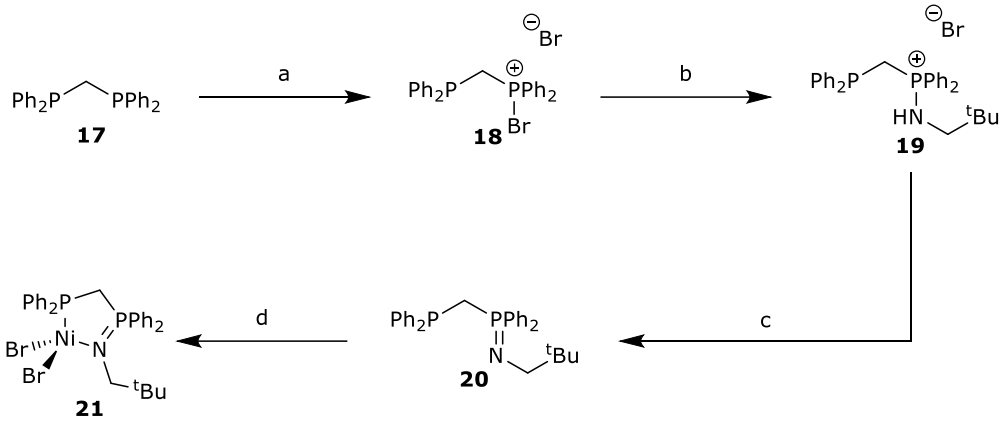

*Scheme 4: Preparation of nickel complex **21** using an iminophosphorane ligand (**20**) synthesised by a Kirsanov reaction.[19] Reagents and conditions a) Br_2, DCM −78 °C, 20 min; b) $^tBuCH_2NH_2$, DCM, −78 °C to r. t., 1 h, 74% (Over two steps); c) n-BuLi, THF, −78 °C to r. t., 20 min; d) [$NiBr_2$(DME)], THF, r. t., 30 min, 80% (over two steps).*

This protocol is typically reserved for instances where the precursor azide required for the Staudinger reaction is not easily accessed.[20] In most instances however, the Staudinger reaction is a milder and more general procedure.

1.2.1.2 Mechanism of the Staudinger Reaction

Staudinger hypothesised in the original publication of 1919 that the reaction proceeds *via* a phosphazide intermediate (**23**), which collapses releasing N_2 to give the iminophosphorane product (**24**).

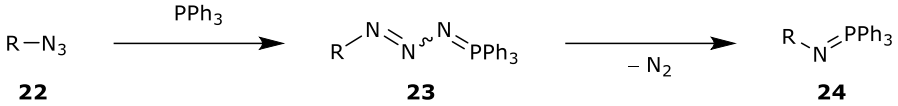

22 **23** **24**

*Scheme 5: Originally proposed reaction mechanism for the Staudinger reaction via phosphazide (**23**).*[1]

More recent mechanistic studies have shown this to be broadly correct whilst offering greater detail. Isotopic labelling experiments with a ^{15}N labelled azide (**25**) found the *N*-Ts bond of the azide was preserved in the iminophosphorane (**26**) (Scheme 6).[21] This data corroborated the authors proposed mechanism whereby a four membered transition state leads to the elimination of N_2.

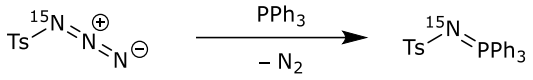

25 **26**

*Scheme 6: Isotopic labelling experiment with ^{15}N labelled azide **25**.*[21]

Kinetic studies by Leffler and co-workers found the phosphazide intermediate to have significant phosphonium character.[22] As a result, it is more accurately depicted as the resonance form **27**. Computational methods have since been applied to further elucidate the mechanism of the Staudinger reaction. The first of these studies were the concurrent

publications of Grützmacher[23] and Rzepa,[24] which established that the *cis*-phosphazide **27** forms preferentially to *trans*. Combining all these elements we arrive at the established mechanism for the Staudinger reaction shown Scheme 7.

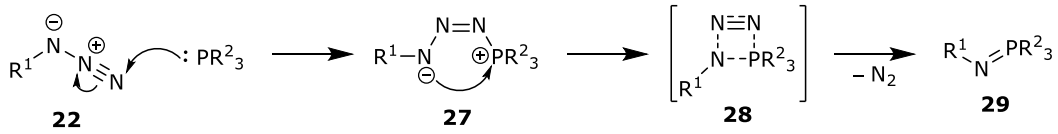

Scheme 7: Reaction mechanism of the Staudinger reaction.

In the vast majority of cases, intermediate phosphazides are unstable and collapse readily to give iminophosphoranes.[10] However, phosphazides may sometimes be observed, for example when reactions are performed very low temperatures.[25] In some instances, phosphazides with bulky substituents and/or substituents which stabilize the charges of the phosphazide, are relatively stable and can be isolated.[26] An early example of this is the phosphazide **30**, which is stable up to 155 °C (Scheme 8).[27] X-ray crystallography determined **30** to exist as the *trans*-phosphazide with zwitterionic character. In this example the electron donating morpholine groups can stabilise the positively charged phosphorus atom. Furthermore, the very electron poor aromatic ring (from the azide) stabilises the negatively charged nitrogen. In addition to electronics, **30** is also stabilised by sterics. The relatively large steric bulk inhibits the rotation about the *N*-*N* bond of the neutral resonance form **31** required to form the *cis*-phosphazide. Consequently, the *trans*-phosphazide is the major isomer and the iminophosphorane cannot form.

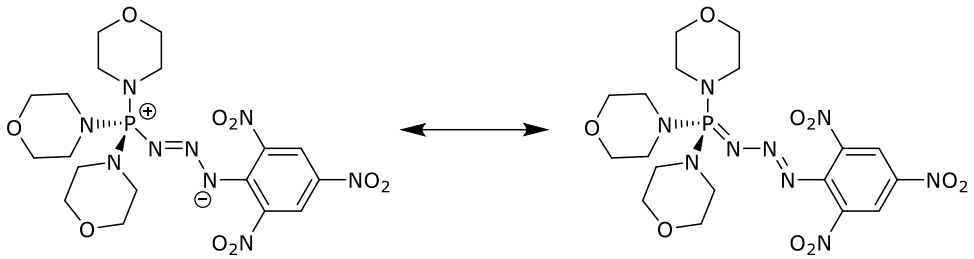

30 **31**

*Scheme 8: Stable and isolable phosphazide **30** and its resonance form **31**.*[27]

Phosphazides are basic and have been shown to interact with organic acids in some instances.[22] Additionally, they are nucleophilic and alkylation of **30** has been achieved with triethyloxonium tetrafluoroborate (Scheme 9).[27]

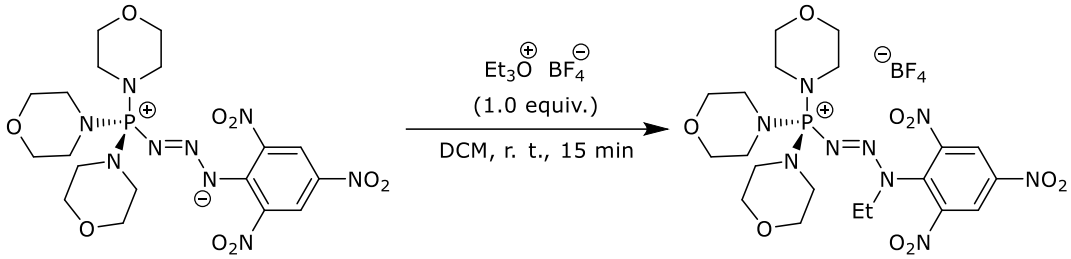

30 **32** - 62%

*Scheme 9: Alkylation of the stable phosphazide **30** using triethyloxonium tetrafluoroborate.*[27]

However, synthesis applications of phosphazides in their own right is not well developed. The chemistry of their iminophosphorane products is significantly more established.

1.2.2 Applications of Iminophosphoranes in Synthesis

The product iminophosphoranes of the Staudinger reaction are nucleophilic and can be trapped with a large number of electrophiles, for instance alkyl

halides.[28] However, the more noteworthy transformations are those which break the nitrogen phosphorus bond, generally eliminating a phosphine oxide in the process. In the original publication of 1919 by Staudinger, a number of such transformations are detailed (Scheme 10).[1] Although experimental details in the paper are sparse, the diverse array of transformations possible for iminophosphoranes was clearly established.

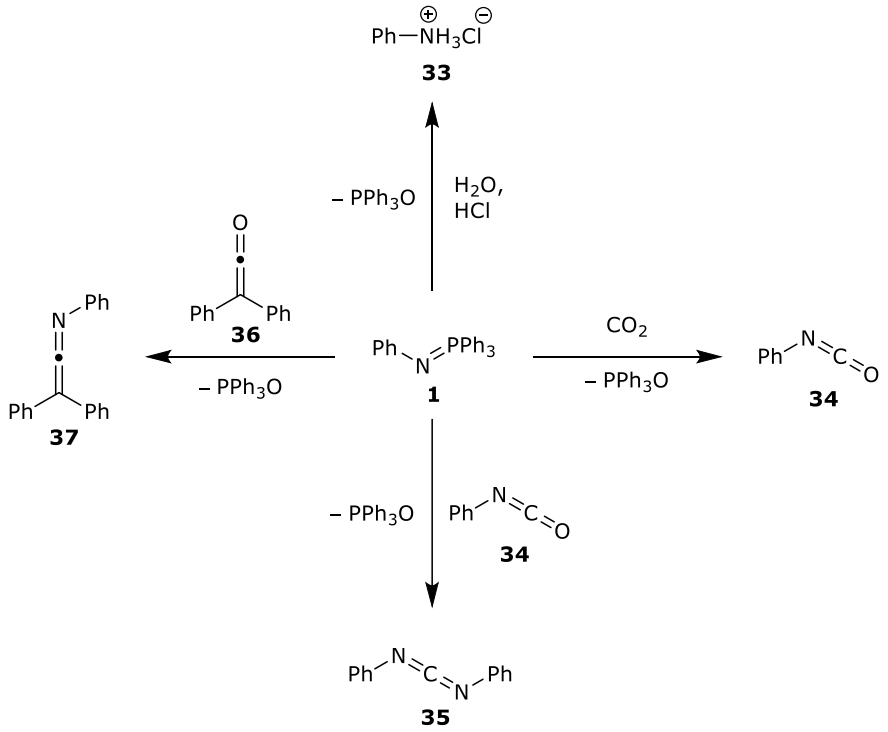

*Scheme 10: Synthetic utility of iminophosphorane **1**, as described in the original paper by Staudinger and Meyer.[1] Note: Reaction equivalents, yields, temperatures, times and solvents not specified.*

Synthesis of aniline (as a HCl salt **33**) was achieved *via* the hydrolysis of the iminophosphorane (**1**), in a process since established as the 'Staudinger reduction' (Scheme 10 top). Carbon dioxide was found to be a suitable electrophile for the preparation of isocyanates (**34**) (Scheme 10 right). Isocyanates themselves could be used to prepare carbodiimides (**35**) (Scheme 10 bottom). Finally, ketenimines (**37**) can be synthesised

when the iminophosphorane is reacted with a ketene (**36**) (Scheme 10 left); incidentally, this was the first preparation of a ketenimine in the literature.

Since this chemistry was first described by Staudinger, substantial research has been undertaken to develop these reactions. Additionally, further suitable electrophiles have been identified expanding the scope of these Staudinger-type reactions. The most significant of these developments shall henceforth be detailed in turn.

1.2.2.1 Staudinger Reduction

As discovered by Staudinger, iminophosphoranes can undergo hydrolysis to form amines, thus allowing the selective reduction of azides. This hydrolysis step may be achieved with water, but sometimes aqueous sodium hydroxide,[29] ammonium hydroxide[30] or hydrochloric acid[31] are used. Other methods are known for the reduction of azides, for example hydrogenation.[32] However, the excellent chemoselectivity and versatility of the Staudinger reduction make it one of the most common methods used. Additionally, its importance as an azide reduction protocol, results in the Staudinger reduction being perhaps the most commonly employed application of iminophosphoranes.

Although first reported as a two-step procedure with isolation of the iminophosphorane prior to reduction, 'one-pot' procedures are commonly employed. Such *in situ* generation and reduction of iminophosphoranes generally does not negatively impact the isolated yields attained.[33] Using this single step method, Vaultier and co-workers were able to reduce the epoxy azide **38** en-route to the natural product (±) α-conhydrine (**40**) (Scheme 11).[34] The chemoselectivity of the Staudinger reaction is clearly

demonstrated in this example with the epoxide unaffected. This transformation would not be possible with a hydride based reductive system such as $LiAlH_4$, which is also used for azide reductions.[35]

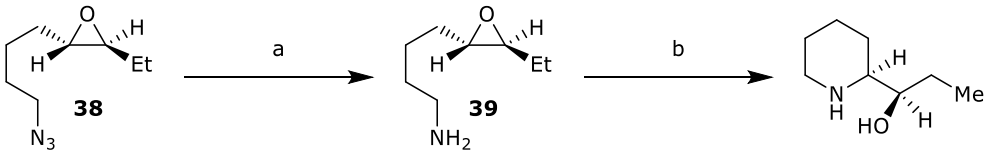

(±) α-conhydrine - **40**

*Scheme 11: Use of a one-pot Staudinger reduction towards the natural product (±) α-conhydrine (**40**).[34] Reagents and conditions a) PPh_3, H_2O, THF, r. t., 18 h, 80%; b) PhMe, 110 °C, 30 h, 90%.*

Protocols have also been developed where organic azides are generated *in situ* and subsequently reduced using the Staudinger reaction. An example of this is shown in Scheme 12, where alkyl halides were converted to amines with no purification of intermediates, thus providing an alternative to the Gabriel synthesis.[31]

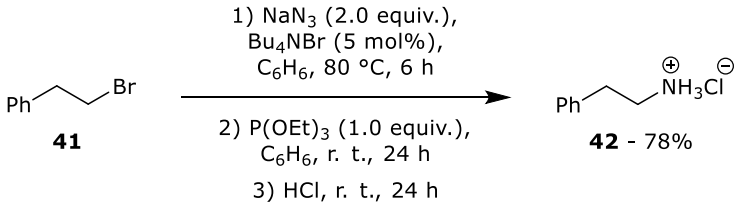

*Scheme 12: One-pot synthesis of amine HCl salt **42**, from alkyl bromide **41**.[31]*

Perhaps the most significant drawback of the Staudinger reduction is the stoichiometric P(V) (typically a phosphine oxide) waste generated. However, a variant catalytic in phosphine was reported by van Delft and co-workers in 2012 (Scheme 13).[36]

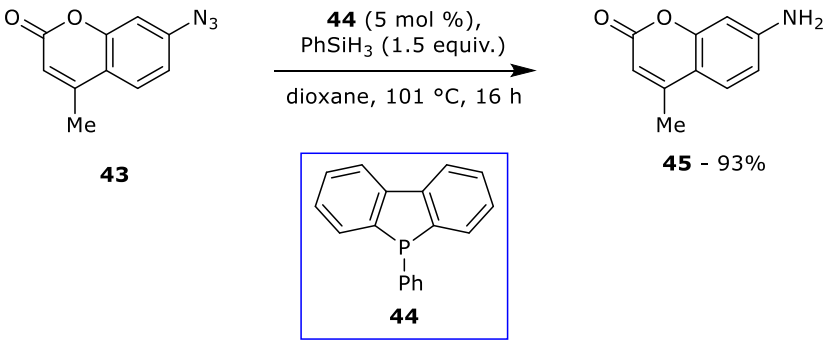

Scheme 13: Example transformation of the catalytic Staudinger reaction.[36]

The mechanism for this reaction is rather interesting and differs from a classical Staudinger reduction (Scheme 14). In this system a sub-stoichiometric quantity of phosphole (**44**) is used to generate the intermediate iminophosphorane (**46**), which is then reduced by the silane (**47**). This results in regeneration of **44** and eliminates a silyated amine (**48**), which is readily hydrolysed on work-up to give the amine product (**49**). Other systems catalytic in a phosphorus reagent, such as O'Brien's catalytic Wittig reaction, utilize a silane to reduce the formed phosphine oxide, thus regenerating the active phosphine.[37] However, in this instance, hydrolysis of the iminophosphorane cannot be performed in the presence of the moisture sensitive silane reductant. Therefore, in this alternative pathway, the iminophosphorane (**46**) is reduced and not hydrolysed, with no phosphine oxide formation occurring.

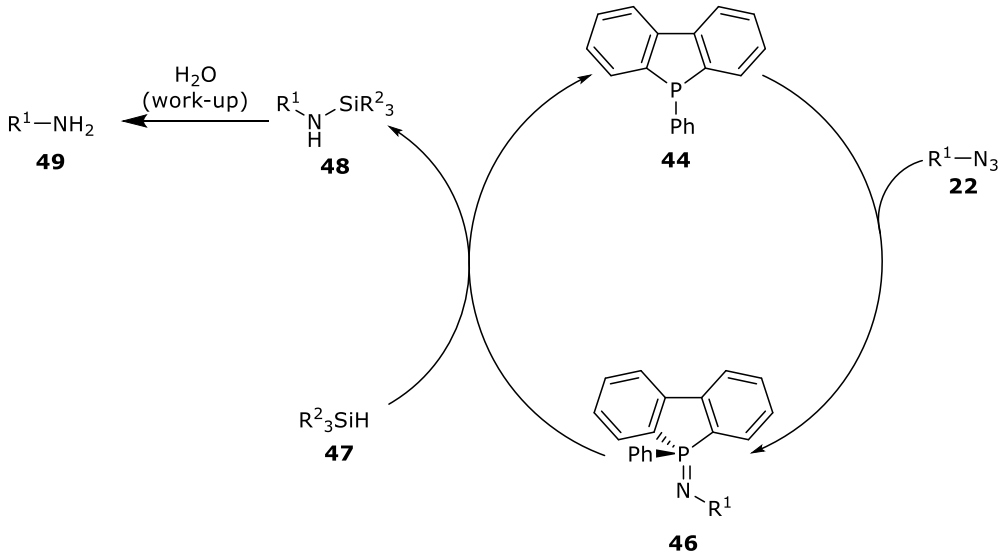

Scheme 14: Proposed cycle for van Delft's catalytic Staudinger reduction.[36]

1.2.2.2 Aza-Wittig Reaction

The aza-Wittig reaction is another very powerful use of iminophosphoranes. By reacting iminophosphoranes (**29**) with carbonyl compounds (**50**), C=N bonds can be constructed, in an analogous fashion to the C=C bond construction of the Wittig reaction (Scheme 15).[38,39] In the context of aza-Wittig reactions, the iminophosphorane is often referred to as an 'aza-Wittig reagent'.[40]

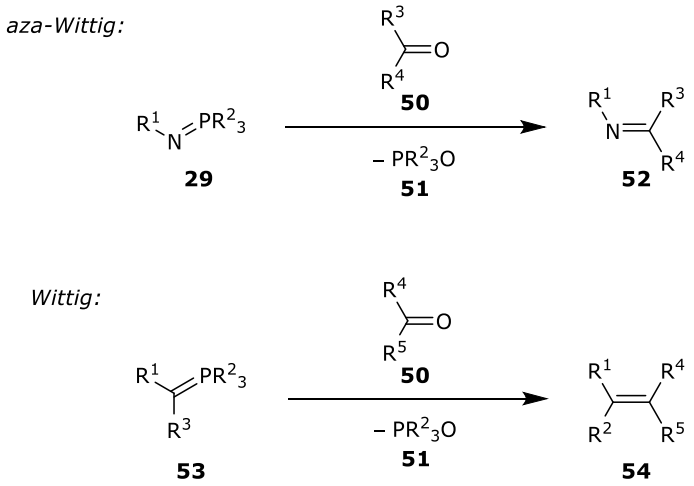

Scheme 15: General reaction schemes for the aza-Wittig and Wittig reactions.

A large number of carbonyl compounds may be used in the aza-Wittig reaction to generate a wide variety of products. The aforementioned reactions of CO_2, isocyanates and ketenes with iminophosphorane **1**, discovered by Staudinger, are examples of the aza-Wittig reaction (Scheme 10, right, bottom and left respectively). A subsequent publication by Staudinger in 1921 expanded the scope of the aza-Wittig reaction to include aldehydes and ketones.[25] Both of these substrates have found extensive use in more recent years. It was also reported that in the same way CO_2 can be used to prepare isocyanates, CS_2 can be used to synthesise isothiocyanates.

Mechanistically, the reaction is similar to that of the Wittig reaction. A number of computational studies have shown that, as is the case with the Wittig reaction, the reaction proceeds *via* a four-membered cyclic intermediate (in this case an oxazaphosphetidine, **55**).[41–44] Collapse of this intermediate eliminates the product (**52**) and phosphine oxide (**51**) (Scheme 16).

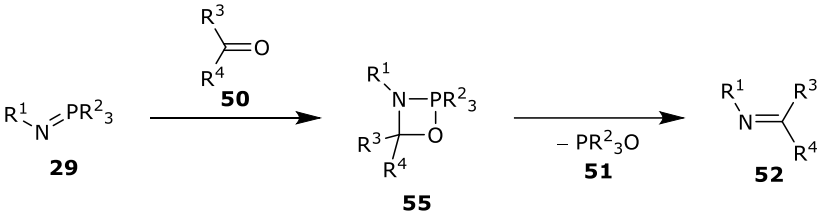

Scheme 16: General mechanism for the aza-Wittig reaction.

In analogy to the Staudinger reaction, the intermediate of this process is generally unstable and cannot be isolated. However, in 2000 Kawashima and co-workers successfully isolated and characterised the stable oxazaphosphetidine **57** (Scheme 17).[45] Thermolysis of **57** yielded the aza-

Wittig products, imine **59** and phosphinate **58**. This therefore provides experimental evidence in support of the reaction mechanism shown in Scheme 16.

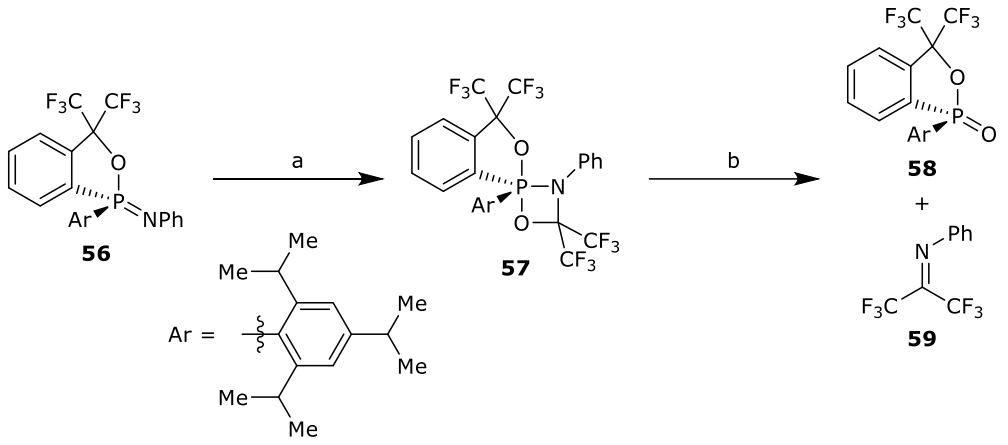

*Scheme 17: Synthesis of the stable oxazaphosphetidine **57** and its thermolysis to the phosphinate **58** and imine **59**.[45] Reagents and conditions a) F_3CCOCF_3, THF, r. t.; b) THF, 150 °C, 90%[a]; [a]Yield determined by ^{19}F NMR spectroscopy. Note: Reaction time and yield for step a, and reaction time for step b not specified.*

Although the imines prepared by the aza-Wittig reaction are often the target compound, significant research has utilised the imine as an *in situ* generated precursor for further chemistry. A relatively simple example of this is the use of a reducing agent, such as $NaBH_4$ to reduce the imine (**62**) to an amine (isolated as HCl salt **63**) (Scheme 18).[46] This effectively being a reductive amination procedure.

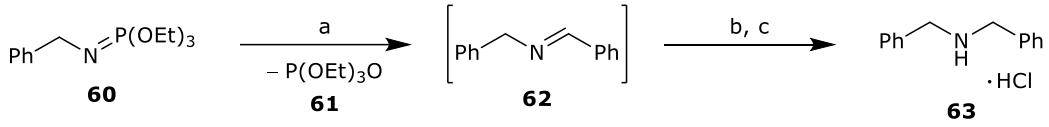

*Scheme 18: Synthesis of amine HCl salt **63** via the reduction of imine **62**, generated in situ via an aza-Wittig reaction.[46] Reagents and conditions a) PhCHO, C_6H_6, 0 °C – r. t., 3 h; b) $NaBH_4$, MeOH, r. t., 24 h; c) HCl work up, 77%[a]; [a]Yield reported from alkyl bromide.*

Interception of the intermediate imine with acyl chlorides has been shown to allow the one-pot formation of enamides from primary azides (Scheme 19).[47] This work by Padwa and co-workers is an excellent example of an aza-Wittig reaction being used to install a good degree of functionality in a single step.

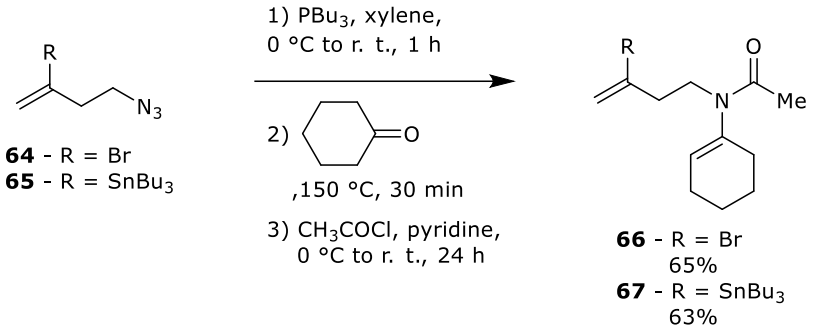

*Scheme 19: Synthesis of enamides **67** and **67** via an acyl chloride intercepted aza-Wittig reaction.[47]*

In situ generated imines have also been used in cyclisation reactions when suitable functionality is incorporated into the substrate. An example of this are the *N*-vinylic iminophosphoranes (**68**-**70**) which can react with two equivalents of ethyl glyoxalate (**71**) to form the heterocycles (**72**-**74**) (Scheme 20).[48] In this example an aza-Wittig reaction with the first equivalent of **71** forms an azadiene which then undergoes a [4+2] cycloaddition with the second equivalent of **71**.

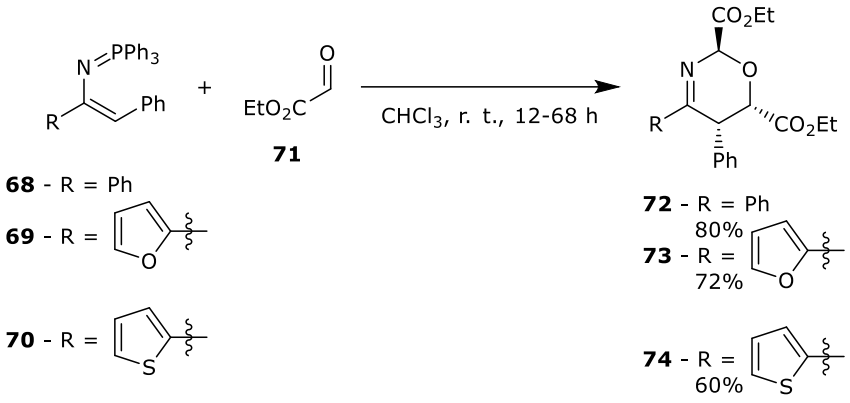

*Scheme 20: Synthesis of heterocycles **72**-**74** via the one pot aza-Wittig and [4+2] reaction of N-vinyl iminophosphoranes **68**-**70** and ethyl glyoxalate (**71**).[48] Note: Single stereoisomers reported in the publication.*

A large amount of research has focussed on intra-molecular aza-Wittig reactions, wherein substrates containing both azide and carbonyl functionality are used to form heterocycles. O'Neil and co-workers employed this strategy towards the construction of the novel tricyclic ring system **76** (Scheme 21).[49]

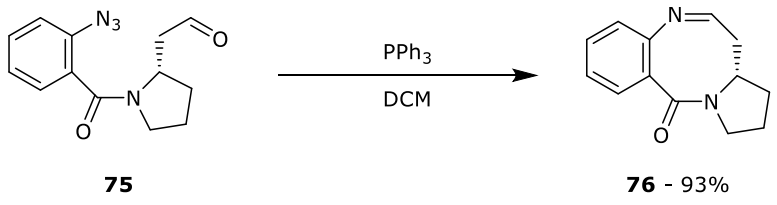

*Scheme 21: Intramolecular aza-Wittig reaction to synthesise the novel heterocyclic system **76**.[49] Note: Reaction temperature, duration and equivalents not specified.*

Such intra-molecular aza-Wittig reactions are a gratifyingly simple means to constructing complex ring systems such as this.

Catalytic variants of the aza-Wittig reaction have been developed in more recent years. The first such example catalytic in the organophosphorus component was developed by Marsden and co-workers in 2008.[50] This

methodology uses a sub-stoichiometric quantity of the phosphine oxide **78** to synthesise a number of benzoxazoles (**79**) *via* an intramolecular aza-Wittig reaction (Scheme 22). The formation of iminophosphoranes from the reaction between isocyanates and phosphine oxides was first reported in 1962 by Monagle and co-workers.[51] Marsden's catalytic aza-Wittig reaction exploits this to allow formation of the iminophosphorane to occur from the phosphine oxide catalyst **78**. The desired aza-Wittig cyclisation then occurs, regenerating the catalyst (**78**) in the process.

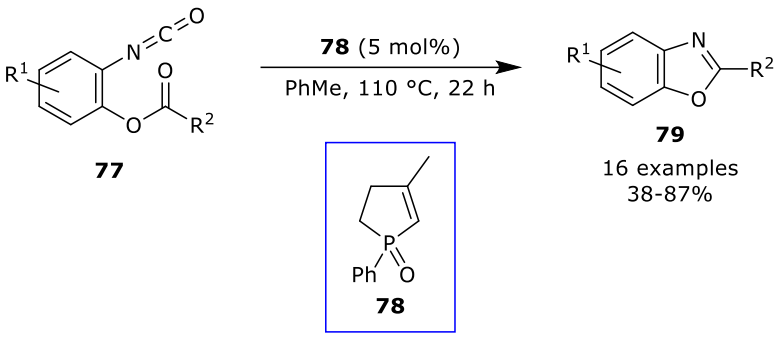

Scheme 22: Marsden's catalytic aza-Wittig reaction.[50]

The authors state that in some instances an intermolecular reaction was observed between the iminophosphorane and the isocyanate **77** forming the carbodiimide (as was reported by Staudinger, Scheme 10 bottom). However, this was overcome by varying concentrations and catalyst loadings. Evidently, this competitive formation of carbodiimides limits the potential to expand this methodology to include intermolecular aza-Wittig reactions.

1.2.2.3 Staudinger Amidation

Another noteworthy use of iminophosphoranes is for the synthesis of amides. First reported by Garcia and co-workers, this method allows the direct synthesis of amides from carboxylic acids with no activating groups required (Scheme 23).[52] Using this process, a number of aliphatic and aromatic azides and carboxylic acids were compatible.

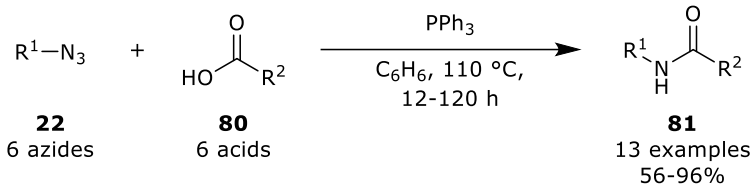

*Scheme 23: Garcia's Staudinger amidation reaction using carboxylic acids (**80**).[52]*

Mechanistically, it was observed that the reaction begins with formation of an iminophosphorane (**24**) which is then protonated by the carboxylic acid (**80**) to form a phosphonium salt (**82**) (Scheme 24). It was then proposed that collapse of the phosphonium salt (*via* phosphorane **83**) yields the amide product (**81**) and triphenylphosphine oxide.

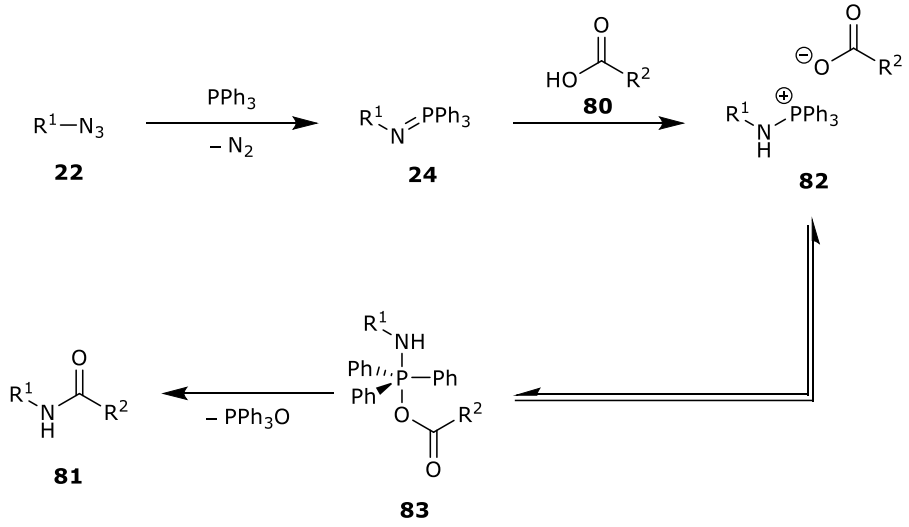

*Scheme 24: Garcia's proposed mechanism for the Staudinger amidation of carboxylic acids, via a phosphonium salt (**82**).[52]*

It was observed that whilst formation of the iminophosphorane (**24**) and its protonation to form the phosphonium salt (**82**) occurred at room temperature, heating was required to from the amide (**81**). Additionally, it was noted that when trifluoroacetic acid was used, despite formation of the relevant phosphonium salt (**82**) being observed, no formation of the amide product occurred. Evidently, the reduced nucleophilicity of the carboxylate anion prevented formation of the product (**81**) in this instance.

Subsequent work within the Denton group has explored the mechanism of this reaction using NMR and DFT studies.[53] As anticipated both the iminophosphorane (**24**) and phosphonium salt (**82**) were observed by ^{31}P NMR spectroscopy for the reaction between benzyl azide, triphenylphosphine and benzoic acid. However, no phosphorane species could be observed spectroscopically. Subsequent DFT studies located both the phosphorane **84** and its reactive conformer **85** as minima in addition to the transition structure **86** (Scheme 25).

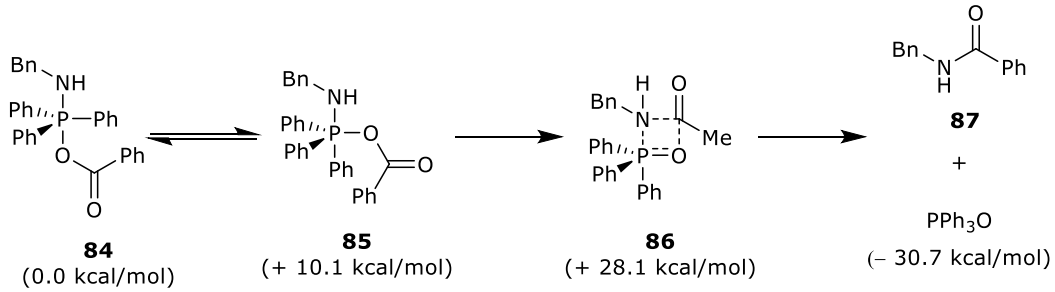

Scheme 25: Final steps of the reaction mechanism for the Staudinger amidation of benzyl azide using benzoic acid, determined by DFT studies.[53]

Although the Staudinger amidation reaction developed by Garcia and co-workers offers an excellent amide synthesis protocol, it possesses one significant drawback: the production of stoichiometric phosphine oxide waste. Ashfeld and co-workers overcame this shortcoming in 2012 by developing a Staudinger amidation process catalytic in triphenylphosphine

(Scheme 26).[54] Through the implementation of phenylsilane as a terminal reductant, only 10 mol% of triphenylphosphine was required with excellent yields obtained.

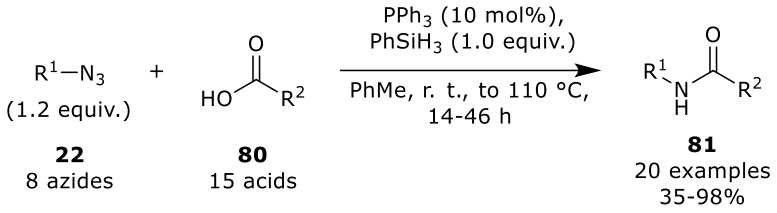

Scheme 26: Ashfeld's catalytic Staudinger amidation of carboxylic acids.[54]

It was proposed that, analogous to O'Brien's catalytic Wittig reaction,[37] the phenylsilane chemoselectively reduces the phosphine oxide, regenerating triphenylphosphine as the catalyst (Scheme 27).

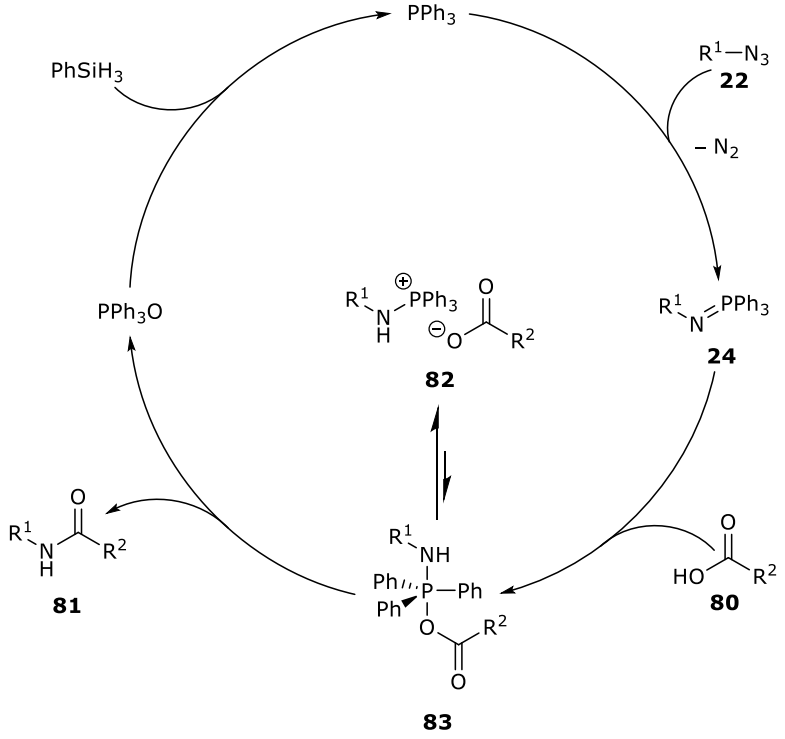

Scheme 27: Ashfeld's proposed mechanism for the triphenylphosphine catalysed Staudinger amidation reaction.[54]

However, recent work within the Denton group has shown phenylsilane does not in fact act as a simple reductant in this process.[53] Instead, phenylsilane was found to react rapidly with the phosphonium salt (**82**), generating a reactive silyl ester species (**89**) after loss of hydrogen from **88**. It was proposed that this silyl ester (**89**) then facilitates the amidation reaction by reducing the iminophosphorane (**24**) (regenerating the triphenylphosphine catalyst) and forming the aminosilylester species (**90**). The aminosilylester **90** ultimately eliminates silanols/siloxanes to give the amide product (**81**).

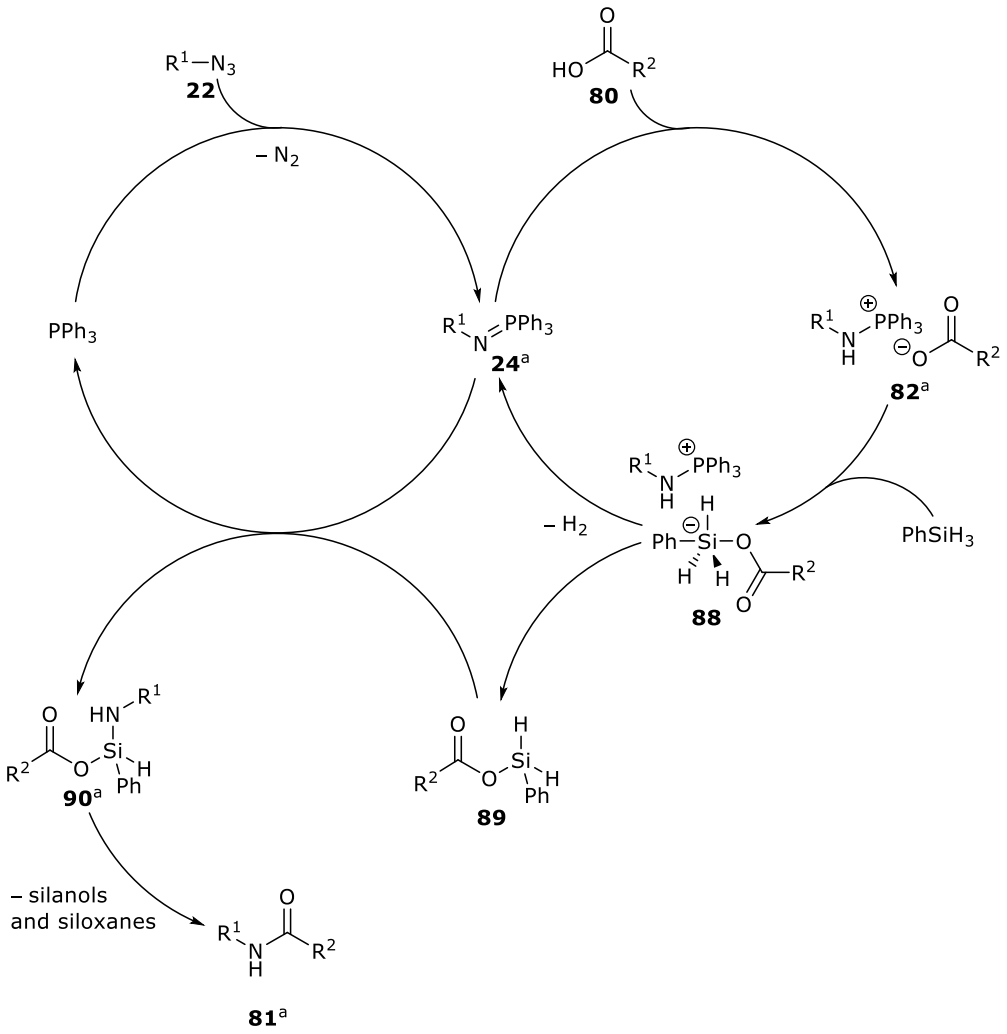

Scheme 28: Denton's proposed catalytic cycle for Ashfeld's triphenylphosphine catalysed Staudinger amidation.[53] [a]Observed by ^{1}H NMR spectroscopy.

1.2.3 Staudinger Ligations

Chemical ligation is an immensely important area in chemical biology for the study of biological systems.[55] Through chemical ligation, bioconjugates can be prepared from a biological sample and a chemical probe (for example an affinity tag such as a FLAG tag).[56] Such chemical ligations often exploit 'biorthogonal chemistry', wherein the ligation uses chemical reactions which do not interfere with the biological system.[57] For this to occur, fast and mild reactions must be performed using functional groups which are otherwise inert within the complex biological system. One such functional group are azides. Azides are almost entirely absent from biological systems and rather inert to the functionality that is present.[58]

1.2.3.1 Non-Traceless Staudinger Ligations

The first use of azide functionality within the field of chemical ligations came in 2000, when Bertozzi and co-workers published the first Staudinger ligation.[59] In this work a Staudinger reaction occurs between the azide (**92**) and a phosphine (**91**) (another biorthogonal functionality), the iminophosphorane (**93**) is then trapped with a tethered ester group to form an amide (**96**). Such trapping of an iminophosphorane with a tethered ester was first described by Bosch and co-workers for the synthesis of lactams.[60] However, it is in the context of chemical ligations where this transformation has found prominence. Subsequent studies have elucidated the mechanism for the Staudinger ligation (Scheme 29).[61]

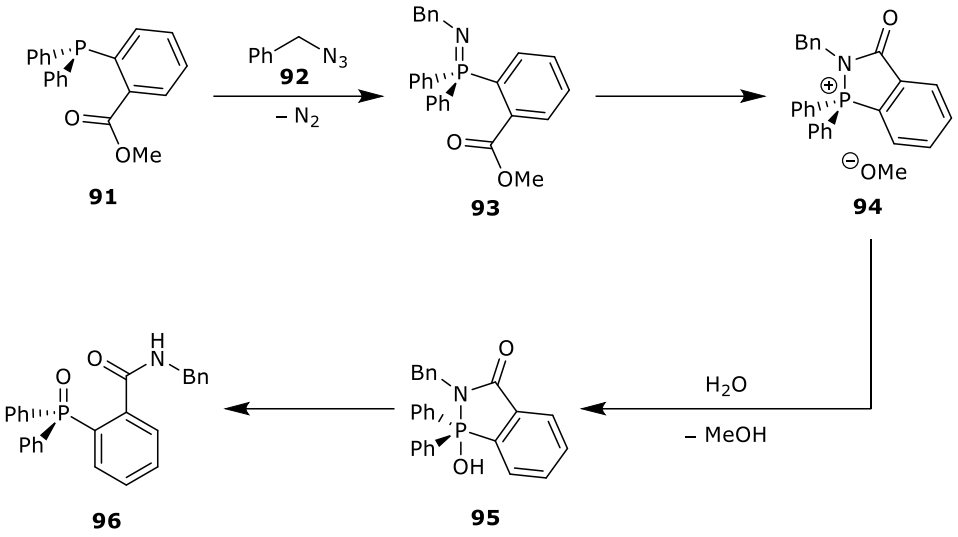

*Scheme 29: Reaction mechanism for the Staudinger ligation reaction of phosphine **91** and benzyl azide (**92**).*[61]

Using this novel and highly influential ligation, Bertozzi and co-workers successfully reacted azide functionalised sialic acids on the cell surface of Jurkat cells (**100**) with a biotinylated phosphine (**99**) (Scheme 30). The biotin-containing phosphine (**99**), itself derived from the phosphine (**97**), acts as a common precursor for labelled phosphines.

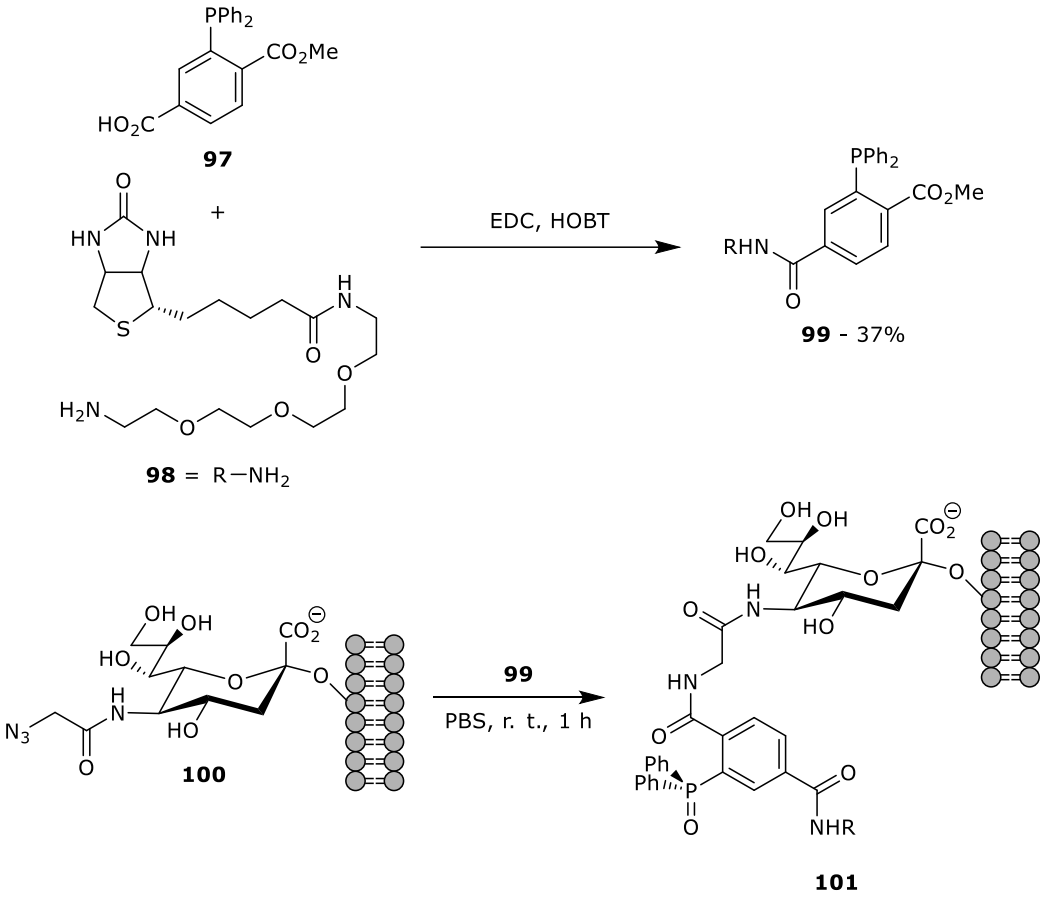

*Scheme 30: Top: Synthesis of the biotin-containing phosphine **99**; Bottom: Application of **99** for the labelling of azide functionalised sialic acids on the cell surface of Jurkat cells (**100**).[59] Note: Reaction time, solvent, temperature and equivalents not specified for the synthesis of **99**; **100** incubated at 20 μM with **99** at 1 mM for synthesis of **101**.*

1.2.3.2 Traceless Staudinger Ligations

The Staudinger ligation has proved an invaluable tool for chemical biology, with numerous investigations making use of it.[62,63] However, the inclusion of a phosphine oxide in the product bioconjugate is neither necessary nor desirable. Subsequent work also by Bertozzi and co-workers developed a 'traceless' Staudinger ligation wherein a cleavable linker is incorporated into the phosphine (**103**).[64] Using this method a proof-of-concept reaction was performed whereby azide modified deoxyadenosine (**102**) was acetylated using **103** (Scheme 31).

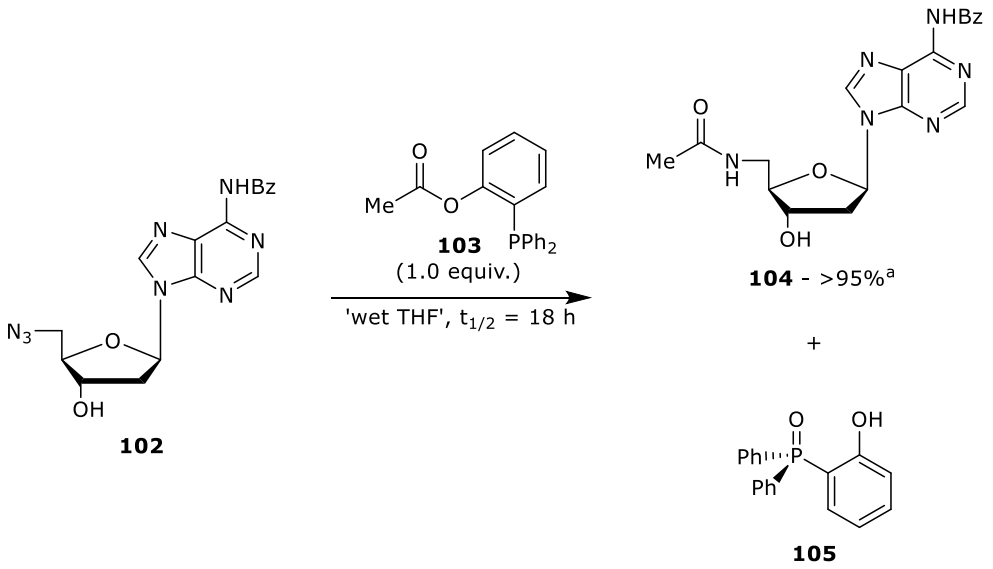

Scheme 31: Example transformation of Bertozzi's traceless Staudinger ligation;[64] [a]Yield determined by HPLC. Note: Reaction temperature not specified.

The orientation of the electrophilic ester group of **103** can be seen to be inverted relative to the original Staudinger ligation reagent **91**. Consequently, upon attack of the iminophosphorane (**106**), cleavage of the ester bond results in the amide and phosphine components only being connected *via* the readily hydrolysed *N-P* bond (**107**) (Scheme 32).

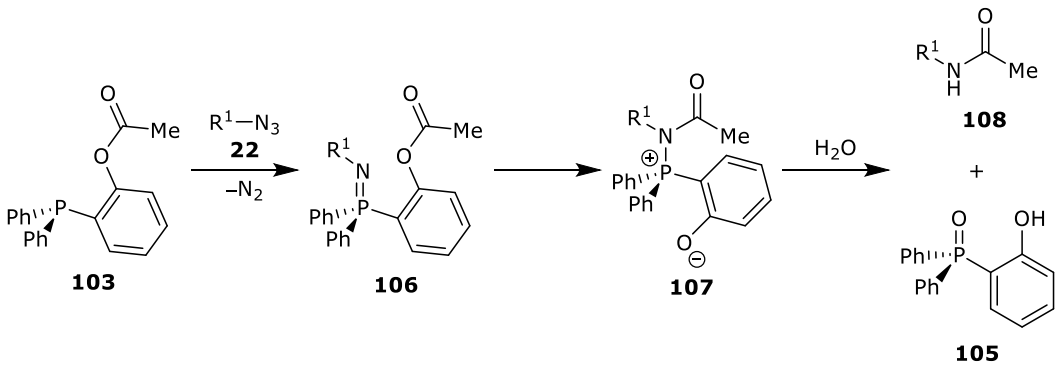

Scheme 32: Reaction mechanism for Bertozzi's traceless Staudinger ligation.[64]

Parallel research was published in the same month by Raines and co-workers, who developed a traceless Staudinger ligation utilising a cleavable thioester linkage (**111**) (Scheme 33).[65] Using this method, peptides can be synthesised in a two-step procedure from thioesters and azides using a phosphine with a thiophenol substituent (**110**). Transthioesterification of the peptide **109**, using excess **110**, forms the thioester **111** which then undergoes the traceless Staudinger ligation in a mechanism analogous to that in Scheme 32.

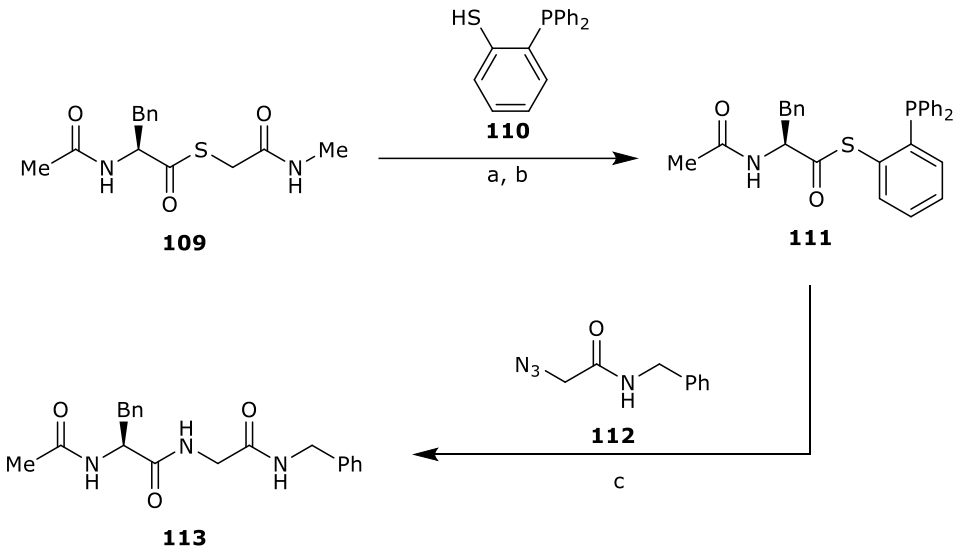

Scheme 33: Example transformation of Raines' traceless Staudinger ligation.[65] Reagents and conditions a) DIEA, DMF, r. t., 12 h; b) DIEA, Merrifield resin, DMF, r. t., 12 h; c) THF:H_2O, r. t., 12h, 35% (yield over two steps).

1.2.3.3 Staudinger-Sulfonamide Ligation

Although the vast majority of Staudinger ligation reactions are used to form amides, variants which install alternative linkers do exist. Two of the most developed of these are the use of phosphite esters to form phosphorimidates,[66] and the application of phosphonites to prepare phosphonamidates.[67] A particularly interesting variant of the Staudinger

ligation was published in 2017 by Ren and co-workers, where an aryl fluorosulfate is used as the tethered electrophile (Scheme 34).[68] In this example the elimination of a fluoride leaving group in a 'SuFEx'[69] process yields a product bearing an aryl sulfamate ester (**115**).

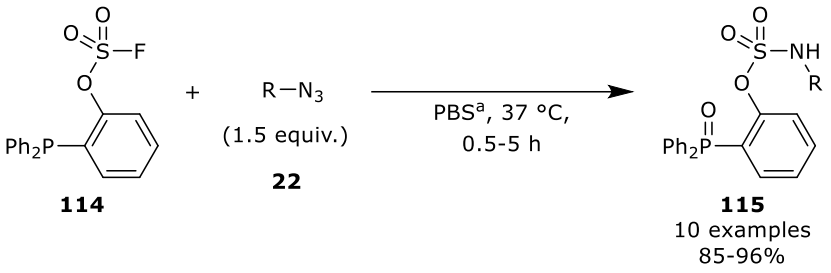

*Scheme 34: Staudinger ligation using the aryl fluorosulfate functionalised phosphine **114** as described by Ren and co-workers.[68] [a]DMSO and/or DMF used in addition to PBS in select examples.*

This is the only instance in the literature of a Staudinger ligation reaction producing a tetrahedral sulfur(VI) linker. Given that the biological systems chemical ligation reactions seek to explore often have tetrahedral geometry linkers (for instance phosphate diesters in DNA),[70] the ability to introduce tetrahedral linkers is of importance.

1.2.4 Project Aims

In the 100 years since the seminal publication of 1919 by Hermann Staudinger, iminophosphoranes have been established as an extremely valuable class of compounds. As shown in section 3, a wealth of Staudinger-type reactions for the synthesis of various structures have been reported. Furthermore, in recent times the Staudinger ligation has become an invaluable tool for the synthesis of bioconjugates in chemical biology.

The aim of this project is to further expand the field of Staudinger-type chemistry. Despite the huge amount of research using iminophosphoranes, further applications have been hypothesised (Scheme 35).

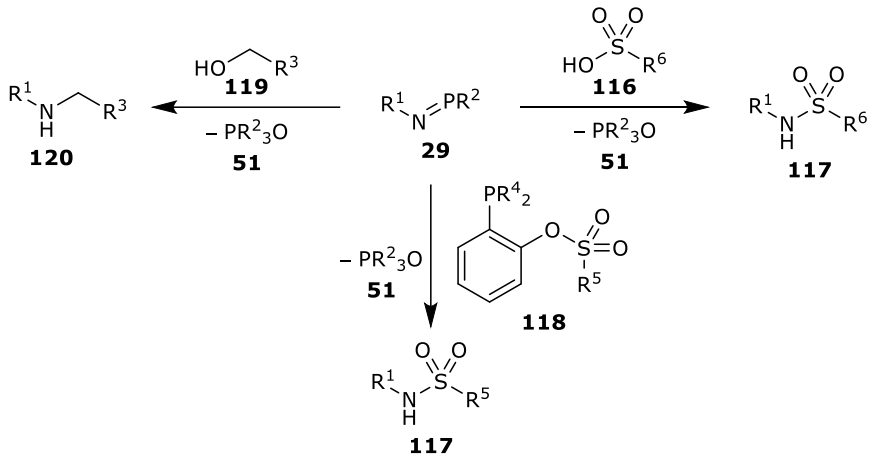

Scheme 35: Proposed novel Staudinger-type methodology. Left: amination using alcohols. Right: sulfonamidation using sulfonic acids. Bottom: traceless Staudinger-sulfonamide ligation

These include a direct Staudinger amination reaction utilising alcohols, which would be a valuable method for amine construction. Secondly, the use of sulfonic acids in a sulfonamidation protocol, analogous to the amidation of carboxylic acids described by Garcia, will be explored. Significantly, this method would allow the replacement of sulfonyl chlorides with sulfonic acids as sulfonamide precursors. Finally, a sulfonamide variant of the traceless Staudinger ligation will be developed, allowing the

synthesis of bioconjugates bearing tetrahedral linkers, with no phosphorus incorporated.

1.3 Results and Discussion

1.3.1 Staudinger Amination

1.3.1.1 Staudinger Amination Using Alcohols

As outlined in chapter one, the synthesis of amines is a highly desirable transformation in organic chemistry. Consequently, we aimed to develop a novel amine synthesis protocol, utilising iminophosphoranes obtained from the versatile Staudinger reaction. It was hypothesised that, as water can be used to hydrolyse iminophosphoranes, primary alcohols could be used in an analogous reaction. Given that the mechanism for the hydrolysis of iminophosphoranes begins with protonation,[71] and the pKa of water is similar to that of alcohols (water = 15.74, ethanol = 15.85, in water)[72], we believed alcohols could be used in a similar mechanism. If this protonation using an alcohol does occur to give the phosphonium salt **121**, then formation of the phosphorane **122** would next occur (Scheme 36).

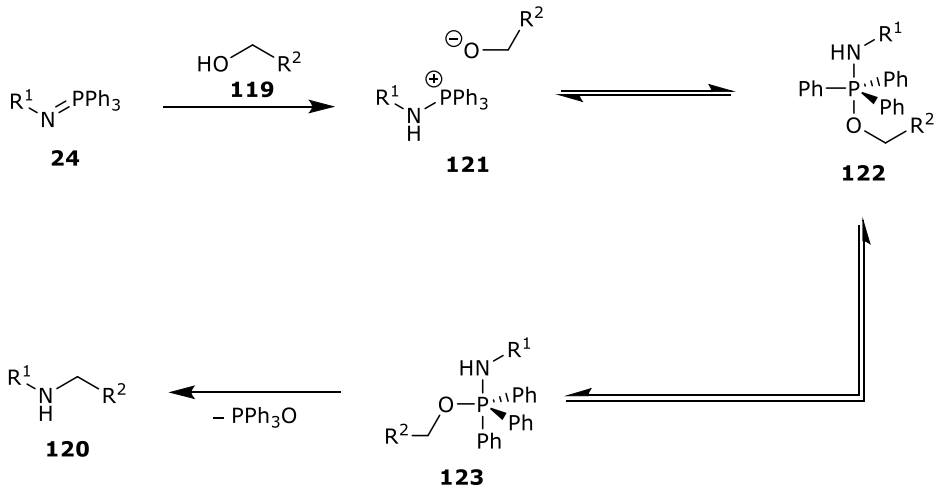

Scheme 36: Proposed mechanism for the Staudinger amination of alcohols.

The mechanism from **122** onwards can be seen to be analogous to the dioxyphosphorane-mediated coupling of amines and alcohols discussed in

chapter one. Therefore, if the initial protonation to form the phosphonium salt **121** can be achieved, the desired amine products should be obtained.

Furthermore, the synthesis of aziridines from 2-azidoalcohols using tertiary phosphines is a known transformation and is essentially the intramolecular version of our desired transformation (Scheme 37).[73]

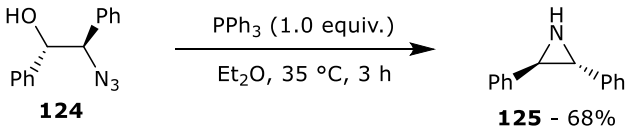

124 **125** - 68%

*Scheme 37: Synthesis of aziridine **125** described by Ittah and co-workers.[73]*

To explore this hypothesis, the iminophosphorane (**126**) was synthesised *via* a Staudinger reaction between benzyl azide (**92**) and triphenylphosphine (Scheme 38). Formation of the iminophosphorane (**126**) was achieved quantitatively (as confirmed by ^{31}P and ^{1}H NMR spectroscopy) after 1 hour at 70 °C.

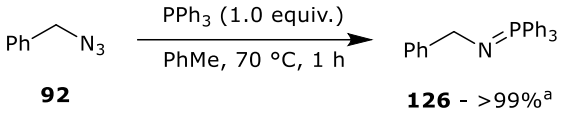

92 **126** - >99%[a]

*Scheme 38: Synthesis of the iminophosphorane **126**. [a]yield determined by ^{1}H and ^{31}P NMR spectroscopy.*

With the iminophosphorane in hand, we explored the proposed Staudinger amination, using 1-decanol as the alcohol.

*Table 1: Attempted Staudinger amination reaction using representative alcohols and iminophosphorane **126**.*

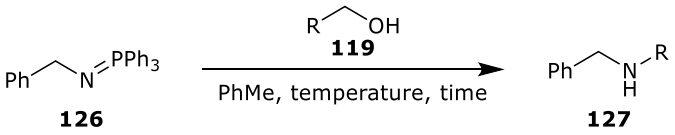

Entry	Alcohol	Time / h	Temperature / °C	Yield / %
1	1-decanol (1 equiv.)	48	r. t.	0
2	1-decanol (1 equiv.)	120	60	0
3	1-decanol (5 equiv.)	24	60	0
4	benzyl alcohol (1 equiv.)	120	60	0
5	trifluoroethanol (20 equiv.)	48	140	0
6	1-decanol (1 equiv.)	3.0	220[a]	0

[a]*Reaction performed using microwave heating*

Unfortunately, no reaction was observed between 1-decanol and **126** at room temperature or 60 °C (Table 1 entries 1 and 2 respectively). Five equivalents of 1-decanol were also used in an attempt to drive the reaction, with no product being obtained (Table 1 entry 3). In the Staudinger reduction, the hydrolysis of *N*-aryliminophosphoranes is accelerated at a lower pH, as protonation of the iminophosphorane occurs more readily.[71] Consequently, two more acidic alcohols in the form of benzyl alcohol and trifluoroethanol were also used (Table 1 entries 4 and 5 respectively). However, in both cases the protonated iminophosphorane was not detected (by ^{1}H and ^{31}P NMR spectroscopy) and no reaction took place. A reaction was also performed at 220 °C, using microwave heating, with no product observed (Table 1 entry 6). In all cases, no product formation occurred, the only reaction observed was a slow Staudinger reduction of **126** to benzylamine, due to the intrusion of water into the reactions. Hydrolysis of the iminophosphorane (**126**) was also observed by ^{31}P NMR spectroscopy, with the formation of triphenylphosphine oxide. As discussed in section 3.2.3, protonation of iminophosphoranes is achieved using carboxylic acids

and is crucial for Garcia's Staudinger amidation method.[52] However, no protonation was observed in any of the aforementioned experiments using alcohols, preventing the desired transformation from occurring.

Due to **126** being inert in the above described reactions, an alternative iminophosphorane (**129**) was synthesised (Scheme 39). The corresponding azide **128** is not commercially available but was easily prepared from the corresponding aniline in excellent yield (Scheme 39). As anticipated synthesis of **129** using the electron rich azide was facile with full conversion achieved after 2 hours at room temperature (Scheme 39).

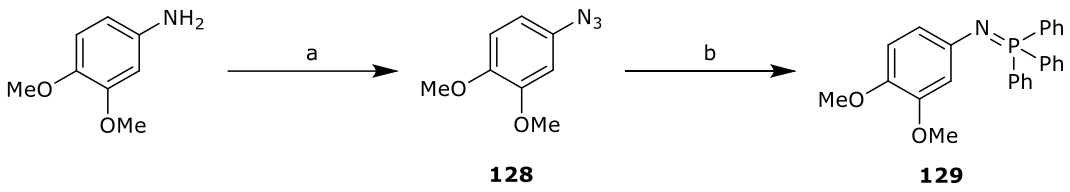

128 **129**

*Scheme 39: Synthesis of iminophosphorane **129**. Reagents and conditions a) $TMSN_3$, t-BuONO, MeCN, r. t., 18 h, 93%; b) PPh_3, $PhCF_3$, r. t., 2 h, >99%[a]; [a]yield of **129** determined by ^1H and ^{31}P NMR spectroscopy.*

The lower basicity of this *N*-aryliminophosphorane (**129**) relative to the *N*-benzyl iminophosphorane (**126**) would be expected to reduce the ability to deprotonate the alcohol. However, it was hoped the electron withdrawing nature of the (albeit electron rich) aromatic ring would make the iminophosphorane more susceptible to nucleophilic attack at phosphorus.

*Table 2: Attempted Staudinger amination reactions using representative alcohols and iminophosphorane **129**.*

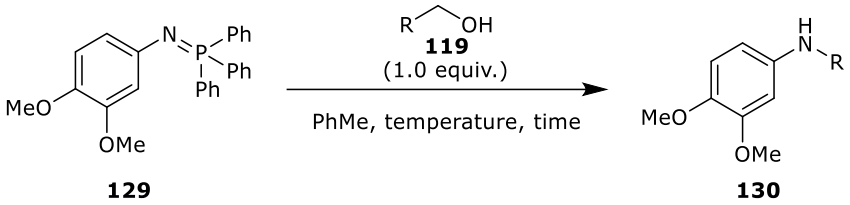

129 **130**

Entry	Alcohol	Time / h	Temp / °C	Yield / %
1	benzyl alcohol	48 then 168	r. t. then 55	0
2	trifluoroethanol	24 then 96	50 then 100	0

However, upon addition of benzyl alcohol no change was observed by ^{31}P NMR spectroscopy after 48 hours at room temperature, or after a further 168 hours at 55 °C (Table 2 entry 1). Similarly, no reaction was observed with trifluoroethanol after 24 hours at 50 °C, or after a further 96 hours at 100 °C (Table 2 entry 2). In contrast to the benzyl azide derived iminophosphorane (**126**) only trace amounts the Staudinger reduction product were observed whilst the iminophosphorane itself was isolable and bench stable. Evidently, the reactivity of **129** is not sufficient for the desired transformation to occur.

As a result of these experiments, it was determined that the ambitious goal of performing Staudinger amination reactions using alcohols was not feasible. Alcohols are fundamentally not acidic enough to protonate the iminophosphoranes used, preventing the desired reaction from occurring. Consequently, an alternative method would need to be devised to synthesise secondary amines from iminophosphoranes.

1.3.1.2 Staudinger Amination Using Esters

Given that the iminophosphoranes **126** and **129** both failed to react with alcohols (Table 1 and Table 2), an alternative method was proposed. Garcia and co-workers noted, in their intermolecular Staudinger amidation publication, that esters such as butyl acetate and ethyl acetate do not react with iminophosphoranes.[52] However, such reactions do occur in intramolecular examples and form the basis of most Staudinger ligations.[62] Additionally, both acyl chlorides[11] and anhydrides[60] have been used as electrophiles with iminophosphoranes to form amides.

Consequently, we proposed that a more electrophilic ester, such as a trifluoroacetate ester (**131**), could act as a suitable electrophile in an intermolecular reaction (Scheme 40).

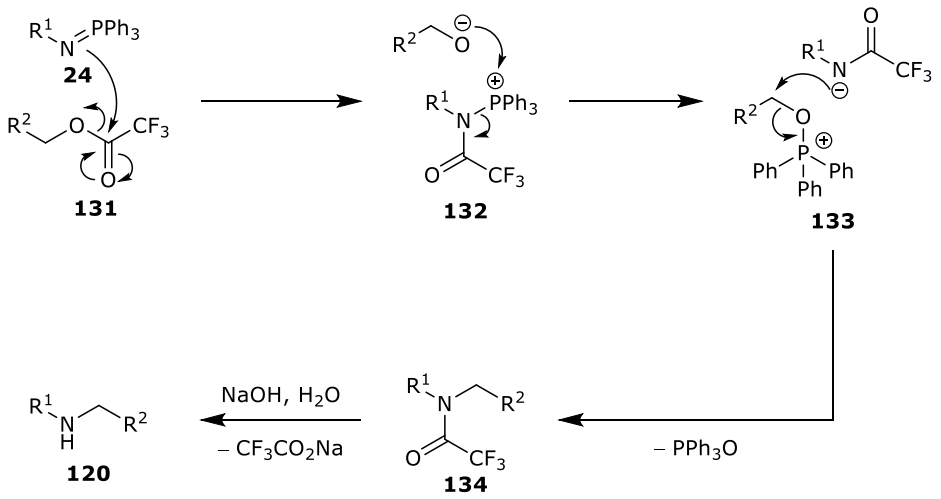

*Scheme 40: Proposed mechanism for the synthesis of amines from iminophosphoranes (**24**) using a trifluoroacetylated alcohol (**131**).*

If the desired intermolecular reaction does occur, then the resulting amidophosphonium salt (**132**) will likely rearrange to the oxyphosphonium salt (**133**). This would be due to the relative energies of the CF_3 stabilised

amide anion compared to the more electronegative, harder, alkoxide ion. Subsequent Arbuzov collapse of the oxyphosphonium salt would give a tertiary amide product and triphenylphosphine oxide. Tertiary trifluoroacetamides such as **134** readily hydrolyse under basic conditions, thus giving the desired secondary amine product. Consequently, trifluoroacetate esters could be used as cleavable activating groups allowing alkylation of iminophosphoranes using alcohols.

To test this concept, benzyl 2,2,2-trifluoroactete (**135**) was synthesised as the activated alcohol using trifluoroacetic anhydride (Scheme 41).

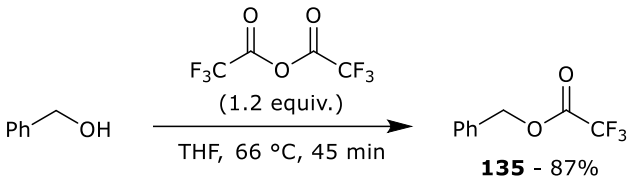

*Scheme 41: Synthesis of benzyl 2,2,2-trifluoroacetate (**135**).*

With this highly electrophilic ester in hand, coupling reactions were then performed with the same *N*-benzyl and *N*-aryl iminophosphoranes as were used in section 4.1.1 (**126** and **129** respectively). In both cases the desired products were successfully isolated (Scheme 42).

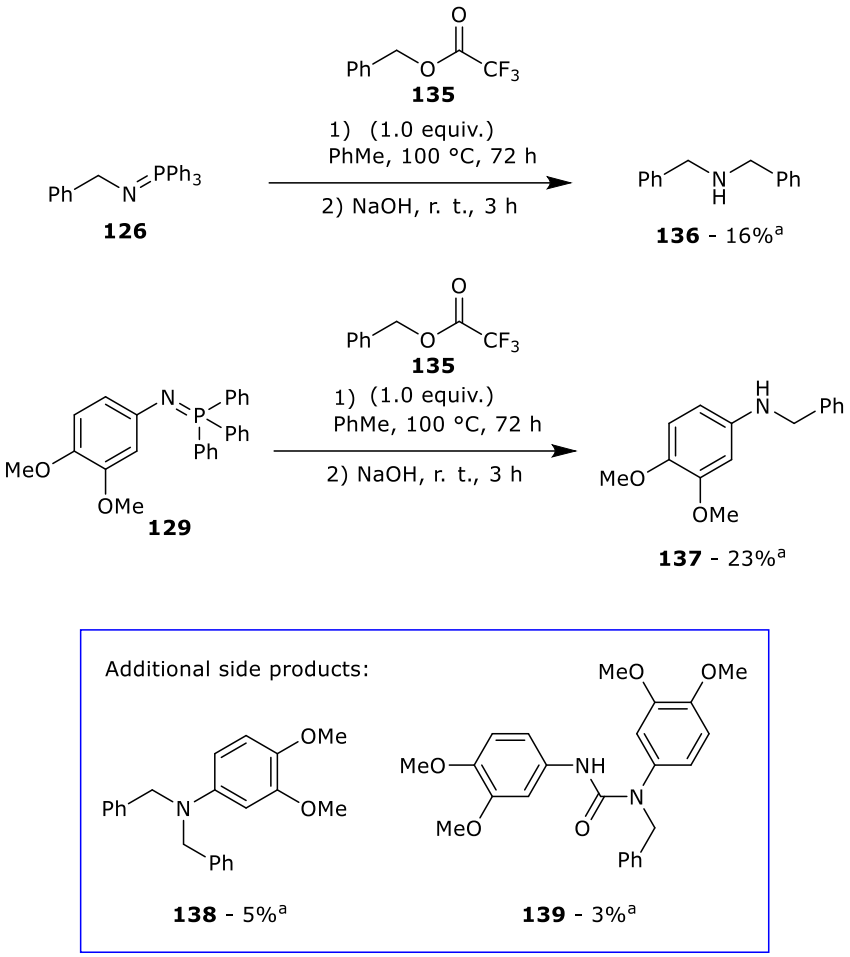

*Scheme 42: Synthesis of amines **136** and **137** via a Staudinger ester coupling. [a]Yields reported from azide.*

Although the successful isolation of product in both cases was very encouraging for this novel method, the yields obtained were disappointing. It can be seen from the reaction using the *N*-aryl iminophosphorane (**129**) that a number of side reactions occurred, leading to the formation of the side-products **138** and **139**, which were both isolated (Scheme 42). The side-product **138** can be seen to form from a reaction between the amine **137** and another equivalent of the ester (**135**) (Scheme 43). Similarly, **139** is presumably the product of a reaction between the iminophosphorane **126** and the trifluoroacetamide intermediate (**140**). These side reactions, in addition to considerable quantities of aniline,

produced *via* a Staudinger reduction, explain the modest yields obtained in the reactions.

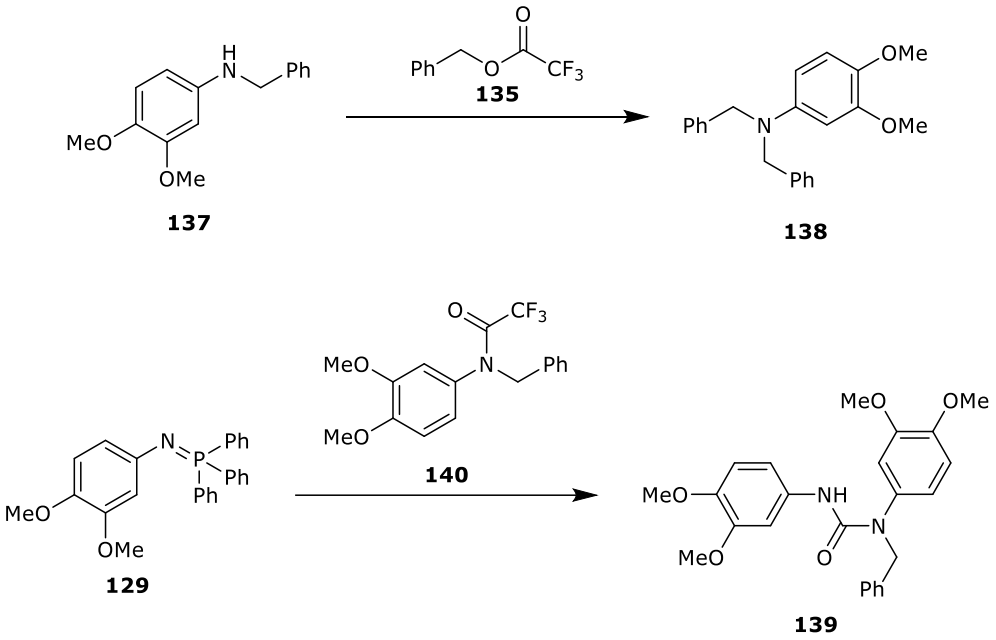

*Scheme 43: Proposed pathway for the formation of the side-products **138** and **139**.*

A multinuclear NMR study of the reaction was conducted, using **126**, to gain an insight into the mechanism of the reaction. As was proposed, an alkoxyphosphonium salt (**141**) was observed by ^{31}P and ^{13}C NMR spectroscopy (Scheme 44). These data correspond well to that reported for a similar compound **142**.[74] The difference between the ^{31}P shifts is most likely due to the difference in counterion. As previously discussed, subsequent Arbuzov collapse of the observed species **141** would yield the desired trifluoroacetamide **134**. On the basis of this evidence, it is likely the reaction occurs through the originally proposed mechanism (Scheme 40) and is not a simple substitution reaction of the iminophosphorane eliminating a trifluoroacetate leaving group.

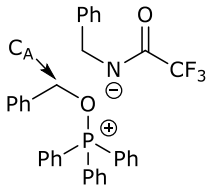

141

^{31}P = 45.6 ppm

$^{13}C_A$ = 119.6 ppm, $^{2}J_{C\text{-}P}$ = 101.5 Hz

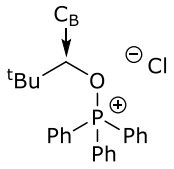

142

^{31}P = 61.9 ppm

$^{13}C_B$ = 118.5 ppm, $^{2}J_{C\text{-}P}$ = 106.6 Hz

*Scheme 44: ^{31}P and ^{13}C NMR data for literature compound **142**[74] and experimental compound **141**.*

Despite the low yields obtained for these reactions, there is considerable potential for this method to offer a new amination protocol. However, the sluggish reactivity observed led to efforts being directed elsewhere.

1.3.2 Staudinger Sulfonamidation

1.3.2.1 Conventionally Heated Reactions

Since coupling reactions between iminophosphoranes and alcohols do not proceed whilst reactions with carboxylic acids are known[52], it was hypothesised that a yet more acidic coupling partner could be used. Therefore, work was undertaken to develop a novel protocol for the synthesis of sulfonamides, using sulfonic acids. Given that sulfonamides are the largest class of antimicrobial agents they represent a target functional group of great significance.[75,76] To date synthetic routes rely almost exclusively on the use of sulfonyl chlorides as precursors.[77] Sulfonyl chlorides are difficult to handle and are not particularly stable to long term storage. Therefore, their replacement with more stable sulfonic acids would be beneficial. However to date there is no known example of a single step direct conversion of a sulfonic acid to a sulfonamide, and very limited examples using sulfonic acid salts.[78,79]

Addition of triflic acid to both **126** and **129** readily formed the protonated iminophosphorane (**143**) as determined by ^{1}H and ^{31}P NMR spectroscopy. However, no further reaction was observed (Scheme 45). The sulfonate conjugate base's very poor nucleophilicity prevents attack at phosphorus and consequently no product is observed. It is worth noting that Garcia reported that trifluoroacetic acid did not yield the desired amide products in their amidation studies.[52] Thus it appears we encountered a similar issue related to the poorer nucleophilicity of the stronger acid.

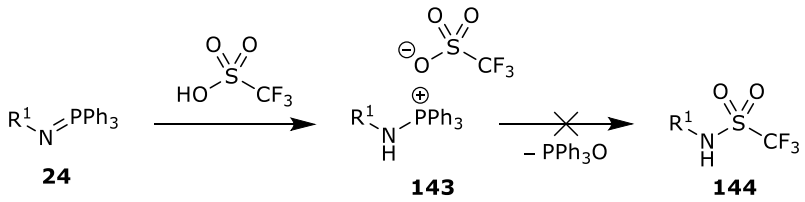

*Scheme 45: Attempted sulfonamidation of an iminophosphorane (**24**) using triflic acid, forming a stable protonated iminophosphorane **143**.*

As a result, the less acidic methanesulfonic acid (with a more nucleophilic conjugate base) was used henceforth. Once again, the protonated iminophosphorane (**145**) was formed immediately, however in this case the subsequent collapse of this species did occur, giving the desired sulfonamide product (**146**) in 40% isolated yield (Scheme 46).

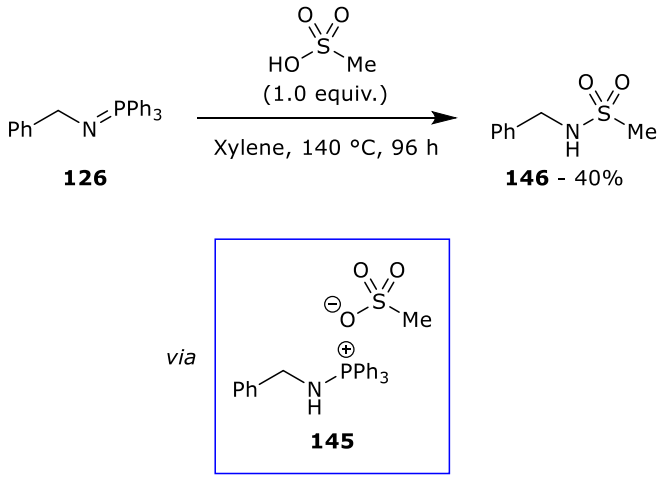

*Scheme 46: Synthesis of N-benzylmethanesulfonamide (**146**), from the iminophosphorane **126**.*

In order to achieve this the reaction was heated to 140 °C for 96 hours. Despite the forcing conditions this was a very promising result, being the first formation of a sulfonamide using a non-activated sulfonic acid. Nevertheless, a solvent screen was performed in an attempt to optimise this process (Table 3).

Table 3: Solvent screen for the synthesis of **146**.

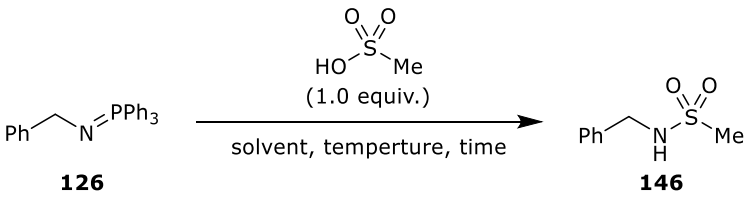

Entry	Solvent	Time / h	Temp / °C	Yield %
1	xylenes	96	140	40
2	DMF	48	130	0
3	1-butanol	96	118	0
4	pyridine	96	116	0
5	PhMe	96	100	0

In the case of all solvents except xylenes, no product formation was observed (Table 3). When the non-polar solvents of xylenes and toluene were employed, the protonated iminophosphorane formed was insoluble, thus impeding the reaction (Table 3 entries 1 and 5). Therefore, a number of high boiling point, polar solvents were used with the aim of overcoming this solubility issue (Table 3 entries 2-4). Although in these examples the protonated iminophosphorane was soluble, no product was obtained at the end of the reaction. In all cases the unreacted protonated iminophosphorane was observed. There are two possible explanations for the lack of reactivity in the polar solvents. Firstly, the protonated iminophosphorane may be too well stabilised by the solvent, preventing nucleophilic attack of the sulfate counterion. Alternatively, the reflux temperatures of these solvents are not sufficiently high to allow the collapse of the protonated iminophosphorane intermediate.

1.3.2.2 Microwave Heated Reactions

1.3.2.2.1 Reaction optimisation

The high temperature and prolonged duration required for the Staudinger sulfonamidation reaction make it a good candidate for microwave chemistry. Microwave chemistry allows for the rapid and uniform heating of solutions to elevated temperatures and has been reviewed extensively.[80–86] Additionally, the use of sealed microwave tubes permits the heating of solvents to temperatures exceeding their boiling points. Consequently, the sulfonamidation of **126** using methanesulfonic acid was further explored using microwave heating.

Reactions were performed in four different solvents of medium polarity (dielectric constants: anisole = 4.3, trifluorotoluene = 9.18, 1,2-dichlorobenzene = 9.93, pyridine = 12.3, relative to xylenes = 2.40).[87]

This was undertaken with a view to solubilising the protonated iminophosphorane (**145**), but not stabilising it and preventing the reaction (Table 4). Furthermore, each solvent has a net dipole moment and consequently is a good microwave absorber. All the reactions were performed at 200 °C for one hour, with the reactions analysed by ^{31}P NMR spectroscopy. Using trifluorotoluene resulted in the greatest formation of triphenylphosphine oxide and was the only reaction where the sulfonamide **146** was clearly detected by ^{1}H NMR spectroscopy (Table 4 entry 2).

*Table 4: Solvent screen for the synthesis of **146** from the microwave heating of **145**.*

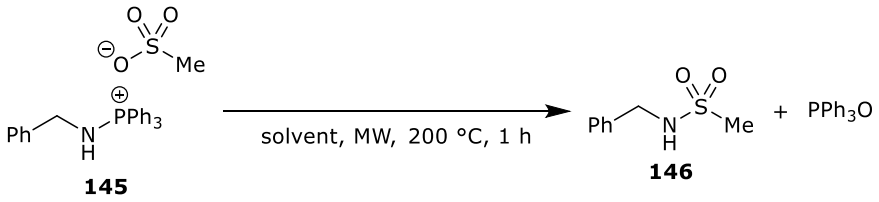

145 **146**

Entry	Solvent	**145** / %[a]	PPh_3O / %[a]
1	PhOMe	88	12
2	$PhCF_3$	49	51
3	1,2-dichlorobenzene	85	15
4	pyridine	74	25

[a]Conversion determined by ^{31}P NMR spectroscopy.

As a result, trifluorotoluene was chosen as the solvent to further explore this reaction. Subsequent experiments found that full consumption of **145** was achieved after three hours at 220 °C, but not at 200 °C. Using these conditions, on a preparative scale, the desired product was obtained in 59% yield from the azide (Scheme 47).

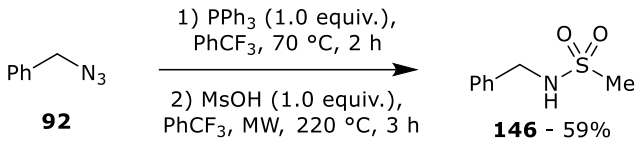

*Scheme 47: Synthesis of N-benzylmethanesulfonamide (**146**) using microwave heating.*

This represents a significant improvement in the yield, whilst greatly reducing the duration of the reaction compared to when conventional heating was used (Scheme 46). Although a very high reaction temperature is used, this is easily achieved using a microwave reactor.

A control experiment was performed using benzylamine and methanesulfonic acid in the absence of any phosphorus species (Scheme 48).

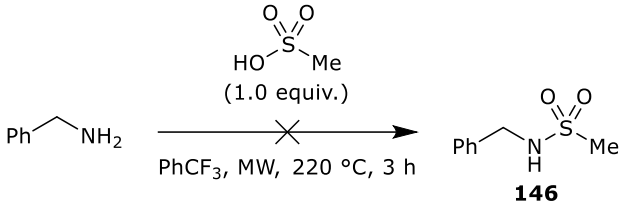

*Scheme 48: Control reaction for the synthesis of **146** in the absence of any phosphorus-containing species.*

This concluded that the product formation is not a result of a Staudinger reduction followed by a condensation reaction under the extreme temperatures.

Further experiments were conducted to optimise the conditions of the reaction (Table 5).

Table 5: Optimisation of the microwave synthesis of **146**.

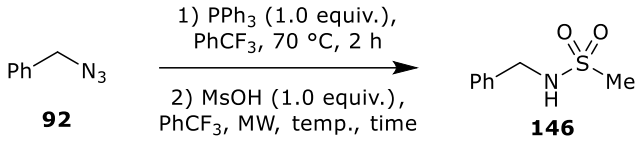

Entry	MsOH equiv.	Time / h	Temp. / h	Yield / %
1	1.0	3.0	220	59
2	1.0	1.0	220	11
3	1.0	5.0	200	54
4	2.0	3.0	220	28

Reducing the reaction duration to one hour resulted in a large decrease in the isolated yield to 11% (Table 5 entry 2). In this case, the intermediate **145** was present at the end of the reaction, clearly indicating that the reaction had not gone to completion. By reducing the reaction temperature to 200 °C the product could be isolated in similar yield (to Scheme 47), at the expense of a longer reaction time of five hours (Table 5 entry 3). Whilst attempts to drive the reaction using two equivalents of methanesulfonic acid proved counterproductive, with a lower yield of 28% obtained (Table 5 entry 4). In this last example a tertiary sulfonamide with two benzyl groups (**147**) was also isolated in 6% yield, somewhat helping to explain the reduced yield of this reaction (Scheme 49).

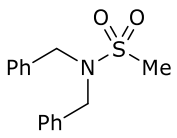

147

*Scheme 49: Tertiary sulfonamide **147** formed as a side-product in the reaction using two equivalents of methanesulfonic acid (Table 5 entry 4).*

As discussed, the formation of the protonated iminophosphorane (**145**) occurs readily at room temperature but formation of the sulfonamide **146** requires very forcing conditions. Additionally, no further phosphorus-containing species (for example *S,O*-phosphoranes) were observed. Therefore, it seems apparent that the nucleophilic attack of the sulfonate counterion to the phosphonium salt is the rate limiting step of the reaction. Consequently, a more electrophilic phosphine could potentially be used to better facilitate nucleophilic attack of the sulfonate, thus accelerating the reaction. To this end a number of different triarylphosphines were employed for synthesis of the model sulfonamide **146** (Table 6).

*Table 6: Screen of phosphines for the Staudinger sulfonamidation of **92**.*

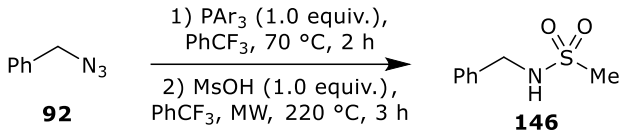

92 **146**

Entry	Ar	Yield / %
1	Ph	59
2	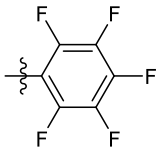	0
3	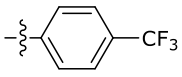	53
4	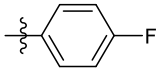	63
5	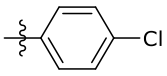	25
6	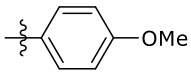	0

The extremely electron poor tris(pentafluorophenyl)phosphine would be expected to form a much more electrophilic phosphonium salt. However, the initial Staudinger reaction to form the iminophosphorane did not occur in this case, consequently no product could form (Table 6 entry 2). The use of both tris(4-trifluoromethylphenyl)phosphine and tris(4-fluorophenyl)phosphine successfully formed the desired product, with comparable yields to that achieved with triphenylphosphine (Table 6 entries 3 and 4 respectively). Tris(4-chlorophenyl)phosphine formed **146**, albeit in a lower yield of 25% (Table 6 entry 5). Additionally, for comparison the more electron rich tris(4-methoxyphenyl)phosphine was used unsuccessfully with no product formation occurring (Table 6 entry 6). In this final instance, the protonated iminophosphorane intermediate was insoluble, prohibiting further reaction.

Although the use of tris(4-fluorophenyl)phosphine gave a marginally elevated yield over that obtained from triphenylphosphine (Table 6 entries 4 and 1 respectively), it is substantially more expensive for only a small increase in performance. However, further experiments were performed to determine if the use of the fluorinated phosphine allowed milder conditions to be employed (Table 7). Reducing the reaction time from three hours to one hour resulted in a small decrease in yield (Table 7 entries 1 and 2 respectively). A reduction in the temperature of the reaction also had a similar effect of lowering the yield (Table 7 entry 3). Given that in the example with the highest yield full consumption of the intermediate **145** was observed, it would appear this yield of 63% is perhaps the limit of the chemistry for this model reaction.

*Table 7: Optimisation of the Staudinger sulfonamidation of **92** using tris(4-fluorophenyl)phosphine.*

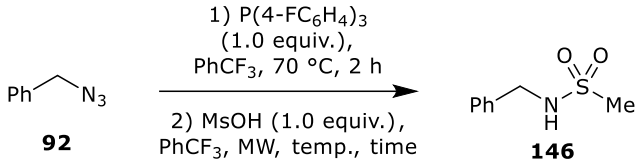

92 **146**

Entry	Time / h	Temp. / h	Yield / %
1	3.0	220	63
2	1.0	220	56
3	3.0	200	53

Due to the aforementioned costs associated with phosphines, exacerbated by the formation of stoichiometric phosphine waste, future reactions were performed using triphenylphosphine and the conditions shown in Table 5 entry 1.

1.3.2.2.2 Substrate scope

Alternative sulfonic acids were also used to explore the substrate scope of the reaction (Table 8). Two more acidic sulfonic acids were used in the form of triflic acid and nonafluorobutane-1-sulfonic acid (Table 8, **149** and **150** respectively). However, in both cases despite the protonated iminophosphorane forming, and being soluble during the reaction, no product was observed. As was the case when triflic acid was employed in the conventionally heated method (Scheme 45), the protonated iminophosphorane was observed unreacted at the end of the reaction. Evidently, in both cases the extremely poor nucleophilicity of the resulting sulfonates are prohibitive for the reaction. Two sulfonic acids bearing amine functionality were also employed unsuccessfully (Table 8, **151** and **152**). Both of these substrates with basic amine functionality, exist not as

a free acid but as zwitterions. Consequently, the ability to protonate the iminophosphorane is reduced. In the case of 3-amino-1-propanesulfonic acid (Table 8, **152**), no protonation of the iminophosphorane was observed by ^{1}H and ^{31}P NMR spectroscopy. Although the protonated iminophosphorane was observed when 4-morpholinepropanesulfonic acid (Table 8, **151**) was used, it was insoluble in the reaction medium and no product was observed.

*Table 8: Substrate scope of the sulfonamidation of **92**.*

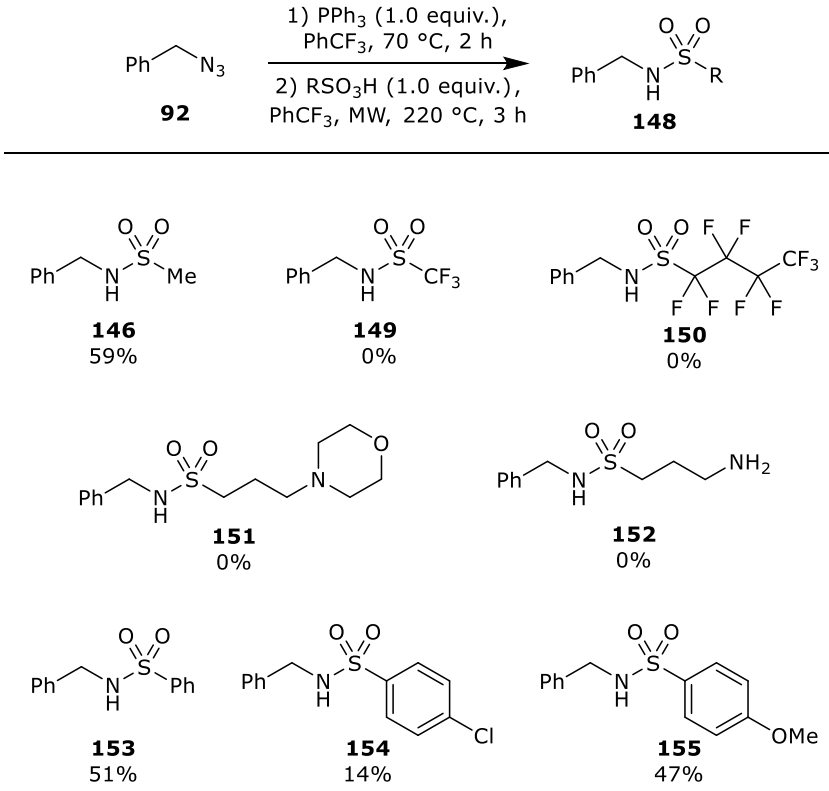

However, the use of aromatic sulfonic acids was successful, with a yield of 51% being obtained using benzenesulfonic acid (Table 8, **153**). The comparatively electron poor aromatic of 4-chlorobenzenesulfonic acid

returned a diminished yield of 14% (Table 8, **154**), whilst the electron rich 4-methoxybenzenesulfonic acid was used to provide the relevant sulfonamide (**155**) in 47% yield. Given that adding an electron withdrawing chlorine substituent lowered the yield of benzenesulfonic acid, it was hoped the electron donating methoxy would increase the yield. However, the yield obtained is comparable to that of benzenesulfonic acid. This suggests that whilst electron withdrawing groups impede the reaction, increasing the nucleophilicity of the sulfonate to exceed that of benzenesulfonate is not conducive to increasing the yield.

The azide component of the reaction was also altered, with the aryl azide **128** used to successfully afford the *N*-aryl sulfonamide **156** (Scheme 50).

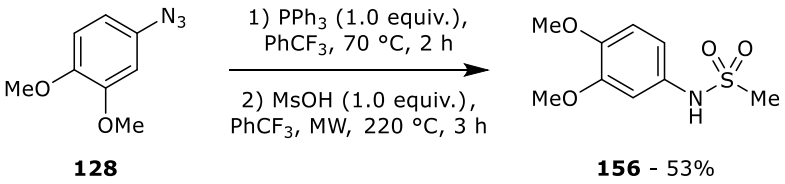

128 **156** - 53%

*Scheme 50: Synthesis of the N-aryl sulfonamide **156** via the Staudinger sulfonamidation of **128**.*

Disappointingly, when benzenesulfonic acid was used with **128**, the resulting protonated iminophosphorane was insoluble in the reaction mixture and no product was observed (Scheme 51).

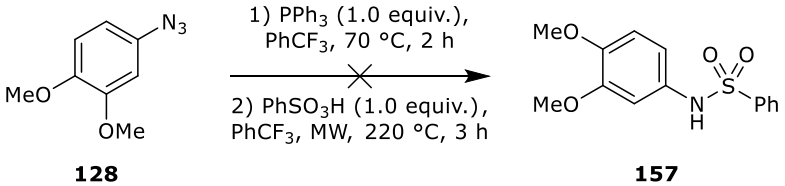

128 **157**

*Scheme 51: Attempted synthesis of the N-aryl sulfonamide **157** via the Staudinger sulfonamidation of **128**.*

This once again highlights the importance of the solubility of the intermediate phosphonium salt. Attempts to overcome this solubility issue with mixtures of trifluorotoluene and DMF or NMP were unsuccessful in all cases. Future work to expand the substrate scope of this novel Staudinger sulfonamidation procedure, should focus on finding a suitable solvent/solvent mixture to solubilise, but not stabilise the protonated iminophosphorane salts.

1.3.3 Traceless Staudinger-Sulfonamide Ligation

1.3.3.1 Outline and Synthesis of the Model Phosphine

To date there is only one example in the literature of a Staudinger ligation reaction giving sulfonamide linked products.[68] As discussed in section 3.3, the tetrahedral linkers offered by sulfonamides are desirable for chemical biology. One major drawback of the work by Ren and co-workers is the incorporation of the phosphine oxide by-product into their products. Therefore, in a similar fashion to the work of Bertozzi[64] and Raines,[65] we aimed to develop a traceless variant of the Staudinger-sulfonamide ligation reaction. To achieve this, it was planned to use the sulfonate ester analogue (**158**) of the ester **103** used by Bertozzi and co-workers (Scheme 52).

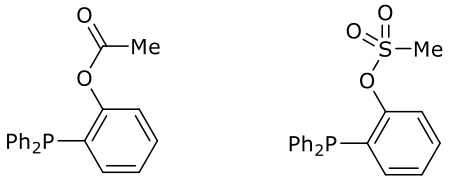

103 **158**

*Scheme 52: Phosphine used in Bertozzi's traceless Staudinger ligation (**103**) and the phosphine to be used in our proposed traceless Staudinger-sulfonamide reaction (**158**).*

If the proposed reaction proves to be the sulfonamide equivalent of Bertozzi's traceless method as intended, then the reaction will occur *via* the mechanism shown in (Scheme 53).

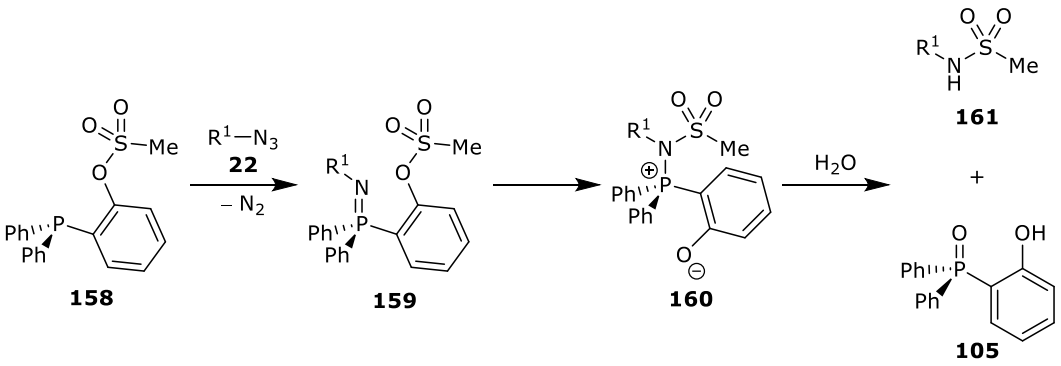

*Scheme 53: Proposed mechanism for the traceless Staudinger-sulfonamide ligation using **158**.*

Attempts to synthesise the phosphine **158** *via* mesylation of **162** resulted in a complex mixture of phosphorus-containing species (Scheme 54).

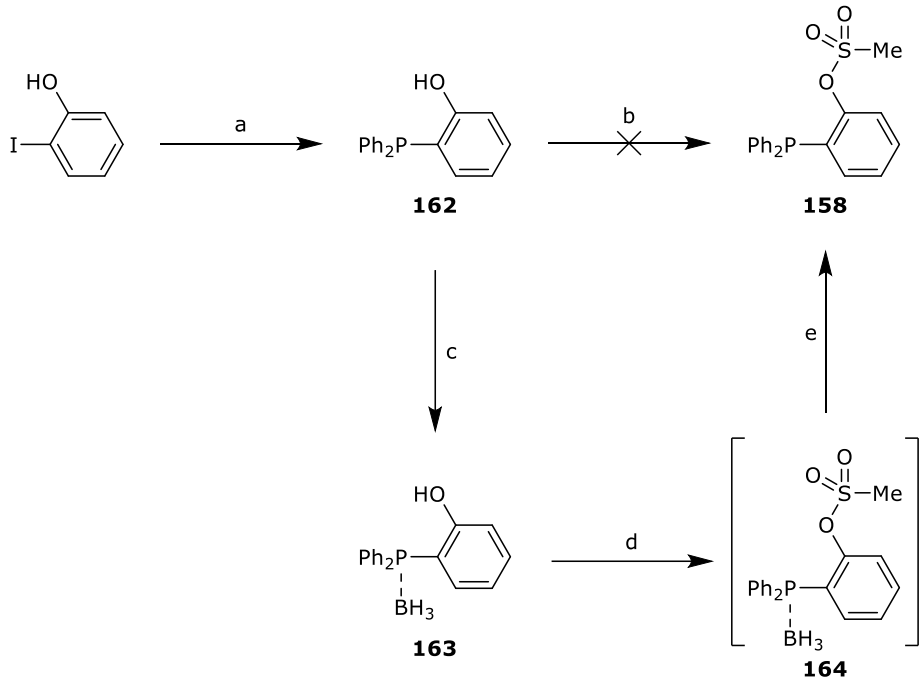

*Scheme 54: Attempted synthesis of phosphine **158** via an unsuccessful direct mesylation of **162** and a successful borane protected route. Reagents and conditions a) PPh_2H, $Pd(OAc)_2$, NaOAc, DMA, 110 °C, 15 h, 76%; b) MsCl, Et_3N, DCM, 0 °C to r. t., 18 h, 0%; c) BH_3.THF, THF, r. t., 18 h, quant.; d) MsCl, KO^tBu, THF, r. t., 18 h; e) MeOH, PhMe, 60 °C, 3 h, 35% (yield over two steps).*

Protection of **162** as the borane adduct **163** allowed mesylation to occur, providing the desired product (**158**) after deprotection in 27% yield over four steps. Using this route, the borane adduct **163** can be used as a general precursor, where various sulfonyl chlorides could be used to prepare an array of phosphines.

Although the synthesis route shown in Scheme 54 provides a good general method for the synthesis of sulfonate ester-containing phosphines, an alternative shorter route can be employed (Scheme 55). By reversing the order of the synthesis and performing the mesylation followed by cross coupling, the desired product (**158**) was obtained in an overall yield of 55%.

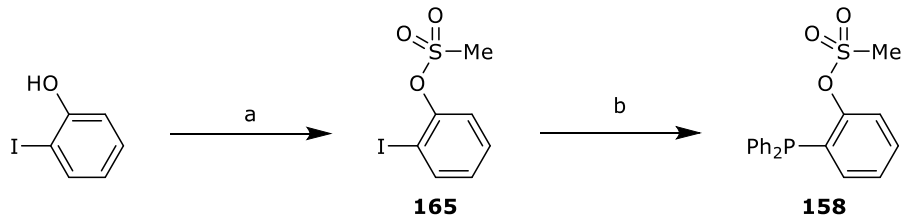

*Scheme 55: Two step synthesis of **158** with no use of protecting groups. Reagents and conditions a) MsCl, KO^{t}Bu, THF, r. t., 18 h, 87%; b) PPh_2H, $Pd(OAc)_2$, NaOAc, DMA, 110 °C, 15 h, 63%.*

With our mesylated phosphine in hand, we then explored the proposed Staudinger-sulfonamide ligation reaction.

1.3.3.2 Application of the Model Phosphine for the Synthesis of Sulfonamides

Upon reaction of **158** with benzyl azide (**92**) a mixture of phosphorus-containing species were observed by ^{31}P NMR spectroscopy

after 8 hours at 70 °C. These were conjectured to be a number of intermediates, possibly including **159** and **160** (Scheme 53). Consequently, sodium hydroxide solution was added, and the reaction heated a further two hours to hydrolyse any intermediates and afford the product. Gratifyingly, the desired product was thus obtained in 54% yield (Scheme 56).

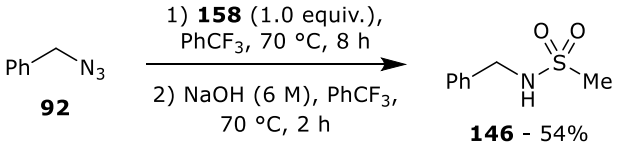

*Scheme 56: Synthesis of **146** using the traceless Staudinger-sulfonamide reaction.*

Two subsequent experiments were performed using toluene as the reaction solvent (Scheme 57). In the first case the reaction was performed under argon and rigorously anhydrous conditions, whilst the second was performed in an open atmosphere. In both cases the reaction yield was increased, to 68% and 60% respectively. Although the reaction performed under anhydrous conditions did give a higher yield, the difference is minor, thus demonstrating the robust nature of the methodology.

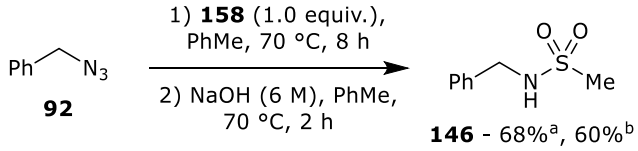

*Scheme 57: Synthesis of **146** using the traceless Staudinger-sulfonamide reaction in toluene. [a]Reaction performed under argon and rigorously anhydrous conditions; [b]Reaction performed in an open atmosphere.*

Two further azides were used in conjunction with **158** to afford the sulfonamides **156** and **166** (Table 9). The *N*-aryl sulfonamide **156** was obtained in a meagre 15% yield, suggesting the lower nucleophilicity and better stabilisation of nitrogen-based anions lowers the reactivity of aryl azides in this methodology. Perhaps this slows transfer of the mesyl group required to convert **159** to **160** (Scheme 53). However, the *N*-alkyl sulfonamide **166** was synthesised in 60% yield, comparable to that observed for the model substrate (**146**).

*Table 9: Substrate scope for the traceless Staudinger-sulfonamide ligation using **158**.*

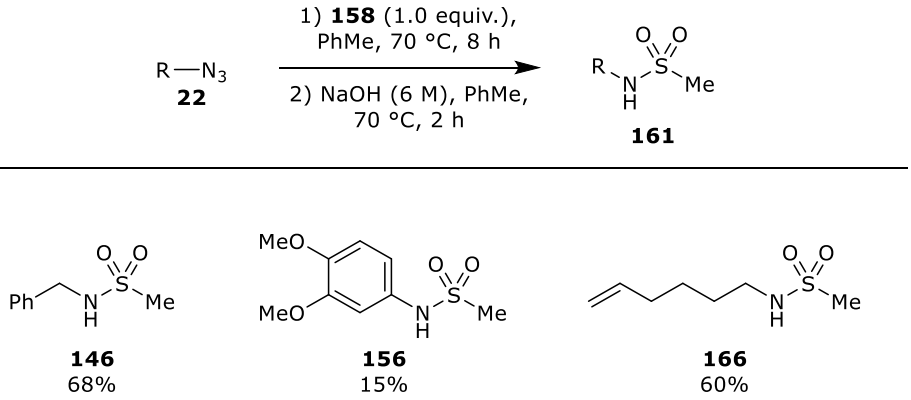

Although these results are very encouraging, the dominant application of Staudinger-ligation reactions is in the field of chemical biology where toluene is not a suitable solvent. Therefore, synthesis of the model substrate was performed in a mixture of DMSO and pH 7.4 buffer, a mixture commonly used in traditional traceless Staudinger ligations (Scheme 58). Moreover, the reaction was performed at a reduced temperature of 37 °C, with no deliberate hydrolysis step using sodium hydroxide. This represents reaction conditions that are suitable to chemical biology.

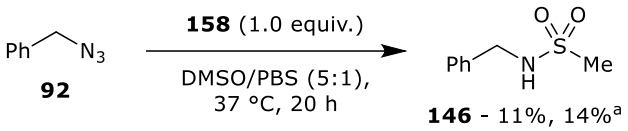

*Scheme 58: Synthesis of **146** using the traceless Staudinger-sulfonamide reaction in DMSO/PBS. [a]1.5 equivalents of benzyl azide (**92**) used.*

Although the yields obtained were considerably lower at 11% and 14% (depending on equivalents of azide used), these preliminary results demonstrate that this novel methodology could potentially be utilized for the synthesis of bioconjugates.

1.3.3.3 Mechanistic Investigations

An alternative pathway to that shown in Scheme 53 that could result in the formation of the desired products, is a Staudinger reduction followed by mesylation of the amine. In order to explore if this possibility is feasible, the relevant mesylated phosphine oxide (**167**) was prepared (Scheme 59).

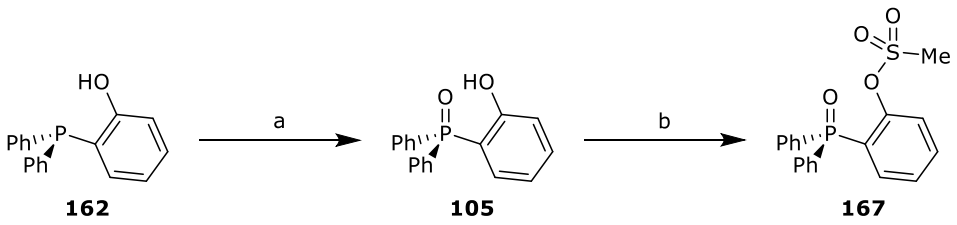

*Scheme 59: Synthesis of the mesylated phosphine oxide **167**, via oxidation of **162** then mesylation of **105**. Reagents and conditions a) H_2O_2, DCM, r. t., 48 h, quant.; b) MsCl, KOtBu, THF, r. t., 40 h, 71%.*

If this alternative pathway is occurring for the synthesis of **146**, then the reaction between benzylamine and **167** must take place under the reaction

conditions to afford **146**. However, this was shown not to be the case, with no product being observed (Scheme 60).

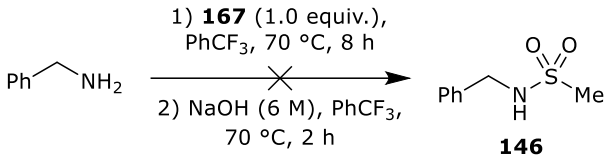

*Scheme 60: Control reaction for the synthesis of **146** from a Staudinger reduction followed by mesylation with the mesylated phosphine oxide **167**.*

A multinuclear NMR study of the reaction was also performed (in deuterated toluene at room temperature). Through ^{1}H, ^{13}C and ^{31}P NMR experiments, in combination with 2D methods, an insight into the mechanism was obtained. Reaction monitoring by ^{31}P NMR spectroscopy showed the consumption of **158** leading to the formation of three final products *via* the iminophosphorane **168** (Figure 1). The three final products of this experiment (which did not include a hydrolysis step with sodium hydroxide) were the phosphine oxide **105**, the sulfonamide-containing phosphonium salt **170** and an unexpected side product **169**. A number of other minor species are observed during the course of the reaction. However, none of these can be attributed to any phosphorane intermediates, which could be expected to form during hydrolysis or *via* intermolecular reactions.

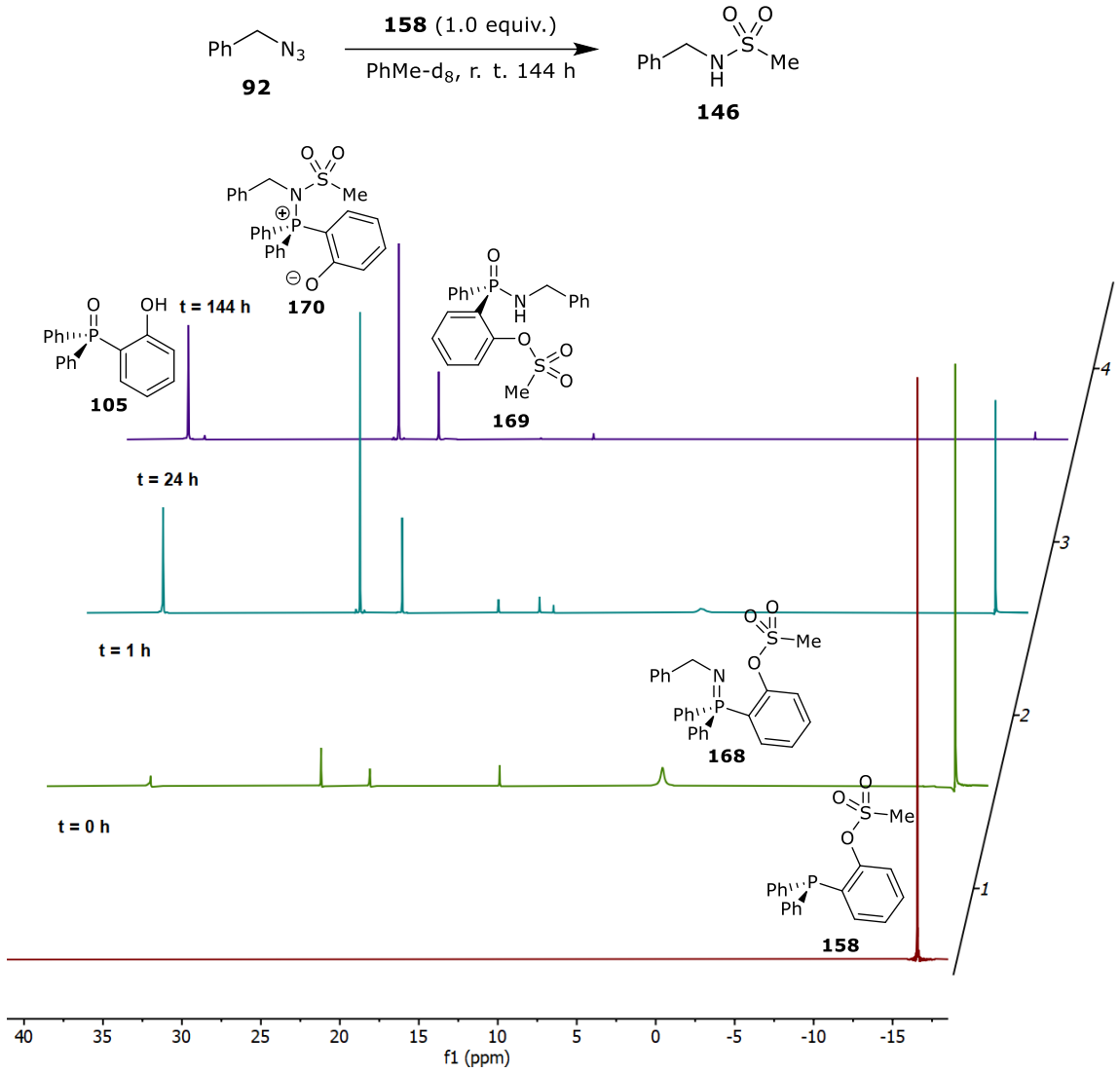

*Figure 1: ^{31}P NMR study of the traceless Staudinger-sulfonamide ligation of benzyl azide (**92**).*

Characteristic ^{1}H and ^{13}C NMR signals for the reaction intermediates (**168** and **170**) and the side-product **169** are shown in Scheme 61.

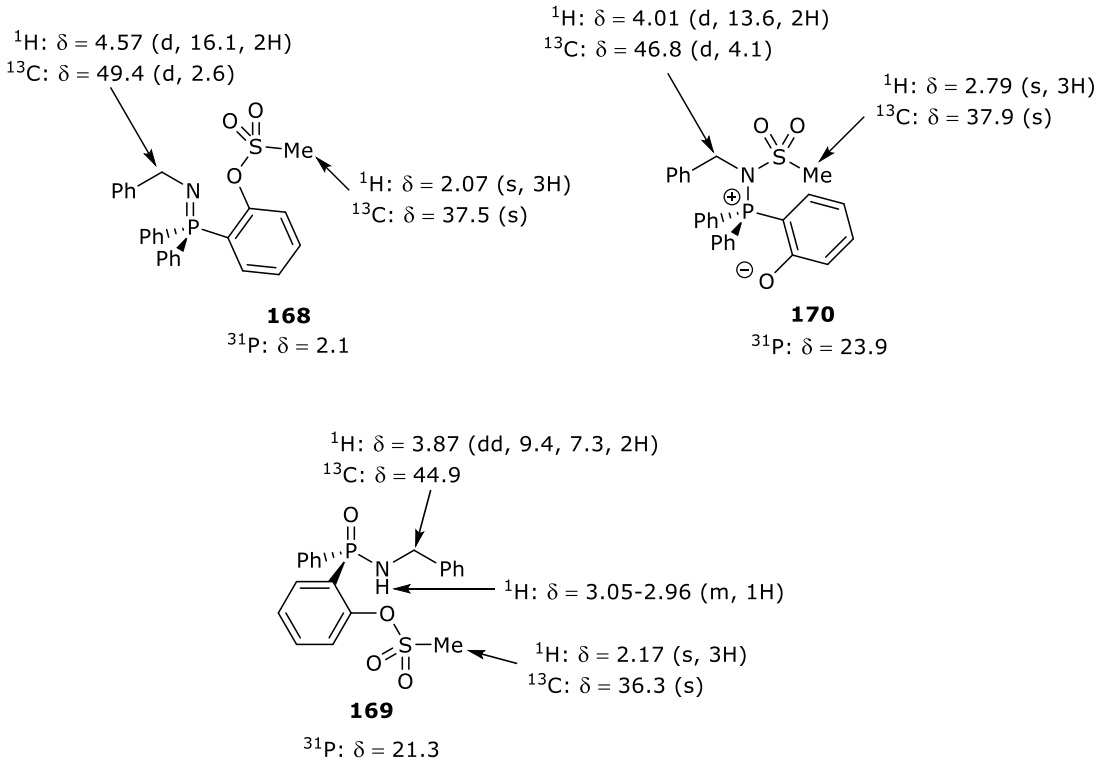

*Scheme 61: Characteristic peaks in the ^{1}H and ^{13}C NMR spectra for the intermediates **168** and **170** in addition to the side product **169**.*

It was originally anticipated that the replacement of an ester with a sulfonate ester in Bertozzi's traceless Staudinger ligation, could allow for the synthesis of sulfonamides by a similar mechanism (Scheme 53). Through our multinuclear NMR study, at a lower reaction temperature, we have successfully shown the formation of the hypothesised intermediates **168** and **170** to occur. Formation of the sulfonamide product **146** was also observed by ^{1}H and ^{13}C NMR spectroscopy, albeit to a lower degree in the absence of the deliberate hydrolysis of **170**. Additionally, a separate experiment has demonstrated that **170** hydrolyses to form the phosphine oxide **105** under the basic conditions typically employed in these reactions. The formation of the side-product **169**, requiring the formal loss of a phenyl substituent, cannot be easily explained. However, the elimination of

benzene from quaternary phosphonium salts, to form tertiary phosphine oxides, under mildly basic conditions is known.[88,89]

1.4 Conclusions and Outlook

An unprecedented Staudinger amination protocol using alcohols was investigated. Although this was ultimately unsuccessful, a novel Staudinger amination method was developed utilising trifluoroacetate esters as activated alcohols. A number of competing side reactions were observed limiting the efficiency of the reaction, future work on this method should focus on overcoming these to improve the reaction yield.

Inspired by the Garcia's Staudinger amidation of carboxylic acids,[52] we have developed a Staudinger sulfonamidation protocol with sulfonic acids. The inherent reduced nucleophilicity of a sulfonate relative to carboxylate, necessitated forcing reaction conditions. However, through the application of microwave heating this method was successfully used to synthesise a number of sulfonamides. Further development of this method to expand the scope of the reaction would require better solubilisation of the intermediate phosphonium salts.

A novel traceless Staudinger ligation method for the synthesis of sulfonamides was also developed. Sulfonamides were obtained in good yields under relatively mild reaction conditions, whilst the potential for the application to chemical biology was demonstrated. Investigations into the mechanism of the reaction found two of the proposed intermediates, consequently suggesting the mechanism is analogous to Bertozzi's original traceless Staudinger ligation. Additional work in this area should focus on the expansion of the substrate scope and reaction optimisation in aqueous media.

1.5 Experimental

1.5.1 General Experimental Procedures

Unless stated otherwise, all reactions were carried out under an atmosphere of argon. All glassware was flame dried or oven dried and allowed to cool under a stream of argon before use. Cooling to 0 °C was effected using an ice-water bath. Cooling to temperatures below 0 °C was effected using dry ice-acetone mixtures. The term petroleum ether refers to the fraction with boiling point of 40 to 60 °C.

Commercially available solvents and reagents were used as supplied with the following exceptions. Toluene, THF and diethyl ether were collected from a solvent tower, where a degassed solvent was passed through two columns of activated alumina and a 7 micron filter under a 4 bar pressure. $CHCl_3$ was stirred with phosphorus pentoxide for 2 h, distilled and stored under an argon atmosphere over activated 4 Å molecular sieves. Reactions were monitored using thin layer chromatography on Merck TLC silica gel 60 F_{254} pre-coated aluminium sheets with fluorescent indicator. Sheets were visualised using ultra-violet light (254 nm) and/or $KMnO_4$ solution, as appropriate. Flash column chromatography was performed using Aldrich silica gel 60, 40–63 μm.

Compounds for which characterisation data matches literature values are denoted by a reference next to the compound name. IR and m. p. data has only been recorded for novel compounds.

Infrared spectra were recorded on the ATR module of a Bruker Alpha spectrometer. Mass spectra were acquired on a Bruker Micromass LCTOF.

Bruker DPX 300, Bruker DPX 400, Bruker AV 400, Bruker AV (III) 400, Bruker AV (III) 400HD or Bruker AV 500 spectrometers were used to record all ^{1}H, ^{13}C, ^{19}F and ^{31}P NMR spectra of dilute solutions of the appropriate compound in the indicated deuterated solvent. All chemical shifts (δ) are reported in parts per million (ppm) relative to residual chloroform (δ_H = 7.26 ppm, δ_C = 77.2 ppm) or benzene (δ_H = 7.16 ppm, δ_C = 128.1 ppm). Coupling constants (*J*) are reported in Hertz and are recorded after averaging. The multiplicity of a ^{1}H NMR signal is designated by one of the following abbreviations: s = singlet, d = doublet, t = triplet, q = quartet and m = multiplet. Where given, reaction conversions were determined by the relative ^{1}H integrations of the product and the appropriate starting material.

Relaxation delays were not measured for solution phase ^{31}P NMR spectroscopy. Consequently, ^{31}P NMR integrals cannot be considered quantitative.

Microwave heated reactions were performed using a Biotage initiator microwave reactor with sealed Biotage 2-5 mL vials.

1.5.2 Experimental Data of Compounds

Benzyl azide (**92**)[90]

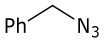

To a solution of sodium azide (1.95 g, 30.0 mmol) in a 4:1 acetone/water mixture (125 mL) was added benzyl bromide (2.34 mL, 20.0 mmol) dropwise over 5 min. The resulting solution was then stirred at r. t. for 18 hours. The reaction mixture was then extracted with Et_2O (3 × 100 mL). The combined organics were washed with brine (150 mL), dried ($MgSO_4$) and concentrated to give **92** (2.58 g, 97 %) as a yellow oil.

^{1}H NMR (400 MHz, $CDCl_3$) δ 7.44 – 7.28 (m, 5H), 4.35 (s, 2H); **^{13}C{^{1}H} NMR** (101MHz, $CDCl_3$) δ 135.5, 128.9, 128.4, 128.3, 54.8; **AT-IR** (neat) ν (cm^{-1}) 3089, 3066, 3032, 2930, 2876, 2089, 1496, 1454, 1349, 1252, 1201, 1078, 1029, 876.

4-Azido-1,2-dimethoxybenzene (**128**)[91]

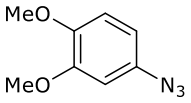

To a solution of 3,4-dimethoxyaniline (1.53 g, 10.0 mmol) in acetonitrile (20 mL) at 0 °C was added *tert*-butyl nitrite (1.19 mL, 15.0 mmol) dropwise over 5 min. Trimethylsilyl azide (1.32 mL, 12.0 mmol) was added dropwise over 5 min at r. t. and the reaction stirred for 18 hours. The reaction mixture was then concentrated *in vacuo*. Flash column

chromatography (4:1, hexane/EtOAc) gave **128** (1.67 g, 93%) as an orange solid.

^{1}H NMR (400 MHz, $CDCl_3$) δ 6.84 (d, *J* = 8.5, 1H), 6.60 (dd, *J* = 8.5, 2.5, 1H), 6.52 (d, *J* = 2.5, 1H), 3.87 (s, 3H), 3.86 (s, 3H); **^{13}C{^{1}H} NMR** (101 MHz, $CDCl_3$) δ 150.1, 146.7, 132.9, 112.2, 110.6, 103.3, 56.3, 56.1; **AT-IR** (neat) ν (cm^{-1}) 2961, 2923, 2846, 2099, 1592, 1507, 1446, 1420, 1339, 1296, 1269, 1234, 1179, 1142, 1116, 1022, 920, 902, 855, 832.

Benzyl 2,2,2-trifluoroacetate (**135**)[92]

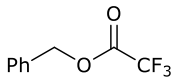

To a solution of benzyl alcohol (310 µL, 3.00 mmol) in THF (5 mL) was added trifluoracetic anhydride (500 µL, 3.60 mmol). The resulting solution was heated to reflux for 45 min. The reaction mixture was then diluted with Et_2O (15 mL), washed with sat. aq. $NaHCO_3$ (3 × 10 mL), dried ($MgSO_4$) and concentrated *in vacuo* to give **135** (532 mg, 87%) as a colourless oil.

^{1}H NMR (400 MHz, $CDCl_3$) δ 7.47 – 7.34 (m, 5H), 5.40 (s, 2H); **^{13}C{^{1}H} NMR** (101 MHz, $CDCl_3$) δ 157.4 (q, *J* = 42.5), 133.3, 129.3, 128.9, 128.7, 114.6 (q, *J* = 286.0), 69.6; **^{19}F NMR** (376 MHz, $CDCl_3$) δ −74.1 (s, 3F); **AT-IR** (neat) ν (cm^{-1}) 1778, 1420, 1346, 1275, 1213, 1136, 1125, 1016, 975.

Dibenzylamine (**136**)[93]

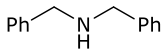

To a solution of triphenylphosphine (262 mg, 1.00 mmol) in dry toluene (2 mL) was added benzyl azide (**92**) (125 μL, 1.00 mmol). The resulting solution was stirred at 70 °C for 2.5 hours. To the reaction mixture was added benzyl 2,2,2-trifluoroacetate (**135**) (204 mg, 1.00 mmol) in dry toluene (2 mL). The reaction mixture was then heated to 100 °C for 72 hours. To the cooled reaction mixture was added 1M NaOH (1 mL) and stirred at r. t. for 2.5 hours. The reaction mixture was then diluted with Et_2O (5 mL) and extracted with 2 M HCl (3 × 5 mL). The combined aqueous layers were neutralised with sat. aq. $NaHCO_3$ (25 mL) and extracted with Et_2O (3 × 30 mL). The combined organic layers were dried ($MgSO_4$) and concentrated *in vacuo*. Flash column chromatography (1:1, petroleum ether/EtOAc) gave **136** (31 mg, 16%) as a colourless oil.

^{1}H NMR (400 MHz, $CDCl_3$) δ 7.42 – 7.28 (m, 10H), 3.86 (s, 4H); **^{13}C{^{1}H} NMR** (101 MHz, $CDCl_3$) δ 140.3, 128.5, 128.2, 127.0, 53.2; **HRMS** (ESI^+) $C_{14}H_{16}N^+$ $[M+H]^+$ calcd. 198.1277, found 198.1290.

N-Benzyl-3,4-dimethoxyaniline (**137**)[94]

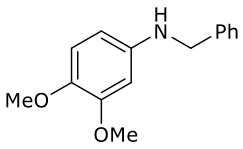

To a solution of triphenylphosphine (262 mg, 1.00 mmol) in dry toluene (2 mL) was added 4-azido-1,2-dimethoxybenzene (**128**) (179 mg, 1.00 mmol). The resulting solution was stirred at r. t. for 2.5 hours. To the reaction mixture was added benzyl 2,2,2-trifluoroacetate (**135**) (204 mg, 1.00 mmol) in dry toluene (2 mL). The reaction mixture was then heated to 100 °C for 72 hours. To the cooled reaction mixture was added 1M NaOH (1 mL) and stirred at r. t. for 2.5 hours. The reaction mixture was then diluted with Et_2O (5 mL) and extracted with 2 M HCl (3 × 5 mL). The combined aqueous layers were neutralised with sat. aq. $NaHCO_3$ (25 mL) and extracted with Et_2O (3 × 30 mL). The combined organic layers were dried ($MgSO_4$) and concentrated *in vacuo*. Flash column chromatography (1:1, petroleum ether/EtOAc) gave **137** (56 mg, 23%) as a colourless oil.

^{1}H NMR (400 MHz, $CDCl_3$) δ 7.44 – 7.29 (m, 5H), 6.77 (d, *J* = 8.5, 1H), 6.31 (d, *J* = 2.7, 1H), 6.20 (dd, *J* = 8.5, 2.7, 1H), 4.32 (s, 2H), 3.84 (s, 3H), 3.83 (s, 3H); δ **HRMS** (ESI^+) $C_{15}H_{18}NO_2^+$ $[M+H]^+$ calcd. 244.1332, found 244.1361.

N-Benzylmethanesulfonamide (**146**)[95]

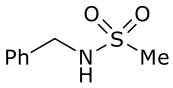

Sulfonic acid conventionally heated method:

To a solution of triphenylphosphine (262 mg, 1.00 mmol) in xylenes (4 mL) was added benzyl azide (**92**) (125 µL, 1.00 mmol). The resulting solution was heated to 70 °C for 3.75 hours. To the reaction mixture was then added methanesulfonic acid (65 µL, 1.0 mmol) and the reaction heated to reflux for 96 hours. The reaction mixture was then diluted with DCM (20 mL) and washed with 2 M NaOH (3 × 7 mL). The combined aqueous layers were extracted with DCM (3 × 20 mL), acidified with 6 M aq. HCl (8 mL) and extracted again with DCM (3 × 20 mL). The combined organic layers were washed with water (3 × 20 mL), dried ($MgSO_4$) and concentrated *in vacuo.* Flash column chromatography (2:3 petroleum ether/EtOAc) gave **146**(73 mg, 40%) as an off white solid.

Sulfonic acid microwave heated method:

To a solution of tris(4-fluorophenyl)phosphine (158 mg, 0.500 mmol) in trifluorotoluene (1 mL) was added benzyl azide (**92**) (67 mg, 0.50 mmol) in trifluorotoluene (1 mL). The resulting solution was heated to 70 °C for 2 hours. To the reaction mixture was then added methanesulfonic acid (32 µL, 0.50 mmol) and the reaction heated to 220 °C in a microwave for 3 hours. The reaction mixture was then diluted with DCM (10 mL) and washed with 2 M NaOH (3 × 3 mL). The combined aqueous layers were

extracted with DCM (3 × 10 mL), acidified with 6 M aq. HCl (4 mL) and extracted again with DCM (3 × 10 mL). The combined organic layers were washed with water (3 × 10 mL), dried ($MgSO_4$) and concentrated *in vacuo.* Flash column chromatography (1:1, hexane/EtOAc) gave **146** (59 mg, 63%) as an off white solid.

Traceless Staudinger-sulfonamide ligation method:

To a solution of benzyl azide (**92**) (27 mg, 0.20 mmol) in toluene (2 mL) was added 2-(diphenylphosphino)phenyl methanesulfonate (**158**) (71 mg, 0.20 mmol). The reaction mixture was heated to 70 °C for 8 hours before 6M NaOH (0.5 mL) was added and the reaction heated at 70 °C for a further 2 hours. The reaction mixture was then neutralised with 1M HCl and extracted with DCM (3 × 10 mL). The combined organic extracts were washed with brine (3 × 30 mL), dried ($MgSO_4$) and concentrated *in vacuo*. Flash column chromatography (24:1, DCM/EtOAc) gave **146** (21 mg, 68%) as an off-white solid.

^{1}H NMR (400 MHz, $CDCl_3$) δ 7.46 – 7.31 (m, 5H), 4.84 (br, 1H), 4.35 (d, *J* = 6.1, 2H), 2.88 (s, 3H); **^{13}C{^{1}H} NMR** (101 MHz, $CDCl_3$) δ 136.68, 128.92, 128.12, 127.91, 47.21, 41.12; **HRMS** (ESI^+) $C_8H_{11}NO_2SNa^+$ $[M+Na]^+$ calcd. 208.0408, found 208.0400.

N-Benzylbenzenesulfonamide (**153**)[96]

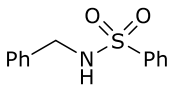

To a solution of triphenylphosphine (262 mg, 1.00 mmol) in trifluorotoluene (2 mL) was added benzyl azide (**92**) (133 mg, 1.00 mmol) in trifluorotoluene (2 mL). The resulting solution was heated to 70 °C for 2 hours. To the reaction mixture was then added benzenesulfonic acid (158 mg, 1.00 mmol) and the reaction heated to 220 °C in a microwave for 3 hours. The reaction mixture was then diluted with DCM (10 mL) and washed with 2 M NaOH (3 × 3 mL). The combined aqueous layers were extracted with DCM (3 × 10 mL), acidified with 6 M aq. HCl (4 mL) and extracted again with DCM (3 × 10 mL). The combined organic layers were washed with water (3 × 10 mL), dried ($MgSO_4$) and concentrated *in vacuo.* Flash column chromatography (4:1, hexane/EtOAc) gave **153** (125 mg, 51%) as a white solid.

^{1}H NMR (400 MHz, $CDCl_3$) δ 7.92 – 7.83 (m, 2H), 7.63 – 7.56 (m, 1H), 7.56 – 7.48 (m, 2H), 7.33 – 7.23 (m, 3H), 7.22 – 7.14 (m, 2H), 4.64 (br, 1H), 4.16 (d, *J* = 6.2, 2H); **^{13}C{^{1}H} NMR** (101 MHz, $CDCl_3$) δ 140.1, 136.3, 132.9, 129.3, 128.9, 128.2, 128.0, 127.3, 47.5; **HRMS** (ESI^-) $C_{13}H_{12}NO_2S^-$ $[M-H]^-$ calcd. 246.0594, found 246.0598.

N-Benzyl-4-chlorobenzenesulfonamide (**154**)[97]

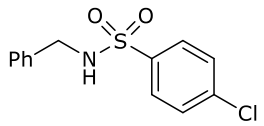

To a solution of triphenylphosphine (262 mg, 1.00 mmol) in trifluorotoluene (2 mL) was added benzyl azide (**92**) (133 mg, 1.00 mmol) in trifluorotoluene (2 mL). The resulting solution was heated to 70 °C for 2 hours. To the reaction mixture was then added 4-chlorobenzenesulfonic acid (193 mg, 1.00 mmol) and the reaction heated to 220 °C in a microwave for 3 hours. The reaction mixture was then diluted with DCM (10 mL) and washed with 2 M NaOH (3 × 3 mL). The combined aqueous layers were extracted with DCM (3 × 10 mL), acidified with 6 M aq. HCl (4 mL) and extracted again with DCM (3 × 10 mL). The combined organic layers were washed with water (3 × 10 mL), dried ($MgSO_4$) and concentrated *in vacuo.* Flash column chromatography (4:1, hexane/EtOAc) gave **154** (40 mg, 14%) as a white solid.

^{1}H NMR (400 MHz, $CDCl_3$) δ 7.82 – 7.76 (m, 2H), 7.51 – 7.44 (m, 2H), 7.33 – 7.24 (m, 3H), 7.21 – 7.16 (m, 2H), 4.70 (br, 1H), 4.20 – 4.11 (m, 2H); **^{13}C{^{1}H} NMR** (101 MHz, $CDCl_3$) δ 139.4, 138.7, 136.0, 129.6, 128.9, 128.7, 128.3, 128.0, 47.5; **HRMS** (ESI^-) $C_{13}H_{11}ClNO_2S^-$ $[M-H]^-$ calcd. 280.0205, found 280.0204.

4-Methoxybenzenesulfonic acid (**171**)[98]

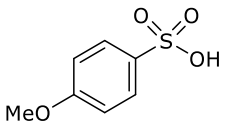

To water (20 mL) was added 4-methoxybenzenesulfonyl chloride (2.07 g, 10.0 mmol) dropwise over 3 min. The reaction mixture stirred at r. t. for 48 hours then heated to reflux for 5 hours. The reaction mixture was concentrated *in vacuo* to give a white solid. The resulting solid was then heated *in vacuo* to 200 °C for 15 min in the presence of $CaCl_2$ to give **171** (1.45 g, 77%) as a red solid.

^{1}H NMR (400 MHz, $CDCl_3$) δ 10.16 – 10.09 (s, 1H), 7.88 – 7.83 (m, 2H), 7.02 – 6.96 (m, 2H), 3.88 (s, 3H); **^{13}C{^{1}H} NMR** (101 MHz, $CDCl_3$) δ 163.8, 130.4, 129.3, 114.5, 55.9; **HRMS** (ESI^-) $C_7H_7O_4S^-$ $[M-H]^-$ calcd. 187.0071, found 187.0069.

N-Benzyl-4-methoxybenzenesulfonamide (**155**)[99]

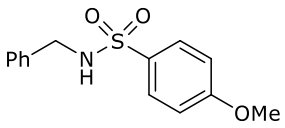

To a solution of triphenylphosphine (262 mg, 1.00 mmol) in trifluorotoluene (2 mL) was added benzyl azide (**92**) (133 mg, 1.00 mmol) in trifluorotoluene (2 mL). The resulting solution was heated to 70 °C for 2 hours. To the reaction mixture was then added 4-methoxybenzenesulfonic acid (**171**) (188 mg, 1.00 mmol) and the reaction heated to 220 °C in a

microwave for 3 hours. The reaction mixture was then diluted with DCM (10 mL) and washed with 2 M NaOH (3 × 3 mL). The combined aqueous layers were extracted with DCM (3 × 10 mL), acidified with 6 M aq. HCl (4 mL) and extracted again with DCM (3 × 10 mL). The combined organic layers were washed with water (3 × 10 mL), dried ($MgSO_4$) and concentrated *in vacuo.* Flash column chromatography (4:1, hexane/EtOAc) gave **155** (131 mg, 47%) as a white solid.

^{1}H NMR (400 MHz, $CDCl_3$) δ 7.84 – 7.79 (m, 2H), 7.36 – 7.23 (m, 3H), 7.22 – 7.17 (m, 2H), 7.02 – 6.94 (m, 2H), 4.55 (t, *J* = 6.1, 1H), 4.12 (d, *J* = 6.1, 2H), 3.88 (s, 3H); **^{13}C{^{1}H} NMR** (101 MHz, $CDCl_3$) δ 163.1, 136.4, 131.6, 129.5, 128.9, 128.1, 128.0, 114.4, 55.8, 47.4; **HRMS** (ESI^-) $C_{14}H_{14}NO_3S^-$ $[M-H]^-$ calcd. 276.0700, found 276.0695.

N-(3,4-Dimethoxyphenyl)methanesulfonamide (**156**)

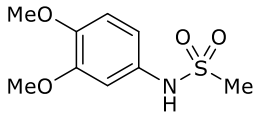

Sulfonic acid microwave heated method:

To a solution of triphenylphosphine (131 mg, 0.500 mmol) in trifluorotoluene (2 mL) was added 4-azido-1,2-dimethoxybenzene (**128**) (90 mg, 0.50 mmol) in trifluorotoluene (1 mL). The resulting solution was stirred at r. t. for 2 hours. To the reaction mixture was then added methanesulfonic acid (32 µL, 0.50 mmol) and the reaction heated to 220 °C in a microwave for 3 hours. The reaction mixture was then diluted with DCM (10 mL) and washed with 2 M NaOH (3 × 3 mL). The combined

aqueous layers were extracted with DCM (3 × 10 mL), acidified with 6 M aq. HCl (4 mL) and extracted again with DCM (3 × 10 mL). The combined organic layers were washed with water (3 × 10 mL), dried ($MgSO_4$) and concentrated *in vacuo.* Flash column chromatography (1:1, petroleum ether/EtOAc) gave **156** (62 mg, 53%) as an off white solid.

Traceless Staudinger-sulfonamide ligation method:

To a solution of 4-azido-1,2-dimethoxybenzene (**128**) (36 mg, 0.20 mmol) in toluene (2 mL) was added 2-(diphenylphosphino)phenyl methanesulfonate (**158**) (71 mg, 0.20 mmol). The reaction mixture was heated to 70 °C for 8 hours before 6M NaOH (0.5 mL) was then added and the reaction heated at 70 °C for a further 2 hours. The reaction mixture was neutralised with 1M HCl then extracted with DCM (3 × 10 mL). The combined organic extracts were washed with brine (3 × 30 mL), dried ($MgSO_4$) and concentrated *in vacuo*. Flash column chromatography (24:1 to 4:1, DCM/EtOAc) gave **156** (7 mg, 15%) as an off-white solid.

^{1}H NMR (400 MHz, $CDCl_3$) δ 6.88 (d, *J* = 2.5, 1H), 6.83 (d, *J* = 8.5, 1H), 6.75 (dd, *J* = 8.5, 2.5, 1H), 6.19 (br, 1H), 3.89 (s, 3H), 3.88 (s, 3H), 2.96 (s, 3H); **^{13}C{^{1}H} NMR** (101 MHz, $CDCl_3$) δ 149.9, 147.9, 129.5, 115.0, 111.7, 107.6, 56.3, 56.2, 39.1; **HRMS** (ESI^-) $C_9H_{12}NO_4S^-$ $[M-H]^-$ calcd. 230.0493, found 230.0493.

2-(Diphenylphosphino)phenol (**162**)[100]

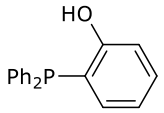

To a solution of 2-iodophenol (2.20 g, 10.0 mmol), palladium(II) acetate (22 mg, 1.0 mol%) and sodium acetate (902 mg, 11.0 mmol) in dimethylacetamide (31 mL) was added diphenylphosphine (1.74 mL, 10.0 mmol) dropwise over 4 min. The reaction mixture was then heated to 110 °C for 15 hours then filtered through celite. Flash column chromatography (9:1, petroleum ether/EtOAc) gave **162** (2.11 g, 76%) as a white solid.

^{1}H NMR (400 MHz, $CDCl_3$) δ 7.40 – 7.28 (m, 11H), 7.01 – 6.95 (m, 1H), 6.96 – 6.90 (m, 1H), 6.92 – 6.85 (m, 1H), 6.15 (d, *J* = 6.6, 1H); **^{13}C{^{1}H} NMR** (101 MHz, $CDCl_3$) δ 159.3 (d, *J* = 18.7), 135.1 (d, *J* = 4.9), 134.9 (d, *J* = 4.1), 133.5 (d, *J* = 18.8), 131.8, 129.2, 128.9 (d, *J* = 7.2), 121.3 (d, *J* = 2.5), 121.1 (d, *J* = 5.4), 115.7 (d, *J* = 1.6); **^{31}P{^{1}H} NMR** (121 MHz, $CDCl_3$) δ −29.1; **HRMS** (ESI^+) $C_{18}H_{15}NaOP^+$ $[M+Na]^+$ calcd. 301.0753, found 301.0752.

2-(Diphenylphosphino)phenol-borane complex (**163**)[101]

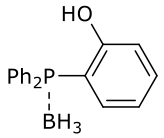

To a solution of 2-(diphenylphosphino)phenol (**162**) (1.39 g, 5.00 mmol) in THF (21 mL) at −78 °C was added borane-THF complex (1.0M in THF, 1.10 mL, 1.10 mmol) dropwise over 3 min. The reaction mixture was stirred at r. t. for 18 hours then concentrated *in vacuo*. Flash column chromatography (4:1, petroleum ether/EtOAc) gave **163** (1.46 g, quantitative) as a white solid.

^{1}H NMR (400 MHz, $CDCl_3$) δ 7.58 – 7.50 (m, 7H), 7.49 – 7.39 (m, 5H), 7.04 – 6.97 (m, 1H), 6.98 – 6.86 (m, 2H), 1.97 – 0.98 (m, 3H); **^{11}B{^{1}H} NMR** (128 MHz, $CDCl_3$) δ −36.6 (d, *J* = 52.4); **^{13}C{^{1}H} NMR** (101 MHz, $CDCl_3$) δ 160.7 (d, *J* = 9.3), 134.5 (d, *J* = 3.2), 134.1 (d, *J* = 1.9), 133.1 (d, *J* = 10.0), 131.8 (d, *J* = 2.4), 129.1 (d, *J* = 10.6), 128.1 (d, *J* = 61.8), 120.8 (d, *J* = 7.8), 118.7 (d, *J* = 6.1), 111.8 (d, *J* = 58.6); **^{31}P{^{1}H} NMR** (162 MHz, $CDCl_3$) δ 13.5 – 11.6 (m); **HRMS** (ESI^-) $C_{18}H_{17}BOP^-$ $[M-H]^-$ calcd. 291.1110, found 291.1121.

2-(Diphenylphosphino)phenyl methanesulfonate (**158**)

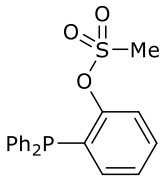

Borane protection route:

To potassium *tert*-butoxide (77 mg, 0.69 mmol) was added 22-(diphenylphosphino)phenol-borane complex (**163**) (155 mg, 0.530 mmol) in THF (5 mL). To the resulting suspension was added methanesulfonyl chloride (53 µL, 0.69 mmol) dropwise over 1 min and the reaction mixture stirred at r. t. for 18 hours. The reaction mixture was then added to sat. aq. $NaHCO_3$ (10 mL), extracted with EtOAc (3 × 20 mL), dried ($MgSO_4$) and concentrated *in vacuo*. Flash column chromatography (85:15, petroleum ether/EtOAc) gave the borane complex **164** (85 mg) as a white solid. The borane complex (**164**) was then dissolved in a 2:1 toluene/methanol mixture (3 mL) and heated to 60 °C for 3 hours then concentrated *in vacuo*. Flash column chromatography (85:15, petroleum ether/EtOAc) gave **158** (66 mg, 35% over two steps) as a white solid.

Two step, no protecting groups route:

To a solution of 2-iodophenyl methanesulfonate (**165**) (894 mg, 3.00 mmol), palladium(II) acetate (7 mg, 1 mol%) and sodium acetate (271 mg, 3.30 mmol) in dimethylacetamide (9 mL) was added diphenylphosphine (522 µL, 3.00 mmol) dropwise over 2 min. The reaction mixture was heated to 110 °C for 15 hours then filtered through celite.

Flash column chromatography (9:1, petroleum ether/EtOAc) gave **158** (671 mg, 63%) as a white solid.

^{1}H NMR (500 MHz, $CDCl_3$) δ 7.49 (ddd, *J* = 8.2, 4.1, 0.9, 1H), 7.45 – 7.29 (m, 11H), 7.20 (td, *J* = 7.6, 1.0, 1H), 6.87 (ddd, *J* = 7.6, 3.8, 1.6, 1H), 3.05 (s, 3H); **^{13}C{^{1}H} NMR** (126 MHz, $CDCl_3$) δ 151.8 (d, *J* = 18.4), 135.2 (d, *J* = 9.9), 134.6, 134.0 (d, *J* = 20.5), 130.8 (d, *J* = 16.9), 130.6, 129.3, 128.8 (d, *J* = 7.3), 127.2, 122.0, 38.7 (d, *J* = 7.7); **^{31}P{^{1}H} NMR** (202 MHz, $CDCl_3$) δ −16.6; **HRMS** (ESI^+) $C_{19}H_{18}O_3PS^+$ $[M+H]^+$ calcd. 357.0709, found 357.0711; **AT-IR** (neat) ν (cm^{-1}) 3065, 3030, 3012, 2923, 1588, 1568, 1465, 1435, 1352, 1329, 1311, 1264, 1202, 155, 1128, 1102, 1069, 998, 967, 863; **m. p.** 102– 104°C.

2-Iodophenyl methanesulfonate (**165**)[102]

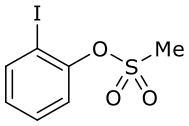

To a solution of 2-iodophenol (2.20 g, 10.0 mmol) and potassium *tert*-butoxide (1.49 g, 13.0 mmol) in THF (88 mL) was added methanesulfonyl chloride (0.99 mL, 13 mmol) dropwise over 5 min. The reaction mixture was then stirred at r. t. for 40 hours. To the reaction was added sat. aq. $NaHCO_3$ (90 mL) and the resulting solution was extracted with EtOAc (3 × 90 mL). The combined organic layers were dried ($MgSO_4$) and concentrated *in vacuo*. Flash column chromatography (9:1, petroleum ether/EtOAc) gave **165** (2.59 g, 87%) as a pink solid.

^{1}H NMR (400 MHz, $CDCl_3$) δ 7.87 (dd, *J* = 7.9, 1.5, 1H), 7.46 (dd, *J* = 8.2, 1.6, 1H), 7.40 (ddd, *J* = 8.2, 7.3, 1.5, 1H), 7.05 (ddd, *J* = 7.9, 7.3, 1.6, 1H), 3.30 (s, 3H); **^{13}C{^{1}H} NMR** (101 MHz, $CDCl_3$) δ 149.6, 140.3, 130.0, 128.9, 123.3, 89.7, 39.5; **HRMS** (ESI^+) $C_7H_7INaO_3S^+$ $[M+Na]^+$ calcd. 320.9053, found 320.9051.

N-(Hex-5-en-1-yl)methanesulfonamide (**166**)[103]

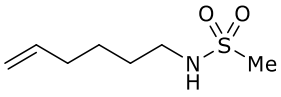

To a solution of 6-azidohex-1-ene (25 mg, 0.20 mmol) in pentane (71 µL) was added 2-(diphenylphosphino)phenyl methanesulfonate (**158**) (71 mg, 0.20 mmol) in toluene (2 mL). The reaction mixture was heated to 70 °C for 8 hours before 6M NaOH (0.5 mL) was then added and the reaction heated at 70 °C for a further 2 hours. The reaction mixture was neutralised with 1M HCl then extracted with DCM (3 × 10 mL). The combined organic extracts were washed with brine (3 × 30 mL), dried ($MgSO_4$) and concentrated *in vacuo*. Flash column chromatography (24:1, DCM/EtOAc) gave **166** (21 mg, 60%) as a colourless oil.

^{1}H NMR (400 MHz, $CDCl_3$) δ 5.77 (ddt, *J* = 16.9, 10.2, 6.7, 1H), 5.01 (apparent dq, *J* = 16.9, 1.6 Hz, 1H), 4.95 (ddt, *J* = 10.2, 2.1, 1.2 , 1H) 4.52 (br, 1H), 3.16 – 3.06 (m, 2H), 2.94 (s, 3H), 2.13 – 2.01 (m, 2H), 1.64 – 1.52 (m, 2H), 1.51 – 1.37 (m, 2H); **^{13}C{^{1}H} NMR** (101 MHz, $CDCl_3$) δ 138.2, 115.2, 43.3, 40.4, 33.2, 29.6, 25.9; **HRMS** (ESI^+) $C_7H_{15}NNaO_2S^+$ $[M+H]^+$ calcd. 178.0896, found 178.0905.

(2-hydroxyphenyl)diphenylphosphine oxide (**105**)[104]

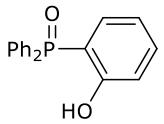

To a solution of 2-(diphenylphosphino)phenol (**162**) (194 mg, 0.700 mmol) in DCM (5 mL) was added aqueous hydrogen peroxide (30% w/v, 114 µL, 1.11 mmol) dropwise over 1 min. The reaction mixture was stirred at r. t. for 48 hours then diluted with DCM (20 mL) and washed with water (2 × 20 mL) and brine (20 mL). The organic layer was then dried ($MgSO_4$) and concentrated *in vacuo* to give **105** (209 mg, quantitative) as a white solid.

^{1}H NMR (400 MHz, $CDCl_3$) δ 11.14 (s, 1H), 7.74 – 7.64 (m, 4H), 7.62 – 7.55 (m, 2H), 7.53 – 7.46 (m, 4H), 7.44 – 7.38 (m, 1H), 7.02 – 6.95 (m, 2H), 6.87 – 6.79 (m, 1H); **^{13}C{^{1}H} NMR** (101 MHz, $CDCl_3$) δ 164.1 (d, *J* = 2.8), 134.5 (d, *J* = 2.1), 132.7 (d, *J* = 2.7), 132.2 (d, *J* = 10.4), 132.1 (d, *J* = 9.9), 131.9 (d, *J* = 105.1), 128.9 (d, *J* = 12.4), 119.2 (d, *J* = 12.4), 118.8 (d, *J* = 7.5), 111.2 (d, *J* = 104.3); **^{31}P{^{1}H} NMR** (202 MHz, $CDCl_3$) δ 39.5; **HRMS** (ESI$^+$) $C_{18}H_{16}O_2P^+$ $[M+H]^+$ calcd. 295.0882, found 295.0879.

2-(Diphenylphosphoryl)phenyl methanesulfonate (**167**)

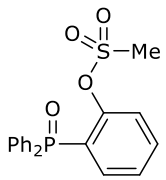

To a solution of (2-hydroxyphenyl)diphenylphosphine oxide (**105**) (147 mg, 0.500 mmol) and potassium *tert*-butoxide (74 mg, 0.65 mmol) in THF (5 mL) was added methanesulfonyl chloride (49 µL, 0.65 mmol) dropwise over 1 min. The reaction mixture was then stirred at r. t. for 40 hours. To the reaction was added Sat. aq. $NaHCO_3$ (5 mL) and the resulting solution was extracted with EtOAc (3 × 5 mL). The combined organic layers were dried ($MgSO_4$) and concentrated *in vacuo*. Flash column chromatography (1:1 to 0:1, petroleum ether/EtOAc) gave **167** (131 g, 71%) as a pink solid.

^{1}H NMR (400 MHz, $CDCl_3$) δ 7.75 – 7.66 (m, 4H), 7.65 – 7.54 (m, 4H), 7.54 – 7.45 (m, 4H), 7.33 – 7.22 (m, 2H), 3.00 (s, 3H); **^{13}C{^{1}H} NMR** (101 MHz, $CDCl_3$) δ 151.9, 135.0 (d, *J* = 8.6), 134.3 (d, *J* = 2.0), 132.3 (d, *J* = 2.8), 132.0 (d, *J* = 107.8), 131.8 (d, *J* = 10.0), 128.8 (d, *J* = 12.5), 126.4 (d, *J* = 11.4), 125.3 (d, *J* = 100.5), 122.4 (d, *J* = 5.5), 38.4; **^{31}P{^{1}H} NMR** (162 MHz, $CDCl_3$) δ 26.4; **HRMS** (ESI$^+$) $C_{19}H_{18}O_4PS^+$ $[M+H]^+$ calcd. 373.0658, found 373.0657; **AT-IR** (neat) ν (cm^{-1}) 3062, 3010, 2925, 2853, 1595, 1570, 1468, 1437, 1357, 1328, 1265, 1200, 1186, 1158, 1135, 1116, 1102, 1072, 1025, 984, 971, 878, 869; **m. p.** 146– 149°C.

1.6 References

1 H. Staudinger and J. Meyer, *Helv. Chim. Acta*, 1919, **2**, 635–646.

2 S. Gosling, C. El Amri and A. Tatibouët, *Synthesis*, 2014, **46**, 1079–1084.

3 J. I. G. Cadogan, R. Gee and R. J. Scott, *J. Chem. Soc. Chem. Commun.*, 1972, 1242.

4 F. D. Marsh and M. E. Hermes, *J. Am. Chem. Soc.*, 1964, **86**, 4506–4507.

5 J. E. Leffler and Y. Tsuno, *J. Org. Chem.*, 1963, **28**, 902–906.

6 R. Neidlein, *Angew. Chem.*, 1966, **78**, 333–334.

7 R. A. Baldwin and R. M. Washburn, *J. Org. Chem.*, 1965, **30**, 3860–3866.

8 B. li Li, P. Mukherjee and R. H. Neilson, *Inorg. Chem.*, 1989, **28**, 605–607.

9 W. L. Lehn, *Inorg. Chem.*, 1967, **6**, 1061–1063.

10 Y. G. Gololobov, I. N. Zhmurova and L. F. Kasukhin, *Tetrahedron*, 1981, **37**, 437–472.

11 I. Bosch, A. González, F. Urpí and J. Vilarrasa, *J. Org. Chem.*, 1996, **61**, 5638–5643.

12 R. Münstedt and U. Wannagat, *Monatshefte für Chemie - Chem. Mon.*, 1985, **116**, 7–18.

13 S. Al-Benna, M. J. Sarsfield, M. Thornton-Pett, D. L. Ormsby, P. J.

Maddox, P. Brès and M. Bochmann, *J. Chem. Soc. Dalton Trans.*, 2000, 4247–4257.

14 C. D. C. J. Smith, C. D. C. J. Smith, N. Nikbin, S. V. Ley and I. R. Baxendale, *Org. Biomol. Chem.*, 2011, **9**, 1927–1937.

15 M. Benhammou, R. Kraemer, H. Germa, J.-P. Majoral and E. J. Navech, *Phosphorus Sulfur Relat. Elem.*, 1982, **14**, 105–119.

16 M. R. Marre, M. Sanchez, J. F. Brazier, R. Wolf and J. Bellan, *Can. J. Chem.*, 1982, **60**, 456–468.

17 J. Breker, P. G. Jones and R. Schmutzler, *Phosphorus Sulfur Silicon Relat. Elem.*, 1990, **53**, 193–202.

18 A. V. Kirsanov, *Izv. Akad. Nauk SSSR.*, 1950, 426–437.

19 A. Buchard, A. Auffrant, C. Klemps, L. Vu-Do, L. Boubekeur, X. F. L. Goff and P. Le Floch, *Chem. Commun.*, 2007, 1502–1504.

20 A. Buchard, H. Heuclin, A. Auffrant, X. F. Le Goff and P. Le Floch, *J. Chem. Soc. Dalton Trans.*, 2009, 1659–1667.

21 H. Bock and M. Schnöller, *Angew. Chem.*, 1968, **80**, 667–668.

22 J. E. Leffler and R. D. Temple, *J. Am. Chem. Soc.*, 1967, **89**, 5235–5246.

23 C. Widauer, H. Grützmacher, I. Shevchenko and V. Gramlich, *Eur. J. Inorg. Chem.*, 1999, **1999**, 1659–1664.

24 M. Alajarin, C. Conesa and H. S. Rzepa, *J. Chem. Soc. Perkin Trans. 2*, 1999, 1811–1814.

25 H. Staudinger and E. Hauser, *Helv. Chim. Acta*, 1921, **4**, 861–886.

26 M. W. P. Bebbington and D. Bourissou, *Coord. Chem. Rev.*, 2009, **253**, 1248–1261.

27 V. P. Kukhar, L. F. Kasukhin, M. P. Ponomarchuk, A. N. Chernega, M. Y. Antipin and Y. T. Struchkov, *Phosphorus Sulfur Silicon Relat. Elem.*, 1989, **44**, 149–153.

28 H. Zimmer and G. Singh, *J. Org. Chem.*, 1963, **28**, 483–486.

29 H. L. Cohen, *J. Polym. Sci. Polym. Chem. Ed.*, 1985, **23**, 1671–1675.

30 W. S. Mungall, G. L. Greene, G. A. Heavner and R. L. Letsinger, *J. Org. Chem.*, 1975, **40**, 1659–1662.

31 A. Koziara, K. Osowska-Pactwicka, S. Zawadzki and A. Zwierzak, *Synthesis*, 1985, **1985**, 202–204.

32 G. W. J. Fleet, P. W. Smith, S. V. Evans and L. E. Fellows, *J. Chem. Soc. - Ser. Chem. Commun.*, 1984, 1240–1241.

33 M. Vaultier, N. Knouzi and R. Carrié, *Tetrahedron Lett.*, 1983, **24**, 763–764.

34 S. Pilard and M. Vaultier, *Tetrahedron Lett.*, 1984, **25**, 1555–1556.

35 M. Bessodes, E. Abushanad and K. Antonakis, *Tetrahedron Lett.*, 1984, **25**, 5899–5902.

36 H. A. van Kalkeren, J. J. Bruins, F. P. J. T. Rutjes and F. L. van Delft, *Adv. Synth. Catal.*, 2012, **354**, 1417–1421.

37 C. J. O'Brien, J. L. Tellez, Z. S. Nixon, L. J. Kang, A. L. Carter, S. R. Kunkel, K. C. Przeworski and G. A. Chass, *Angew. Chem. Int. Ed.*, 2009, **48**, 6836–6839.

38 G. Wittig and G. Geissler, *Justus Liebigs Ann. Chem.*, 1953, **580**,

44–57.

39 G. Wittig and U. Schollkopf, *Chem.Ber.*, 1954, **87**, 1318–1330.

40 F. Palacios, C. Alonso, D. Aparicio, G. Rubiales and J. M. de los Santos, *Tetrahedron*, 2007, **63**, 523–575.

41 F. P. Cossío, C. Alonso, B. Lecea, M. Ayerbe, G. Rubiales and F. Palacios, *J. Org. Chem.*, 2006, **71**, 2839–2847.

42 Y. Xue, D. Xie and G. Yan, *J. Phys. Chem. A*, 2002, **106**, 9053–9058.

43 J. Koketsu, Y. Ninomiya, Y. Suzuki and N. Koga, *Inorg. Chem.*, 1997, **36**, 694–702.

44 W. C. Lu, C. B. Liu and C. C. Sun, *J. Phys. Chem. A*, 1999, **103**, 1078–1083.

45 N. Kano, X. J. Hua, S. Kawa and T. Kawashima, *Tetrahedron Lett.*, 2000, **41**, 5237–5241.

46 T. Gajda, A. Koziara, K. Osowska-Pacewicka, S. Zawadzk and A. Zwierzak, *Synth. Commun.*, 1992, **22**, 1929–1938.

47 M. P. Cassidy, A. D. Özdemir and A. Padwa, *Org. Lett.*, 2005, **7**, 1339–1342.

48 F. Palacios, C. Alonso and G. Rubiales, *J. Org. Chem.*, 1997, **62**, 1146–1154.

49 I. A. O'Neil, C. L. Murray, A. J. Potter and S. B. Kalindjian, *Tetrahedron Lett.*, 1997, **38**, 3609–3610.

50 S. P. Marsden, A. E. McGonagle and B. McKeever-Abbas, *Org. Lett.*, 2008, **10**, 2589–2591.

51 J. J. Monagle, T. W. Campbell and H. F. McShane, *J. Am. Chem. Soc.*, 1962, **84**, 4288–4295.

52 J. Garcia, F. Urpí and J. Vilarrasa, *Tetrahedron Lett.*, 1984, **25**, 4841–4844.

53 K. G. Andrews and R. M. Denton, *Chem. Commun.*, 2017, **53**, 7982–7985.

54 A. D. Kosal, E. E. Wilson and B. L. Ashfeld, *Angew. Chem. Int. Ed.*, 2012, **51**, 12036–12040.

55 J. A. Prescher and C. R. Bertozzi, *Nat. Chem. Biol.*, 2005, **1**, 13–21.

56 H. C. Hang, C. Yu, M. R. Pratt and C. R. Bertozzi, *J. Am. Chem. Soc.*, 2004, **126**, 6–7.

57 E. M. Sletten and C. R. Bertozzi, *Angew. Chem. Int. Ed.*, 2009, **48**, 6974–6998.

58 R. J. Griffin, *Prog. Med. Chem.*, 1994, **31**, 121–232.

59 E. Saxon and C. R. Bertozzi, *Science*, 2000, **287**, 2007–2010.

60 I. Bosch, P. Romea, F. Urpí and J. Vilarrasa, *Tetrahedron Lett.*, 1993, **34**, 4671–4674.

61 F. L. Lin, H. M. Hoyt, H. Van Halbeek, R. G. Bergman and C. R. Bertozzi, *J. Am. Chem. Soc.*, 2005, **127**, 2686–2695.

62 C. I. Schilling, N. Jung, M. Biskup, U. Schepers and S. Bräse, *Chem. Soc. Rev.*, 2011, **40**, 4840–4871.

63 M. Köhn and R. Breinbauer, *Angew. Chem. Int. Ed.*, 2004, **43**, 3106–3116.

64 E. Saxon, J. I. Armstrong and C. R. Bertozzi, *Org. Lett.*, 2000, **2**, 2141–2143.

65 B. L. Nilsson, L. L. Kiessling and R. T. Raines, *Org. Lett.*, 2000, **2**, 1939–1941.

66 R. Serwa, L. Wakening, G. Del Signore, M. Mühlberg, I. Claußnitzer, C. Weise, M. Gerrits and C. P. R. Hackenberger, *Angew. Chem. Int. Ed.*, 2009, **48**, 8234–8239.

67 M. R. J. Vallée, P. Majkut, I. Wilkening, C. Weise, G. Müller and C. P. R. Hackenberger, *Org. Lett.*, 2011, **13**, 5440–5443.

68 G. Ren, Q. Zheng and H. Wang, *Org. Lett.*, 2017, **19**, 1582–1585.

69 J. Dong, L. Krasnova, M. G. Finn and K. Barry Sharpless, *Angew. Chem. Int. Ed.*, 2014, **53**, 9430–9448.

70 I. R. Lehnman, *Science*, 1974, **186**, 790–797.

71 S.-Y. Pyun, Y.-H. Lee and T.-R. Kim, *Kinet. Catal.*, **46**, 21–28.

72 W. Reeve, C. M. Erikson and P. F. Aluotto, *Can. J. Chem.*, 1979, **57**, 2747–2754.

73 Y. Ittah, Y. Sasson, I. Shahak, S. Tsaroom and J. Blum, *J. Org. Chem.*, 1978, **43**, 4271–4273.

74 R. M. Denton, J. An, B. Adeniran, A. J. Blake, W. Lewis and A. M. Poulton, *J. Org. Chem.*, 2011, **76**, 6749–6767.

75 M. A. Navia, *Science*, 2000, **288**, 2132–2133.

76 L. C. Bouchez, S. R. Dubbaka, M. Turks and P. Vogel, *J. Org. Chem.*, 2004, **69**, 6413–6418.

77 A. Kolaczek, I. Fusiarz, J. Lawecka and D. Branowska, *Chemik*, 2014, **68**, 620–628.

78 S. Caddick, J. D. Wilden and D. B. Judd, *J. Am. Chem. Soc.*, 2004, **126**, 1024–1025.

79 N. Eid, I. Karamé and B. Andrioletti, *Eur. J. Org. Chem.*, 2018, **2018**, 5016–5022.

80 D. M. P. Mingos and D. R. Baghurst, *Chem. Soc. Rev.*, 1991, **20**, 1–47.

81 R. A. Abramovitch, *Org. Prep. Proced. Int.*, 1991, **23**, 683–711.

82 S. Caddick, *Tetrahedron*, 1995, **51**, 10403–10432.

83 S. A. Galema, *Chem. Soc. Rev.*, 1997, **26**, 233.

84 C. O. Kappe, *Angew. Chem. Int. Ed.*, 2004, **43**, 6250–6284.

85 A. De La Hoz, Á. Díaz-Ortiz and A. Moreno, *Chem. Soc. Rev.*, 2005, **34**, 164–178.

86 P. Lidström, J. Tierney, B. Wathey and J. Westman, *Tetrahedron*, 2001, **57**, 9225–9283.

87 A. A. Maryott and E. R. Smith, *Table of dielectric constants of pure liquids*, National Bureau Of Standards, Gaithersburg MD, 1951.

88 P. Calcagno, B. M. Kariuki, S. J. Kitchin, J. M. A. Robinson, D. Philp and K. D. M. Harris, *Chem.: Eur. J.*, 2000, **6**, 2338–2349.

89 M. Mečiarov, Š. Toma, A. Loupy and B. Horváth, *Phosphorus Sulfur Silicon Relat. Elem.*, 2008, **183**, 21–33.

90 L. Campbell-Verduyn, P. H. Elsinga, L. Mirfeizi, R. A. Dierckx and B.

L. Feringa, *Org. Biomol. Chem.*, 2008, **6**, 3461–3463.

91 A. S. Kumar, M. A. Reddy, M. Knorn, O. Reiser and B. Sreedhar, *Eur. J. Org. Chem.*, 2013, 4674–4680.

92 Z. Yang and J. Zhou, *J. Am. Chem. Soc.*, 2012, **134**, 11833–11835.

93 P. R. Sultane, T. B. Mete and R. G. Bhat, *Org. Biomol. Chem.*, 2014, **12**, 261–264.

94 E. J. Hennessy and S. L. Buchwald, *J. Am. Chem. Soc.*, 2003, **125**, 12084–12085.

95 Z. Li, L. Jin and C. Cai, *Org. Biomol. Chem.*, 2017, **15**, 1317–1320.

96 T. Liu, D. Zheng, Z. Li and J. Wu, *Adv. Synth. Catal.*, 2017, **359**, 2653–2659.

97 M. Zhu, K. I. Fujita and R. Yamaguchi, *Org. Lett.*, 2010, **12**, 1336–1339.

98 K. Bahrami, M. M. Khodaei and J. Abbasi, *Synthesis*, 2012, **2012**, 316–322.

99 M. H. S. A. Hamid, C. L. Allen, G. W. Lamb, A. C. Maxwell, H. C. Maytum, A. J. A. Watson and J. M. J. Williams, *J. Am. Chem. Soc.*, 2009, **131**, 1766–1774.

100 F. Blume, S. Zemolka, T. Fey, R. Kranich and H. G. Schmalz, *Adv. Synth. Catal.*, 2002, **344**, 868–883.

101 C. Mamat, A. Flemming, M. Köckerling, J. Steinbach and F. R. Wuest, *Synthesis*, 2009, 3311–3321.

102 T. Ritter, K. Stanek, I. Larrosa and E. M. Carreira, *Org. Lett.*, 2004, **6**, 1513–1514.

103 T. H. Jepsen, M. Larsen and M. B. Nielsen, *Tetrahedron*, 2010, **66**, 6133–6137.

104 N. Qi, N. Zhang, S. R. Allu, J. Gao, J. Guo and Y. He, *Org. Lett.*, 2016, **18**, 6204–6207.